Universidade de Aveiro Departamento de Química
2014

Flávio Alberto da Silva Figueira

Porfirinas expandidas e sua avaliação como quimiossensores de aniões

Expanded porphyrins and their evaluation as anion chemosensors

Tese apresentada à Universidade de Aveiro para cumprimento dos requisitos necessários à obtenção do grau de Doutor em Química, realizada sob a orientação científica do Doutor João Paulo Costa Tomé, Investigador Principal do Departamento de Química da Universidade de Aveiro, e do Doutor José Abrunheiro da Silva Cavaleiro, Professor Catedrático do Departamento de Química da Universidade de Aveiro.

Este trabalho de doutoramento foi financiado pela FCT (Fundação para a Ciência e Tecnologia) através da bolsa de doutoramento SFRH/BD/46788/2008

o júri

presidente

Prof. Doutor João Manuel Nunes Torrão
Professor Catedrático do Departamento de Línguas e Culturas da Universidade de Aveiro

Prof. Doutor Carlos Alberto Mateus Afonso
Professor Catedrático da Faculdade de Farmácia da Universidade de Lisboa

Prof. Doutora Amélia Pilar Grases Santos Silva Rauter
Professora Associada com Agregação do Departamento de Química e Bioquímica da Faculdade de Ciências da Universidade de Lisboa

Prof. Doutor Augusto Costa Tomé
Professor Associado com Agregação do Departamento de Química da Universidade de Aveiro

Prof. Doutora Maria Manuela Marques Raposo
Professora Associada do Departamento de Química da Universidade do Minho

Doutor João Paulo Costa Tomé
Investigador Principal do Departamento de Química da Universidade de Aveiro

Doutor Mário Jorge Ferreira Calvete
Investigador Auxiliar do Departamento de Química da Faculdade de Ciências e Tecnologia da Universidade de Coimbra

Doutora Andreia Sofia Filipe Farinha
Investigadora de Pós-Doutoramento do Departamento de Química da Universidade de Aveiro

agradecimentos

First, has been an honour to work with Doctor João Paulo Costa Tomé, who induces the 'excited state' in his students, inspiring them to achieve great things. With his patience and vast knowledge, I learned many experimental and analysis skills needed to complete this doctoral work.
I would also like to thank Professor José A. S. Cavaleiro for being my co-supervisor, for extracting my best work and for showing me a world of opportunities within this field.
I also valued the assistance and expertise of Doctor Andreia Farinha, mainly during the analysis of the anion binding data; Prof. Artur Silva, particularly in the analysis of the NMR data; Prof Augusto Tomé, for the expertise in Diels-Alder reactions and Doctor Filipe Paz for the many tentative X-Ray analyses of my compounds.
I admire most of my colleagues and friends from the Porphyrins and Phthalocyanines materials research group that have made research, fun and friendly.
I need to thank my parents, brothers, and all the friends who have followed me through these last few years without whom this journey would have been infinitely harder.
Finally, This work would not be possible without the collective effort of friends, family and colleagues that supported me in this venture.

palavras-chave

Porfirinas expandidas, Pentafirinas, Safirina, Hexafirina, Porfirinas invertidas, Bipirrol, dipirrometano, Reações Diels-Alder e de Adição de Michael, Quimiossensores/Sensores de aniões.

resumo

Porfirinas expandidas são análogos sintéticos das porfirinas, diferindo destes apenas por possuírem um core contendo no mínimo 17 átomos.

A expansão do core resulta em vários sistemas com novas características electrónicas e espectrais, e numa extraordinária química de coordenação. Em muitos casos é também possível interação supramolecular com um ou vários aniões. Outra característica interessante é a possibilidade destes macrociclos acomodarem mais do que um estado de oxidação variando as suas características de aromaticidade e planaridade sem antecedentes na química de macrociclos tetrapirrólicos e derivados.

Este trabalho discute diversas rotas de síntese de macrociclos expandidos e sua derivatização, bem como a síntese de precursores bipirrólicos sobejamente conhecidos pela sua utilização como precursores na síntese de Porfirinas expandidas. Para este fim, unidades do tipo bipirrolico foram funcionalizadas através de adições de Michael. Estes pequenos compostos foram também derivatizados através de condensações de Knoevenagel para aplicação em coordenação de aniões demonstrando reconhecimento de diferentes aniões mediante uma variação de cor específica. No seguimento destes estudos de reactividade por Diels-Alder e/ou adições de Michael obtiveram-se novos derivativos do tipo safirina com substituições no interior do macrociclo.

Tendo em vista a síntese de compostos com reconhecimento de aniões e potencial aplicação em PDT/PDI e catálise, macrocrociclos do tipo pentafirina e hexafirina foram derivatizados com diversos nucleófilos. Neste último, a introdução de grupos amino na sua periferia conduziu a um aumento drástico da capacidade de interação com aniões em solventes polares. Estudos de RMN com os compostos capazes de reconhecer aniões possibilitou a sua total caracterização estrutural demonstrando estruturalmente os grupos que participam no reconhecimento de aniões.

Todos os compostos presentes sintetizados foram caracterizados estruturalmente com recurso a diversas técnicas espectroscópicas, nomeadamente: à ressonância magnética nuclear de protão, carbono 13 e de flúor 19, à absorção no Ultravioleta-Visível, à espectrometria de massa e sempre que possível a análise de raio-X de monocristal.

.

keywords

Expanded Porphyrin, pentaphyrin, Saphyrin, Hexaphyrin, Inverted Porphyrin, Bipyrroles, dipyrromethane, Diels-Alder, Aza-Michael Addition and Michael Addition Reactions, Anions Chemosensors/Sensors

abstract

Expanded porphyrins are synthetic analogues of porphyrins, differing from the last ones and other naturally occurring tetrapyrrolic macrocycles by containing a larger central core, with a minimum of 17 atoms, while retaining the extended conjugation features that are a tremendous feature of these biological pigments. The core expansion results in various systems with novel spectral and electronic features, often uniques. Most of these systems can also coordinate cations and/or anions, and in some cases they can bind more than one of these species. In many cases, these molecules display structural features, such as non-planar structures, that have no antecedents in the chemistry of porphyrins or related macrocyclic compounds.

This work will discuss several synthetic approaches for the synthesis of expanded porphyrins, namely the construction of new building blocks by Michael addition, as well as potential synthetic routes towards expanded porphyrins.

The synthesis of smaller oligopyrrolic compounds namely, bipyrroles and dipyrromethanes, not only were developed for the synthesis of expanded porphyrins as they were also used in Knoevenagel condensations furnishing chromogenic compounds able to recognize different anions in solution.

Also, an approach to the synthesis of novel expanded porphyrins namely sapphyrins has been done by aza-Michael additions. Several synthetic routes towards the synthesis of pyridyl and pyridinium *N*-Fused pentaphyrins and hexaphyrins have been explored in order to achieve compounds with potential applications in catalysis and PDI, respectively.

Studies on the synthesis of compounds with potential anion binding properties, led to the structural characterization and NMR anion binding studies of [28]hexaphyrins functionalized with several diamines in the *para* position of their pentafluorophenyl groups. These compounds allow NH hydrogen bond interactions with various anions. All synthesized compounds were fully characterized by modern spectroscopic techniques.

Index

List of abbreviations

Ac – Acetyl Group

ATP - Adenosine 5'-triphosphate

BP – Bipyrrole

CDI – N,N'-Carbonyldiimidazole

COSY – Homonuclear correlation spectroscopy

d – Doublet

dd – Doublet of doublets

D-A – Diels-Alder

DDQ – 2,3-Dichloro-5,6-dicyanobenzoquinone

DIPEA – Diisopropiletilamine

DMAD – Dimethylacetilenedicarboxylate

DMF – Dimethylformamide

DMSO – Dimethylsulfoxide

DNA - Deoxyribonucleic acid

DPM - Dipyrromethane

EDA - 1,2-Diaminoethane

Equiv. – Equivalents

EG – Ethylene glycol

EtOH – Ethanol

ESI-MS – Electrospray ionization mass spectrometry

EWG- Electron withdrawing group

J – Coupling constant

HOBT – *N*-Hydroxybenzotriazole

HOMO – Highest occupied molecular orbital

HSQC - Heteronuclear Single Quantum Correlation

K – Affinity constant

m – Multiplet

MALDI (TOF)– Matrix-assisted laser desorption/ionization time of flight

MW – Microwave

MS – Molecular sieves

Me – Methyl

MeOH – Methanol

NLO–Nonlinear optics

PA – Propargyl alcohol

PD - 1,3-Propanedithiol

Pd/C – Palladium on activated charcoal

PDT – Photodynamic therapy

PDI– Photodynamic inactivation

q – Quartet

LUMO – Lowest unoccupied molecular orbital

MO – Molecular orbital

NMR – Nuclear magnetic ressonance

RNA - Ribonucleic acid

s – Singlet

t – Triplet

TFA – Trifluoroacetic acid

THF – Tetrahydrofuran

rt – Room temperature

TBA - Tetrabutylamonium

TLC – Thin layer chromatography

TMS – Tetramethylsilane

TsOH – *p*-Toluenesulfonic acid

UV-Vis – Ultraviolet–Visible spectroscopy

δ – Chemical shift

ε – Molar absorptivity

λ – Wavelength

2PA - Two-photon absorption

1. Introduction

1. Introduction

1.1. General considerations

Porphine (Fig. 1.1) represents one of the most widely studied family of macrocycles, amongst all known macrocyclic ring systems, called porphyrins [1].

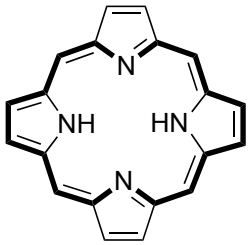

1.1

Figure 1.1: Porphine structure **1.1**.

This group of chemical compounds of which many occur in nature, such as in green leaves, red-blood cells, in bio-inspired synthetic catalysts and devices, are heterocyclic macrocycles. These highly colored tetrapyrrolic pigments normally referred as "pigments of life" play diverse and critical role in nature, ranging from electron transfer, oxygen transport, photosynthetic processes and catalytic substrate oxidation.

Porphyrins are aromatic compounds, obeying to Hückel's rule for aromaticity, possessing 18n+4 π electrons that are delocalized over the macrocycle. The macrocycle, therefore, is a highly-conjugated system, and, as a consequence, deeply colored. The name porphyrin comes from a Greek word for purple. The parent porphyrin is porphine, and substituted porphines are called porphyrins [2].

Interest in this naturally occurring tetrapyrrolic macrocycle is broadly based in its multiple biological functions as well as its ability to function as an excellent metal-complex ligand. In general, all macrocycles containing pyrroles that are not naturally occurring may be defined as porphyrin analogues. This definition has generally been further restricted by the porphyrin research community to encompass systems that either contains four or more pyrroles and some degree of conjugation or that possesses only four pyrroles but little or no conjugation.

Traditionally, the first of these two groups are represented by porphyrin analogues that are contracted, expanded or isomeric regarding to the porphyrin itself, such as corrole (**1.2**), sapphyrin (**1.3**) and porphycene (**1.4**) (Fig. 2) [1].

The second main set of porphyrin analogues has been largely restricted to calix[4]pyrroles (octaalkylporphyrinogens, **1.5**) and to stable systems with formal oxidation states that are intermediate between those of porphyrinogens and porphyrins (*e.g.* the calixphyrins (**1.6**), and higher homologues) (Fig. 1.2) [1,3].

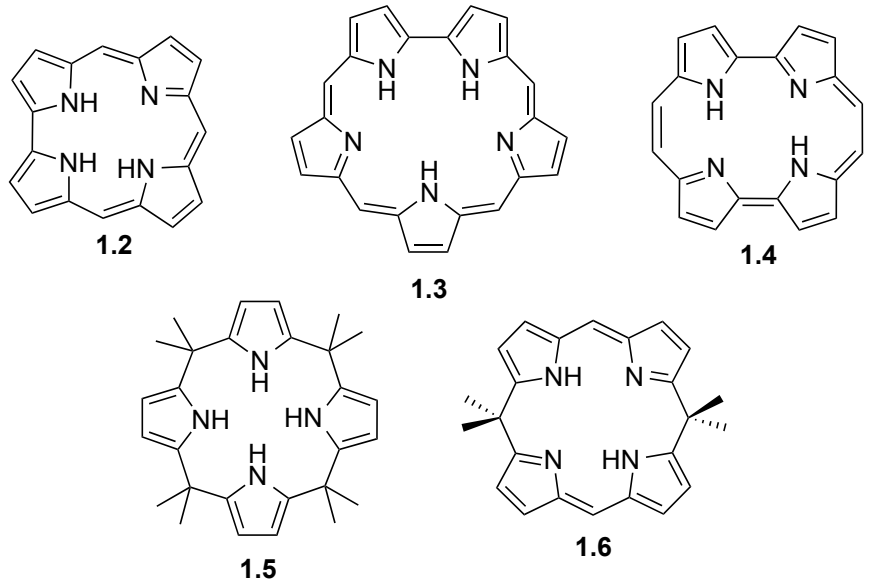

Figure 1.2: Porphyrin analogue structures.

The interdisciplinary interest generated by the porphyrins resulted in the syntheses of modified porphyrin analogues (Fig. 1.3). The most important modifications can be obtained in the periphery, including *β* (**1.7**) and *meso* (**1.8**) positions of the parent macrocycles or in the core (**1.9**), where one or more core nitrogen atoms, of parent porphyrin, are substituted with chalcogen atoms (O, S, Se and Te) [4].

Considering other different class of porphyrin analogues it's possible to find in the literature *N*-confused porphyrins (**1.10**) which have one or more of the core nitrogens pointing out of the ring and *N*-fused porphyrins (**1.11**) derived from *N*-confused porphyrin by appropriate synthetic modifications [5-10].

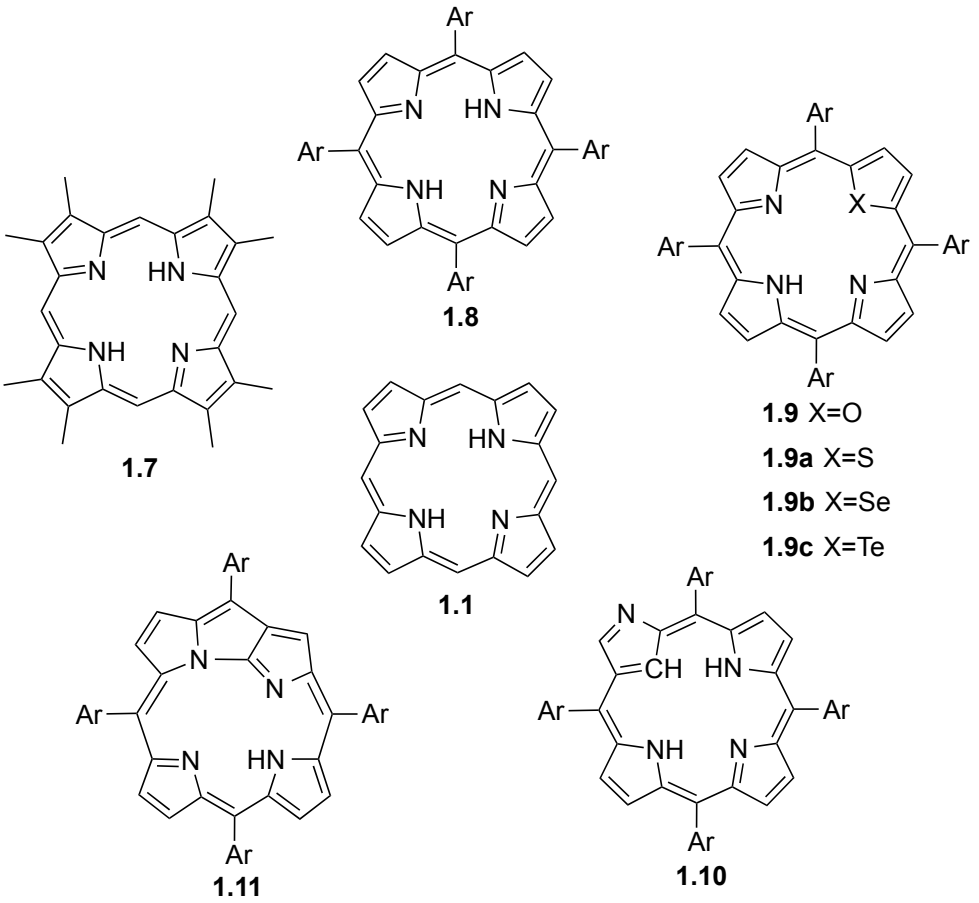

Figure 1.3: Modified porphyrin analogues.

In many aspects, the origin of porphyrin analogue chemistry can be traced back to early studies involving the structure of vitamin B12 (**1.12**). Present in this key natural product is the cobalt corrin, the stable octadecahydro analogue of corrole **1.2**. This latter contracted porphyrin was primarily synthesized by A. W. Johnson in 1960 and has remained a subject of intense interest ever since (Fig. 1.4) [11].

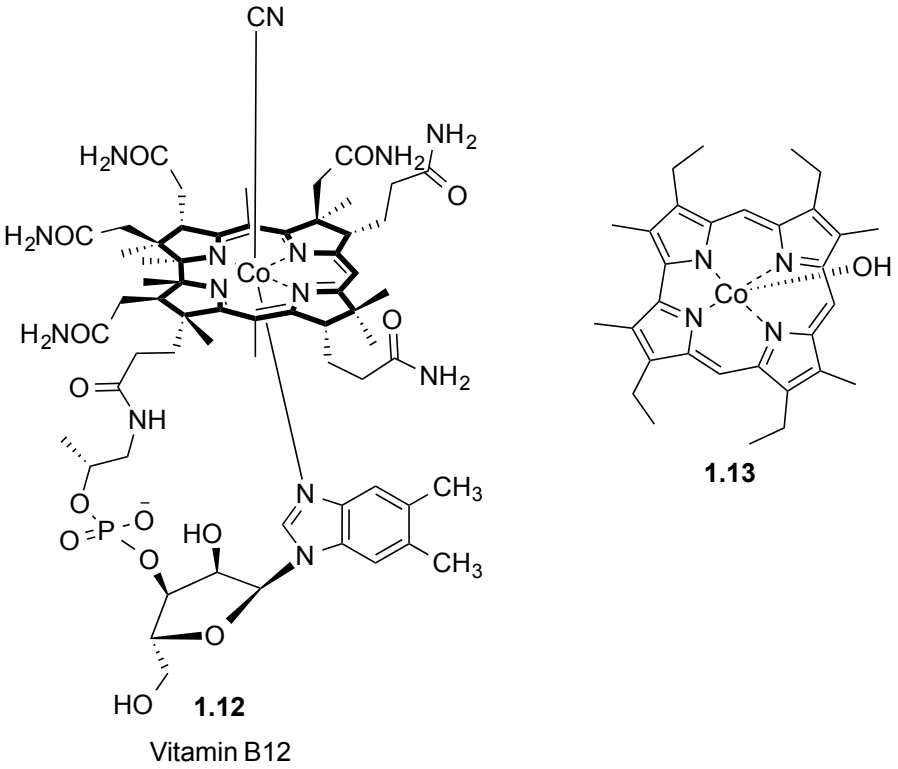

Figure 1.4: Vitamin B_{12} and corrole structures.

The complex **1.13** (Fig. 1.4) obtained by A. W. Johnson displayed a complex and rich coordination chemistry that is not equivalent to the one shown by porphyrins. For instance, corroles have been found to stabilize high-valent states of a variety of transition metals including Cr, Mn, Fe, Co, and Cu [12]. Unfortunately, difficulties associated with synthesis, manipulation and characterization of corrole and its metal complexes limited at the time further developments on this chemistry.

However, more recently, efficient syntheses of *meso*-aryl-substituted and other more classic corroles served to alter this situation in a impressive way [13]. Much of the attention dedicated to these systems is based on their similarity to porphyrins and the anticipation that they could show the prosperous coordination chemistry found on porphyrins [14].

On an unusual level, the electronic structure of various larger, or expanded porphyrin systems, in particular their similarities and differences to porphyrins, have made them an object of profound study [15]. Another factor motivating the study of conjugated expanded porphyrins is that they often exhibit absorbance bands that are red-shifted relatively to those of porphyrin. This quality, which is attributed to an enlarged π

conjugation pathway, has led into consideration that some expanded porphyrins could find use as therapeutics on PDT [16]. Related properties, including a facilitated reduction, have led to the testing of one particular expanded porphyrin (motexafin gadolinium) as an adjuvant for radiation therapy [17,18].

Another area of interest, without precedence in the porphyrin area, is focused on the unexpected discovery that expanded porphyrins can operate as anion receptors. This result revealed that these systems have a huge potential in several applications, including anion sensing and transport (for example, drug delivery), as well as chromatography-based purification of anions [18,19].

1.2. Expanded Porphyrins: Historical Overview

In the early efforts devoted to the synthesis of corrole, Woodward and his coworkers isolated by chance pentapyrrolic macrocycle attributed to structure **1.3**. This compound, containing 22 π electrons in its aromatic periphery, was found to be deep blue in the solid state and intense green in organic solution. This led Woodward to term this group of macrocycles 'sapphyrins'. Sapphyrin **1.16** was obtained in the 4+1 condensation reaction between the linear tetrapyrrolic precursor, bipyrrolyldipyrromethane **1.14** and 3,4-dimethylpyrrole-2,5-dicarbaldheyde (**1.15)** in acid medium as shown in scheme 1.1 [20].

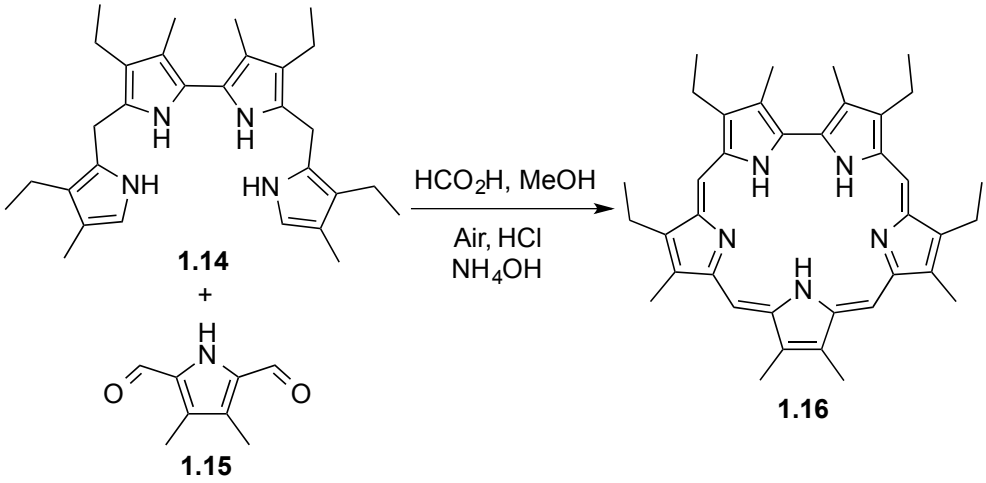

Scheme 1.1

Woodward's and Broadhurst´s groups, independently, also reported a 3+2 condensation involving bipyrrole dialdehyde with a tripyrrane catalysed by acid, followed

by air oxidation, which became the most widely used methodology for the synthesis of sapphyrins [20,21].

Woodward and coworkers, using diformyl bipyrrole **1.17** and tripyrromethane dicarboxilic acid **1.18** produced the desired sapphyrin **1.19** in 35% yield. This synthesis implemented an alternative 3+2 methodology (Scheme 1.2) [21].

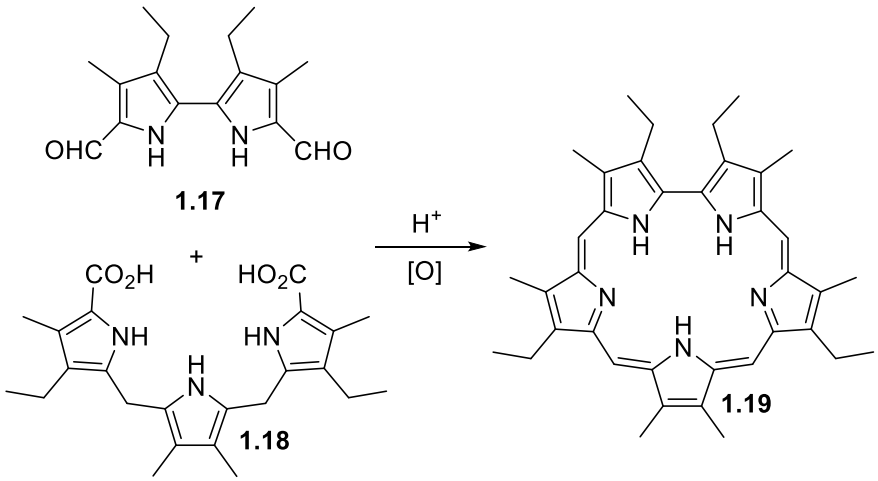

Scheme 1.2

While these syntheses of sapphyrin were made possible, the monotonous nature of the synthesis of these precursors, acted as an obstacle to the continuous study of these porphyrin analogues. However, later in the 90s Sessler and coworkers developed a simple, three-step, high-yield synthesis of the dicarboxyl-substituted tripyrranes **1.24** and **1.25**, which involved the near quantitative condensation between 3,4-diethylpyrrole (**1.20**) and the corresponding benzyl pyrroles **1.21a** and **1.21b** (Scheme 1.3) [22].

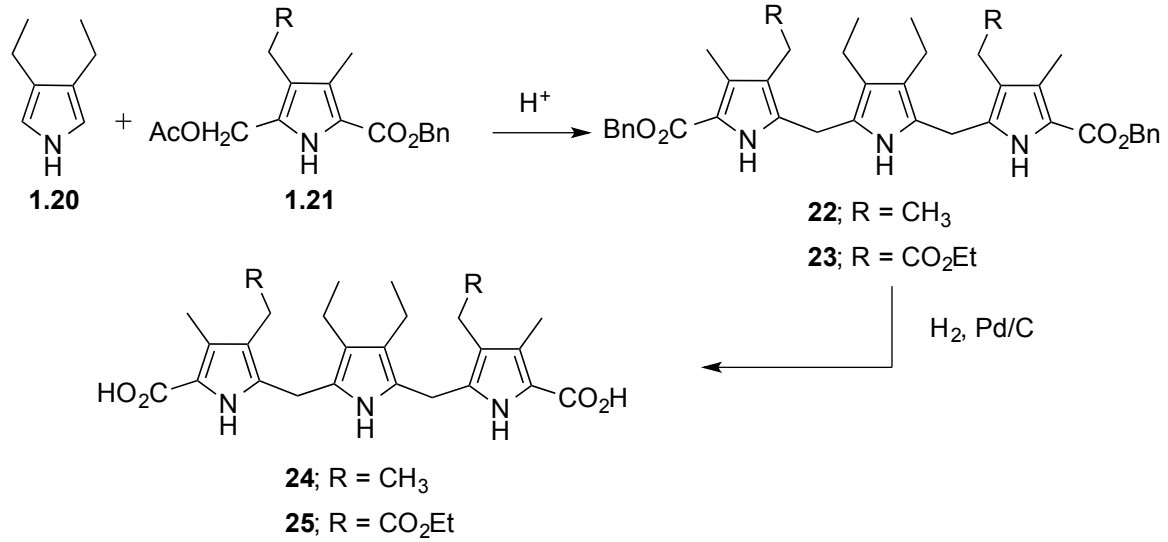

Scheme 1.3

The diformyl bipyrrole was prepared from the direct Ullmann coupling of 5-iodopyrrole-2-carboxylate **1.27** and consequent functionalization as depicted in scheme 1.4.

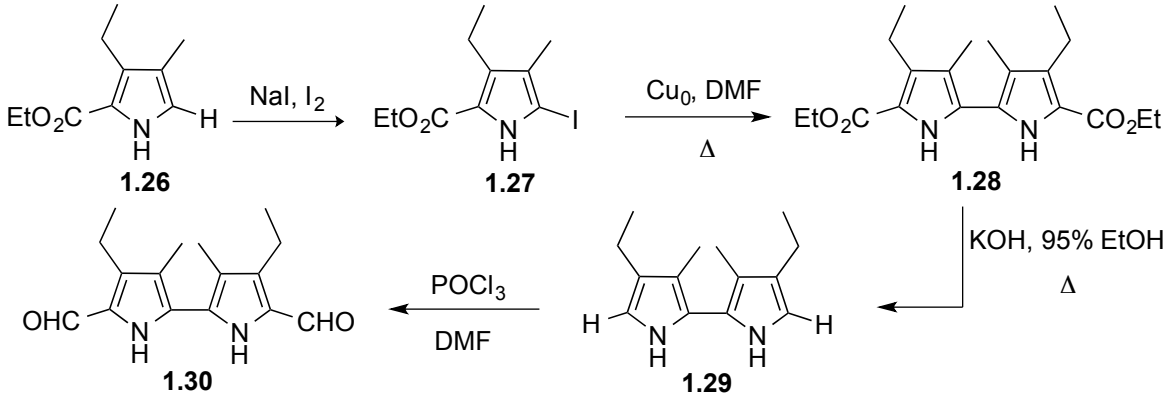

Scheme 1.4

However, the complexity inherent in the synthesis of the initial pyrroles led to the use of a Barton-Zard pyrrole synthesis providing an easy way to prepare the α-free pyrrole **1.26** with a higher yield [23,24]. This allowed the rational synthesis of 22 π sapphyrins **1.31** and **1.32**, using stable precursors in higher overall yields (Scheme 1.5) [22].

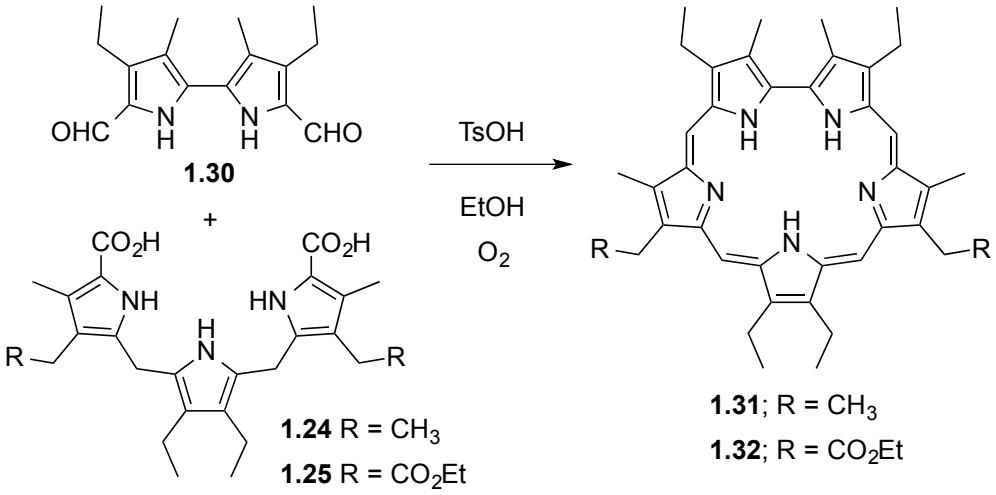

Scheme 1.5

These syntheses here referred, have not only succeeded in building efficient synthetic methods, but also pioneered the synthesis of stable building blocks, such as tripyrranes, dipyrromethanes, and quaterpyrroles, required for the synthesis of expanded porphyrins.

1.3. Synthesis of expanded porphyrins: overview

1.3.1. Developments in the synthesis of Building Blocks

The synthesis of new expanded macrocycles, can be approached by two general strategies, namely: i) the use of different combinations of pyrrole units and bridging carbons, and ii) synthesizing new building blocks, which can replace pyrroles. Most of the classic expanded porphyrins were synthesized using a combination of these approaches.

Furthermore, cyclic [25,26] and linear π conjugated oligo- and poly-pyrrolic systems are of growing relevance in materials science, supramolecular chemistry, and nanotechnology. For instance, they have found application in anion binding [27], cation coordination [28], conducting polymers [29], liquid crystals [30], and nonlinear optics [31,32].

Traditionally, bipyrroles, terpyrroles, and quaterpyrroles have been synthesized by performing Vilsmeier condensations and consequent dehydrogenation of the cyclic imine intermediaries (Scheme 1.6, Route A) [33-35], the cyclization of pyrrolic 1,4-diketones

[36,37] (Scheme 1.6, Route B) and the already referred Ullmann coupling used by Sessler and coworkers in the synthesis of diformyl bipyrrole **1.30** (Scheme 1.5).

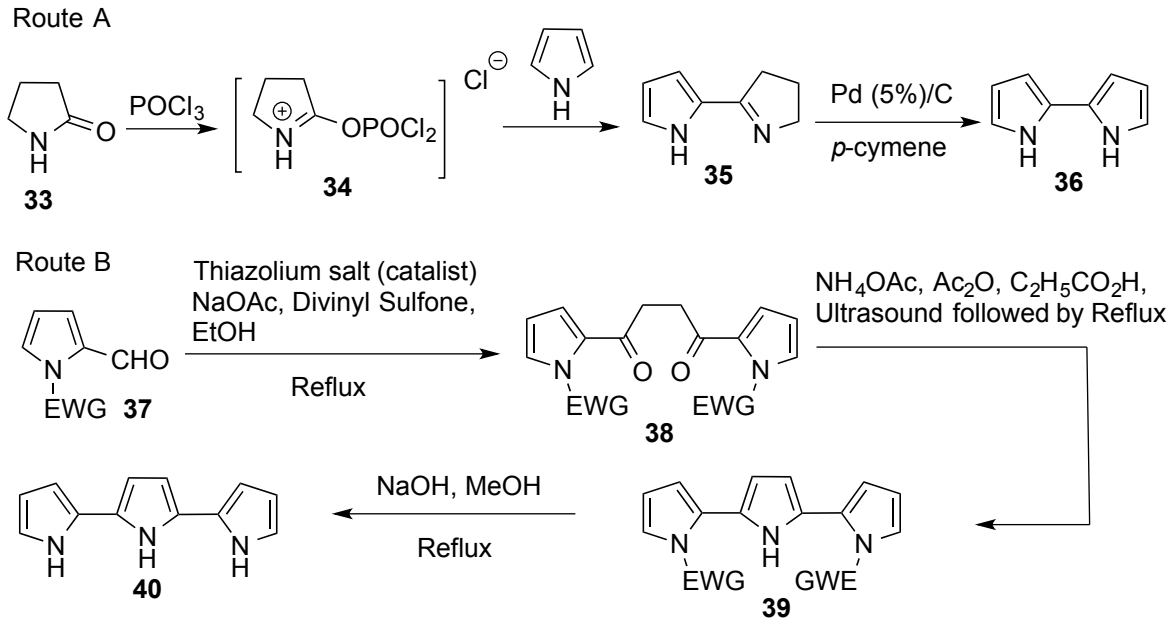

Scheme 1.6

Other methods of synthesis like the classical Knorr [38], Paal-Knorr [39,40], strategies to 1,3-dipolar cycloaddition procedures with activated alkynes and alkenes [41-43] and multi-component protocols [44], are also used for this purpose.

While attempting to synthesize new building blocks to construct expanded porphyrins, Sessler and coworkers found that the treatment of a α-free pyrrole with $FeCl_3$ or $Na_2Cr_2O_7$ yielded an azafulvalene, which, after $NaBH_4$ reduction, furnished the corresponding bipyrrole in moderate yields. Interested in these developments, Sessler and coworkers tested whether oligopyrroles, larger than bipyrroles, could be synthesized by oxidative couplings. Therefore, Sessler described in 2005 the synthesis and structural characterization of quaterpyrroles and sexipyrroles obtained via the oxidative homocoupling of bi- and terpyrroles mono-α-free using potassium ferricyanide (Scheme 1.7). The synthesis was obtained dissolving compounds **1.43** and **1.44** in methylene chloride and treated with potassium ferricyanide dissolved in a saturated aqueous sodium bicarbonate solution. Stirring this biphasic mixture at room temperature afforded the oxidized quaterpyrrole **1.45** and sexipyrrole **1.46** in relatively good yields [45]. Further reduction of these compounds led to the final compounds **1.47** and **1.48**, respectively.

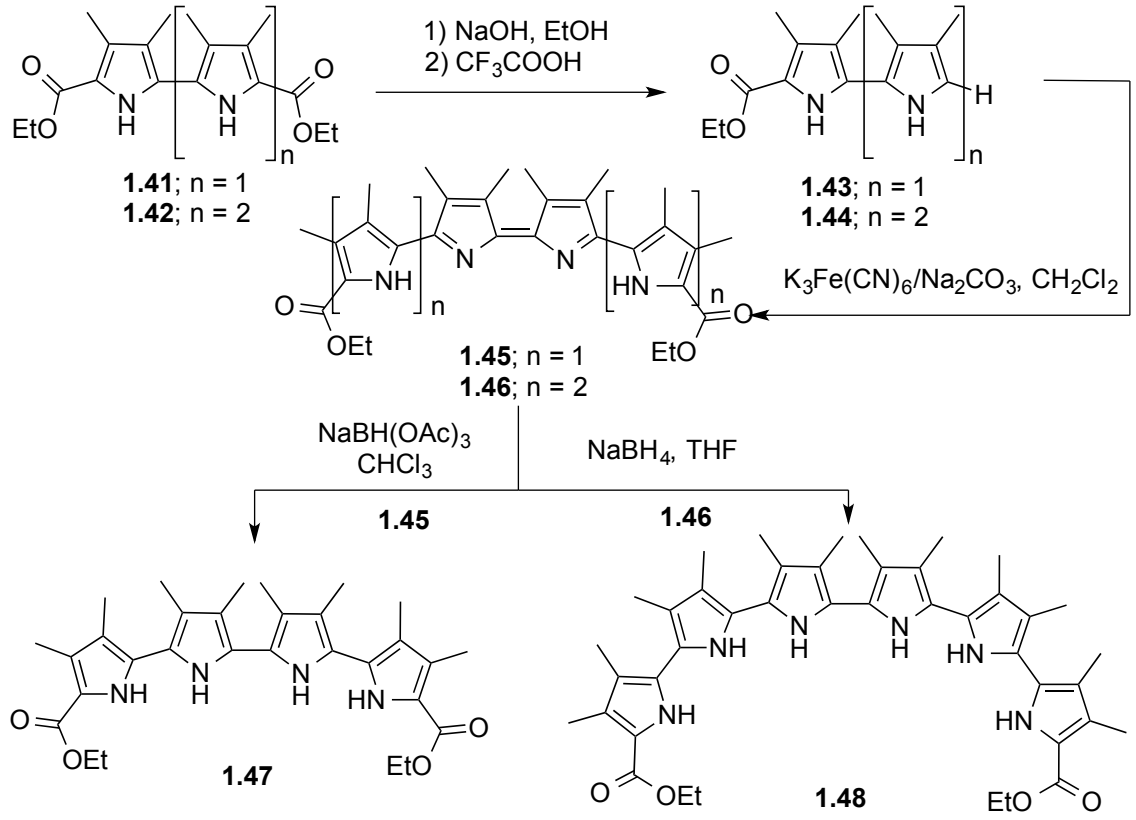

Scheme 1.7

However, these authors have noted that such approach would only be useful for the preparation of even numbered oligopyrroles (number of pyrroles = 2, 4, 6, 8…). For this reason in the same article this author also explored the enolate coupling, 1,4-dicarbonyl cyclization method used to generate terpyrroles [36], could be generalized to construct higher-order oligopyrroles. This would provide several general strategies to obtain oligopyrroles. Consequently the synthesis of a pentapyrrole (**1.51**) was obtained through enolate coupling, and Knorr-like cyclization of the resulting 1,4-diketones (Scheme 1.8) [45].

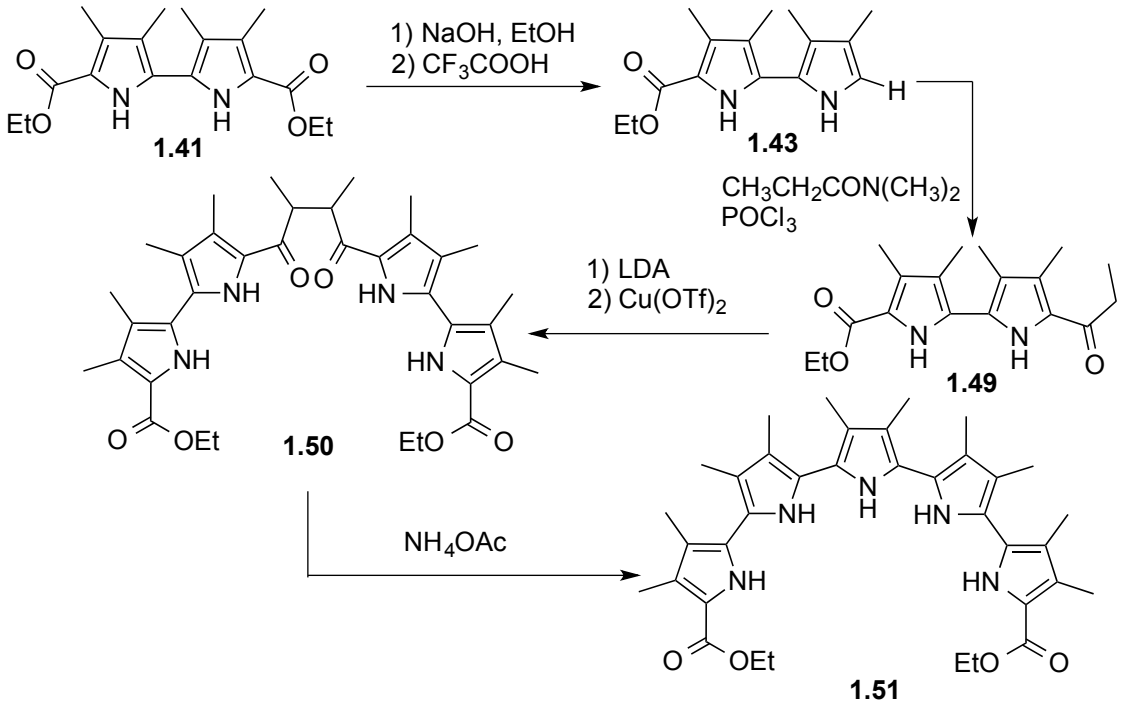

Scheme 1.8

Interestingly, the use of similar oxidative couplings described previously with open-chain pyrrole precursors by Sessler and coworkers has allowed the preparation of several new expanded porphyrins, including isoamethyrin [46], heptaphyrin (1.0.0.1.0.0.0) and octaphyrin(1.0.0.0.1.0.0.0), and more recently a series of cyclo[*n*]pyrroles [47].

While several advancements were achieved in the synthesis of new expanded macrocycles with the acyclic moieties presented until now, several researchers have also found analogous methodologies for the synthesis of even more complex expanded structures, increasing almost exponentially the structural diversity of these compounds. For instance, also pyrrole moieties containing methine bridges between pyrroles and several functionalizations in the *β*-pyrrolic and *meso* positions have already been reported. Some examples of these building blocks are shown in figure 1.5 [48].

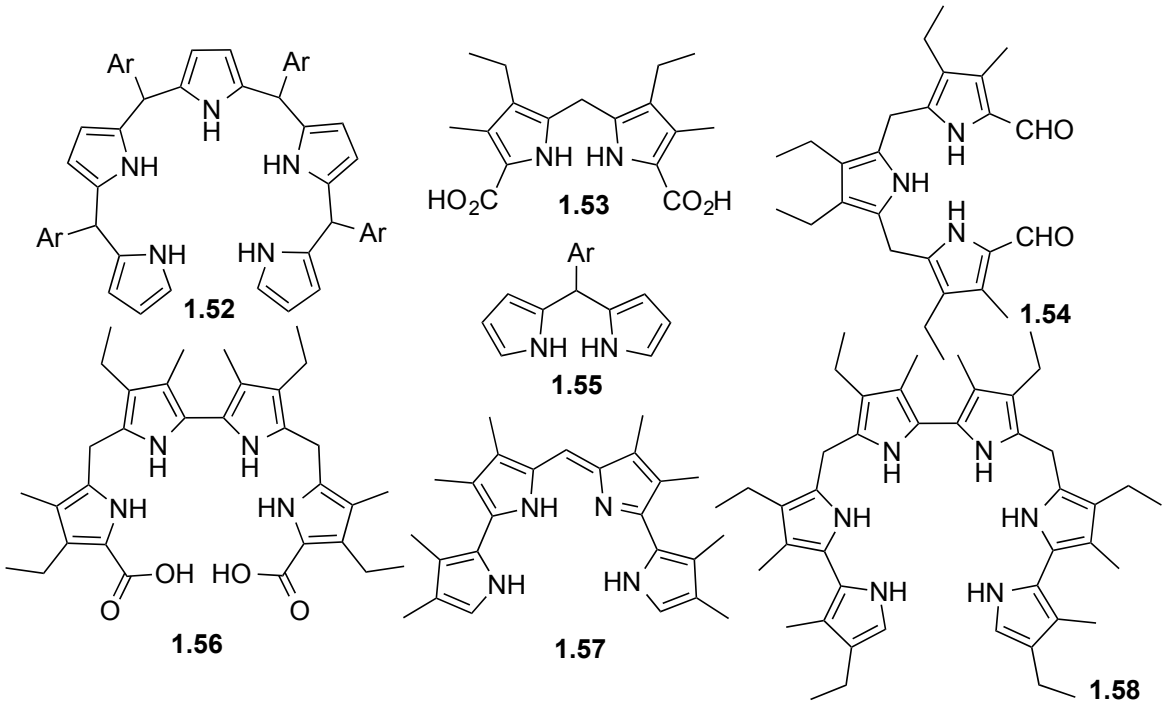

Figure 1.5: Example of building blocks used in the synthesis of expanded macrocycles.

Also syntheses involving building blocks with inverted pyrrole units have been achieved by Heo and coworkers (Scheme 1.9) [49]. Initially used for the synthesis of *N*-confused porphyrins by a 3+1 condensation method, tripyrrin precursor **1.62** latter allowed the synthesis of a doubly *N*-confused hexaphyrin by a 3+3 condensation method by Furuta and coworkers. This work is discussed further ahead in the hexapyrrolic expanded porphyrins section.

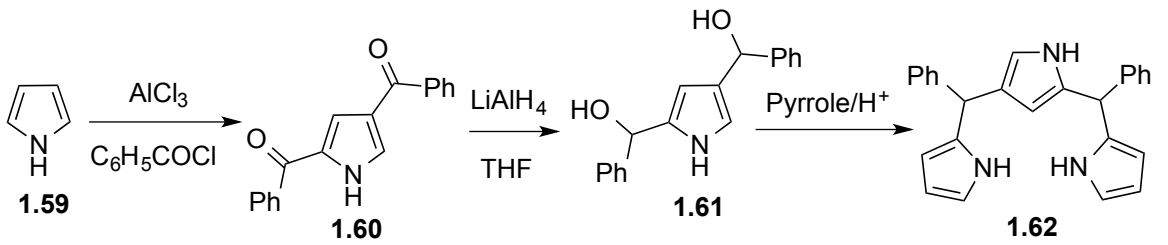

Scheme 1.9

The increased availability of these building blocks allowed the synthesis of expanded porphyrins, and also extended tremendously the structural diversity amongst this family of macrocycles. Interestingly the attention devoted to this kind of macrocycles has increased after the synthesis of sapphyrin in enough quantities to be studied in detail and might be considered the first of its kind. In particular, it allowed that structural analyses

could be carried out, showing that the protonated forms of sapphyrin were potential anion-binding agents [19,50].

However, it is clear that the anion binding properties of sapphyrin show that the fact of possessing a larger cavity, allows an easier protonation, and the free pyrrole NH subunits, if not deprotonated, are good hydrogen bond donors for such classic Lewis basic anions such as fluoride, chloride and phosphate. This shows the enormous importance that sapphyrins have in a large variety of molecular recognition applications [19].

1.4. Synthesis and applications of expanded Porphyrins

Expanded porphyrins are synthetic analogues of the porphyrins, and differ from these tetrapyrrolic macrocycles by containing a larger central core with a minimum of 17 atoms.

The concept of core expansion is to produce systems with new spectral and electronic features, cation-coordination properties, and, in many cases, the ability to bind anions in certain protonation states. In many cases, they also display structural features, such as nonplanar "figure-eight" conformations, that have no precedent in the chemistry of porphyrins or related macrocyclic compounds. In this chapter several synthetic approaches being employed to synthesize expanded porphyrins as well as their various properties and applications are going to be discussed.

1.4.1. Pentapyrrolic systems

Expanded porphyrins containing five pyrrolic units that can be connected by different type of bridges, and of which can differ on the number of carbons, are known as pentapyrrolic systems. These variations gave rise to the synthesis of several macrocycles containing five pyrrolic rings by several research groups. Some of these macrocycles are shown in Fig. 1.6 [20,51-53].

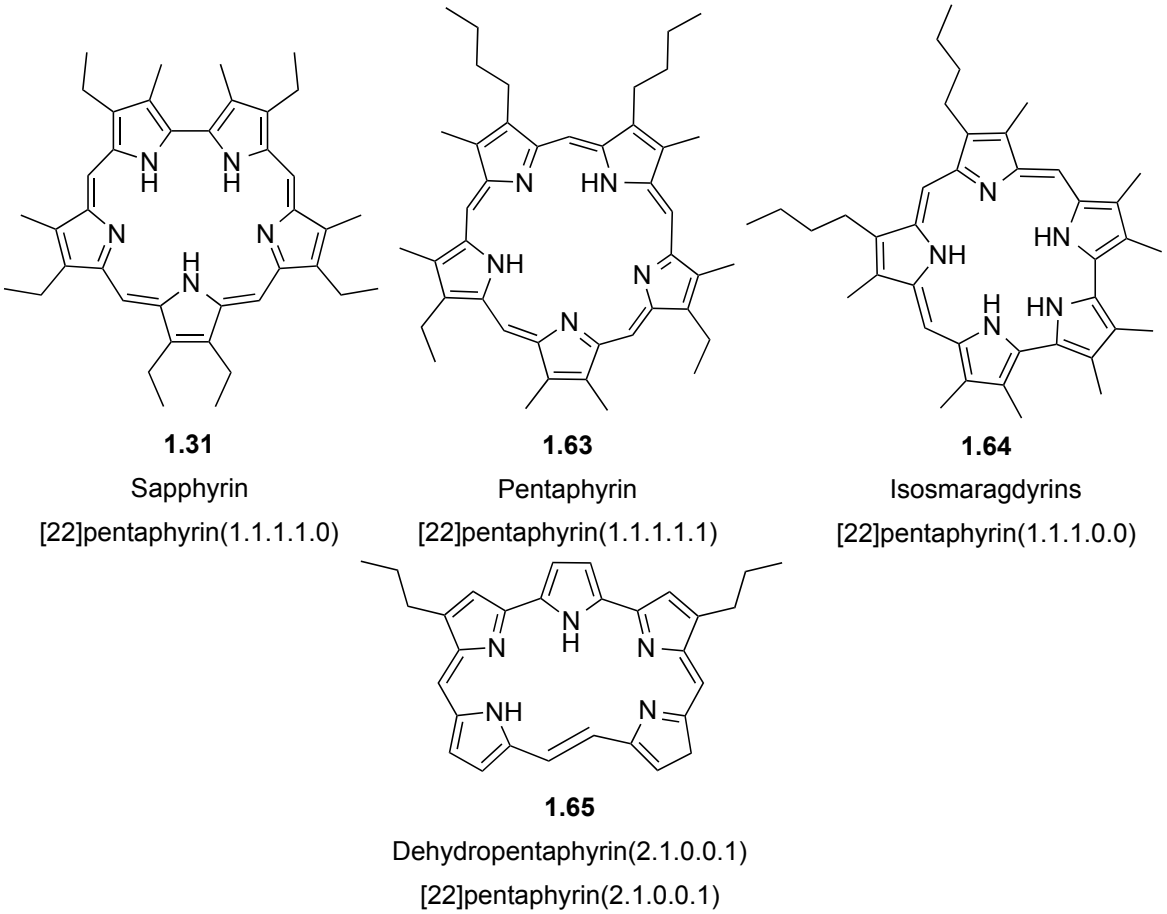

Figure 1.6: Pentapyrrolic macrocycles.

In analogy to the smaller tetrapyrrolic family of macrocycles, the same structural variations were made with pentapyrrolic systems. Two different types of pentapyrrolic systems are identified in the literature depending on the location of the substituents. They can either be *β*-substituted or *meso*-substituted [19].

1.4.1.1. β-substituted pentapyrrolic systems

As referred previously, the preparation of sapphyrin with increased yields marked an historical achievement allowing the spectroscopical study of this structure. In fact, pentapyrrolic macrocycles are among the most studied macrocycles in the general area of expanded porphyrins (Fig. 1.6) [19,51,54,55]. This availability allowed several structural studies where it was possible to notice that this parent porphyrin (**1.31**) was able to establish anion binding interactions, as it can be seen by inspection of the resolved structure (Fig. 1.7) [19,22].

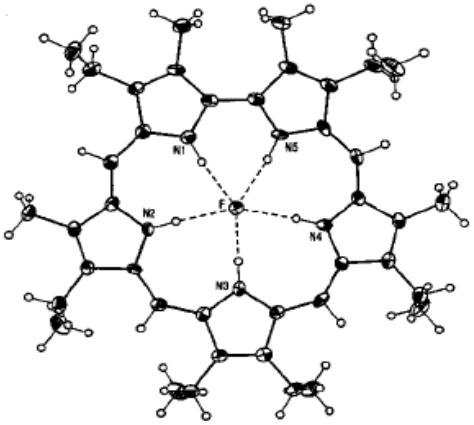

Figure 1.7: DRX Structure of sapphyrin **1.31** binding a fluoride anion.

In this structure, the nitrogen and the fluoride atoms were found to be almost coplanar, with a mean deviation of only 0.03 Å, while the bound fluoride center was found to be at the distance of a hydrogen-bonding of all five nitrogens. This finding guided the authors of this study to question whether if other anions could coordinate in this manner. An attempt with chloride showed the formation of sapphyrin dihydrochloride salt **1.31** [56].

The two chloride anions are too large to be inserted in the sapphyrin plane. In this way they bound in the opposite faces of the diprotonated sapphyrin macrocycle by hydrogen bonding (Fig. 1.8).

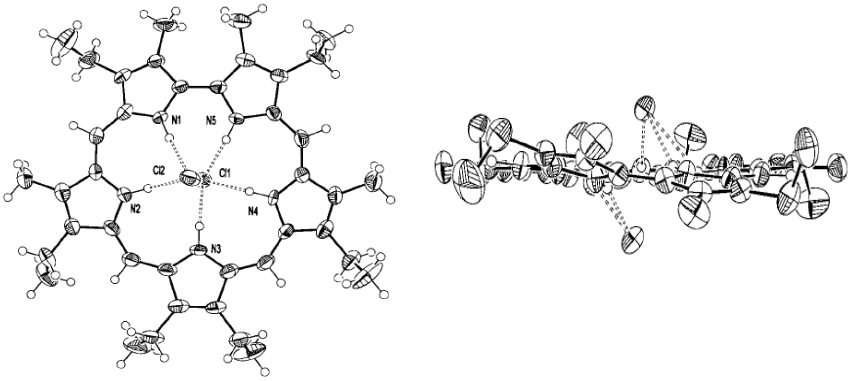

Figure 1.8: DRX Structure of sapphyrin **(1.31)** binding two chloride anions.

In solution (dichloromethane and methanol) studies of the protonated forms of sapphyrin, demonstrated that the visual absorbance of fluoride coordinated sapphyrin spectra had a maximum slightly shifted (446 nm) comparing to the maximum showed for the chloride coordinated sapphyrin (456 nm). This variation in the visible spectra was a

first indication of the amplitude and interaction of these anions with sapphyrin **1.31**. This feature was again observed when the association constants were calculated for these anions. These calculations showed a clear selectivity of 3 orders of magnitude for fluoride over chloride anions (2.8 x 10^5 and 1 x 10^2 M^{-1} respectively), and were considered fully consistent with the stabilized plane designed, seen in the solid-state structure.

In an attempt to synthesize new *β*-substituted analogues that would improve the results of demonstrated by **1.31**, several covalently linked sapphyrin dimers were introduced by Sessler *et al.* This first generation of sapphyrin dimers **1.66-1.68** was designed to function as "pacman" receptors. The synthesis of these receptors (Fig. 1.9) was accomplished by the induced coupling of the mono acid sapphyrin precursors with 1,3-diaminopropane, (*S*)-2,2´-diamino-1,1´-binaphthalene and (1*S*,2*S*)-1,2-diaminocyclohexane moieties respectively.

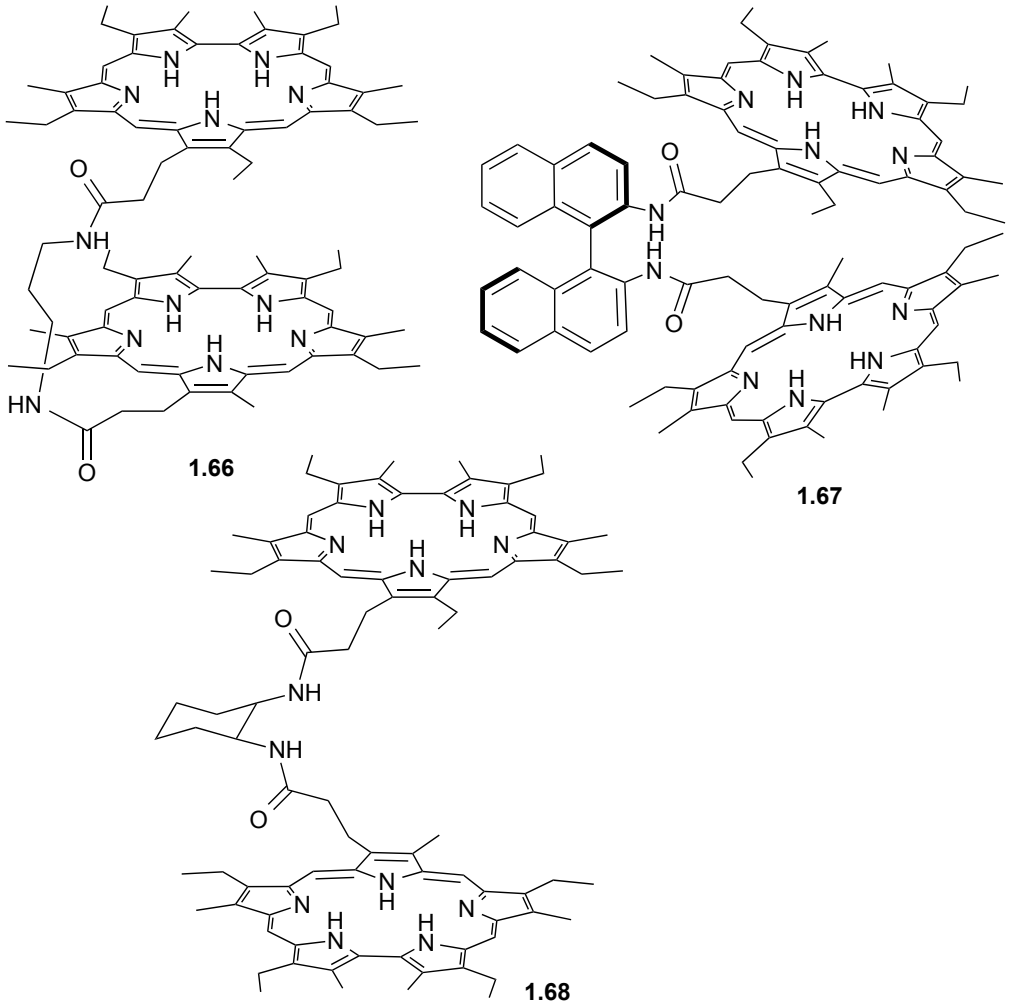

Figure 1.9: First generation of sapphyrin dimers.

The mono linked covalent dimer **1.66** displayed unique attributes in the visible absorbance spectra, where precisely two Soret-like maxima in both methanol (422 and 441 nm) and dichloromethane (426 and 450 nm) where found. The cause of these two bands was consistent with the existence of two different conformational states, the "*open*" and "*sandwich-like*" forms. These characteristics allowed this sapphyrin dimer to coordinate bigger anions such as dicarboxylate anions causing the Soret band with the higher wavelength maximum to increase in intensity at the expense of the lower wavelength one. This kind of behavior was consistent with a binding model where the dicarboxylate substrate is coordinated inside the sapphyrin with a *"sandwich-like"* form [57]. Encouraged by the successful results obtained with system **1.66**, other sapphyrin based dimeric receptors were prepared based on the use of more rigid, chiral spacers. Such systems, envisioned both more selective di-anion recognition and enantio-selective chiral dicarboxylate anion binding. Interestingly, in part this was achieved. Dimer **1.67** has shown higher affinities for dicarboxylate anions and an excellent affinity towards substrates that differ in one carbon length.

These two new sapphyrin dimers **1.67** and **1.68** not only have shown the same properties of their congener **1.66** in terms of visible absorbance spectra but also an increase in glutamate and aspartate anions affinity, especially for dimer **1.67**. Not only the synthesis of chiral spacers has been attempted in order to increase selectivity in dicarboxylate anions recognition. In a recent work the same authors showed a double linked dimer with (1*S*,2*S*)-1,2-diaminocyclohexane moieties where the fact of being a more pre-organized cyclic system, emphasized the importance of a good size and shape match between the receptor and the substrate. This cyclic sapphyrin dimer **1.71** was prepared with 46% yield from the sapphyrin bis-acid **1.69** and the di-(1*S*,2*S*)-1,2-diaminocyclohexane sapphyrin **1.70** upon activation with CDI and HOBT (Scheme 1.10) [58].

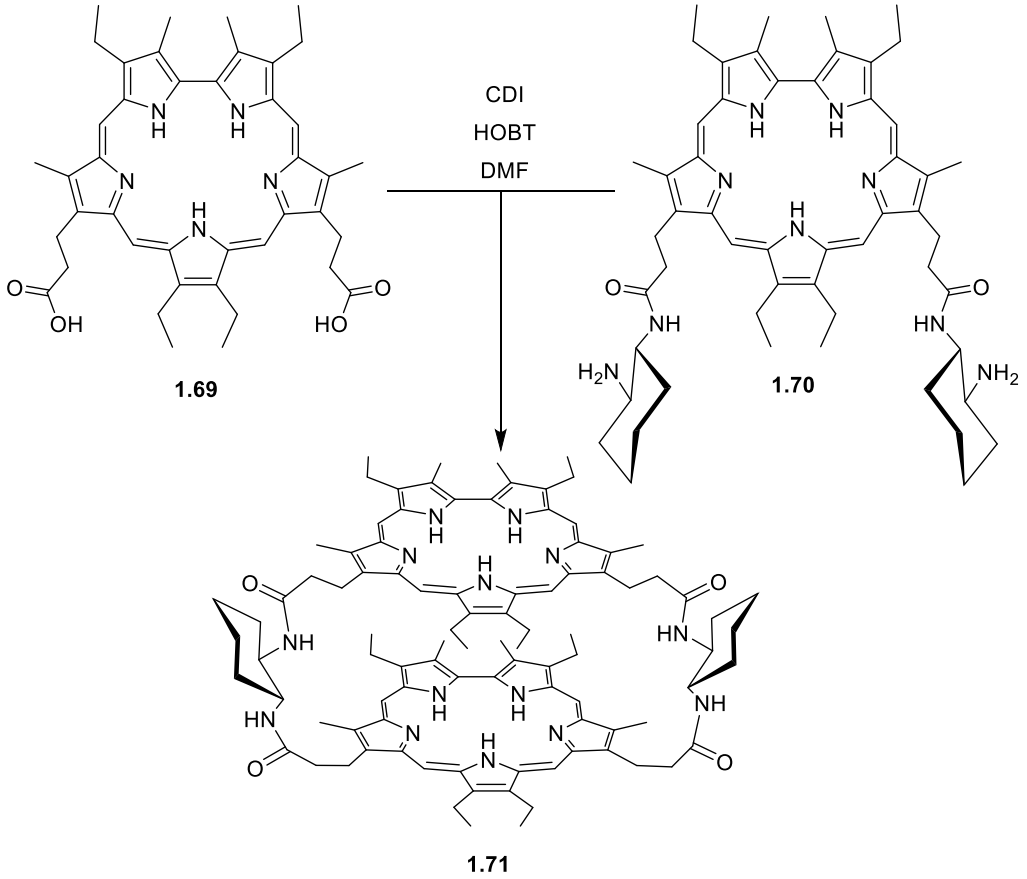

Scheme 1.10

As expected the visible absorbance spectrum of this cyclic dimer **1.71** differs from its previous analogs **1.66-1.68**. The spectra showed only one maximum Soret band that confirmed that regardless of the solvent the structure of this dimer remains in "sandwich like" form.

Important to refer is that this cyclic dimer exhibited recognition of *N*-protected amino acids, as evidenced by the association constants listed in table 1.1.

Table 1.1: Association constants of **1.71** with different *N*-protected amino acids.

1.71	**Anion** Solvent: 5% CH_3OH in CH_2Cl_2	***K*** **(M^{-1})**
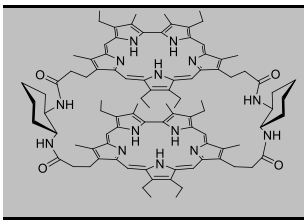	*N*-CBZ-*L*-ASP	1.6 x 10^4
	N-CBZ-*D*-ASP	9700
	N-CBZ-*L*-GLU	3800
	N-CBZ-*D*-GLU	1.6 x 10^4

In table 1.1 is possible to note that the recognition ability of this sapphyrin dimer **1.71** is enantioselective due to the different association constants between the *L*- and *D*-enantiomers of the same protected amino acid.

As a consequence of possessing 22 π electron aromatic conjugation pathway, sapphyrins have a relatively high yield of singlet oxygen formation and near infrared absorbance properties [59]. This generation of singlet oxygen has been found to catalyze the photocleavage of DNA effectively, by compounds (**1.72** and **1.73**) (Fig. 1.10) [60,61].

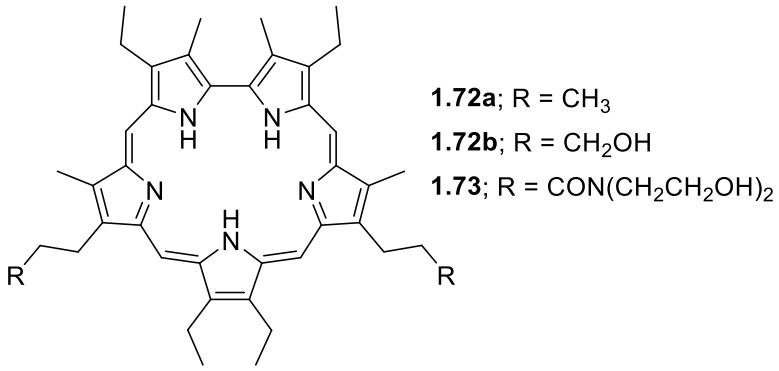

Figure 1.10: Sapphyrin derivatives capable of catalyzing the photocleavage of DNA.

The water soluble sapphyrin **1.73** was able to cleave DNA upon irradiation at wavelengths above 600 nm, whereas for the use *in vivo*, the 600-900 nm region is preferable, because body tissues are more transparent to this wavelength range. Compounds **1.72** and **1.73** have also shown ability to interact with nucleic acids by several modes of interaction, including phosphate chelation of the phosphodiester backbone and hydrophobic interactions with the nucleotide bases. Therefore these compounds represent potential candidates for use in oligonucleotide affinity enhancement studies [62].

Using similar methodologies to synthesize water soluble sapphyrins, Kral *et al.* developed a synthetic route that allows the attachment of four hydroxyl groups to a pentaphyrin skeleton [63]. Specifically, it was centered on the condensation of the bis-acid dipyrromethane **1.75** with the diformyl tripyrrane **1.74** [64]. This gave rise to the tetraacetate pentaphyrin **1.76** that, subsequent to the hydrolytic removal of the acetate blocking groups, gave the desired tetrahydroxy pentaphyrin **1.77** in 56% overall yield (Scheme 1.11).

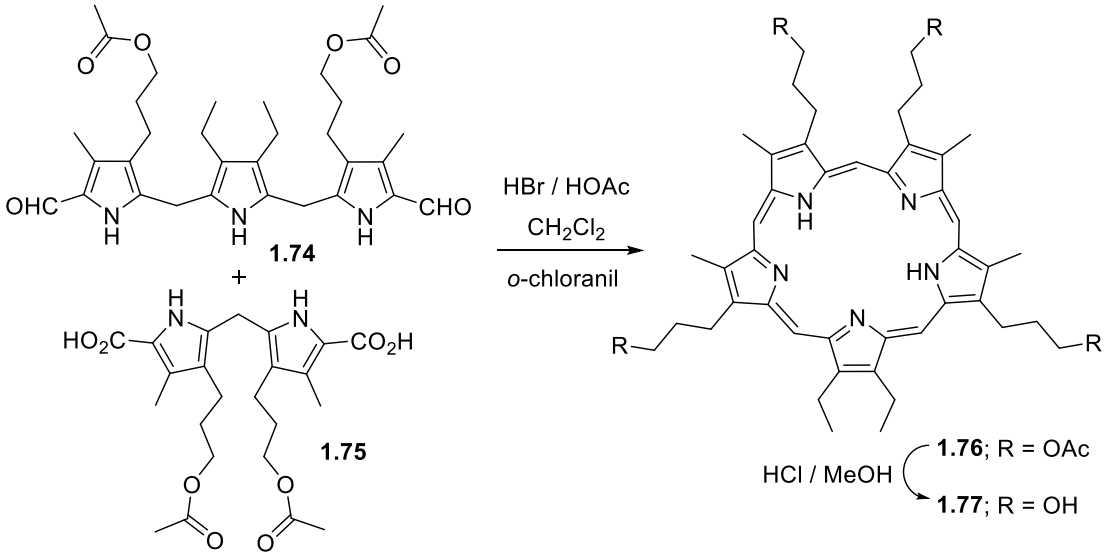

Scheme 1.11

Recently, Naumovski *et al.* reported the anti-cancer activity of several sapphyrin derivatives in hematologic cell lines and tumors, confirming that sapphyrins possess intrinsic anticancer activity that is independent of their photosensitizing properties (Fig. 1.11) [65].

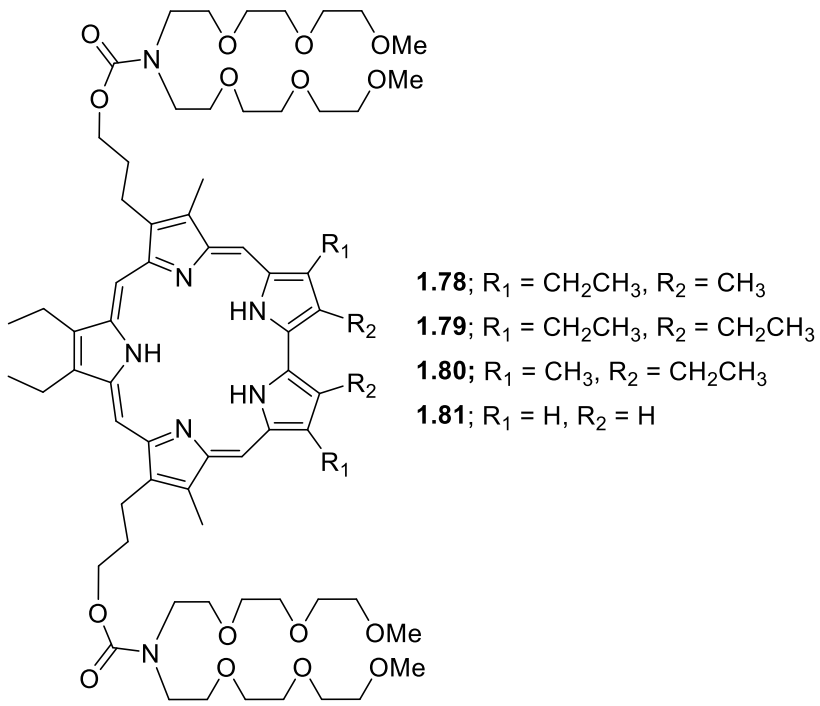

Figure 1.11: Sapphyrin derivatives with anti-cancer activity.

These studies showed that sapphyrins **1.78-1.81** induce apoptosis in numerous cell lines, including those derived from lymphoma, leukemia, and multiple myeloma, in the absence of light. The biochemical pathway through which these sapphyrins induce apoptosis has not yet been fully elucidated, however similar to other stress-inducing stimuli, sapphyrin treatment was found to result in the phosphorylation of p38MAPK, which may then transduce either survival or death signals.

Recently, several hydrophilic sapphyrin analogues have been evaluated as new drug candidates for the treatment of solid tumors (Fig. 1.12) [66]. These compounds **1.82-1.85** were found to inhibit the proliferation of adherent cancer cell lines *in vitro* at relatively low doses, leading to cell death within a few days. Treatment of A549 cells with sapphyrin **1.84** has elucidated the formation of ROS (reactive oxygen species) and resulted in wide-spread decreasing in transcript levels in four hours.

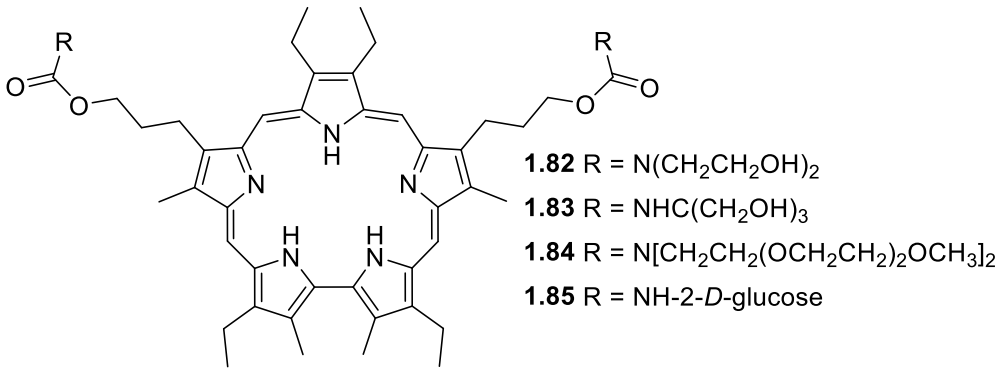

Figure 1.12: Hydrophilic sapphyrin derivatives.

Also relevant is the synthesis of stretched pentapyrrolic macrocycles systems. In 2009 Zhang and co-workers have developed new building blocks allowing an increased number of carbons between pyrrole units. Attempting to obtain tetrapyrrolic derivatives they have noticed that reacting pyrrole bisacrylaldehyde **1.86** and dipyrromethane **1.53** the reaction do not undergo in 1+1 condensation. In fact several combinations of equivalents can be achieved and the most interesting in this case is that even using the same equivalents of both reactants the reaction occurred between 2 eq. of **1.53** and 1 eq. of **1.86**, yielding the stretched analogue sapphyrin **1.87** (Scheme 1.12) [67].

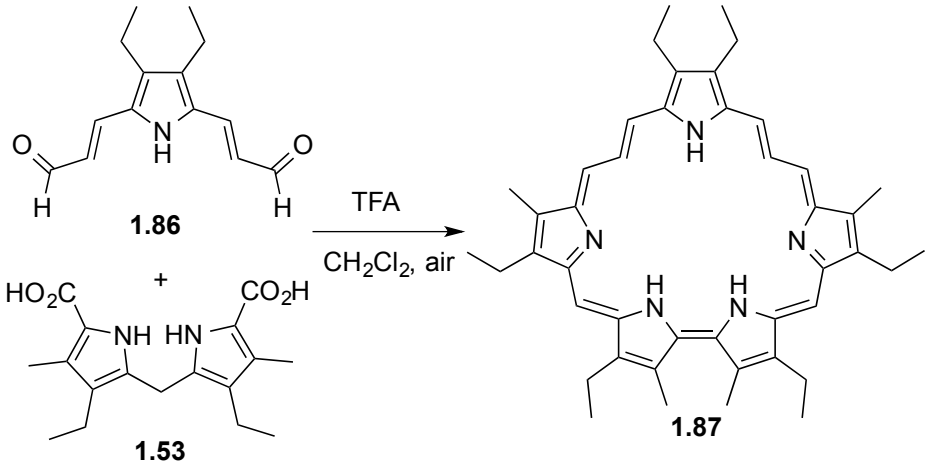

Scheme 1.12

Until now no further studies in macrocycle **1.87** have been performed but this new expanded porphyrin has a large cavity that can be useful for anion binding applications. Also the long exhibited wavelength absorptions (solvent: chloroform, Soret band at 535 nm and Q bands at 684, 754 and 840 nm) possibly will make it a suitable candidate for use as photosensitizer in photodynamic therapy.

While research for new *β*-pyrrolic substituted pentaphyrins has led to a considerable effort in the most recent years, several research groups have been devoted to developing strategies that allow access to various pentapyrrolic macrocycles and heteroatom analogues that bear *meso*-substituents.

1.4.1.2. Meso-substituted pentapyrrolic systems

Latos–Grazynski and coworkers reported the first *meso*-tetraphenyl sapphyrin (**1.88**) from the reaction of benzaldehyde **1.88** and pyrrole **1.59** in 1:3 molar ratio under oxidative acid catalysis in 10% yield (Scheme 1.13). This synthesis have shown that *meso*-aryl sapphyrins, when compared with *β*-substituted sapphyrins, can also show an enormous structural diversity. For example, **1.89** exhibits an inverted structure in which the pyrrole ring, in an opposite direction to the bipyrrole subunit, has undergone a 180° ring flipping, instead of exhibiting a structure without any ring inversion like in the *β*-substituted sapphyrins [68].

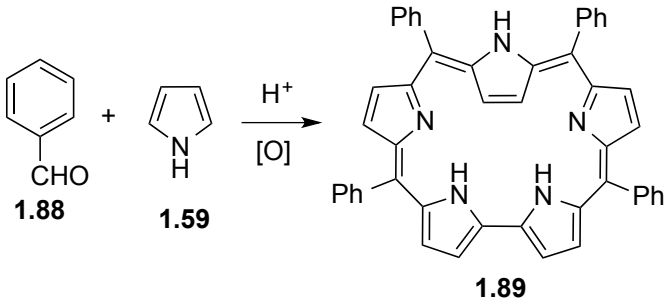

Scheme 1.13

It has been shown that it is possible to convert an inverted structure to a normal structure in favorable cases by simple chemical modification. For example, Latos-Grazynski *et al.* using ^{1}H-NMR have shown that the inverted structure **1.89** can be converted to the normal structure **1.89** by simple di-protonation (Scheme 1.14) [69]. Here, the inverted pyrrole ring undergoes a 180° ring flipping upon protonation of the adjacent pyrrole nitrogens.

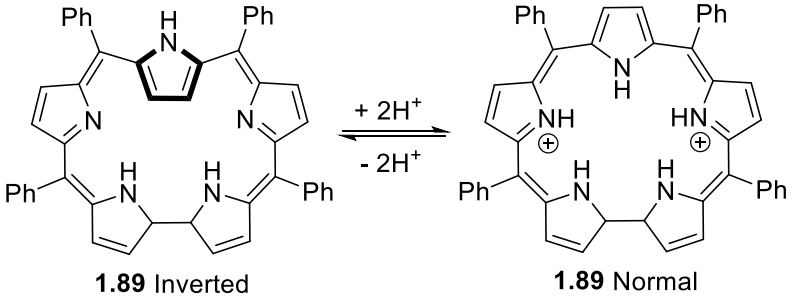

Scheme 1.14

However, some core-modified sapphyrins **1.90-1.92** do not exhibit ring flipping upon protonation, and the structures either remain inverted or normal (Fig. 1.13).

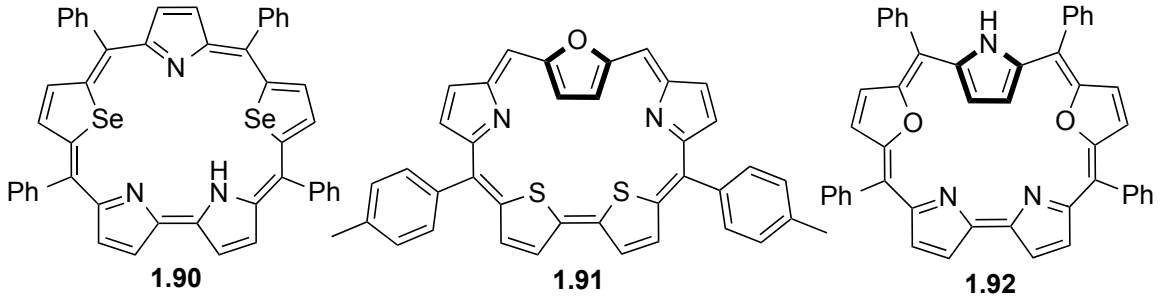

Figure 1.13: *Meso*-substituted core modified sapphyrin structures.

The ^{1}H-NMR and X-ray structure analyses revealed that larger core size and the presence of smaller heteroatoms (N or O) adjacent to the heterocyclic ring leads to inverted

structure, while the presence of bigger heteroatoms (S or Se) leads to normal structure. For example, when the adjacent ring next to the inverted ring contains a small heteroatom like N and O, the ring is inverted as in **1.89**, **1.91** and **1.92**, while in **1.90** the macrocycle acquires a normal structure, due to the increase in size of the adjacent ring heteroatom's (S or Se).

Attractively, heterocore *meso*-substituted sapphyrins have also encountered their space in biomedical applications. Chandrashekar and co-workers have examined the uptake of *meso*-substituted heterocore sapphyrin derivatives into human erythrocytes tissue [70]. This water soluble *meso*-substituted sapphyrin, namely ammonium salt of 5,10,15,20-tetrakis(*meso*-*p*-sulfonatophenyl)-25,27,29-trithiasapphyrin was prepared from trithiasapphyrin **1.95** in dichloromethane, while chlorosulfonic acid was added slowly with vigorous stirring. After refluxing for 48 h, the excess of chlorosulfonic acid decomposed by addition of ice-cold water. The mixture was cooled at 5 °C and filtered and the precipitated water soluble derivative of modified sapphyrin **1.96** was purified by two successive reprecipitations from methanol/acetone. The dark brown crystals of **1.96** were obtained in 48% yield and identified by spectroscopic techniques. The synthetic methodology is outlined in scheme 1.15 [71].

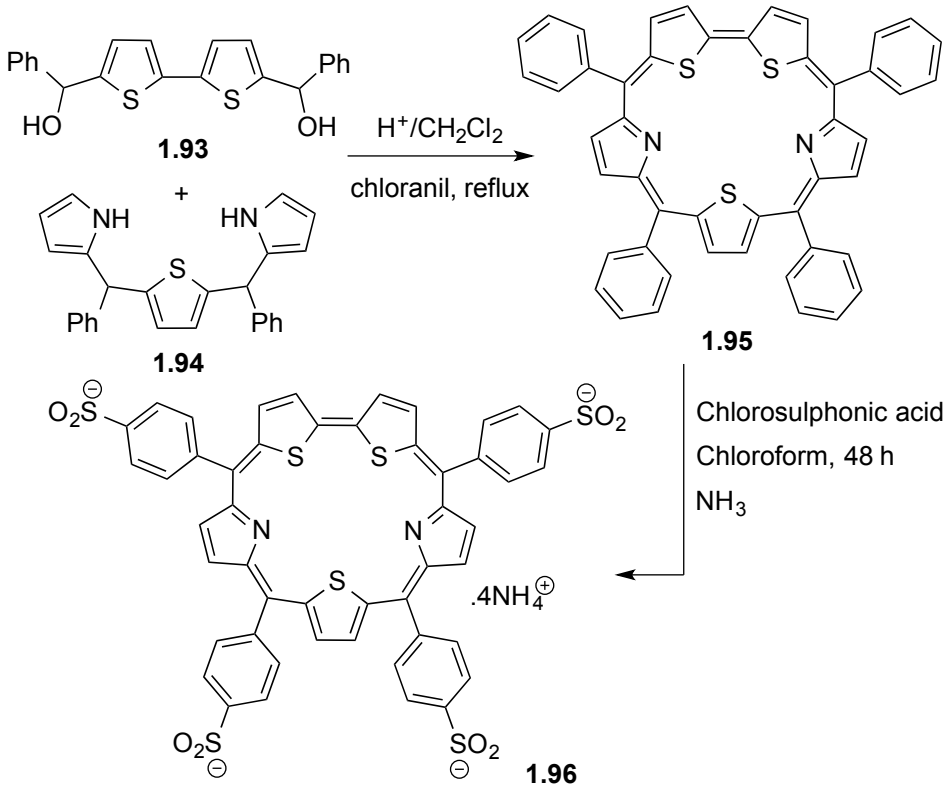

Scheme 1.15

This new photosensitizer **1.96** had a wide absorption across the entire visible region with the Soret band centered on 513 nm. The Q-bands for the same compound are at 610 and 837 nm. In analogy to sapphyrins, they have a relatively greater absorption in the clinically useful red region (600-800 nm) and a photodynamic efficiency mainly dependent on the drug uptake. Experiments with cell cultures and animal tumor models found that its rate of release from tissues was faster than what is seen for Photofrin®.

1.4.1.3. N-confused and N-fused pentapyrrolic systems

Sessler *et al.* used a [3 + 2] approach to generate double *N*-confusion in sapphyrin **1.99** (Scheme 1.16), where the two pyrroles of the bipyrrole unit are inverted [72]. The synthesis of this inverted sapphyrin **1.99** was accomplished *via* the acid-catalyzed 3+2 condensation between the 3,3`-bipyrrole dialdehyde **1.97** and tripyrromethane diacid **1.24**. Although the expected product of this condensation was product **1.98**, all efforts to isolate this intermediate failed. Presumably, this product **1.99** arises from the nucleophilic attack of MeOH to one of the tautomers of intermediate **1.98**. After chromatography on silica gel and treatment with aqueous NH_4Cl, the inverted sapphyrin **1.99** was obtained in 8-9% yield.

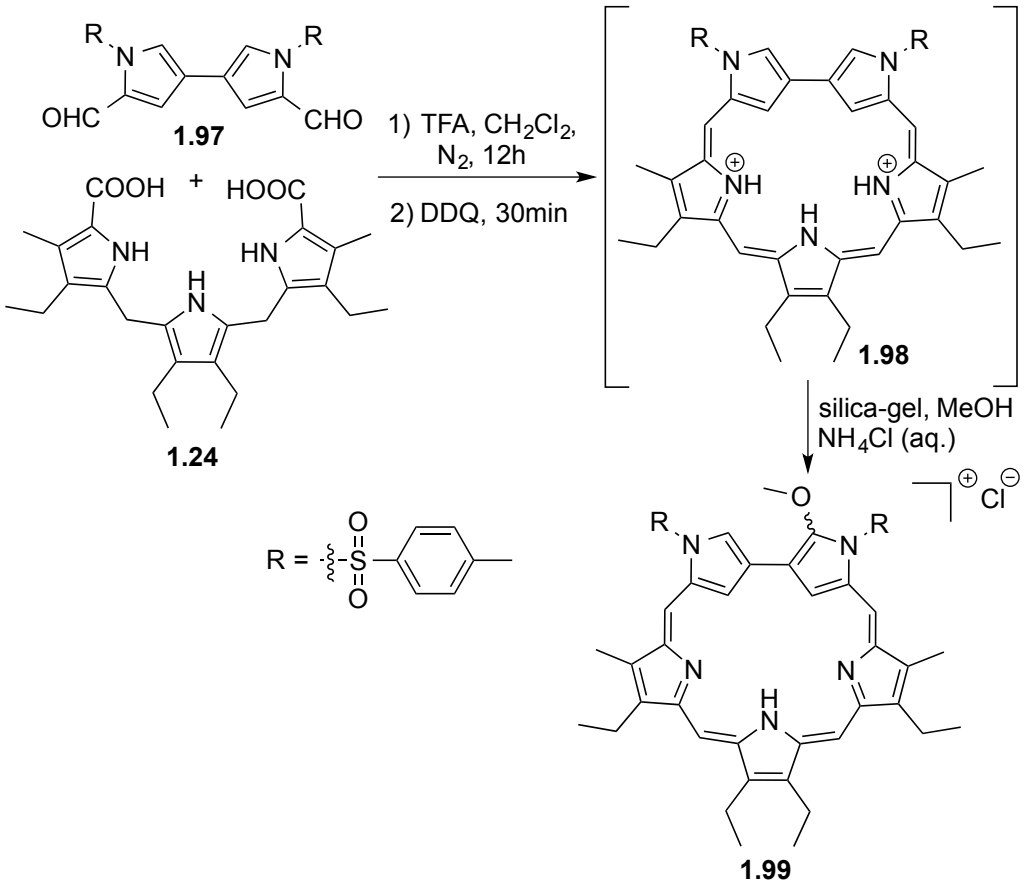

Scheme 1.16

Osuka and coworkers first reported that *meso*-aryl pentaphyrin exists in the form of an *N*-fused pentaphyrin [73]. The Rothemund-type condensation reaction of pyrrole with pentafluorobenzaldehyde resulted in oxidized and reduced forms of *N*-fused pentaphyrins along with other products. The oxidized form of the *N*-fused pentaphyrin **1.101** shows an aromatic behavior while the reduced form **1.100** shows an anti-aromatic behavior. Interestingly they are inter-convertible (Scheme 1.17).

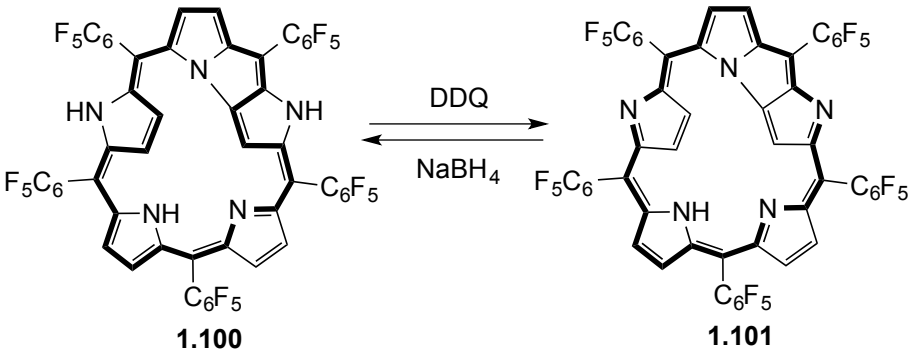

Scheme 1.17

In another attempt for the synthesis of *N*-confused pentaphyrin, Furuta *et al.* obtained product **1.104,** which contain the fused tripentacyclic with four nitrogens pointing inward. Further, oxidation of **1.104** resulted in formation of **1.105**, which isomerized into the double *N*-fused pentaphyrin **1.106** (Scheme 1.18) [74]. Fascinatingly, isomerization takes place with loss of aromaticity and the resulting pentaphyrin **1.106** is non-aromatic.

These systems have been successfully used in coordination chemistry. For example structure **1.100** bearing rhodium ions are already described in literature [75,76].

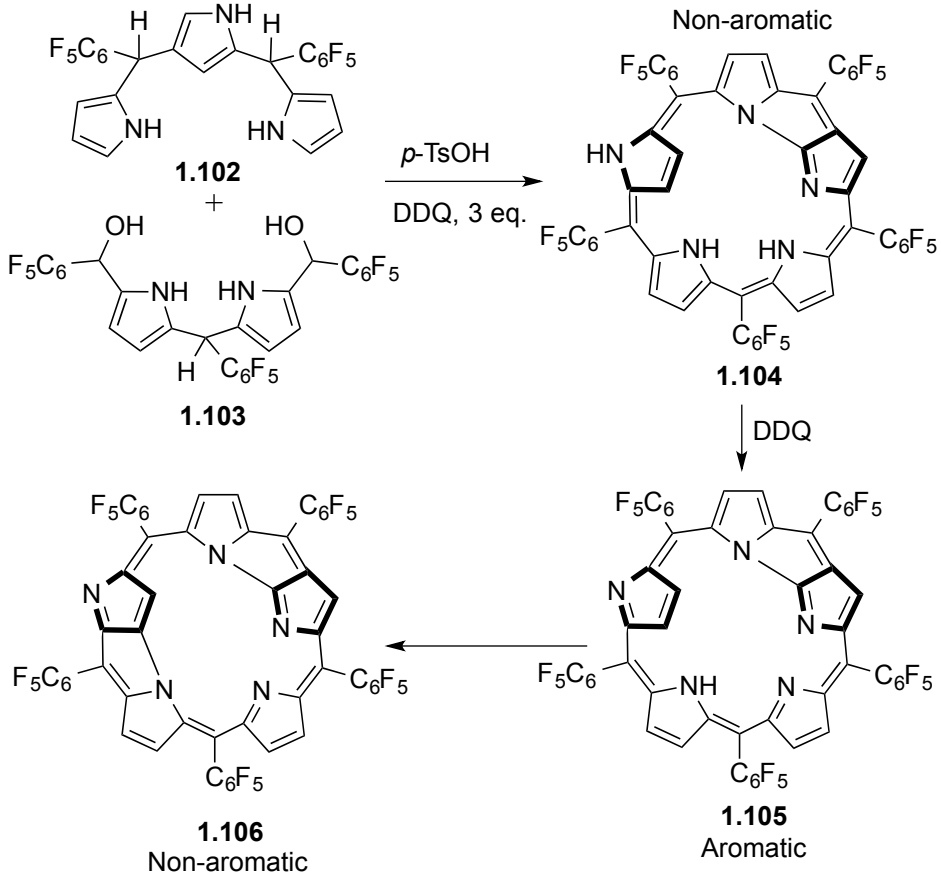

Scheme 1.18

1.4.2. Hexapyrrolic systems

An initial demonstration that expanded porphyrins could have more than five pyrroles was reported by Sessler *et al.*, with the introduction of rubyrin [77,78]. This expanded porphyrin **1.107** which is a [26]hexaphyrin(1.1.0.1.1.0) was synthesized in 1991 by condensing the tetrapyrrolic precursor **1.56** with diformyl bipyrrole **1.30** under acid catalysis and subsequent air oxidation as shown in scheme 1.19.

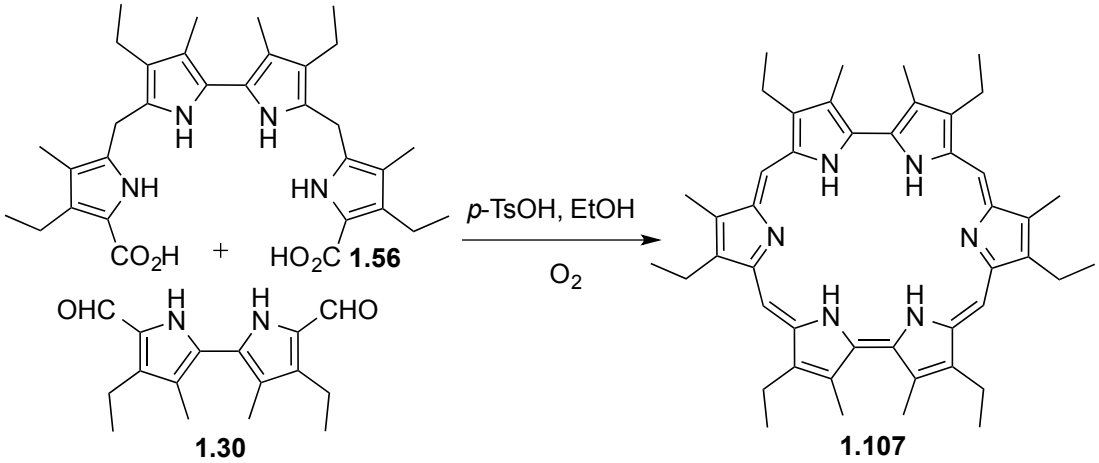

Scheme 1.19

Almost at the same time, Gossauer and coworkers introduced hexaphyrins. This synthesis was possible by the acid catalysed 3+3 condensation of free tripyrranes **1.108** and **1.109** with tripyrrane dialdehydes **1.110** and **1.111**, respectively, followed by oxidation with a mixture of I_2/*p*-benzoquinone (scheme 1.20) [79]. Through this reaction they have isolated the hexapyrrolic macrocycles **1.112** and **1.113** together with minor quantities of the corresponding pentaphyrins. As a result of the substitution pattern on the precursor tripyrranes **1.108-1.111**, the macrocycles **1.112** and **1.113** are obtained in two isomeric forms, structures **A** and **B**, in equal proportions [15].

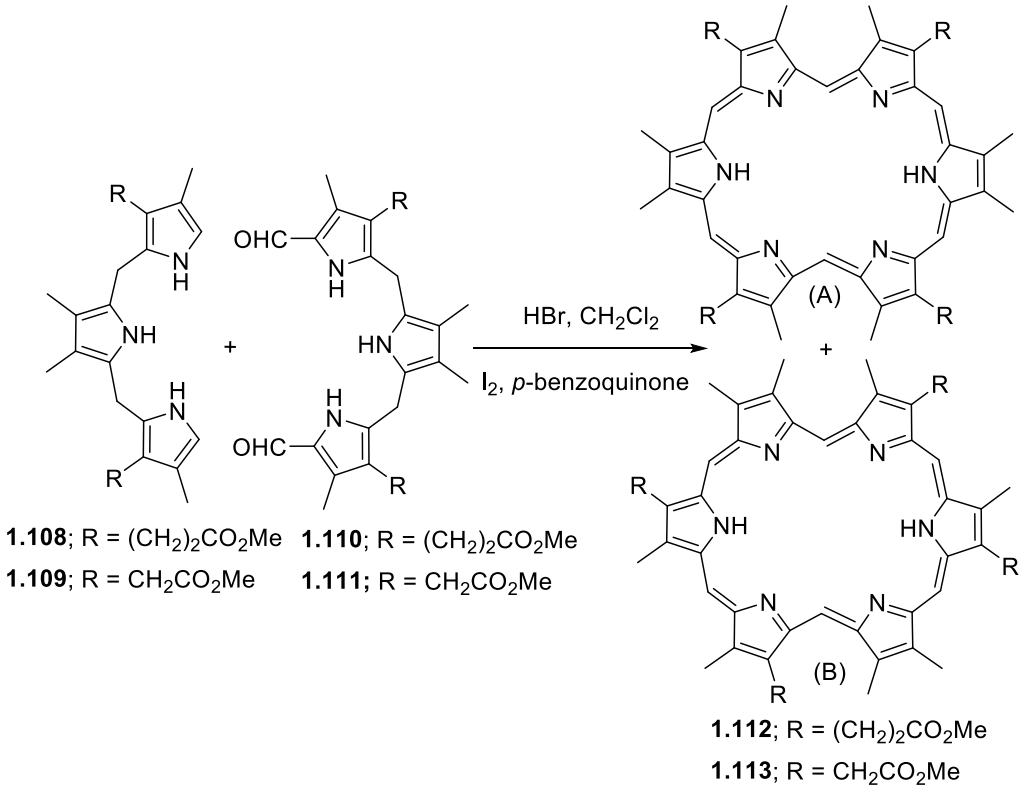

Scheme 1.20

In analogy with pentapyrrolic systems, the hexapyrrolic systems exhibit an even higher structural diversity, since the structure of the resulting macrocycle is influenced by the nature of the link, the number of *meso*-carbons linking the six heterocyclic rings, and the nature of the heteroatoms (Fig. 1.14) [80-82].

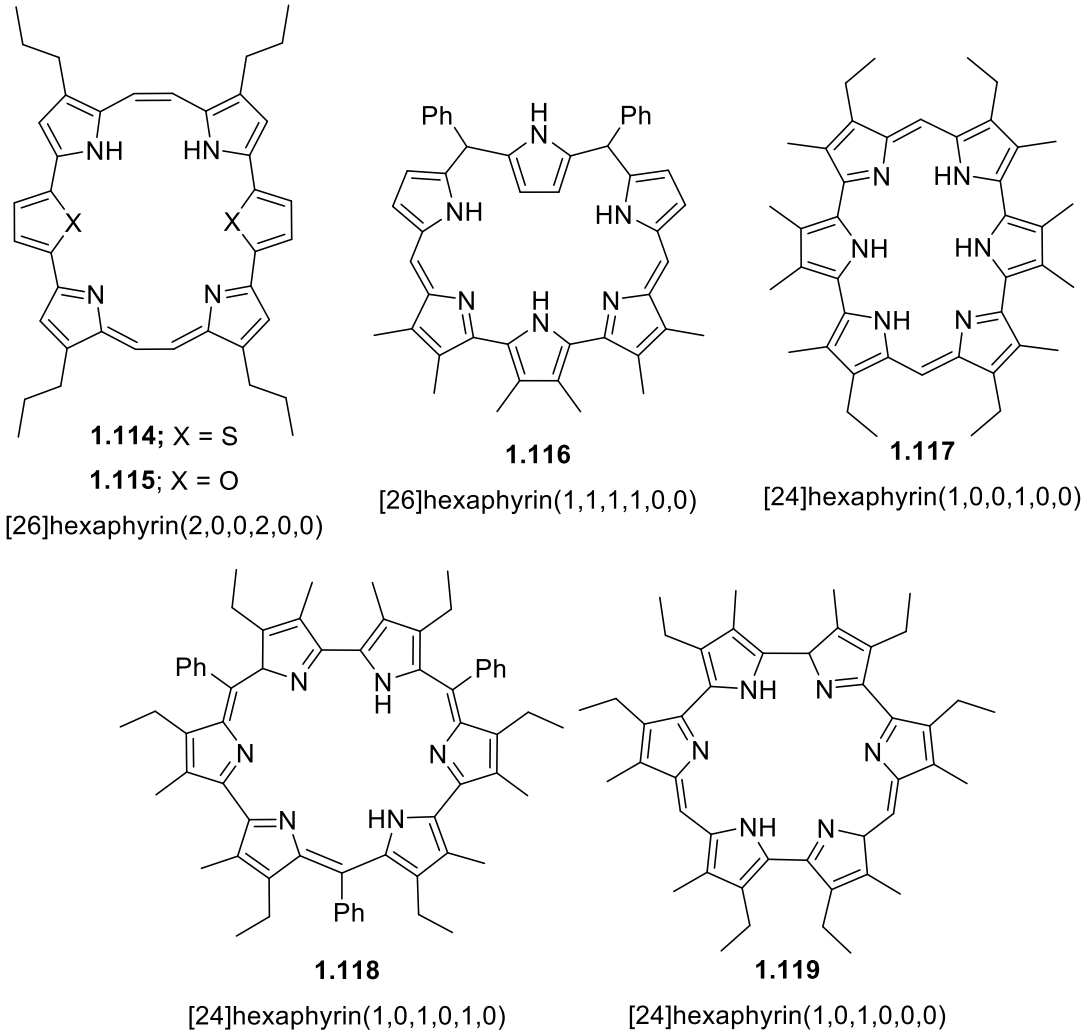

Figure 1.14: Hexapyrrolic systems.

1.4.2.1. β-substituted hexapyrrolic systems

Investigations on the coordination chemistry of hexaphyrins have provided an insight into their dynamic behavior. The flexibility of this molecular framework has been displayed by the isolation of the bimetallic Zn and Pd chelates of hexaphyrins **1.112-1.113** in which two different geometrical arrangements were found to be predominant (Schemes 1.21 and 1.22). Treatment of the isomeric mixture of **1.112** with $ZnCl_2$ furnished the symmetrical bimetallic zinc complex **1.120** (Scheme 1.21) [15]. Interestingly, the same methodology when applied to the crude mixture of hexaphyrin **1.113** gave the less symmetric isomer **1.121**.

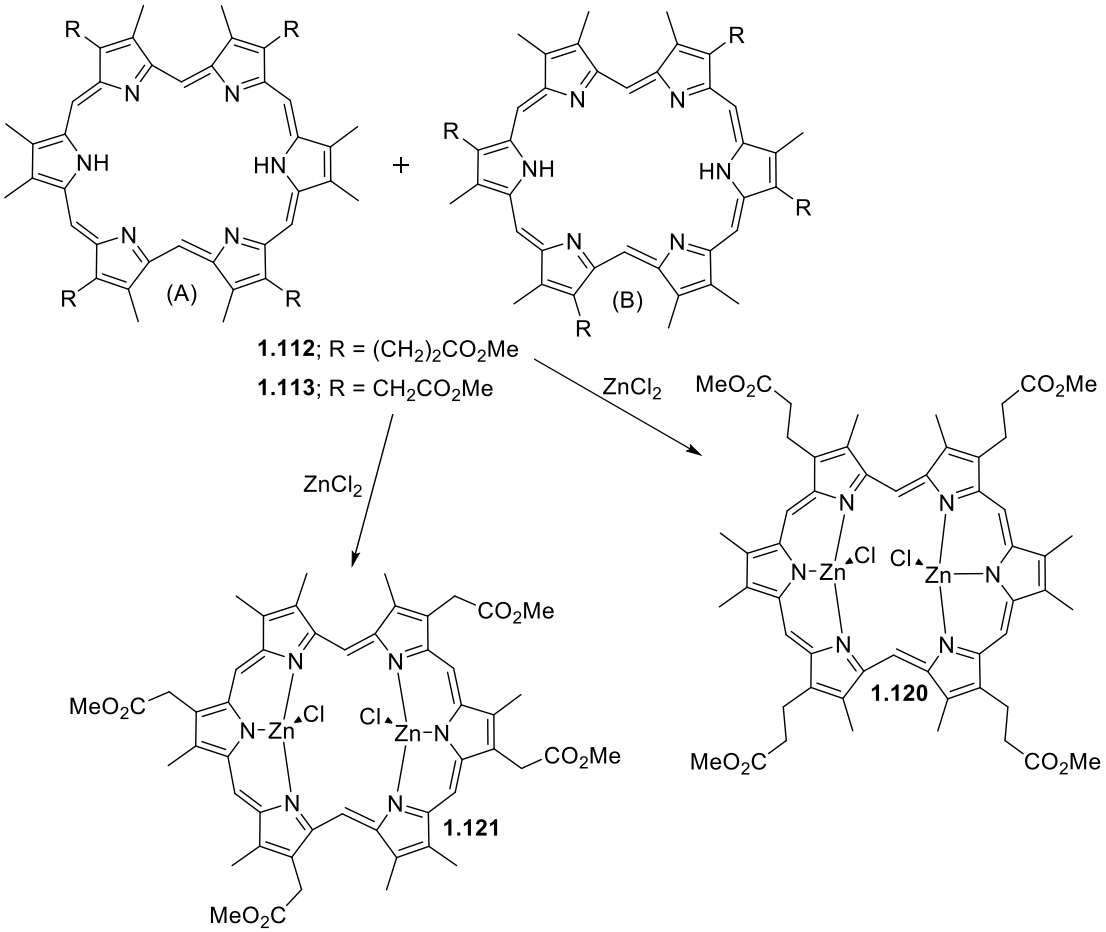

Scheme 1.21

On the other hand, with Pd, a totally different representation emerged. Treatment of basified crude reaction mixtures of hexaphyrins **1.112** or **1.113** with ammonium-tetrachloropalladate furnished the bis-palladium complexes **1.122** and **1.123** (Scheme 1.22). Unexpected was their unusual geometry where it seems that in order to accommodate the square-planar geometry around the d^8 Pd centers, the two central pyrrolic rings coordinated to these metal atoms have rotated through 180° [15].

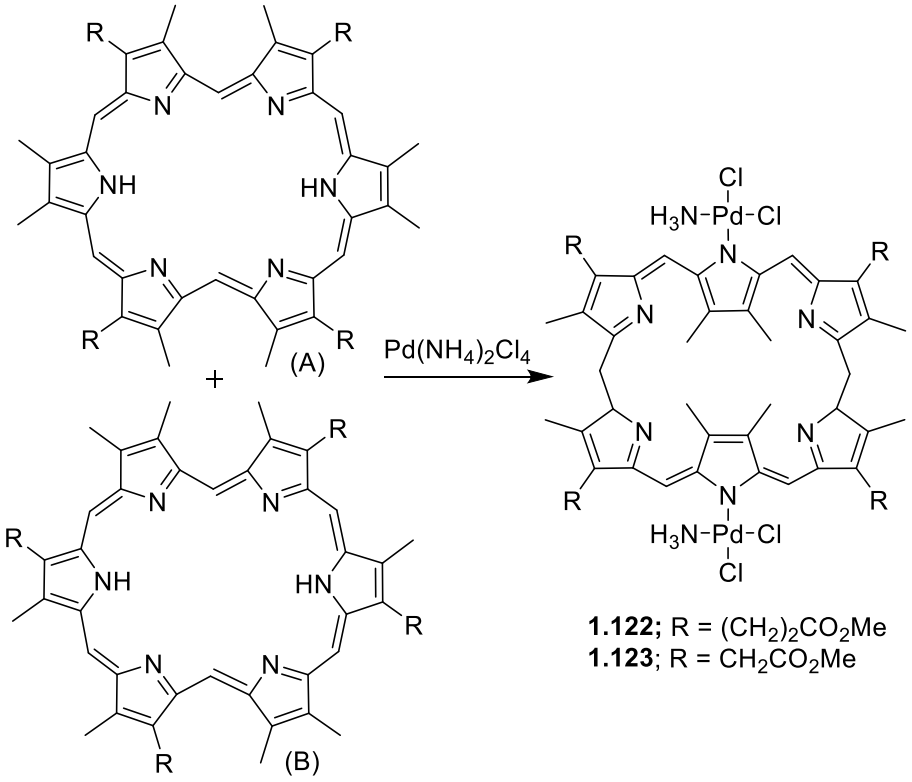

Scheme 1.22

This dynamic behavior led other authors to the synthesis of hexaphyrin analogues to apply in coordination chemistry. A noteworthy work was developed by Sessler and coworkers in the area of actinides coordination by hexapyrrolic systems [83]. During these efforts in 1995, this author synthesized a hexapyrrolic macrocycle containing terpyrrolic subunits [84]. The procedure involved the condensation of a diformylterpyrrole **1.124**, with a terpyrrole **1.125**, in the presence of trifluoroacetic acid. Treatment of the resulting amethyrin–TFA salt with NaOH, followed by crystallization from MeOH, furnished compound **1.117** in 90% yield (Scheme 1.23)[85].

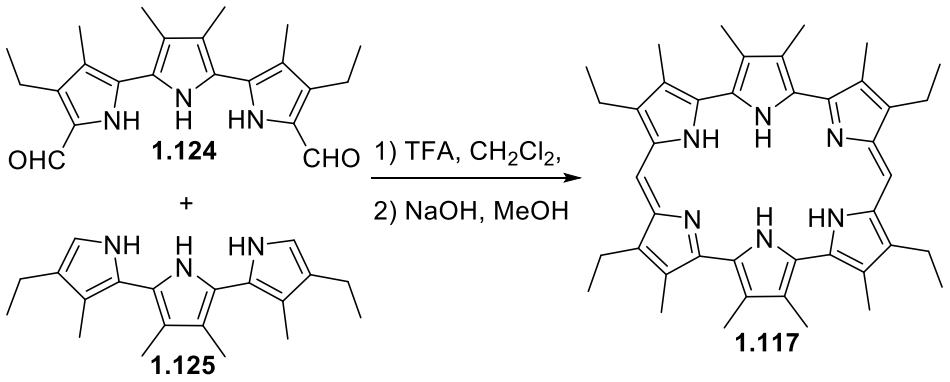

Scheme 1.23

To this 24 π electron system, [24]hexaphyrin(1.0.0.1.0.0), was assigned the trivial name amethyrin (**1.117**) and so far, it has proved to be rather unique among expanded porphyrins since it possesses a rich metallation chemistry. For instance, as summarized in scheme 1.24), this hexapyrrolic system can form stable cobalt **1.126**, zinc **1.127**, copper **1.128** and uranyl **1.129** complexes. [83,86].

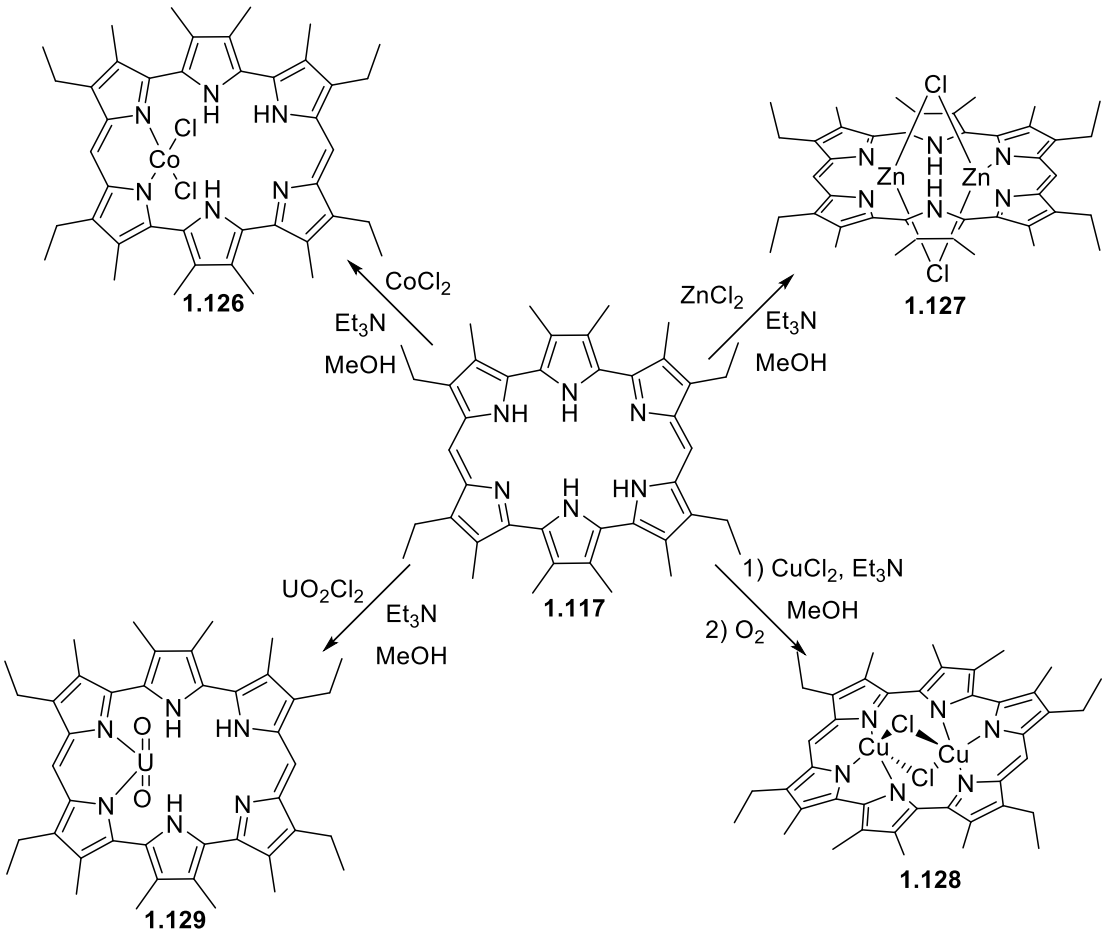

Scheme 1.24

Latter, isoamethyrin ([24]hexaphyrin(1.0.1.0.0.0)]; **1.119**) was prepared and studied as ligand for the actinide cations, uranyl (UO_2^{2+}.) and neptunyl (NpO_2^{+}) [46].

The synthesis of isoamethyrin was obtained by treatment of **1.58** with aqueous $Na_2Cr_2O_7$ in TFA followed by purification on column chromatography and protonation with HCl. This procedure gives rise to isoamethyrin **1.119** in the form of its diprotonated salt in 77% yield (Scheme 1.25).

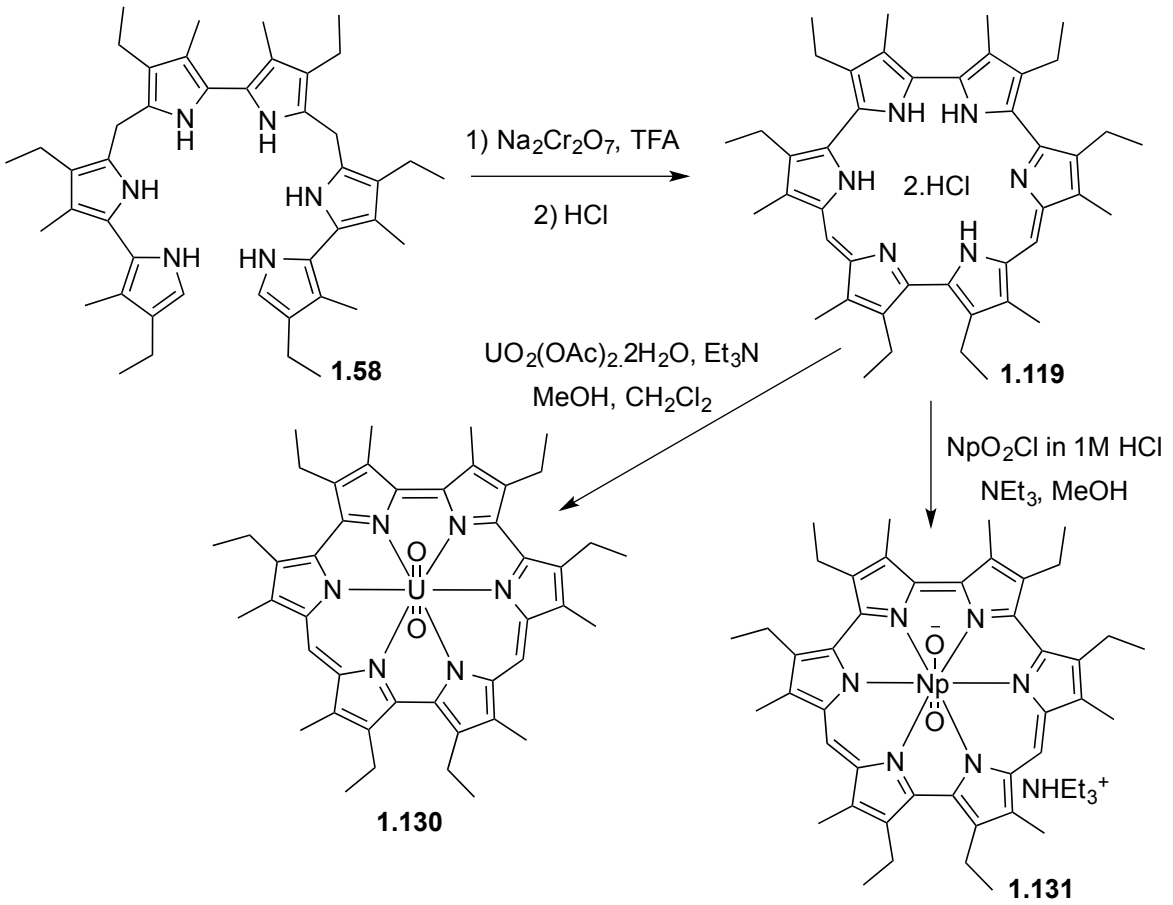

Scheme 1.25

Subsequent addition of $UO_2(OAc)_2{\cdot}2H_2O$ in the presence of base yielded the uranyl complex **1.130** in 74% yield (Scheme 1.25). The latter reaction, is preceded by an oxidation producing what is formally an aromatic [22]hexaphyrin(1.0.1.0.0.0) dianionic ligand. Also in the same scheme is possible to notice the synthesis of a neptunyl complex **1.131** obtained by treating **1.119** with a solution of neptunyl (V) chloride in the presence of base.

Unlike the previous uranyl system **1.129**, formed after more than a day of heating, the uranyl complex **1.130** was formed from this new derivative **1.119** within minutes and do not required the application of heat, or the use of an inert atmosphere to be generated. Further, this ligand is relatively easy to synthesize, requiring only one-third of the synthetic steps required to produce sapphyrin. This makes it potentially attractive in actinide coordination-based applications and waste remediation [83].

1.4.2.2. Meso-substituted hexapyrrolic systems

Like *meso*-substituted sapphyrins, *meso*-substituted rubyrins also show a structure where one or two pyrrole rings are inverted. In analogy with the parent *meso*-substituted sapphyrins, *meso*-aryl rubyrin **1.132** shows similar behavior upon protonation. For example, it has been shown that the ring flipping in rubyrin **1.132** upon protonation depends on the nature of acid used (Scheme 1.26). Protonation by HCl leads to 180° ring flipping of two inverted pyrrole rings **1.133**, while use of TFA leads to simultaneous flipping of two inverted rings to normal and two normal rings to inverted **1.134** [87].

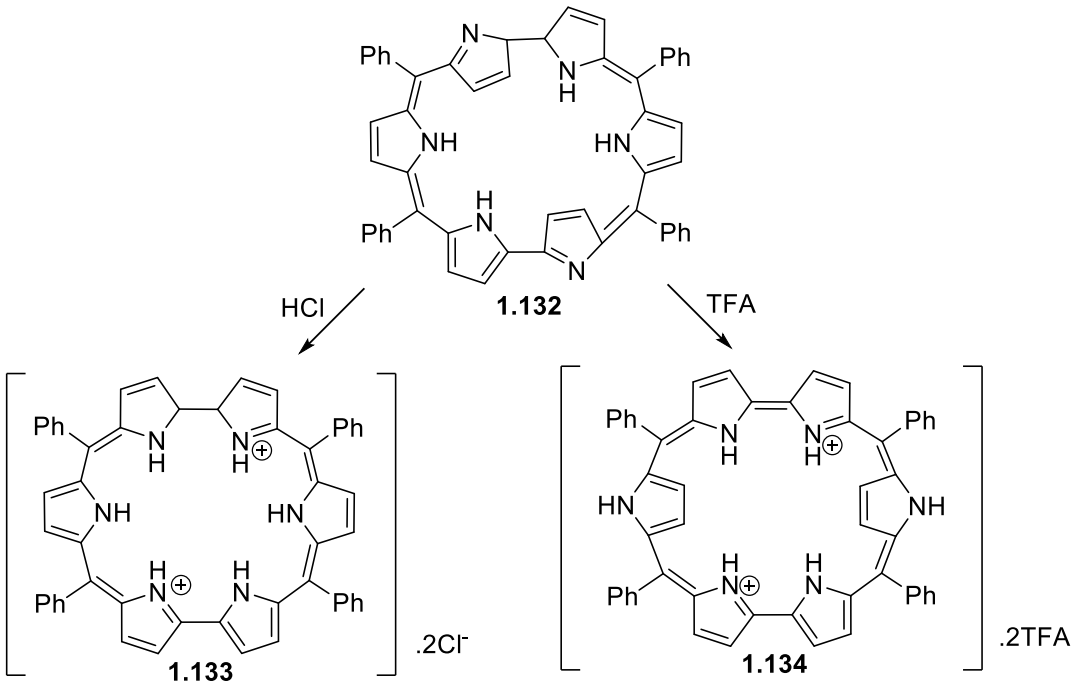

Scheme 1.26

One of the most interesting additions to the family of hexapyrrolic macrocycles was described by Cavaleiro and co-workers and was a minor product from the modified Rothemund method [88]. Condensation of pentafluorobenzaldehyde (**1.135**) with pyrrole

(**1.57**) in a mixture of boiling acetic acid and nitrobenzene enabled [26]hexaphyrin(1.1.1.1.1.1) **1.137** to be isolated in approximately 1% yield. The expected porphyrin **1.136** was also obtained in 15% yield (Scheme 1.27).

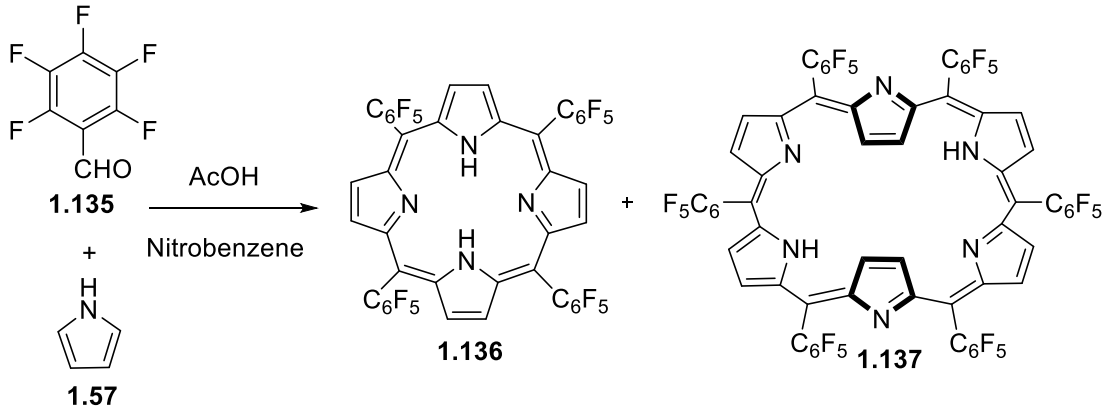

Scheme 1.27

The yield was later improved by using the ring size selective synthesis [89]. Treatment with $TsNHNH_2$, [26]hexaphyrin **1.137** was easily reduced to [28]hexaphyrin **1.138**, which could be quantitatively oxidized back with DDQ to the original [26]hexaphyrin (Scheme 1.28).

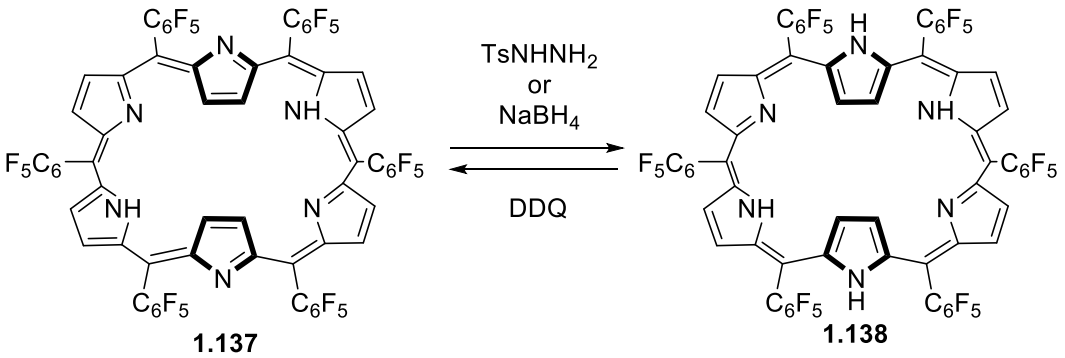

Scheme 1.28

Recently, studies concerning the response of expanded porphyrins in the presence of different cationic ions in methanol or a mixture of methanol/water it was found that this latter hexaphyrin **1.137** could act as chemodosimeter for Ag^+ ions via near-infrared luminescence above 900 nm, a region that is free from the optical interference in the visible wavelength range induced by the commonly used matrix and other organic compounds [90].

The presence of six *meso*-carbon bridges makes hexaphyrins flexible molecules, and therefore generally they adopt different conformations. *Meso*-substituted hexaphyrins reported in the literature (Fig. 1.15) were found to exhibit, rectangular conformations, consisting in two opposite, inverted pyrroles with nitrogen atoms pointing outward and four pyrroles in the corner positions with nitrogen atoms pointing inward as in **1.137, 1.138**, **1.139** and **1.140** or a *figure eight* conformation as in **1.141** [68,91,92].

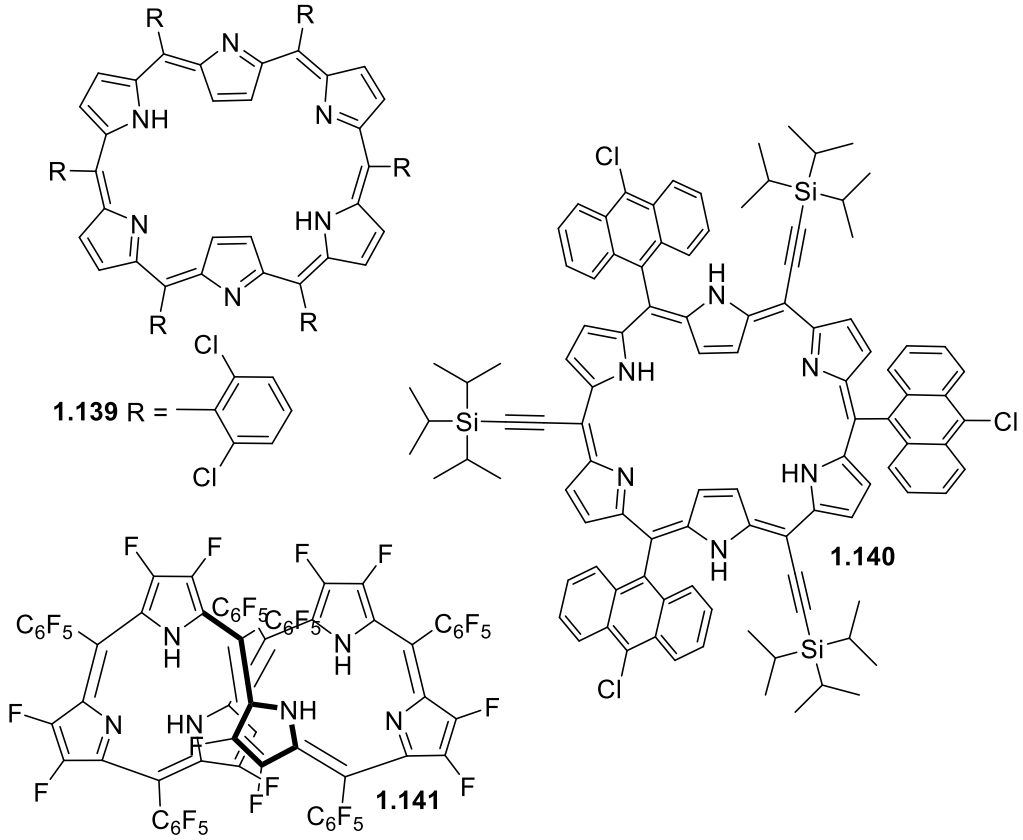

Figure 1.15: *Meso*-substituted hexaphyrins.

Interestingly, 28 π hexaphyrin **1.140** reported by Anderson *et al.*, which presented two different *meso*-substituents, does not show aromatic character despite its inverted structure [91]. These observations reveals that the subtle changes on the periphery of hexaphyrin can affect the aromatic nature as well as the conformation. In fact aromaticity is a fundamental concept in organic chemistry. The Huckel rule is very useful in these cases, and helps us to predict that cyclic [4n+2]π and [4n]π conjugated systems should be aromatic and antiaromatic, respectively, given that their π systems lie on two-sided normal planes. On the other hand, Mobius aromaticity, which complements the Huckel aromaticity, predicts that the above [4n+2] and [4n] Huckel rule should be reversed for

those π systems that lie on a singly twisted Mobius topology. However, the realization of Mobius aromatic systems is difficult, since the implementation of two conflicting structural features, that is, cyclic full π conjugation and a singly twisted topology, within a single macrocycle is not easy.

In recent years, *meso*-aryl-substituted expanded porphyrins have emerged as a remarkably effective platform to realize stable Mobius aromatic systems. The attributes of these porphyrins include conformational flexibility, which allows flipping of the constitutional pyrrole rings.

Normally phosphorus insertion into porphyrinoids has proved a useful means to realize fully reduced annulenic π conjugation. Optimistic with these results, Osuka and co-workers attempted the reaction of *meso*-pentafluorophenyl [28]hexaphyrin **1.138** with $POCl_3$ (100 equiv.) in the presence of triethylamine at room temperature for 24 h, which gave a monophosphorus hexaphyrin **1.143** in approximately 65% yield after aqueous workup (Scheme 1.29).

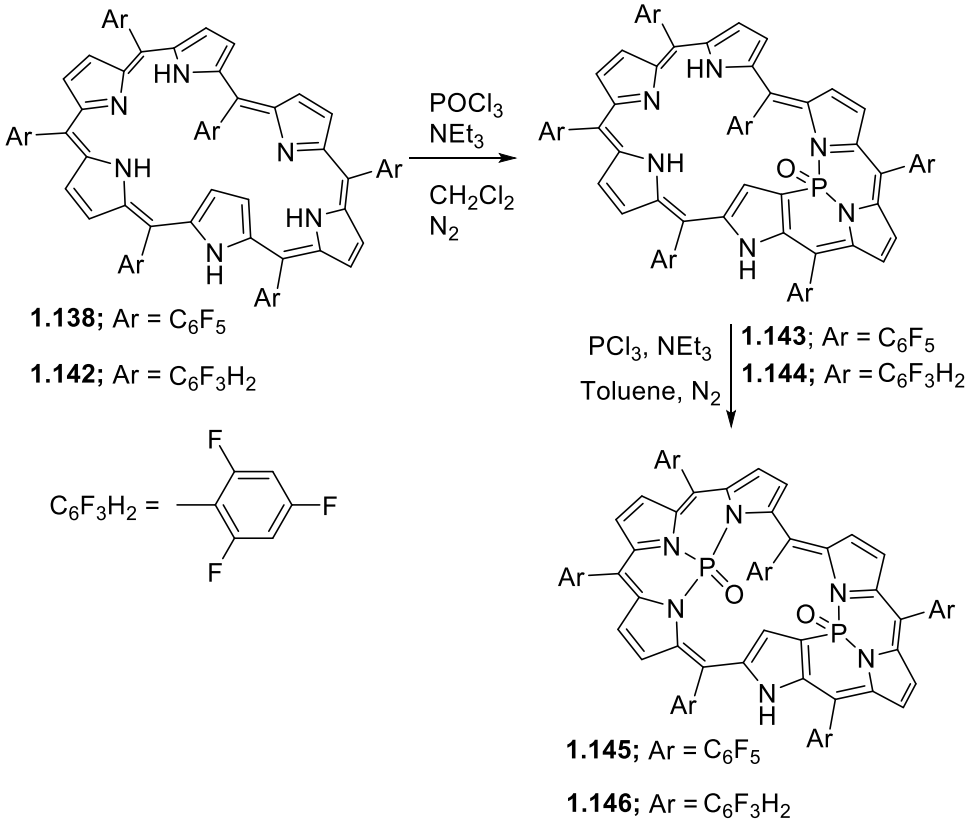

Scheme 1.29

Further treatment of **1.143** with PCl_3 (50 equiv.) in the presence of triethylamine at 80 ºC for 1 h gave the bisphosphorus [30]hexaphyrin **1.145** in approximately 46% yield. In the same manner, phosphorus complexes **1.144** and **1.146** were obtained from *meso*-(2,4,6-trifluorophenyl) substituted [28]hexaphyrin **1.142** in 24 and 10% yield, respectively (Scheme 1.29).

This work not only has shown bis-phosphorus complexes of hexaphyrin **1.145** and **1.146**, but also identified the first examples of a structurally well-characterized and stable [4n]π Mobius antiaromatic molecules, in which the two incorporated phosphoramide moieties play an important role in rigidifying the twisted Mobius conformations rendering highly reduced stable hexaphyrins **1.145** and **1.146** as it also validates the reversibility of Huckel rule upon changing the number of π electrons between [4n+2] and [4n] for cyclic conjugated molecules with a twisted Mobius topology [93,94].

1.4.2.3. N-confused and N-fused hexapyrrolic systems

Recently Osuka's group reported a double *N*-fused *meso*-aryl substituted [28]hexaphyrin(1.1.1.1.1.1) [95]. Compound **1.147** was obtained in 55% yield by refluxing **1.137** in chlorobenzene in the presence of Fe(III) acetylacetonate (Scheme 1.30).

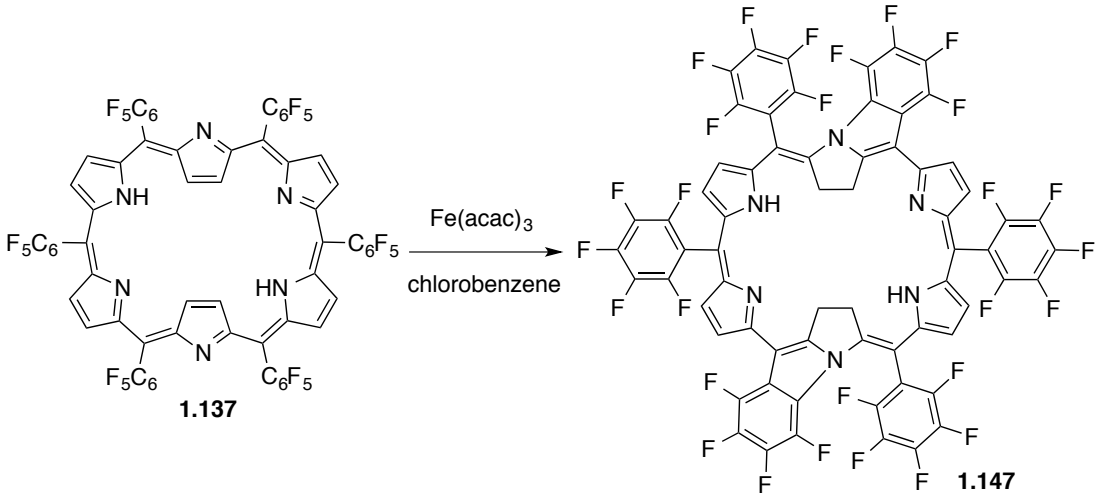

Scheme 1.30

It is important to note that [28]hexaphyrin, **1.138** a reduced form of **1.137**, could not be converted into **1.147** under the reaction conditions depicted above. Furuta *et al.* reported the first examples of double *N*-confused hexaphyrins **1.149-1.152** [96]. When *N*-confused tripyrrane **1.148** was treated with pentafluorobenzaldehyde in the presence of *p*-

TsOH, followed by oxidation with *p*-chloranil, *meso*-hexakis(pentafluorophenyl)-substituted doubly *N*-confused hexaphyrins, **1.149** and **1.150**, were obtained as brown solids in 7 and 3% yields, respectively (Scheme 1.31).

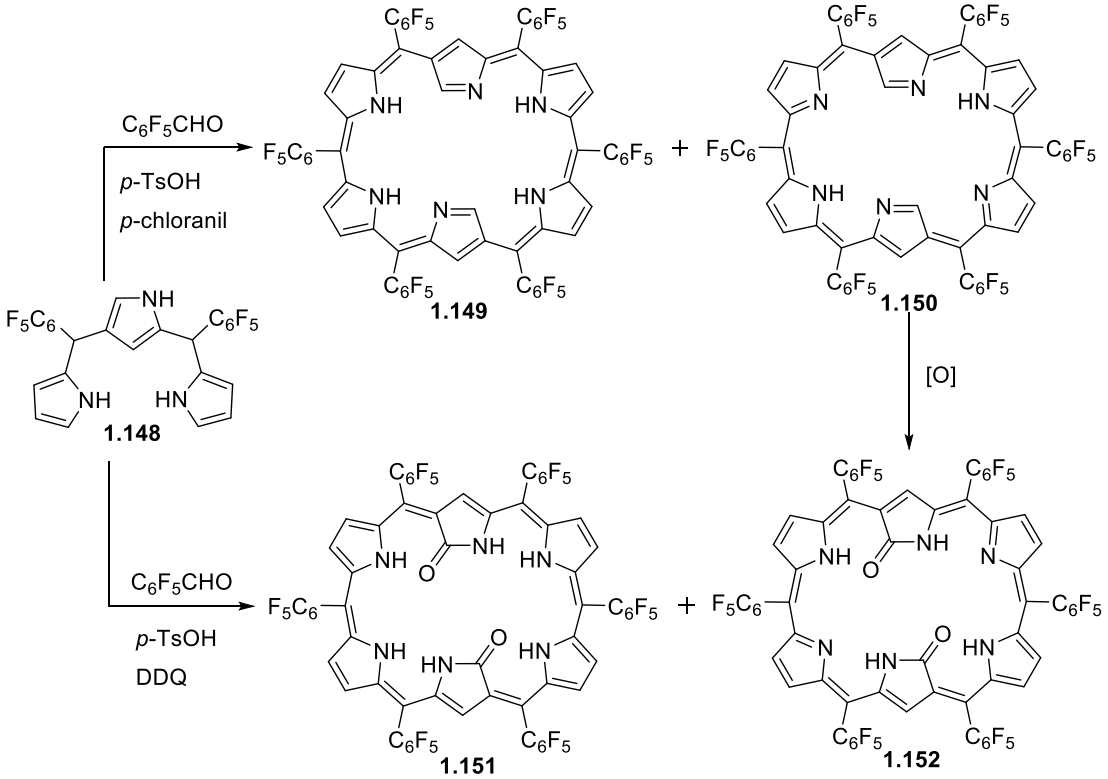

Scheme 1.31

Interestingly, the nature of these hexaphyrins was found to be dependent on the nature of the oxidant used in the reaction. On varying the oxidizing agent from *p*-chloranil to DDQ in the condensation reaction, two different products (**1.151** and **1.152**) were obtained as greenish solids in 7 and 10% yields, respectively (Scheme 1.31). However, **1.150** was quite unstable and gradually oxidizes into amide 1.**152** in CH_2Cl_2 solution at room temperature.

Recently Osuka and coworkers were able to synthesize **1.152**, from [26]hexaphyrin **1.137** [97]. This was accomplished adding CuCl to a solution of **1.137** in pyridine under aerobic conditions. After usual workup followed by chromatographic separation through a silica gel column, a reddish solid was isolated as a sole major product **1.153** (Scheme 1.32).

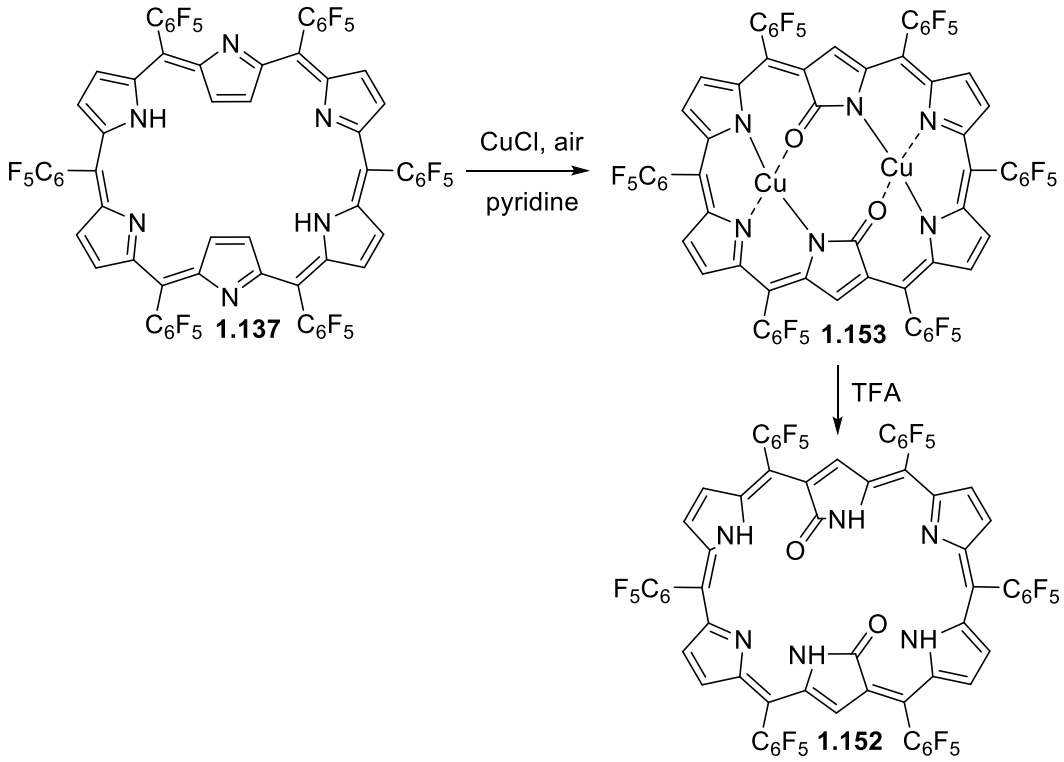

Scheme 1.32

After quantitative demetallation to its free base, upon treatment with TFA, all the structural data confirmed that this compound as exactly identical to that prepared by the previous stepwise synthesis (**1.152**) [96]. Although the yield of **1.152** by this method is modest (24.4%), this reaction is far superior to the previous synthesis in terms of the easy procedure and ready availability of **1.152**. *N*-Confused porphyrinic macrocycles have been so far prepared by an accidental coupling reaction of an aryl aldehyde with pyrrole at *β*-position or by means of a designed route using *N*-confused mono- or oligopyrrolic precursors [15]. In this respect, this procedure is quite attractive, since it opens up a new entry to *N*-confused expanded porphyrins from normal expanded porphyrins by means of an unprecedented pyrrole rearrangement.

1.4.3. Higher order systems

There are only very few reports on expanded porphyrins containing seven pyrrolic units till date. Some of the seven pyrrolic units reported so far are shown in figure 1.16 [98-100].

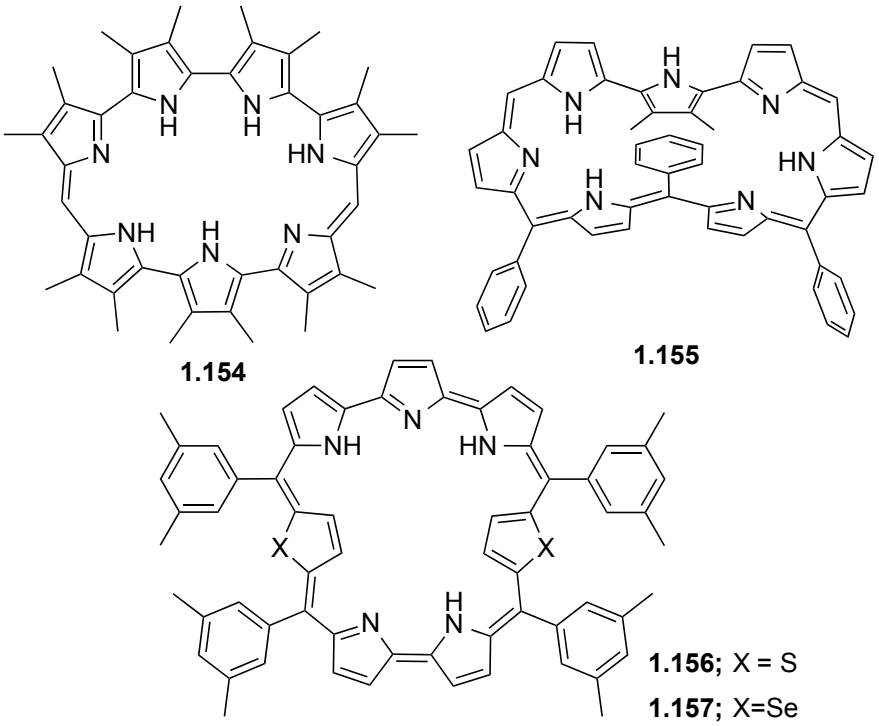

Figure 1.16: Heptapyrrolic Systems.

These compounds can also be classified as non-aromatic and aromatic systems. Heptaphyrin **1.154** is non-aromatic while **1.155**, **1.156** and **1.157** are aromatic [25].

Larger macrocycles containing eight, ten, twelve and sixteen pyrrolic units have also been reported. The octaphyrins **1.158–1.160** were reported by Vogel's group and they were found to exist in chiral figure eight conformations like depicted in figure 1.17 [101].

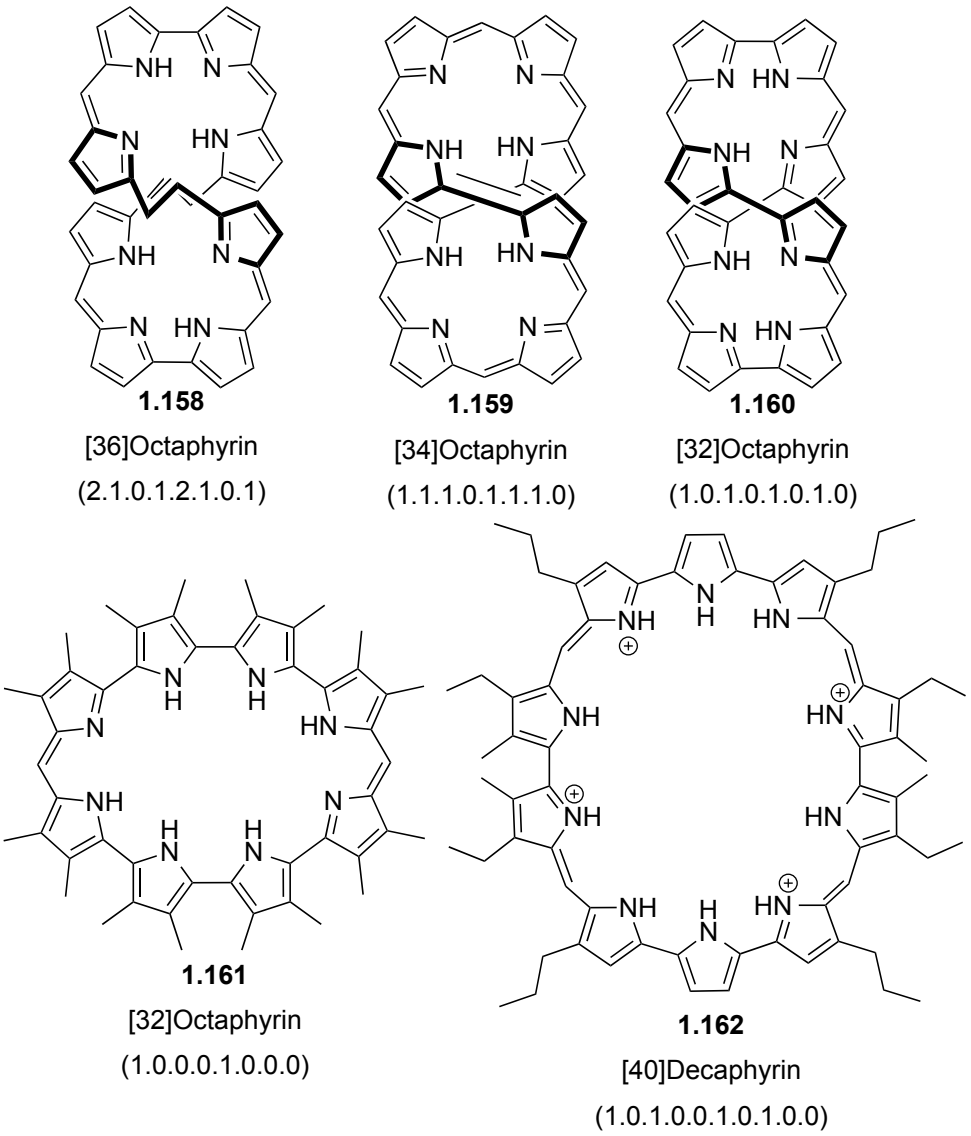

Figure 1.17: Octa- and deca-pyrrolic systems.

Compound **1.159** in spite of having 34 π aromatic pathway, revealed no diamagnetic ring current and planarity associated with aromatic character in solution and solid state. This may be interpreted as the lack of overall aromaticity arising from nonplanarity and ring size [102]. Another [32]octaphyrin(1.0.0.0.1.0.0.0) (**1.161**) was reported by Sessler *et al.* [99]. This compound was also nonaromatic and nonplanar but it does not adopt a figure eight conformation unlike other octaphyrins reported.

Expanded porphyrins having ten pyrrolic units, turcasarin **162**, named for its bright turquoise color in organic solvent, and was synthesized by Sessler and coworkers [81]. This compound **1.162** has 40 π electrons in its conjugate pathway and has the scientific name [40]decaphyrin(1.0.1.0.0.1.0.1.0.0).

In 2007 researchers also found evidences that expanded macrocycles namely cyclo[8]pyrroles **1.163-1.165** (Fig. 1.18) can also act as liquid crystals. Interestingly, this feature only occurs in two expanded porphyrin mesophases derived from imine-linked oligopyrrolic macrocycles and neither of them is aromatic.

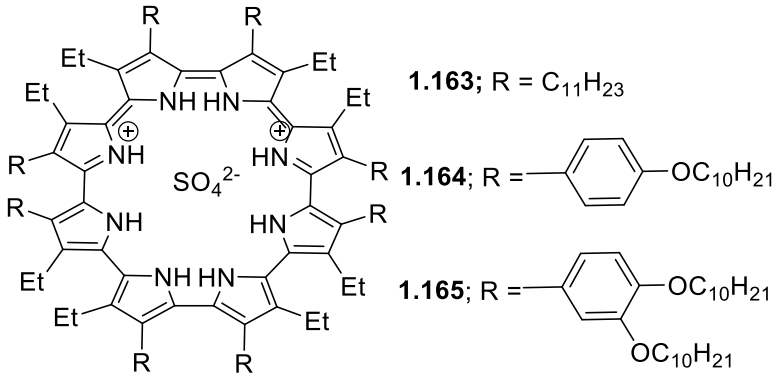

Figure 1.18: Oligopyrrolic macrocycles.

Normally, expanded porphyrin cores are very often nonplanar and highly flexible, and such characteristics are unfavorable for the formation of discotic mesophases. However, expanded porphyrins, are electron-rich aromatic species, and the use of appropriate molecular partners like electron deficient aromatic molecules allows a face-centered stacking arrangement. This approach allowed the formation of liquid crystalline mesophases based on aromatic expanded porphyrin systems.

Interestingly the use of several combinations of electron deficient acceptors (trinitrofluorenone, trinitrobenzene, trinitrophenol and trinitrotoluene) with cyclo[8]pyrrole derivatives provided the formation of hexagonal columnar mesophases (Fig. 1.19).

Figure 1.19: Cyclo[8]pyrroles hexagonal columnar mesophases.

These resulting systems are structurally interesting due the optical properties of these new mesophases. Furthermore these systems can potentially be interesting materials for molecular electronic and photovoltaic applications.

In 1999, Setsune *et al.* carried out a condensation between tetraethylbipyrrole **1.166** and 2,6-dichlorobenzaldehyde (**1.167**) under conditions of acid catalysis and in the presence of Zn^{2+} ions. They obtained a complex mixture that contained, among other products, [48]dodecaphyrin(1.0.1.0.1.0.1.0.1.0.1.0) (**1.170**) and [64]hexadecaphyrin(1.0.1.0.1.0.1.0.1.0.1.0.1.0.1.0) **1.171** (Scheme 1.33) [103].

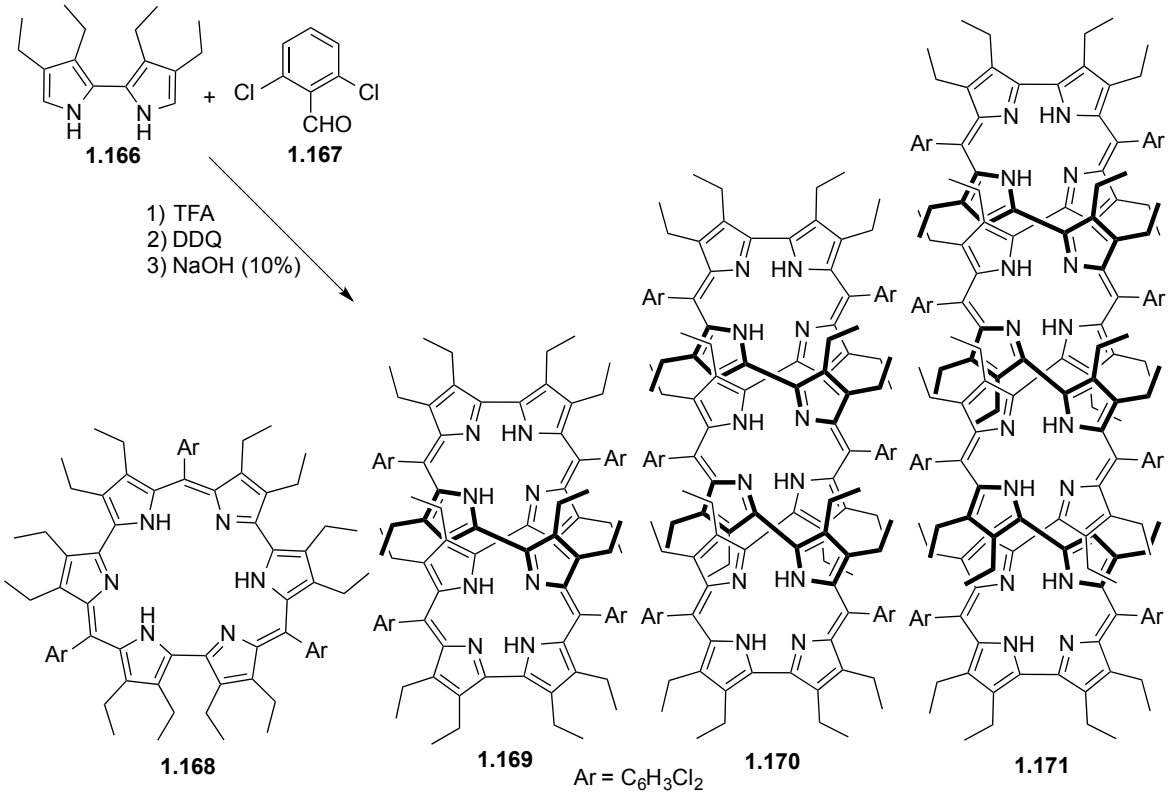

Scheme 1.33

By employing a different synthetic strategy, namely the use of a highly reactive bis(azafulvene) species, Setsune and Maeda also succeeded in preparing expanded porphyrins with up to 24 pyrrole rings [104].

This synthesis was accomplished by adding to a solution of dimethyl-2,20-bis(6-phenylazafulvenyl)methane **1.172** in CH_2Cl_2, the bipyrrole **1.173**. After oxidation with DDQ, the reaction mixture was purified by column chromatography to give isocorrole **1.174** in 27.8% yield. The higher homologues **1.175-1.179** containing 8, 12, 16, 20 and 24 pyrrole units, respectively, were separated by gel permeation chromatography in 9.5, 5.8, 3.2, 2.5 and 1.5% yield, respectively (Scheme 1.34).

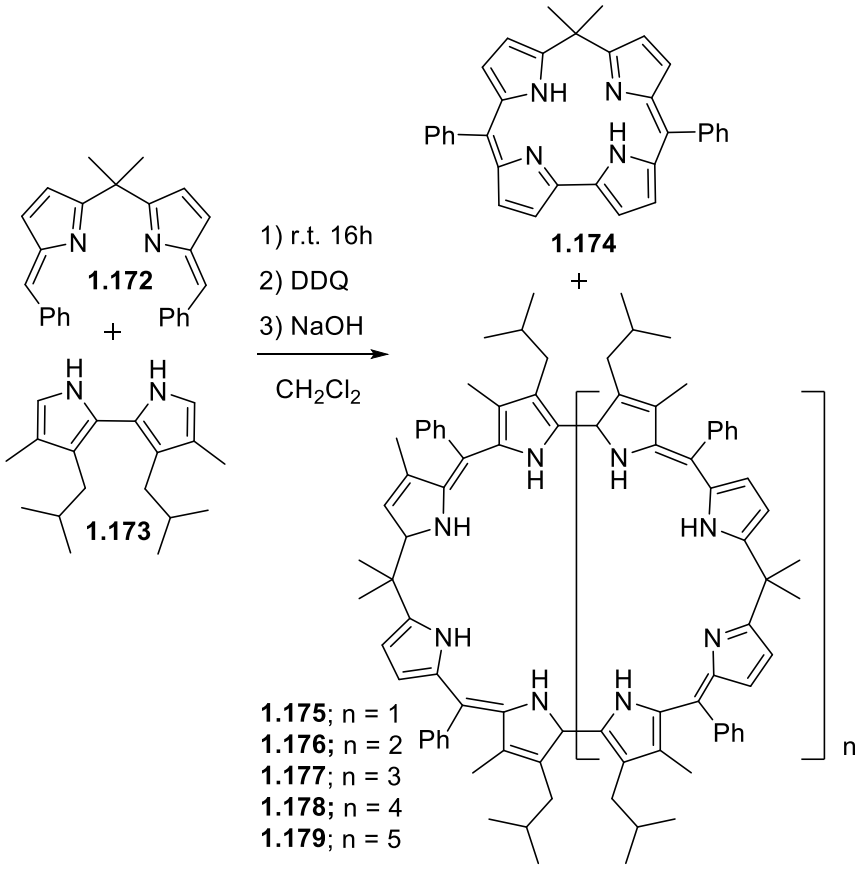

Scheme 1.34

These systems are of enormous scientific interest, not only because of their appealing structures, but also because of their nonplanar conformations that can make them chiral. They also represent the logical extension of the deca- and octapyrrolic systems with figure-eight structures and underline the fact that as larger these systems get higher is the level of conformational complexity.

1.5. Anion Binding Receptors

1.5.1. General considerations

Even though initially ignored in terms of their importance, anions are abundant in the entire world and have been nowadays associated with numerous roles. Pollutant anions, phosphate and nitrate present in fertilizers are responsible for the eutrophication of rivers and pertechnetate produced during the reprocessing of nuclear fuel and its subsequent discharge to the seas, are a matter of environmental concern [105-108].

They are also associated with numerous biochemical processes like transport, recognition and transformations at a cellular level.

For example, anions are crucial in the formation of the majority of enzyme–substrate complexes as well as in the interaction between proteins and DNA or RNA. Phosphocreatine, ATP and other high-energy anionic phosphate derivatives are at the center of important processes as biosynthesis, molecular transport, and muscle contraction. A small disturbance in these processes is associated with a variety of diseases like osteoporosis, Alzheimer's and cystic fibrosis.

More recently, attention has turned to the use of anions in templation, anion-directed self-assembly, catalysis, and ion-pair recognition [109].

The interaction of anions with porphyrins and expanded porphyrins has been thoroughly reviewed in the literature [19,110]. This field gained attention in the early 1990's with the first reports of diprotonated sapphyrins to bind halides, as well as bind and transport phosphates [56,111].

Sapphyrin is an expanded porphyrin that has a cavity equipped to host small anionic guests, when in their protonated form this feature is also observed in cyclo[8]pyrrole family,.

Porphyrins, on the other hand, because of their smaller cavity usually need to be synthetically elaborated to bind anions. An assessment of the literature involving porphyrin-based anion receptors shows a propensity for the functionalization of porphyrins to provide a source of hydrogen bond donors that allow anionic guest recognition. Urea subunits and amine moieties are particularly popular in this regard [112-114].

In fact, the supramolecular chemistry of anions by pyrrole-containing entities has been extended to structures containing a huge set of functionalizations with unusual binding abilities. Gale and coworkers have discussed these structures in several reviews [115-120]. Nevertheless despite of the efforts directed towards receptors design, strategies for receptors with high affinity and specificity for a given substrate are still rare.

This breach is due to the complexities of the weak forces involved in binding, the precise requirement of conformational factors and the numerous non-covalent interactions makes impossible to predict if a certain molecule can act or not as a receptor for a specific guest [121].

Molecular engineering of receptors requires a precise control of binding interactions, correct cavity size and solvation including other parameters. For instance, anions are larger than isoelectronic cations and therefore have a lower charge to radius ratio [109]. This means that electrostatic binding interactions are less effective than they would be for the smaller cation. Additionally, anions may be sensitive to pH values (becoming protonated at low pH, so losing their negative charge), thus receptors must function within the pH window of their target anion. Furthermore, anionic species have a wide range of geometries and therefore a higher degree of design may be required to make receptors complementary to their anionic guest.

One pathway for successful molecular design is the synthesis of pre-organized receptors that will have an energetic advantage over other flexible structures [122,123]. This makes the design of highly pre-organized and rigid receptors with accurate atomic level complementarity with the guest molecule extremely complex. Therefore, the advantages of using semi-rigid systems over rigid systems lay in the ability to adopt favorable conformations to fit the guest molecule. With this design is possible to create receptors for a specific guest molecule with simple modulation of the receptor [124].

1.5.2. Anion Transport across membranes

A cell membrane is essentially an interface analogous to that formed between two immiscible liquid phases. This has made so-called U-Tube experiments popular in the study of ion transport. A U-tube experiment consists of a hydrophobic phase flanked by two aqueous phases in which transporter assisted movement of an anion from one aqueous phase through an organic phase to another aqueous phase can be observed. This type of experiment was used by Sessler and coworkers to demonstrate the capability of sapphyrin (**1.31**) to act as an inter membrane anion transporter and as a result, demonstrate anticancer activity, in analogy with prodigiosin.

This was performed using a U-tube type aqueous I – dichloromethane – aqueous II model membrane system where sapphyrins could be used as an anion carrier of phosphate and different halides [125-127].

1.5.3. Anion extraction

Besides convenience in predicting biological activity, there are a plethora of environmental reasons for removing anions from aqueous solutions through extraction or related solvent separation processes since anionic species are also noteworthy as pollutants and toxins [128,129].

For instance, receptors that can act as sulfate anion extractants are highly desirable, as the sulfate anion is a problematic species in the eutrophication of rivers. In this regard, in 2007, a study conducted by Sessler and Moyer showed that **1.163** could mediate sulfate exchange under interfacial conditions in the presence of a phase transfer catalyst (Figure 20) [130]. The findings that **1.163** was able to extract sulfate selectively in the presence of high levels of nitrate shown that **1.163** had the ability to overcome the so-called Hofmeister bias, in this case, the inherent propensity for nitrate to partition before sulfate. While the kinetics is slow, hindering the ability for near-application, this was the first example where this level of selectivity has been observed in a sulfate *vs* nitrate extraction experiment [131].

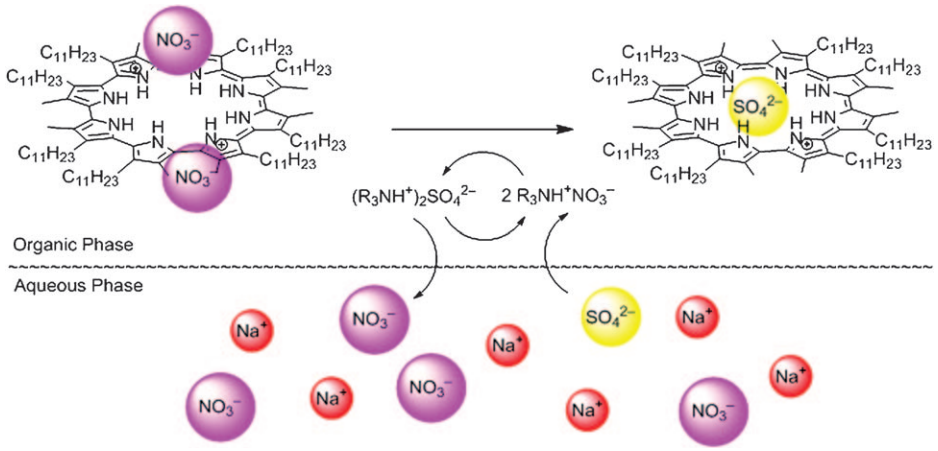

Figure 1.20: Schematic showing anion exchange and subsequent phase transfer of sulfate as induced by **1.163**.

Among other potential pollutants, the tetrahedral oxoanions, pertechnetate and perrhenate, are also especially important. Pertechnetate, TcO_4^-, the most stable form of the radioactive element technetium, is among the most hazardous of all radiation-derived contaminants, due to its long half-life and good environmental mobility [132,133].

There is consequently a strong need for receptors that can assist in the remediation of this species. Protonated forms of sapphyrins **1.73** showed to be effective in binding phosphate anions, and in the photocleavage of DNA. While these features were fully studied by sapphyrins **1.69**, **1.72,** and **1.73** (Fig. 1.10 Section 1.4.1.1), Sessler and co-workers considered also the possibility of sapphyrin **1.73** serve as a receptor for pertechnetate [134]. To test this hypothesis, binding studies were carried out in a mixture of 2.5% methanol–water at an initial pH of 7.0. Under these conditions, **1.73** exists predominantly in its mono-protonated form and was found to interact with TcO_4^- as inferred from UV-Vis spectrophotometric titrations.

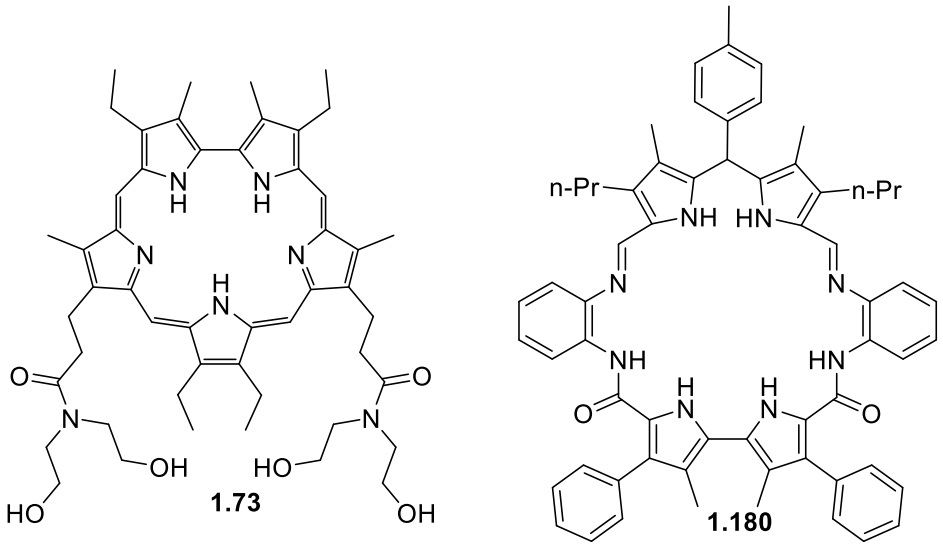

Figure 1.21: Compounds able to recognize TcO_4^-.

The spectroscopic changes seen upon the addition of the pertechnetate anion were found to differ dramatically from those induced by the addition of either pure water or dilute nitric acid. The binding profiles were consistent with a 1:1 binding mode and gave rise to a calculated $K_a = 3900\ M^{-1}$.

Another example of a pyrrole-based receptor capable of binding the pertechnetate anion was published by Katayev *et al.* [135]. This system, consisting of receptor **1.180**, is not conjugated giving a certain degree of freedom in this sensor making it capable to bind perrhenate anion in acetonitrile solution with a $K_a = 124000\ M^{-1}$.

Other strategies to achieve transport/extraction involve the use of a mechanism, in which a cation and anion are co-transported by a neutral carrier containing sites for cation and anion binding.[136,137] This is provided by easy-to-synthesize receptors, such as calix[4]pyrrole, which can also be used in liquid-liquid anion extractions [138,139].

Furthermore, immobilized calix[4]pyrroles have shown to be particularly promising as extractants of anions and ion pairs from aqueous to organic solution [140-142].

1.5.4. Anion Sensing

Supramolecular chemistry has always been associated with possible applications. With the aim of advancing chemical sensor technology, considerable attention has also been focused on the design of receptors with the ability to selectively bind and sense the anion recognition event through a macroscopic electrochemical or optical response.

1.5.4.1. Electrochemical Sensors

Three major strategies can be applied to the electrochemical detection of receptor–anion complexes. The first is the extraction of a charged guest into a membrane by a non electroactive host and detection of the resulting membrane potential (ion-selective electrodes (ISEs), chemically modified field-effect transistors (CHEMFETs), potentiometric sensors). The second is the detection of a current/potential perturbation of the properties of a redox-active host on complex formation (voltammetric/amperometric sensors) and finally the third strategy comprises the production of a chemically modified electrode (CME) consisting of a redox-active matrix and an anion-selective binding site.

Amongst these strategies, the first was widely experimented in expanded porphyrin chemistry. Umezawa and Sessler studied the potentiometric response of membranes using expanded porphyrins towards carboxylate and inorganic anions. The expanded porphyrins used in these studies included saphyrin **1.31**, triphenylrosarin **1.118** and rubyrin **1.107** (Figure 1.22).

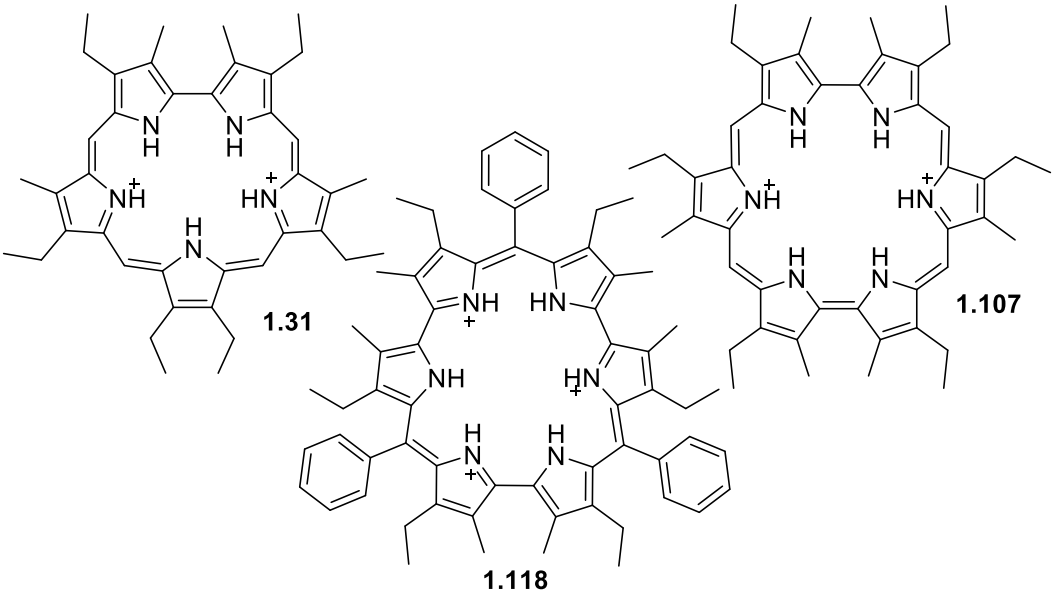

Figure 1.22: Expanded porphyrins incorporated in PVC membranes.

The prepared PVC membranes containing the expanded porphyrins **1.31**, **1.118** and **1.107** were subjected to pH titrations with and without a guest anion in the sample solution showed that protonation of the expanded porphyrins at the surface of the electrode membrane was a prerequisite for accommodating the guest anions and yielding their potential responses. The electrodes strongly responded to benzoates, but rather less to inorganic anions and saturated aliphatic organic carboxylates. The selectivity sequences for the sapphyrin based electrode were found bind preferably fluoride over chloride and bromide [143,144]. The same kind of electrodes have been developed with a different set of macrocyclic compounds, in this regard calix[4]pyrroles where Kral *et al.* were also able to recognize several inorganic anions al low pH [145].

Until now the use of redox active species coupled with expanded porphyrins for anion binding is yet to be developed, nevertheless it is possible to find in the literature several other compounds, which have, been widely studied in this regard [146-148].

1.5.4.2. Optical Sensors

The high sensitivity of spectrometric techniques for sensing target guest species has stimulated an enormous amount of interest in the covalent attachment of organic and inorganic luminophores or the use of the target guest intrinsic photochemical properties in recognition of different anions.

Examples of anion-responsive systems have combined a wide range of fluorophores with calixpyrroles and the use of expanded porphyrins chemistry characteristics for anion recognition [149-151].

In fact, this area is probably the most developed and the one where it is possible to find more published examples of anion recognition in the literature.

For instance, water-soluble derivatives of sapphyrin appeared as a fluorescent sensor for phosphate in 2003 (fig 1.23)[152].

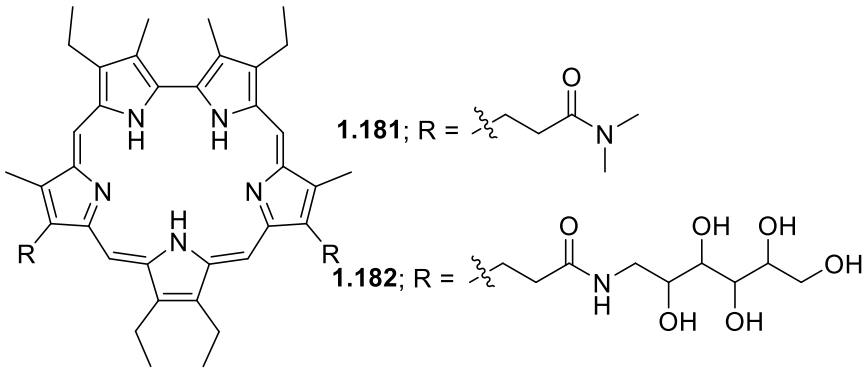

Figure 1.23: Fluorescent sensor for phosphate based on sapphyrins.

This phosphate-sensing ability was based on a fluorescence quenching effect caused by the inherent 'aggregation' of sapphyrins. Upon phosphate binding, sapphyrin deaggregates, thus resulting in a higher concentration of the monomeric form, which is significantly fluorescent.

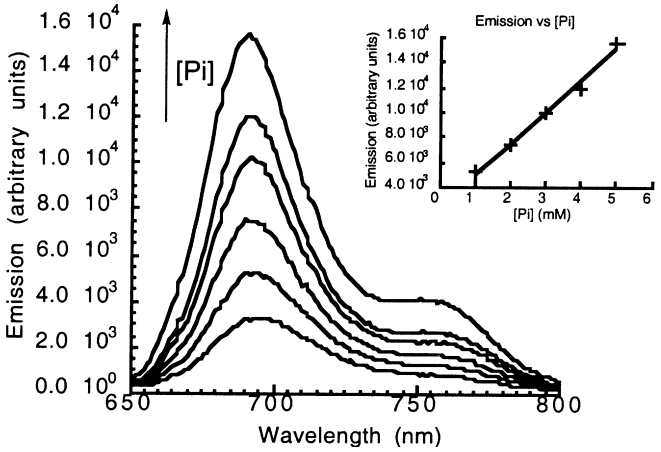

Figure 1.24: Increase in fuorescence intensity seen when sapphyrin **1.182** is titrated with increasing quantities of phosohate in water at pH 7.0 ($\lambda_{excit.}$ = 450 nm). The inset shows a plot of the emission intensity vs. [Phosphate].

The underlying aggregation effect was studied through addition of sodium dodecyl sulfate, a well-known surfactant (fig 1.24). At high concentrations of sapphyrin, the UV-Vis spectra displayed a Soret band at around 410 nm that was attributed to higher order aggregates. Upon addition of sodium dodecyl sulfate, these higher aggregates break into dimers, which are characterized by a red-shifted Soret band at 420 nm. Further addition of sodium dodecyl sulfate results in a Soret band at 450 nm, characteristic of the monomeric species.

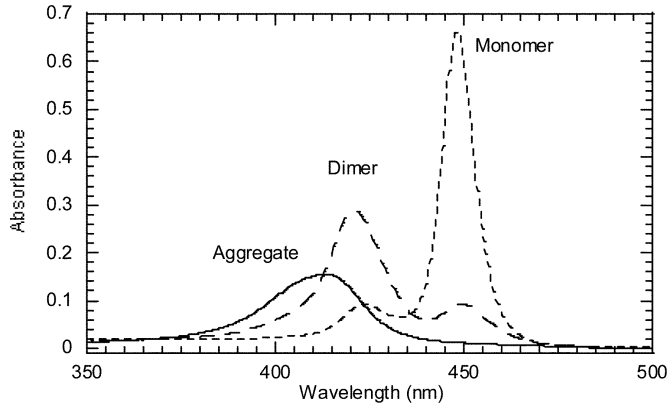

Figure 1.25: Absorbance spectra of sapphyrin **1.181** as recorded in 10 mM PIPES buffer (pH 7.0) in the presence of 0, 0.1, and 10 mM sodium dodecyl sulfate (SDS). These spectra are ascribed to the presence of three different prominent aggregations states, monomer, dimer, and "aggregate"

Other examples making use of cyclo[8]pyrroles (**1.163**), rubyrins (**1.107**), triphenyl rosarins (**1.118**), and smadagirins (**1.64**) are also able to bind different inorganic anions in solution and were all verified by spectrophotometric techniques and in the solid state [149,153].

1.5.4.2.1. Optical Sensors: Colorimetric Sensors

Nowadays, the development of colorimetric anion sensing is particularly challenging since visual detection can give immediate qualitative information and is becoming increasingly appreciated in terms of quantitative analysis.

One approach to reach an effective colorimetric anion sensor consists of two parts. One part is an anion-binding site employing various combinations of anion receptor units and the other is the chromophore part, which converts the binding events or recognition phenomena to optical signals Fig 1.26 [154,155].

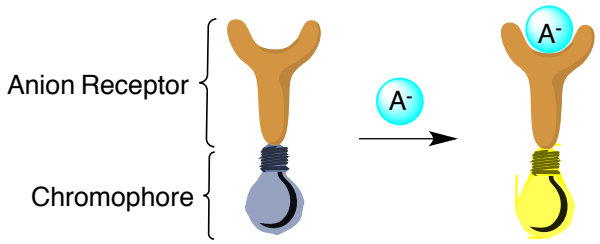

Figure 1.26: Principle for the construction of colorimetric anion binding systems.

While in the previous section is possible to find several example of expanded porphyrins for sensing anions through spectrophotometric detection, the colorimetric aspects of sensing are only developed in expanded calix[n]pyrroles which are the non-aromatic congeners of expanded porphyrins [150,156,157].

In fact, in this particular area Sessler and coworkers developed a series of acyclic (**1.183)** and cyclic dipyrrylquinoxalines (**1.184**) in which the presence of both the NH donor functionality and a built-in quinoxaline chromophore, led the authors to mononitor these derivatives in the detection of fluoride anions. These compounds showed a dramatically color change when in the presence of fluoride anions while there was no response to other halogen anions. Following the same principles Panda and coworkers, recently synthesized a series of expanded calix[4]pyrroles by Mcmurray coupling of diformylated dipyrromethanes. In this series **1.185** displayed colorimetric sensing of fluoride ion in polar aprotic solvents as it's possible to note in figure 1.27.

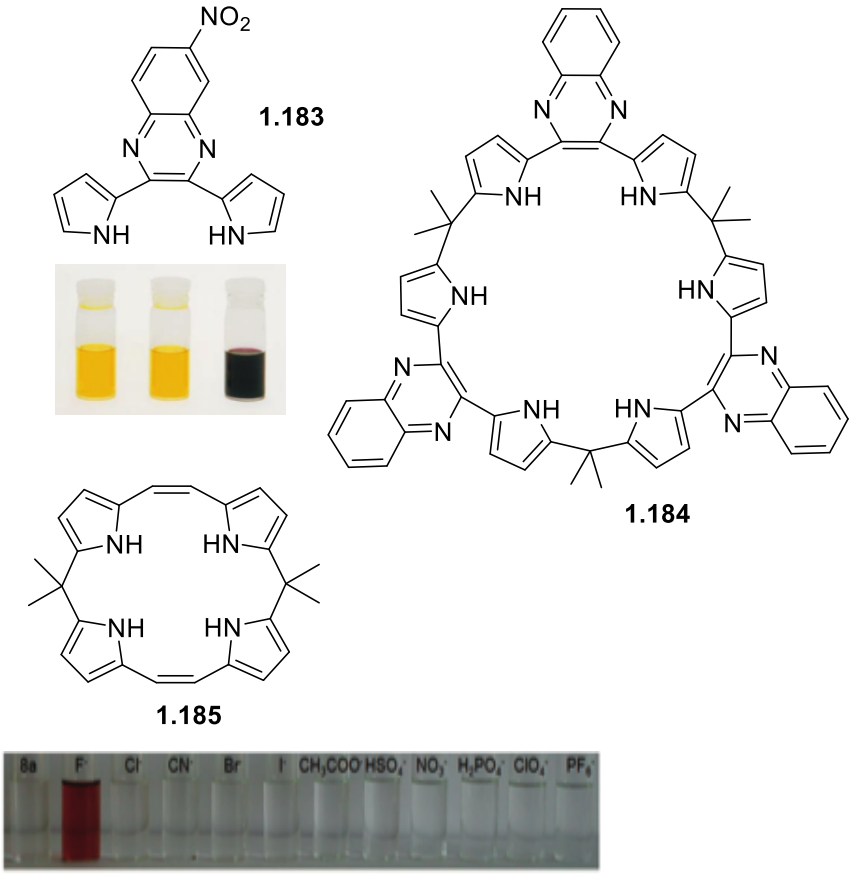

Figure 1.27: Expanded colorimetric macrocycles and their colour change upon addition of fluoride anions.

Many other entities with colorimetric capabilities in the detection of anions can be found and has already been been a subject of several interesting reviews [155].

1.6. Aims of this thesis

Expanded porphyrins are a theme of relevant research years and has become the subject of study for many researchers. The interest in these systems lies in their potential applications in various fields including anion recognition, photodynamic therapy (PDT), MRI contrast agents, near infrared dyes, and two photon absorption materials (TPA), due to their extended π conjugation and increased cavity size [158, 159].

Therefore, the global goal of this project comprises the development of new targeted expanded porphyrins, mainly for anion recognition, biomedical and catalysis applications. From a chemical standpoint, the new expanded porphyrins will be used as chemosensors, based on their previous reports that show high binding specificity for

certain anion species. The most suitable new molecules will be also explored as ligands for new catalysts and as photosensitizes, for new cancer photodynamic therapy or/and on photodynamic inactivation of microorganisms agents.

The introduction of adequate motifs and "bio"compatible units on their periphery can be useful in directing these motifs towards specific applications, such as anion recognition, drug administration and transport through the organism and across the cell membranes, and as ligand for catalytic active metals. For this, the main photo -physical, -chemical and biological studies of these new molecules were planned. To achieve this main goal, the present PhD work was divided in tree specific aims being the overall goals the synthesis and anion studies of these new compounds, as stated below:

Specific Aim 1- Develop robust precursors that enable rapid development of new compounds based on expanded porphyrins. For that Vilsmeier, Knovenagel, Diels-Alder reactions and others were carried out on adequate precursors (Fig. 1.28). From these studies first impressions using these motifs in anion binding interactions allow the rapid development of simple compounds with chromogenic characteristics.

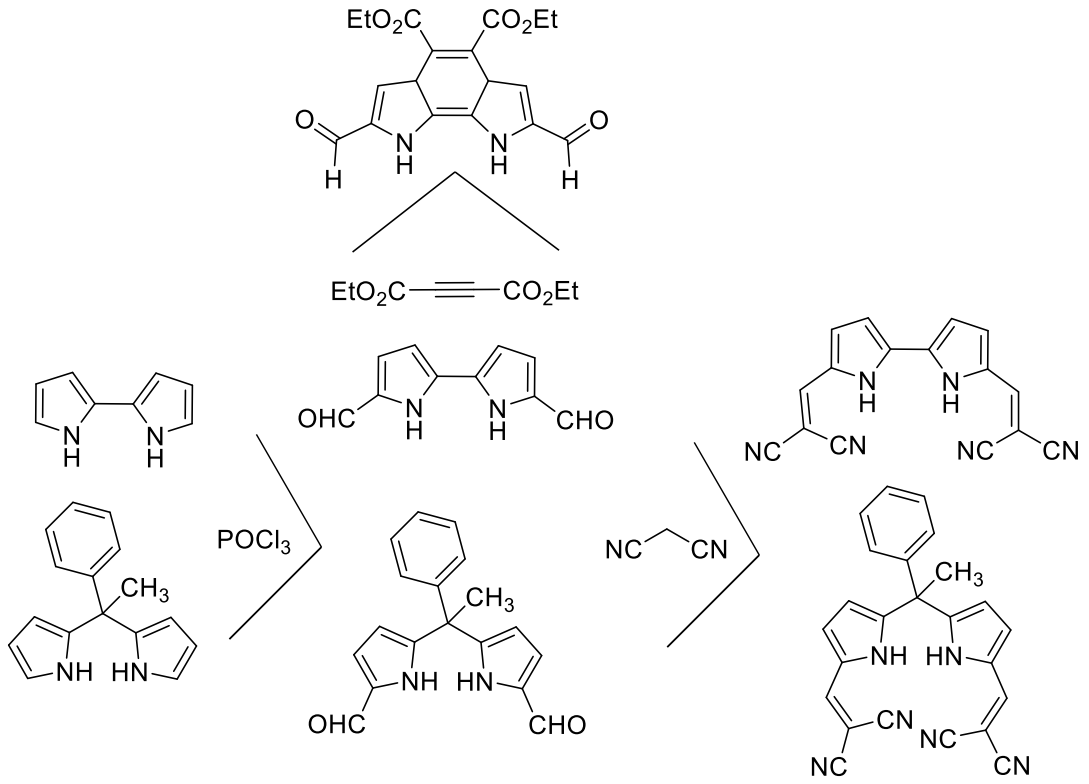

Figure 1.28: Example of possible target precursors

Specific Aim 2- Synthesis and characterization of new pentaphyrins and hexaphyrins. Again based on the literature and to our previous results, we expect that these new porphyrinoids, having a larger macrocycle, and adequate motifs will show higher and probably strong supramolecular interactions with anions in different media (Fig. 1.29) and with multiple pyridyl and pyridinium groups eventually useful for molecular frameworks building blocks and as cationic photosensitizes for PDI (Figure 1.30).

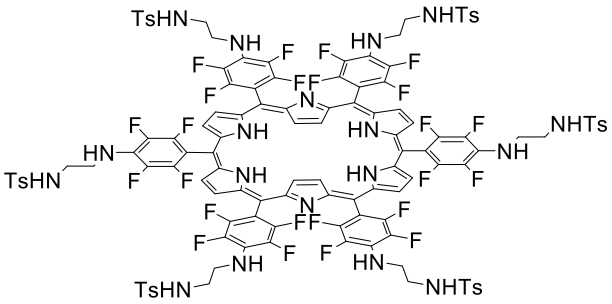

Figure 1.29: Example of possible target anion chemosensor structures

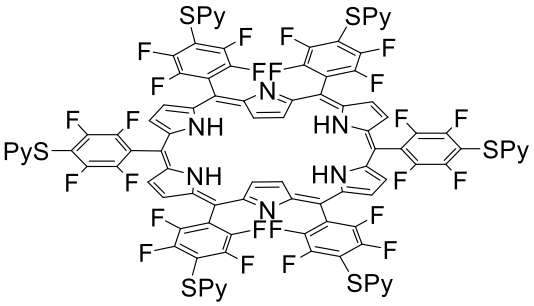

Figure 1.30: Example of possible multipyridyl and cationic compounds

Specific Aim 3 – study the anion binding properties of all new chemosensors and prepared sensors (Figure 1.31). The anion binding properties of the new compounds/materials will be investigated in order to screen the best hosts and determine if they are advantageous compared to present technologies. UV-visible absorbance and NMR will be the main study methodologies. These preliminary studies, will guide the synthesis and the selection of the most effective host systems.

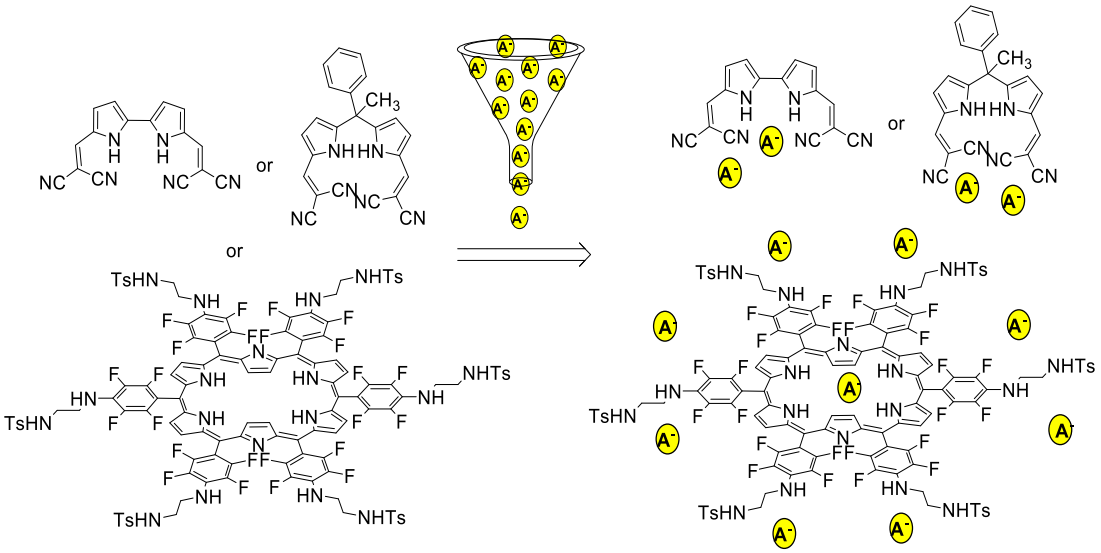

Figure 1.31: Example of target chemosensors

1.7. References

1. Kadish KM, Smith KM and Guilard R. *The Porphyrin Handbook*; Academic Press, 2000

2. Sessler JL. *J. Porphyrins Phthalocyanines* 2000; **4**: 331-336.

3. Montforts FP, Gerlach B and Hoper F. *Chem. Rev.* 1994; **94**: 327-347.

4. Chmielewski PJ and Latos-Grazynski L. *Coord. Chem. Rev.* 2005; **249**: 2510-2533.

5. Furuta H, Ishizuka T, Osuka A and Ogawa T. *J. Am. Chem. Soc.* 1999; **121**: 2945-2946.

6. Pacholska-Dudziak E, Skonieczny J, Pawlicki M, Szterenberg L, Ciunik Z and Latos-Graynski L. *J. Am. Chem. Soc.* 2008; **130**: 6182-6195.

7. Pawlicki M and Latos-Grazynski L. *Chem. Rec.* 2006; **6**: 64-78.

8. Furuta H, Asano T and Ogawa T. *J. Am. Chem. Soc.* 1994; **116**: 767-768.

9. Furuta H, Maeda H and Osuka A. *Chem. Commun.* 2002: 1795-1804.

10. Harvey JD and Ziegler CJ. *Coord. Chem. Rev.* 2003; **247**: 1-19.

11. Johnson AW and Price R. *J. Chem. Soc.* 1960: 1649-1653.

12. Ghosh A, Wondimagegn T and Parusel ABJ. *J. Am. Chem. Soc.* 2000; **122**: 5100-5104.

13. Gross Z, Simkhovich L and Galili N. *Chem. Commun.* 1999: 599-600.

14. Sessler JL and Tomat E. *Acc. Chem. Res.* 2007; **40**: 371-379.

15. Jasat A and Dolphin D. *Chem. Rev.* 1997; **97**: 2267-2340.

16. Sessler JL, Hemmi G, Mody TD, Murai T, Burrell A and Young SW. *Acc. Chem. Res.* 1994; **27**: 43-50.

17. Sessler JL and Miller RA. *Biochem. Pharmacol.* 2000; **59**: 733-739.

18. Iverson BL, Thomas RE, Kral V and Sessler JL. *J. Am. Chem. Soc.* 1994; **116**: 2663-2664.

19. Sessler JL and Davis JM. *Acc. Chem. Res.* 2001; **34**: 989-997.

20. Bauer VJ, Clive DLJ, Dolphin D, Paine JB, Harris FL, King MM, Loder J, Wang SWC and Woodward RB. *J. Am. Chem. Soc.* 1983; **105**: 6429-6436.

21. Broadhurst Mj, Johnson AW and Grigg R. *J. Chem. Soc., Perkin Trans. 1* 1972: 2111-2116.

22. Sessler JL, Cyr MJ, Lynch V, Mcghee E and Ibers JA. *J. Am. Chem. Soc.* 1990; **112**: 2810-2813.

23. Sessler JL, Johnson MR, Creager SE, Fettinger JC and Ibers JA. *J. Am. Chem. Soc.* 1990; **112**: 9310-9329.

24. Barton DHR, Crich D, Lobberding A and Zard SZ. *J. Chem. Soc., Chem. Commun.* 1985: 646-647.

25. Sessler JL and Seidel D. *Angew. Chem. Int. Ed.* 2003; **42**: 5134-5175.

26. Sessler JL and Tomat E. *Acc. Chem. Res.* 2007; **40**: 371-379.

27. Sessler JL, Camiolo S and Gale PA. *Coord. Chem. Rev.* 2003; **240**: 17-55.

28. Plitt P, Gross DE, Lynch VM and Sessler JL. *Chem. Eur. J.* 2007; **13**: 1374-1381.

29. Nadeau JA and Swager TA. *Tetrahedron* 2004; **60**: 7141-7146.

30. Stepien M, Donnio B and Sessler JL. *Angew. Chem. Int. Ed.* 2007; **46**: 1431-1435.

31. Yoon ZS, Kwon JH, Yoon MC, Koh MK, Noh SB, Sessler JL, Lee JT, Seidel D, Aguilar A, Shimizu S, Suzuki M, Osuka A and Kim D. *J. Am. Chem. Soc.* 2006; **128**: 14128-14134.

32. Rath H, Sankar J, PrabhuRaja V, Chandrashekar TK, Nag A and Goswami D. *J. Am. Chem. Soc.* 2005; **127**: 11608-11609.

33. Rapoport H and Castagno.N. *J. Am. Chem. Soc.* 1962; **84**: 2178-2181.

34. Rapoport H and Holden KG. *J. Am. Chem. Soc.* 1962; **84**: 635-642.

35. Rapoport H, Castagno.N and Holden KG. *J. Org. Chem.* 1964; **29**: 883-885.

36. Merrill BA and Legoff E. *Abstr. Pap. Am. Chem. S.* 1989; **197**: 261-264.

37. Merrill BA and Legoff E. *J. Org. Chem.* 1990; **55**: 2904-2908.

38. Shiner CM and Lash TD. *Tetrahedron* 2005; **61**: 11628-11640.

39. Minetto G, Raveglia LF and Taddei M. *Org. Lett.* 2004; **6**: 389-392.

40. Banik BK, Samajdar S and Banik I. *J. Org. Chem.* 2004; **69**: 213-216.

41. Bashiardes G, Safir I, Barbot F and Laduranty J. *Tetrahedron Lett.* 2004; **45**: 1567-1570.

42. Arrieta A, Otaegui D, Zubia A, Cossio FP, Diaz-Ortiz A, de la Hoz A, Herrero MA, Prieto P, Foces-Foces C, Pizarro JL and Arriortua MI. *J. Org. Chem.* 2007; **72**: 4313-4322.

43. Bergner I and Opatz T. *J. Org. Chem.* 2007; **72**: 7083-7090.

44. Balme G. *Angew. Chem. Int. Ed.* 2004; **43**: 6238-6241.

45. Sessler JL, Aguilar A, Sanchez-Garcia D, Seidel D, Kohler T, Arp F and Lynch VM. *Org. Lett.* 2005; **7**: 1887-1890.

46. Sessler JL, Seidel D, Vivian AE, Lynch V, Scott BL and Keogh DW. *Angew. Chem. Int. Ed.* 2001; **40**: 591-594.

47. Kohler T, Seidel D, Lynch V, Arp FO, Ou ZP, Kadish KM and Sessler JL. *J. Am. Chem. Soc.* 2003; **125**: 6872-6873.

48. Misra R and Chandrashekar TK. *Acc. Chem. Res.* 2008; **41**: 265-279.

49. Heo PY, Shin K and Lee CH. *Tetrahedron Lett.* 1996; **37**: 197-200.

50. Sessler JL, Cyr M, Furuta H, Kral V, Mody T, Morishima T, Shionoya M and Weghorn S. *Pure Appl. Chem.* 1993; **65**: 393-398.

51. Rexhausen H and Gossauer A. *Chem. Commun.* 1983: 275-275.

52. Sessler JL, Davis JM and Lynch V. *J. Org. Chem.* 1998; **63**: 7062-7065.

53. Weghorn SJ, Lynch V and Sessler JL. *Tetrahedron Lett.* 1995; **36**: 4713-4716.

54. Sessler JL, Eller LR, Cho WS, Nicolaou S, Aguilar A, Lee JT, Lynch VM and Magda DJ. *Angew. Chem. Int. Ed.* 2005; **44**: 5989-5992.

55. Roitman L, Ehrenberg B, Nitzan Y, Kral V and Sessler JL. *Photochem. Photobiol.* 1994; **60**: 421-426.

56. Shionoya M, Furuta H, Lynch V, Harriman A and Sessler JL. *J. Am. Chem. Soc.* 1992; **114**: 5714-5722.

57. Kral V, Andrievsky A and Sessler JL. *J. Am. Chem. Soc.* 1995; **117**: 2953-2954.

58. Sessler JL, Andrievsky A, Kral V and Lynch V. *J. Am. Chem. Soc.* 1997; **119**: 9385-9392.

59. Springs SL, Gosztola D, Wasielewski MR, Kral V, Andrievsky A and Sessler JL. *J. Am. Chem. Soc.* 1999; **121**: 2281-2289.

60. Magda D, Wright M, Miller RA, Sessler JL and Sansom PI. *J. Am. Chem. Soc.* 1995; **117**: 3629-3630.

61. Sessler JL, Sansom PI, Kral V, OConnor D and Iverson BL. *J. Am. Chem. Soc.* 1996; **118**: 12322-12330.

62. Iverson BL, Shreder K, Kral V, Smith DA, Smith J and Sessler JL. *Pure Appl. Chem.* 1994; **66**: 845-850.

63. Kral V, Brucker EA, Hemmi G, Sessler JL, Kralova J and Bose H. *Bioorg. Med. Chem.* 1995; **3**: 573-578.

64. Sessler JL, Johnson MR and Lynch V. *J. Org. Chem.* 1987; **52**: 4394-4397.

65. Naumovski L, Sirisawad M, Lecane P, Chen J, Ramos J, Wang Z, Cortez C, Magda D, Thiemann P, Boswell G, Miles D, Cho DG, Sessler JL and Miller R. *Mol. Cancer Ther.* 2006; **5**: 2798-2805.

66. Wang Z, Lecane PS, Thiemann P, Fan Q, Cortez C, Ma X, Tonev D, Miles D, Naumovski L, Miller RA, Magda D, Cho DG, Sessler JL, Pike BL, Yeligar SM, Karaman MW and Hacia JG. *Molecular Cancer* 2007; **6**: 1-12.

67. Zhang ZJ, Ferrence GM and Lash TD. *Org. Lett.* 2009; **11**: 1249-1252.

68. Narayanan SJ, Sridevi B, Chandrashekar TK, Vij A and Roy R. *J. Am. Chem. Soc.* 1999; **121**: 9053-9068.

69. Misra R and Chandrashekar TK. *Acc. Chem. Res.* 2008; **41**: 265-279.

70. Parmeswaran D, Pushpan SK, Srinivasan A, Kumar MR, Chandrashekar TK and Ganesan S. *Photochem. Photobiol.* 2003; **78**: 487-495.

71. Pushpan SK, Venkatraman S, Anand VG, Sankar J, Parmeswaran D, Ganesan S and Chandrashekar TK. *Curr. Med. Chem.* 2002; **2**: 187-207.

72. Sessler JL, Cho DG, Stepien M, Lynch V, Waluk J, Yoon ZS and Kim D. *J. Am. Chem. Soc.* 2006; **128**: 12640-12641.

73. Shin JY, Furuta H and Osuka A. *Angew. Chem. Int. Ed.* 2001; **40**: 619-621.

74. Srinivasan A, Ishizuka T and Furuta H. *Angew. Chem. Int. Ed.* 2004; **43**: 876-879.

75. Mori S, Shin JY, Shimizu S, Ishikawa F, Furuta H and Osuka A. *Chem. Eur. J.* 2005; **11**: 2417-2425.

76. Shimizu S and Osuka A. *Eur. J. Inorg. Chem.* 2006: 1319-1335.

77. Sessler JL, Morishima T and Lynch V. *Angew. Chem. Int. Ed.* 1991; **30**: 977-980.

78. Sessler JL, Morishima T and Lynch V. *Abstr. Pap. Am. Chem. S.* 1991; **202**: 58-59.

79. Sessler JL and Burrell AK. *Top. Curr. Chem.* 1992; **161**: 177-273.

80. Sessler JL, Seidel D, Bucher C and Lynch V. *Chem. Commun.* 2000: 1473-1474.

81. Sessler JL, Gebauer A and Weghorn SJ. *The Porphyrin Handbook*; Kadish KM, Smith KM, Guilard R ed.; Academic Press: San Diego, CA, 1999; Vol. 2, 55–124

82. Sessler JL, Weghorn SJ, Morishima T, Rosingana M, Lynch V and Lee V. *J. Am. Chem. Soc.* 1992; **114**: 8306-8307.

83. Sessler JL, Vivian AE, Seidel D, Burrell AK, Hoehner M, Mody TD, Gebauer A, Weghorn SJ and Lynch V. *Coord. Chem. Rev.* 2001; **216**: 411-434.

84. Weghorn SJ, Sessler JL, Lynch V, Baumann TF and Sibert JW. *Inorg. Chem.* 1996; **35**: 1089.

85. Sessler JL, Weghorn SJ, Hiseada Y and Lynch V. *Chem. Eur. J.* 1995; **1**: 56-67.

86. Sessler JL, Vivian AE, Seidel D, Burrell AK, Hoehner M, Mody TD, Gebauer A, Weghorn SJ and Lynch V. *Coordin Chem Rev* 2001; **216**: 411-434.

87. Shimizu S, Cho WS, Sessler JL, Shinokubo H and Osuka A. *Chem. Eur. J.* 2008; **14**: 2668-2678.

88. Neves MGPMS, Martins RM, Tome AC, Silvestre AJD, Silva AMS, Felix V, Drew MGB and Cavaleiro JAS. *Chem. Commun.* 1999: 385-386.

89. Shin JY, Furuta H, Yoza K, Igarashi S and Osuka A. *J. Am. Chem. Soc.* 2001; **123**: 7190-7191.

90. Zhu XJ, Fu ST, Wong WK and Wong WY. *Tetrahedron Lett.* 2008; **49**: 1843-1846.

91. Krivokapic A and Anderson HL. *Org. Biomol. Chem.* 2003; **1**: 3639-3641.

92. Shimizu S, Shin JY, Furuta H, Ismael R and Osuka A. *Angew. Chem. Int. Ed.* 2003; **42**: 78-82.

93. Stepien M, Sprutta N and Latos-Grazynski L. *Angew. Chem. Int. Ed.* 2011; **50**: 4288-4340.

94. Saito S and Osuka A. *Angew. Chem. Int. Ed.* 2011; **50**: 4342-4373.

95. Suzuki M, Taniguchi R and Osuka A. *Chem. Commun.* 2004: 2682-2683.

96. Srinivasan A, Ishizuka T, Osuka A and Furuta H. *J. Am. Chem. Soc.* 2003; **125**: 878-879.

97. Suzuki M, Yoon MC, Kim DY, Kwon JH, Furuta H, Kim D and Osuka A. *Chemistry-a European Journal* 2006; **12**: 1754-1759.

98. Anand VRG, Pushpan SK, Srinivasan A, Narayanan SJ, Sridevi B, Chandrashekar TK, Roy R and Joshi BS. *Org. Lett.* 2000; **2**: 3829-3832.

99. Sessler JL, Seidel D and Lynch V. *J. Am. Chem. Soc.* 1999; **121**: 11257-11258.

100. Bucher C, Seidel D, Lynch V and Sessler JL. *Chem. Commun.* 2002: 328-329.

101. Vogel E, Broring M, Fink J, Rosen D, Schmickler H, Lex J, Chan KWK, Wu YD, Plattner DA, Nendel M and Houk KN. *Angew. Chem. Int. Ed.* 1995; **34**: 2511-2514.

102. Vogel E, Broring M, Fink J, Rosen D, Schmickler H, Lex J, Chan KWK, Wu YD, Plattner DA, Nendel M and Houk KN. *Angew. Chem. Int. Ed.* 1995; **34**: 2511-2514.

103. Setsune J, Katakami Y and Iizuna N. *J. Am. Chem. Soc.* 1999; **121**: 8957-8958.

104. Setsune J, Tsukajima A and Watanabe J. *Tetrahedron Lett.* 2006; **47**: 1817-1820.

105. McKee V, Nelson J and Town RM. *Angew. Chem. Int. Ed.* 2003; **32**: 309-325.

106. Glidewell C. *Chem. Br.* 1990; **26**: 137-140.

107. Moss B. *Chem Ind-London* 1996: 407-411.

108. Katayev EA, Kolesnikov GV and Sessler JL. *Angew. Chem. Int. Ed.* 2009; **38**: 1572-1586.

109. Beer PD and Gale PA. *Angew. Chem. Int. Ed.* 2001; **40**: 486-516.

110. Sessler JL, Camiolo S and Gale PA. *Coord. Chem. Rev.* 2003; **240**: 17-55.

111. Furuta H, Cyr MJ and Sessler JL. *J. Am. Chem. Soc.* 1991; **113**: 6677-6678.

112. Jagessar RC, Shang MY, Scheidt WR and Burns DH. *J. Am. Chem. Soc.* 1998; **120**: 11684-11692.

113. Calderon-Kawasaki K, Kularatne S, Li YH, Noll BC, Scheidt WR and Burns DH. *J. Org. Chem.* 2007; **72**: 9081-9087.

114. Rodrigues JMM, Farinha ASF, Muteto PV, Woranovicz-Barreira SM, Paz FAA, Neves MGPMS, Cavaleiro JAS, Tome AC, Gomes MTSR, Sessler JL and Tome JPC. *Chem. Commun.* 2014; **50**: 1359-1361.

115. Gale PA. *Coord. Chem. Rev.* 2001; **213**: 79-128.

116. Caltagirone C and Gale PA. *Chem. Soc. Rev.* 2009; **38**: 520-563.

117. Gale PA. *Chem. Soc. Rev.* 2010; **39**: 3746-3771.

118. Wenzel M, Hiscock JR and Gale PA. *Chem. Soc. Rev.* 2012; **41**: 480-520.

119. Gale PA, Busschaert N, Haynes CJE, Karagiannidis LE and Kirby IL. *Angew. Chem. Int. Ed.* 2014; **43**: 205-241.

120. Gale PA. *Chem. Commun.* 2011; **47**: 82-86.

121. Haridas V, Sahu S and Venugopalan P. *Tetrahedron* 2011; **67**: 727-733.

122. Bisson AP, Lynch VM, Monahan MKC and Anslyn EV. *Angew. Chem. Int. Ed.* 1997; **36**: 2340-2342.

123. Lee S, Hua YR, Park H and Flood AH. *Org. Lett.* 2010; **12**: 2100-2102.

124. Lee CH, Na HK, Yoon DW, Won DH, Cho WS, Lynch VM, Shevchuk SV and Sessler JL. *J. Am. Chem. Soc.* 2003; **125**: 7301-7306.

125. Sessler JL, Ford DA, Cyr MJ and Furuta H. *Chem. Commun.* 1991: 1733-1735.

126. Kral V, Andrievsky A and Sessler JL. *Chem. Commun.* 1995: 2349-2351.

127. Kral V and Sessler JL. *Tetrahedron* 1995; **51**: 539-554.

128. Stephan H, Gloe K, Schiessl P and Schmidtchen FP. *Supramol. Chem.* 1995; **5**: 273-280.

129. Katayev EA, Ustynyuk YA and Sessler JL. *Coord. Chem. Rev.* 2006; **250**: 3004-3037.

130. Eller LR, Stepien M, Fowler CJ, Lee JT, Sessler JL and Moyer BA. *J. Am. Chem. Soc.* 2007; **129**: 11020.

131. Rambo BM and Sessler JL. *Chem. Eur. J.* 2011; **17**: 4946-4959.

132. Yoshihara K. *Top. Curr. Chem.* 1996; **176**: 17-35.

133. Icenhower JP, Qafoku NP, Zachara JM and Martin WJ. *Am. J. Sci.* 2010; **310**: 721-752.

134. Gorden AEV, Davis J, Sessler JL, Kral V, Keogh DW and Schroeder NL. *Supramol. Chem.* 2004; **16**: 91-100.

135. Katayev EA, Boev NV, Khrustalev VN, Ustynyuk YA, Tananaev IG and Sessler JL. *J. Org. Chem.* 2007; **72**: 2886-2896.

136. Chrisstoffels LAJ, de Jong F, Reinhoudt DN, Sivelli S, Gazzola L, Casnati A and Ungaro R. *J. Am. Chem. Soc.* 1999; **121**: 10142-10151.

137. Santos SM, Costa PJ, Lankshear MD, Beer PD and Felix V. *J. Phys. Chem. B* 2010; **114**: 11173-11180.

138. Levitskaia TG, Marquez M, Sessler JL, Shriver JA, Vercouter T and Moyer BA. *Chem. Commun.* 2003: 2248-2249.

139. Fowler CJ, Haverlock TJ, Moyer BA, Shriver JA, Gross DE, Marquez M, Sessler JL, Hossain MA and Bowman-James K. *J. Am. Chem. Soc.* 2008; **130**: 14386.

140. Aydogan A, Coady DJ, Lynch VM, Akar A, Marquez M, Bielawski CW and Sessler JL. *Chem. Commun.* 2008: 1455-1457.

141. Zyryanov GV, Kinstle TH and Anzenbacher P. *Synlett* 2008: 1171-1174.

142. Aydogan A, Coady DJ, Kim SK, Akar A, Bielawski CW, Marquez M and Sessler JL. *Angew. Chem. Int. Ed.* 2008; **47**: 9648-9652.

143. Lin XM, Umezawa K, Tohda K, Furuta H, Sessler JL and Umezawa Y. *Anal. Sci.* 1998; **14**: 99-108.

144. Umezawa K, Tohda K, Lin XM, Sessler JL and Umezawa Y. *Anal. Chim. Acta* 2001; **426**: 19-32.

145. Kral V, Sessler JL, Shishkanova TV, Gale PA and Volf R. *J. Am. Chem. Soc.* 1999; **121**: 8771-8775.

146. Beer PD. *Acc. Chem. Res.* 1998; **31**: 71-80.

147. Beer PD, Gale PA and Chen GZ. *J. Chem. Soc., Dalton Trans.* 1999: 1897-1909.

148. Beer PD and Cadman J. *Coord. Chem. Rev.* 2000; **205**: 131-155.

149. Sessler JL, Cyr M, Furuta H, Kral V, Mody T, Morishima T, Shionoya M and Weghorn S. *Pure Appl. Chem.* 1993; **65**: 393-398.

150. Sessler JL, Tvermoes NA, Davis J, Anzenbacher P, Jursikova K, Sato W, Seidel D, Lynch V, Black CB, Try A, Andrioletti B, Hemmi G, Mody TD, Magda DJ and Kral V. *Pure Appl. Chem.* 1999; **71**: 2009-2018.

151. Miyaji H, Anzenbacher P, Sessler JL, Bleasdale ER and Gale PA. *Chem. Commun.* 1999: 1723-1724.

152. Sessler JL, Davis JM, Kral V, Kimbrough T and Lynch V. *Org. Biomol. Chem.* 2003; **1**: 4113-4123.

153. Pareek Y, Ravikanth M and Chandrashekar TK. *Acc. Chem. Res.* 2012; **45**: 1801-1816.

154. Suksai C and Tuntulani T. *Chem. Commun.* 2005; **255**: 163-198.

155. Suksai C and Tuntulani T. *Chem. Soc. Rev.* 2003; **32**: 192-202.

156. Mahanta SP, Kumar BS, Baskaran S, Sivasankar C and Pandet PK. *Org. Lett.* 2012; **14**: 548-551.

157. Anzenbacher P, Try AC, Miyaji H, Jursikova K, Lynch VM, Marquez M and Sessler JL. *J. Am. Chem. Soc.* 2000; **122**: 10268-10272.

158. Cumpston BH, Ananthavel SP, Barlow S, Dyer DL, Ehrlich JE, Erskine LL, Heikal AA, Kuebler SM, Lee IYS, McCord-Maughon D, Qin JQ, Rockel H, Rumi M, Wu XL, Marder SR and Perry JW. *Nature* 1999; **398**: 51-54.

159. He GS, Tan LS, Zheng Q and Prasad PN. *Chem. Rev.* 2008; **108**: 1245-1330.

2 Synthesis of acyclic precursors

2. Synthesis of acyclic precursors

2.1. General considerations

As already discussed in the introduction one of the objectives of this work relied on the synthesis of several pyrrolic units to be used as building blocks in the construction of expanded macrocycles. To synthesize new expanded macrocycles, two general strategies have been relied on, namely: i) the use of different combinations of pyrrole units and bridging carbons, and ii) synthesizing new building blocks, which can replace pyrroles. Most of the classic expanded porphyrins were synthesized using a combination of these approaches. All the systems synthesized in this thesis are comprised of two pyrroles being called bipyrroles (BP) when there is a direct link between two pyrroles in the α position or dipyrromethanes (DPM) when there is a carbon between the two pyrroles interconnected by their alpha positions. The synthetic pathways used in the synthesis of bipyrrolic units are already known: Vilsmeier condensation of pyrrole and 2-pyrrolidinone and consequent dehydrogenation of the cyclic imine intermediaties or the cyclization of pyrrolic 1,4-diketones and Ullmann coupling of the corresponding iodopyrroles (Scheme 6, Section 1.3.1).

Likewise, DPM are widely used as essential building blocks for the synthesis of a variety of functional porphyrins and (contracted and expanded) porphyrin analogues [1-7]. Furthermore, DPM are the precursors of BODIPY dyes (boron dipyrromethenes), which are currently receiving increasing attention due to their valuable properties, such as the relatively high absorption coefficients and fluorescence quantum yields, high (photo)chemical stability, and improved synthetic availability [8-10].

Meso-substituted DPM are usually prepared via a one-flask method based on the acid-catalyzed (*e.g.* trifluoroacetic acid) condensation of an appropriate aldehyde with an excess of pyrrole used as solvent. Flash chromatography is required, in most of the cases, to obtain the DPMs in high purity [11,12]. The efficient preparation of these dipyrrolic building blocks requires an excess of pyrrole to ensure an optimal yield of the DPM (over the higher oligocondensates, *e.g.* tripyrromethane). One simple methodology requires the use of acidic aqueous media (HCl) and the required DPM can be isolated in essentially pure form by a simple filtration from the (cooled) reaction mixture. Precipitation of the

DPM from the aqueous layer as it is formed, forces the reaction to completion and protects the product from further reactions [13].

2.1.1. Synthesis of acyclic precursors: experimental results

Until now the work developed in the area of building blocks is still limited and there is room for improvement, especially in reducing the number of steps in the preparation of coupling partners and increasing the functional group tolerance.

For this reason our group is particularly interested in expanding the scope of building blocks, exploring new routes of synthesis and functionalization of bipyrrolic units. Therefore, to fulfill our objectives we prepared BP **1.36** synthesized previously by Rapoport and coworkers already shown in the introduction (Scheme 1.6, Route A) and here highlighted again in scheme 2.1 [14-16].

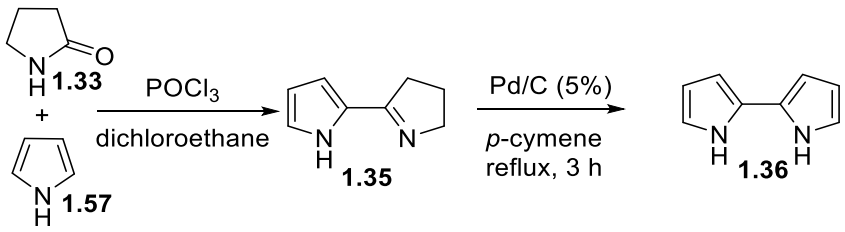

Scheme 2.1

The first step of this reaction was obtained easily with a dropwise addition of $POCl_3$ to a mixture of pyrrolidin-2-one (**1.33**) and pyrrole (**1.57**) dissolved in dichloromethane at 0 ºC. After the complete addition of $POCl_3$ the reaction was allowed to continue at room temperature for 3 hours. Neutralization of the reactional mixture with a solution of NaAcO in water followed by workup with $CHCl_3$ furnished a white powder after crystallization in 60% yield. After removal of all the solvents under vacuum, compound **1.35** was dissolved in *p*-cymene with Pd (5%) charcoal allowing it to be oxidize under reflux. After 3 h under N_2 atmosphere **1.35** was converted to the corresponding fully aromatic BP **1.36** (η = 30%).

Product **1.36** was characterized by ^{1}H and ^{13}C-NMR and the corresponding data are given in Fig. 2.1 and 2.2, respectively. As expected, after this step all the signals are displayed in the aromatic area of the ^{1}H-NMR spectrum (Fig. 2.1).

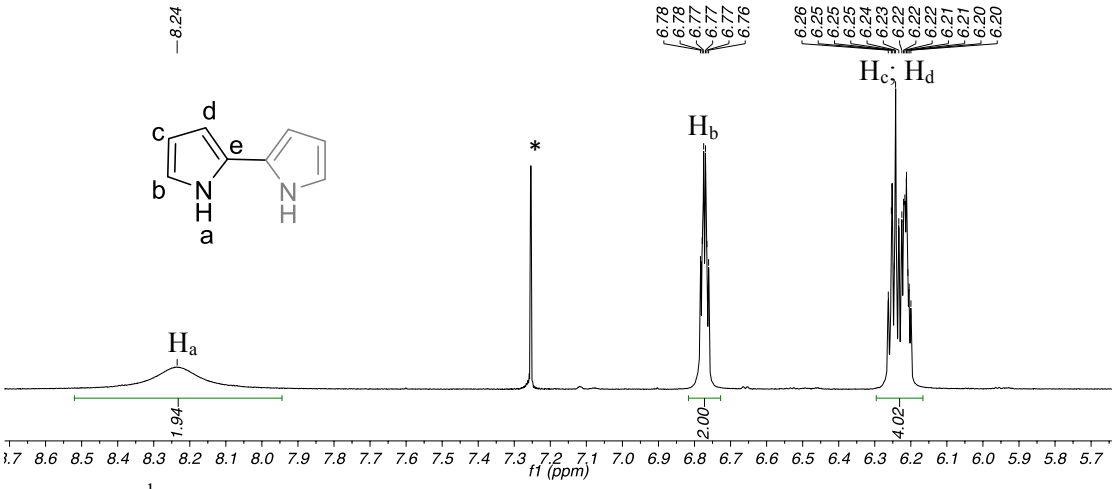

Figure 2.1: ^{1}H-NMR spectrum of compound **1.36**, ***** stands for $CHCl_3$.

Being a completely symmetrical molecule the signals due the *β*- and *α*-positions of the pyrrole units are discriminated in two signals, a multiplet at δ 6.26-6.20 ppm integrating for 4 protons (H_c and H_d,) and a doublet of doublets at δ 6.77 ppm (J = 2.6 and 1.6 Hz) integrating for 2 protons (H_b), respectively. It is also possible to note a broad signal characteristic of NH protons at δ 8.24 ppm, integrating for the two NH protons of compound **1.36** (H_a).

Also in ^{13}C-NMR this feature can be found (Fig 2.2). The symmetry of the molecule makes the spectra simples to analyze and as expected only signals in the aromatic zone of the spectra can be found. The signal due the quaternary carbons is the most shifted at δ 125.9 ppm (C_e) and the signals due the *α*-positions can be found at δ 117.6 ppm (C_b). The other two signals are attributed to the carbons in the *β*-pyrrolic positions at δ 109.4 (C_d) and 103.5 ppm (C_c).

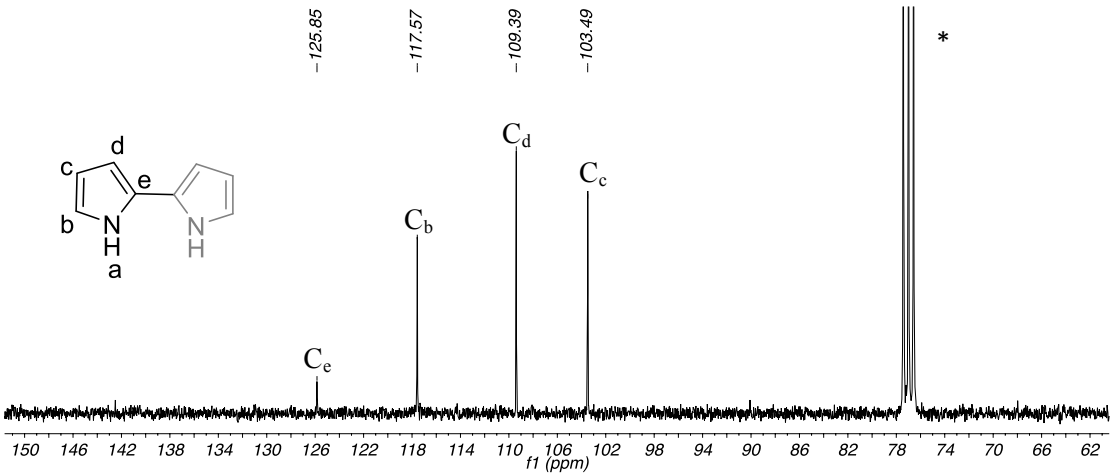

Figure 2.2: ^{13}C-NMR spectrum of compound **1.36**, ***** stands for $CHCl_3$.

The synthesis of precursors from the DPM family was also achieved by conventional methodologies and efforts in order to provide generalization in the methodology was also attempted. The methodologies discussed in the overview section were fully achieved with aldehydes/ketones **2.1-2.5** and different ratios of pyrrole and reaction times (Scheme 2.2).

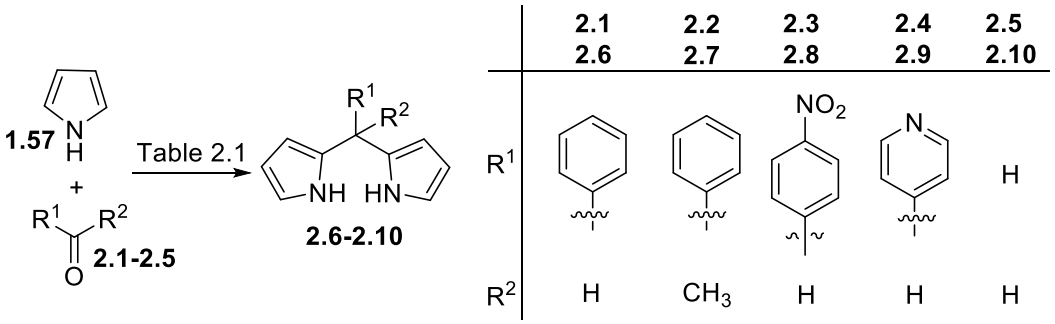

Scheme 2.2

Synthetically, these intermediates are synthesized from the readily available distilled pyrrole, used in large excess, and the corresponding aldehyde/ketone **2.1-2.4** in aqueous acidic media (HCl, 0.18 M) furnishing compounds **2.6-2.9**. The yields vary from moderate to good and are possible to obtain up to 5 grams in one reactional batch (Table 2.1). The precipitated aryl-DPM can be isolated directly from the reaction mixture in an essentially pure state by simple filtration, with exception for compound **2.9**, which needed to be purified over silica-gel with CH_2Cl_2:MeOH (95:5) as solvent before crystallization from a mixture of H_2O:EtOH (1:1).

Table 2.1: Conditions used in the preparation of DPM **2.6-2.10**.

DPM	Aldehyde/Ketone	Ratio (Pyrrole:aldehyde /Ketone)	Time (h)	Yield (%)
2.6	**2.1**	3:1	4	82
2.7	**2.2**	3:1	4	76
2.8	**2.3**	3:1	2	95
2.9	**2.4**	5:1	6	42
2.10	**2.5**	25:1*	5 min.	40

*Pyrrole is used as solvent in the reaction.

Attempts to obtain compound **2.10** using similar methods as the one already discussed, proved to be unsuccessful. This DPM was then obtained using a methodology extensively studied by Lindsey, where formaldehyde is dissolved in pure pyrrole at 60 ºC [17]. After this 0.1 eq. of TFA is added and the reaction is left under vigorous stirring during 5 minutes. Work up of the mixture with a 0.1 M solution of NaOH and vacuum evaporation of the excess of pyrrole provides an orange oil, which was purified over silica gel (hexane/CH_2Cl_2/NEt_3, (75:24:1) furnishing **2.10** as white needles in 40% yield, taking into account the consumed pyrrole.

The ^{1}H-NMR spectra of compounds **2.6-2.10** are presented in fig. 2.3. Here, for instance, the peripheral *α*-, *β*-pyrrolic signals are delimited between δ 5.70-6.0 and 6.80-6.10 ppm, respectively.

These signals, for clarity are enclosed in the corresponding colored boxes in fig. 2.3. As for the signals due to the aryl groups positioned at the *meso* position of these units, these may be displayed as doublets each one integrating for two protons when the aryl group is substituted in the *para* position (**2.8** and **2.9**) or a set of multiplets which combined integrates for 5 protons, when the aryl group is a phenyl (**2.6** and **2.7**).

The only exceptions are the signals attributed to the group positioned at the *meso* position of aryl-DPM **2.7** which is a CH_3 group appearing as a sharp singlet integrating 3 protons at highfield (δ 2.05 ppm), and DPM **2.10** where the absence of a phenyl group at this position makes the signal a sharp singlet less shifted to high field integrating for 2 protons at δ 3.91 ppm. The remaining signals are broad singlets highly shifted to low field, attributed to the NH groups.

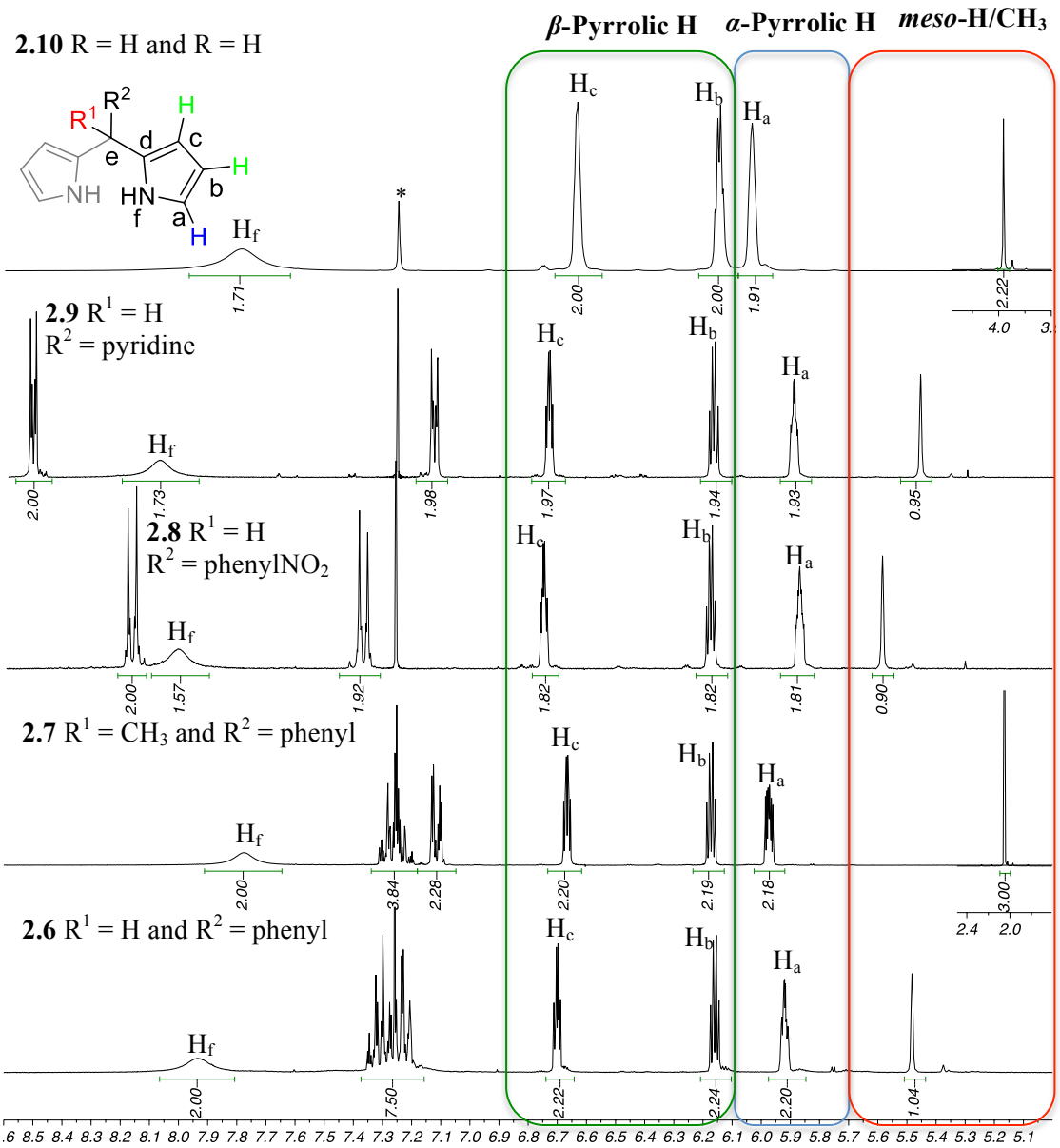

Figure 2.3: ^{1}H-NMR spectra of compounds **2.6-2.10**, * stands for $CHCl_3$.

While these precursors can be achieved easily, their stability at room temperature is quite low. The highly reactive α-positions, sensitivity to light and ease oxidation makes their storage, for long periods of time, difficult. Two different methodologies can be found on literature to stabilize these pyrrolic precursors. Methods like incorporation in tetrapyrrolic macrocycles or the use of electron withdrawing groups in the α-positions of these units have shown to be easy methods to obtain simple and stable precursors. Here the choice was based on the introduction of an electron withdrawing group on the α-positions which not only would stabilize a highly reactive precursor as it served the purpose of protecting these positions from side reactions when attempting further functionalization in these units (Scheme 2.3).

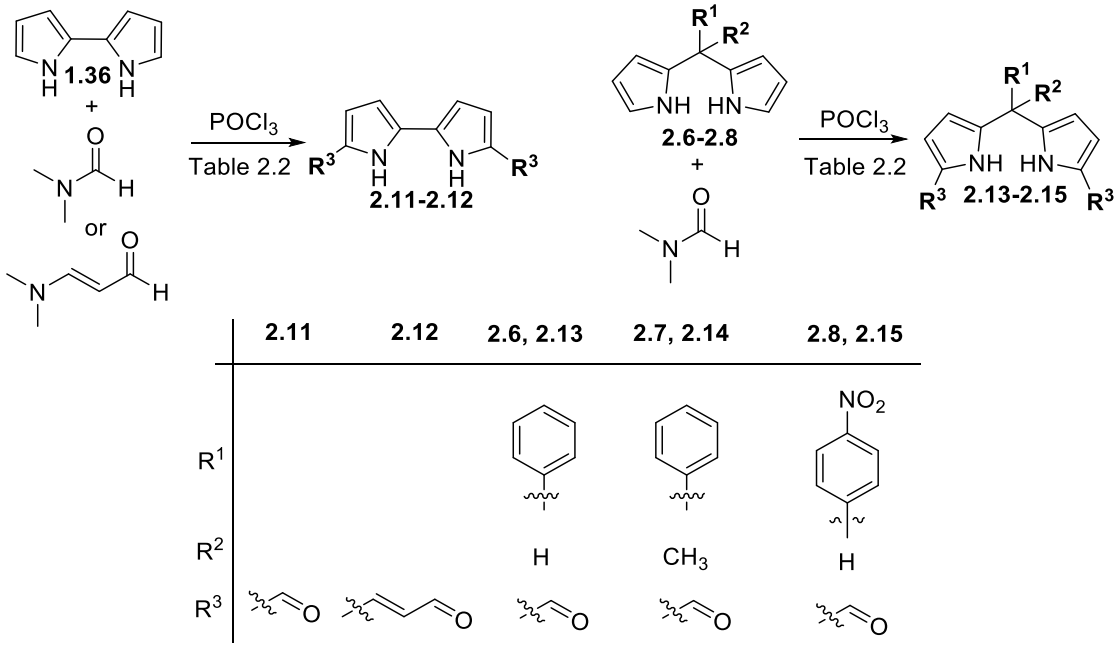

Scheme 2.3

With the above view in mind, we performed Villsmeyer-Hack reactions with the *α*-free compounds **1.36**, **2.6**, **2.7** and **2.8**.

In the selected route to the diformyl- BP and diformyl-DPM (Scheme 2.3), the preparation of the Vilsmeyer reagent (DMF/$POCl_3$) and the way it is added to the reaction play a pivotal role in the sequence.

Synthetically, these intermediates are synthesized from the readily available DPM *vi*a well-established procedures in pyrrole chemistry. The general sequence starts with dissolution of the corresponding BP or DPM unit in DMF or dimethylaminoacrolein and the addition of $POCl_3$ dropwise at 0 ºC. After a combination of temperatures and reaction times (Table 2.3), further hydrolysis with the corresponding base furnishes the desired diformyl derivatives.

However these conditions only worked for compound **2.11**. When similar conditions were attempted to obtain compound **2.12**, changing DMF for dimethylaminoacrolein a dark insoluble solid was obtained, while complex mixtures over TLC analysis were achieved when attempts were made with compounds **2.6-2.8**. After new attempts using room temperature and a combination of different bases such as NaOH for the hydrolysis of the iminium salts compound **2.12**, was achieved. This last approach used again in DPM **2.6-2.8** also did not provide the desired diformylated precursors (**2.13-2.15**).

The most obvious approach to tackle this problem was to prepare the Villsmeyer reagent prior to the addition of the DPM. In these instances, the synthesis starts off with the preparation of the Villsmeyer reagent at 0 ºC under nitrogen atmosphere during 30 min. At this time, DPM **2.6-2.8** are added dropwise dissolved in CH_2Cl_2 during 45 min. After complete addition of the corresponding DPM the reaction is allowed to stir at room temperature for another 45 minutes. Further hydrolysis of the iminium salts is accomplished adding an aqueous saturated solution of Na_2CO_3. After 6 hours reaction, extraction with ethyl acetate and purification over silica gel furnished the desired diformyl-DPM **2.13-12.15** in moderate to good yields (Table 2.2).

Table 2.2: Conditions used in the preparation of dipyrrolic compounds **2.11-2.15**.

Compound	Temperature (ºC)	Time (min.)	Base (Aqueous solutions)	Time (h)	Yield (%)
2.11	60	60	NaOAc[a]	2	84
2.12	25	180	NaOH[b]	6	82
2.13	25	45	Na_2CO_3[a]	6	60
2.14	25	45	Na_2CO_3[a]	6	65
2.15	25	45	Na_2CO_3[a]	6	63

a) Saturated solutions of these bases were used in the synthesis; b) 1M NaOH solution was prepared dissolving about 4 g of NaOH in 100 mL of water.

The ^{1}H-NMR conclusively manifests the presence of compounds **2.11-2.15**. Here, for clarity the diformyl BP **2.11** and diformylethynilated BP **2.12** are discussed separately from the diformyl DPM units **2.13-2.15**. On the ^{1}H-NMR (Fig. 2.4) spectra of compounds **2.11** and **2.12**, it is possible to assign all the signals for these compounds. The key differences compared with the starting material **1.36** are related with the presence of aldehyde groups in the *α*-pyrrolic positions in both compounds while in compound **2.12** there´s still the additional signals due the ethylene bridge between the pyrroles and the aldehyde groups.

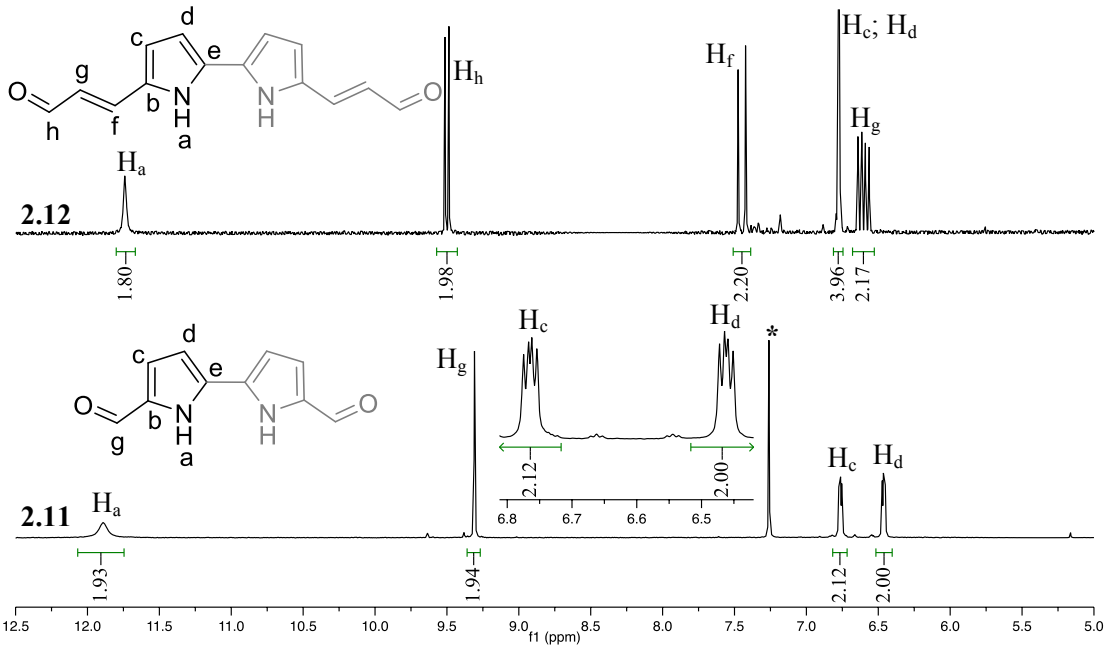

Figure 2.4: ^{1}H-NMR spectra of compounds **2.11** ($CDCl_3$) and **2.12** (DMSO-d_6) *stands for $CHCl_3$.

As a result of this substitution pattern the signals of the *β*-pyrrolic protons appear at low field, in the aromatic zone of the spectra two doublet of doublets integrating each one for two protons at δ 6.76 and 6.46 ppm for **2.11** (corresponding to H_c and H_d, respectively, expansion in figure 2.4) and a doublet integrating for four protons at δ 6.68 ppm for **2.12** (corresponding to H_c and H_d). The signal attributed to the aldehyde group is displayed as a sharp singlet for compound **2.11** (H_g) at δ 9.32 ppm or a doublet for compound **2.12**, (H_h) at δ 9.55 ppm, integrating for two protons in both spectra, as expected. Moreover, in compound **2.12** is possible observe a doublet at δ 7.45 ppm attributed to H_f, and a doublet of doublets at δ 6.60 ppm corresponding to H_g, both integrating for 2 protons due to the presence of the ethylene spacer between the aldehyde and the pyrroles.

There is a remarkable resemblance when the ^{1}H-NMR of compounds **2.13**-**2.15** are compared with their non-formylated counterparts. These similarities are depicted in figure 2.5 and most of the signals don't show much difference. In contrast, further analysis of these spectra shows unmistakably the disappearance of the signals attributed to the *α*-pyrrolic protons, and the presence of a shifted singlet integrating for two protons to lower field in the spectra (around δ 9.5 ppm) normally attributed to the CHO signal.

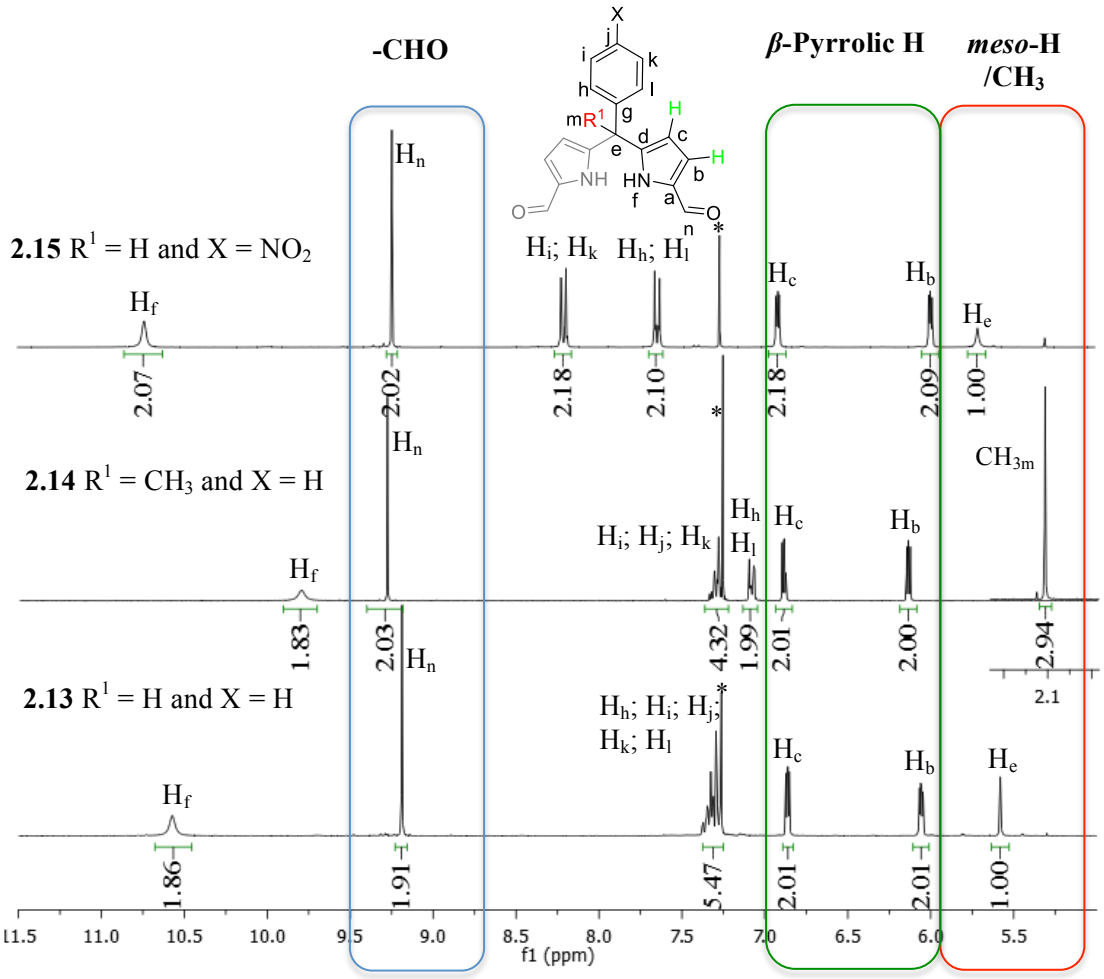

Figure 2.5: ^{1}H-NMR spectra of compounds **2.13-2.15** ($CDCl_3$) * stands for $CHCl_3$.

The last statement is further supported with ^{13}C-NMR where it is possible to note the presence of a signal around δ 178.0-180.0 ppm attributed to the CHO group for compounds **2.13-2.15**.

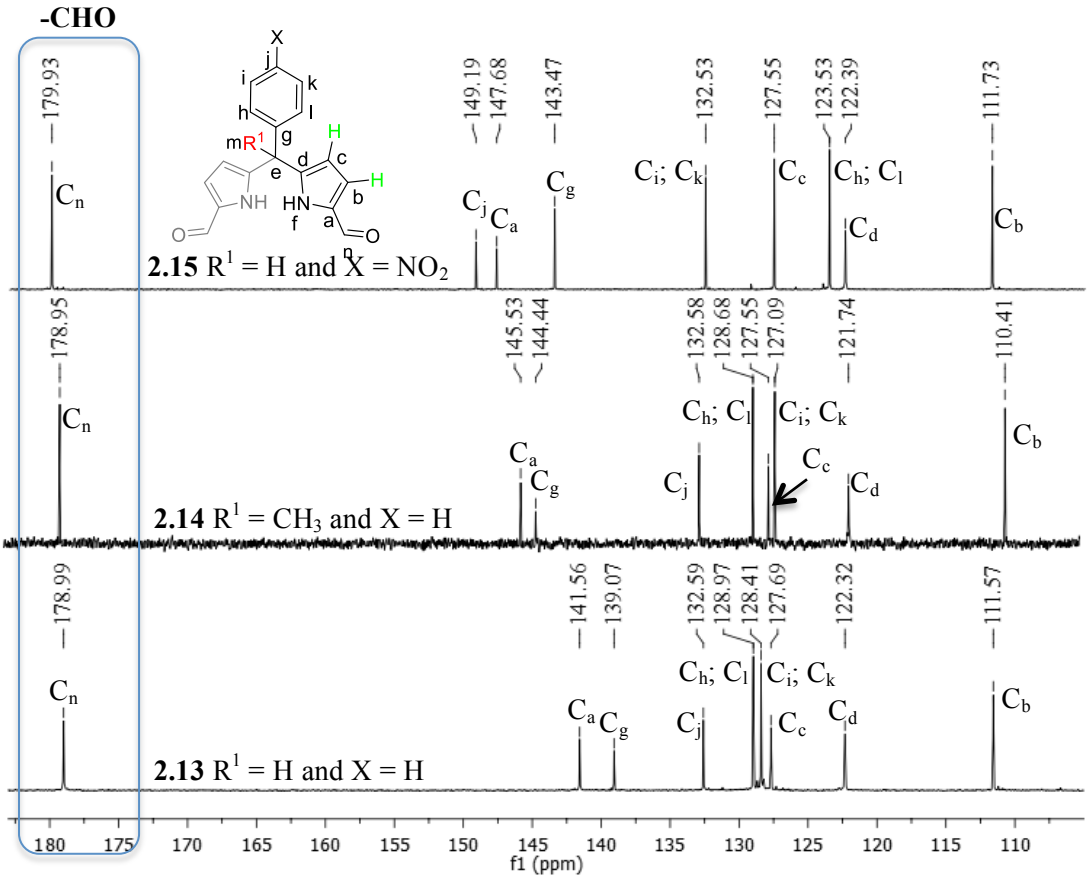

Figure 2.6: ^{13}C-NMR spectra of compounds **2.13**-**2.15** ($CDCl_3$).

Encouraged by the simple methodologies used for the synthesis of precursors **2.11** and **2.12** we anticipated the possibility of synthesizing a series of small synthons that would provide us compounds that could be used in colorimetric recognition of anions by means of Knoevenagel reactions or the use of Diels-Alder (D-A) reaction to further increase the conjugation of these compounds. This type of reaction was expected to form new carbon-carbon bonds between a dienophile (good dienophiles often bear one or two of the following substituents: CHO, COR, COOR, CN, C=C, Ph, or halogen) and a diene (BP unit).

2.2. Knoevenagel condensation on acyclic precursors

2.2.1. General considerations

The synthesis of materials that may establish supramolecular interactions with anions is an important field of research in organic chemistry, with an increasing interest

due to the need to find, for instance, compounds that can bind and transport anions across lipid bilayer membranes or cleaner methods for waste treatment [18-21].

For this purpose, pyrrole units are particularly attractive since the N–H protons remain in place over a wide pK_a range making possible their use as a hydrogen bond donor group within a large pH window. Also, the reasonably easy functionalization and incorporation into elaborate cyclic and acyclic systems are reasons to have into account when synthesizing this kind of receptors [22].

In the last few years, efforts to develop chromogenic anion sensors with varying substrate selectivity and different colorimetric response patterns have been a field of active research [23,24]. Such systems generally consist of two parts. One part is an anion-binding site employing various combinations of anion receptor units. The other is the chromophore part, which converts the binding events or recognition phenomena to optical signals. These two parts can be either covalently attached or intermolecularly linked to each other. In this area of development, compounds like calix[4]pyrroles and DPM structures have been used for this end [25-28].

Inspired in some of these works, which showed pronunced changes in color in the presence of anions, we considered the combination of Knoevenagel reactions using malononitrile and indane-1,3-dione moieties with the dipyrrolic compounds synthesized in the previous section. It was expected that the highly conjugated, push-pull chromophores would provide improved sensing performance (both binding and signaling) as well as insight into the photophysical and thermodynamic processes taking place in such materials.

2.2.2. Knoevenagel condensations on acyclic precursors: experimental results

As stated, compound **2.11** with malononitrile and indane-1,3-dione could provide compounds with strong visual differentiation upon addition of different anions. Part of our studies on anion binding and colorimetric agents led to the synthesis of bipyrrolic structures through Knoevenagel condensations (Scheme 2.4).

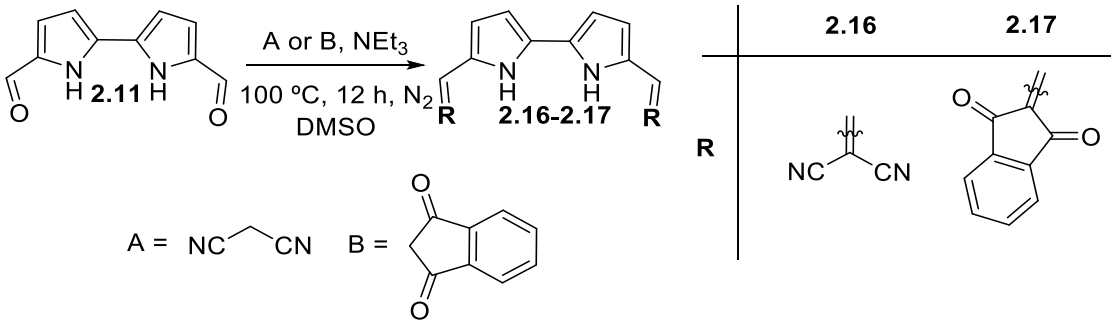

Scheme 2.4

These syntheses were attempted in several solvents and conditions being the initial attempts in THF at room temperature insufficient to obtain the desired compounds. In fact the BP synthon **2.11** is highly stable at temperatures below 100 ºC. Compound **2.16** was obtained, dissolving **2.11** and malononitrile (6 eq.) in DMSO with a catalytic amount of NEt_3 at 100 ºC for 12 h. The same conditions used with idane-1,3-dione were insufficient in the synthesis of precursor **2.17**, leading to complex mixtures when subject to TLC analysis and most of the starting material untouched. In fact several efforts to obtain **2.17** were attempted before its synthesis.

Initially the increase of reaction temperature was the rational conclusion, highlighting the differences in reactivity between the two Knoevenagel nucleophiles used in these reactions. Unfortunately, an increase in temperature up to 120 ºC and longer periods of reaction did not achieve the desired progress. While these attempts were made a different approach was also attempted based on the concept that the H_2O formation in the reaction progress was hindering the equilibrium. The following reactions were then made in the presence of molecular sieves 4A. However this also did not gave the anticipated results. Further attempts were made, but in this case a different base was used. Piperidine a recognized organocatalyst in Knoevenagel reactions and it has been used successfully in several reactions of this type. This catalytic activity related with piperidine is associated with the formation of an intermediary imine compound, which is more reactive than the aldehyde group of the starting material. In fact, this methodology allowed a full conversion of the starting material into a more polar orange compound over the TLC at rt during 6 h.

The use of the NMR technique allowed us to validate the presence of compounds **2.16** and **2.17** and these results are depicted in figures 2.7 and 2.8.

The simplicity of the ^{1}H-NMR spectrum of compound **2.16** is shown in the next figure, where it's possible to note the disappearance of the peak previously attributed to the

CHO group normally depicted around δ 9.50 ppm. In fact this substitution pattern is corroborated with the appearance of a new singlet less shifted at δ 7.82 attributed to proton H_f. The remaining signals of the spectra are the *β*-pyrrolic protons at δ 7.49 (H_d) and 7.06 ppm (H_c) each one of them integrating for 2 protons, and the signal due to the NH groups (singlet at 12.76, H_a).

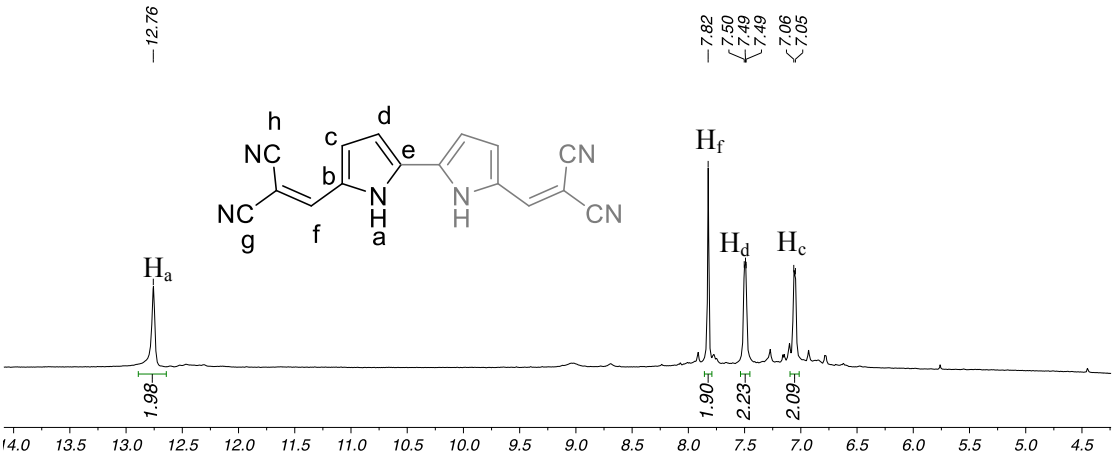

Figure 2.7: [1]H-NMR spectrum of compounds **2.16** (DMSO-d_6).

In terms of NMR spectroscopy the same is observed in compound **2.17** where the signal at δ 9.50 ppm disappears giving place to a singlet integrating for two protons at δ 7.78 ppm (H_f), a similar shift when compared with compound **2.16**.

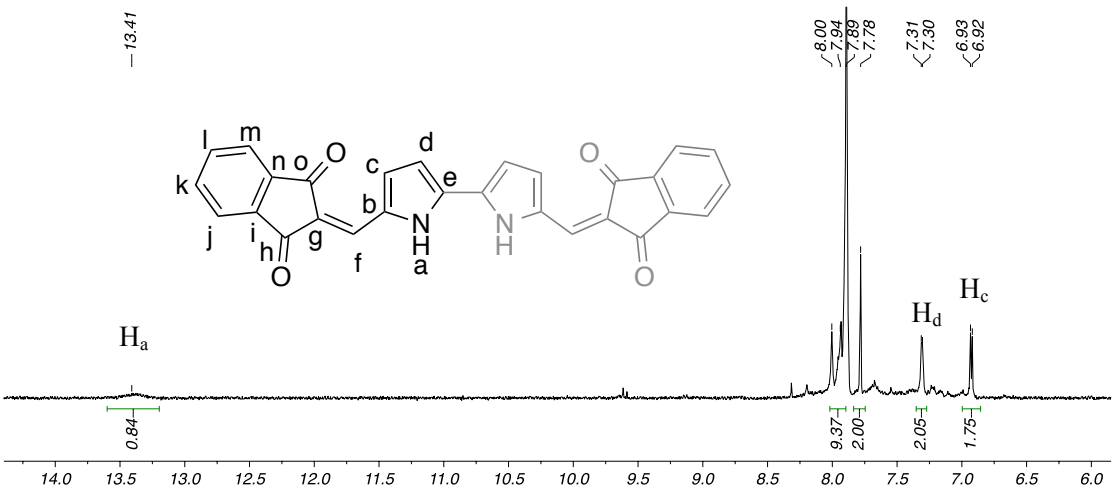

Figure 2.8: [1]H-NMR spectrum of compounds **2.17** (DMSO-d_6).

The success in the synthesis of the previous compounds prompted the synthesis of other acyclic pyrrolic systems with the same methodology. For this end DPM **2.13** and

2.14, where the increased distance between the pyrroles was expected to bind larger anions and to give different specificities were also synthesized (Scheme 2.5).

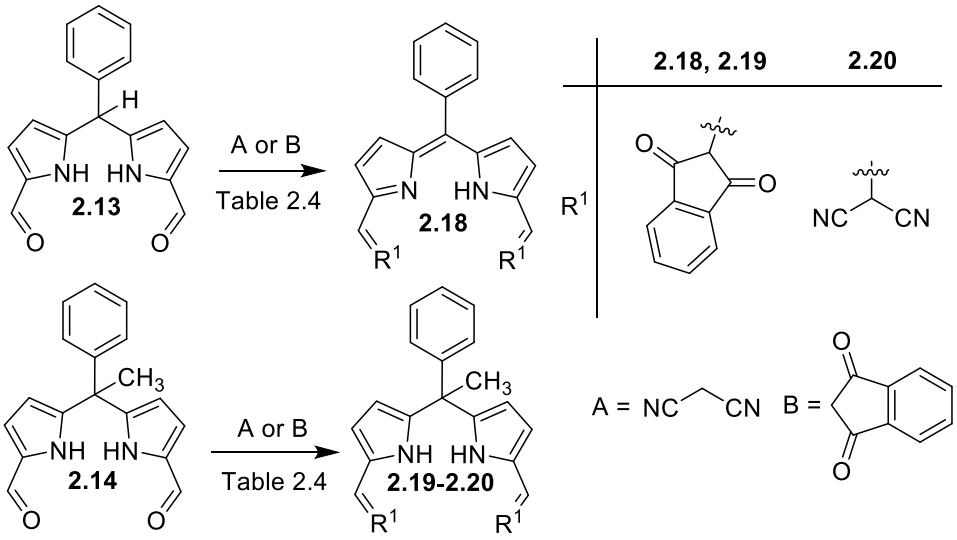

Scheme 2.5

Here the solubility factor was completely different from the previous analogues. DPM **2.13** and **2.14** were highly soluble in organic media furnishing the desired compounds with yields around 60% using CH_2Cl_2 as solvent, in different times of reaction for each kind of substituent (table 2.3). DPM **2.13** reaction with malononitrile was subject of several attempts changing the bases and the solvents used in the reaction, nevertheless the final outcome was similar no compound desired were isolated. Further examination showed that long periods of reaction or purification over flash silica gel lead to the decomposition of the potential products of the reaction (examples of the conditions attempted are summarized in table 2.3). While compound **2.18** was possible to be fully characterized, mostly because this product precipitated directly from the reaction media with hexane, avoiding post-reaction treatment that would eventually decompose it. Nonetheless it was obtained in 32% yield and its structure is associated to a dipyrromethene and not the expected DPM.

On the contrary compounds **2.19** and **2.20** were obtained easily using the conditions in table 2.3. These last derivatives proved to be stable at workbench conditions for long periods of time in the solid state and in solution.

Table 2.3: Knoevenagel reactional conditions used for compounds **2.18**-**2.20**.

DPM	Base	Time (h)	Solvent	Yield (%)	Final Product
2.13	NEt_3	6	CH_2Cl_2	32	**2.18**
2.13	NEt_3	6	CH_2Cl_2	-	-
2.13	NEt_3	3	THF	-	-
2.13	Na_2CO_3	12	CH_2Cl_2	-	-
2.13	DIPEA	3	THF	-	-
2.13	DIPEA	6	CH_2Cl_2	-	-
2.14	NEt_3	6	CH_2Cl_2	58	**2.19**
2.14	NEt_3	8	CH_2Cl_2	73	**2.20**

The ^{1}H and ^{13}C NMR spectra of compounds **2.18**-**2.20** are in accordance with the expected structures and were further corroborated with bi-dimensional techniques (COSY and HQSC). In figure 2.9 the ^{1}H-NMR spectrum of **2.18** is elucidated.

DPM **2.18** is structurally similar to its counterpart **2.19**. However, the resonance peaks in the ^{1}H-NMR spectra were severely broadened when compared with its counterpart ^{1}H-NMR (**2.19**, fig 2.10). Nevertheless, it was possible to attribute all the signals due the indane-1,3-dione moieties all in one multiplet integrating for 8 protons. As for the remaining signals it is possible to note the same behavior as the previous compounds. The disappearance of the signal attributed to the CHO and the appearance of a new one at higher field (δ 7.73 ppm). The remaining signals are attributed to the DPM framework. It is also possible to note the disappearance of the signal attributed to the *meso* proton, which resonates at δ 5.58 ppm in the starting material (**2.13**). Furthermore mass spectrometry showed an *m/z* = 534.2 corresponding to $[M+H]^+$ of structure **2.18**.

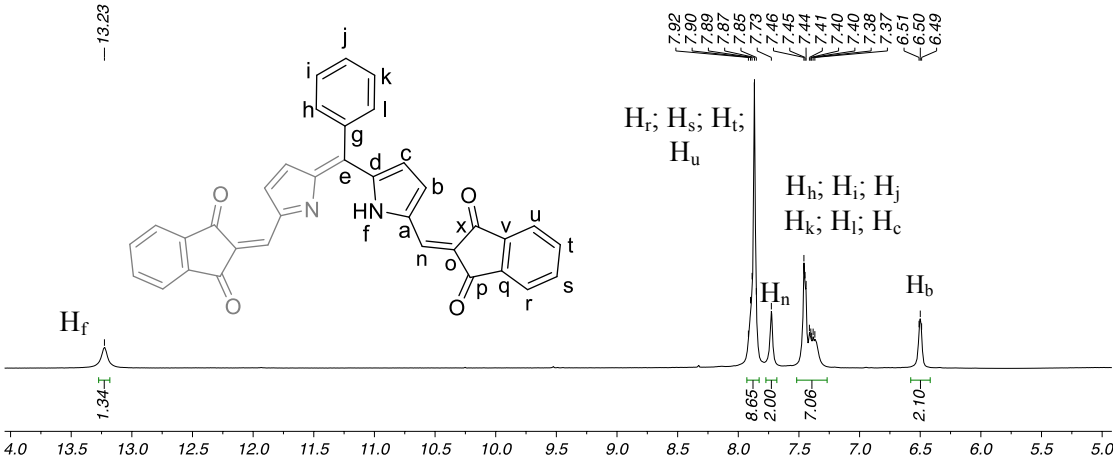

Figure 2.9: ^{1}H-NMR spectrum of compound **2.18** in DMSO-d_6.

On the ^{1}H-NMR (figure 2.9) spectrum of **2.19**, it is possible to assign all the signals for this compound. The main differences to the starting material are related with presence of the aromatic protons present in the indane-1,3-dione moieties. As a result of this substitution, the additional protons results in a complex spectrum with several coupling and unresolved signals. For instance, as it is possible to see fig. 2.10, the signals for the protons H_b and H_c in the starting material **2.14** were doublets. Now, they appear as quartets showing a coupling constant between them (J = 4.0 Hz). Looking closely to the expansion in figure 2.10 is possible to note the multiplet between δ 7.72 and 7.62 ppm, attributed to the protons (H_n, H_s and H_t), and the other two multiplets to the remaing signals of the indane-1,3-dione moieties H_u (δ7.87-7.84 ppm) and H_r (δ 7.78-7.75 ppm). The remaining signals have been attributed unambiguously.

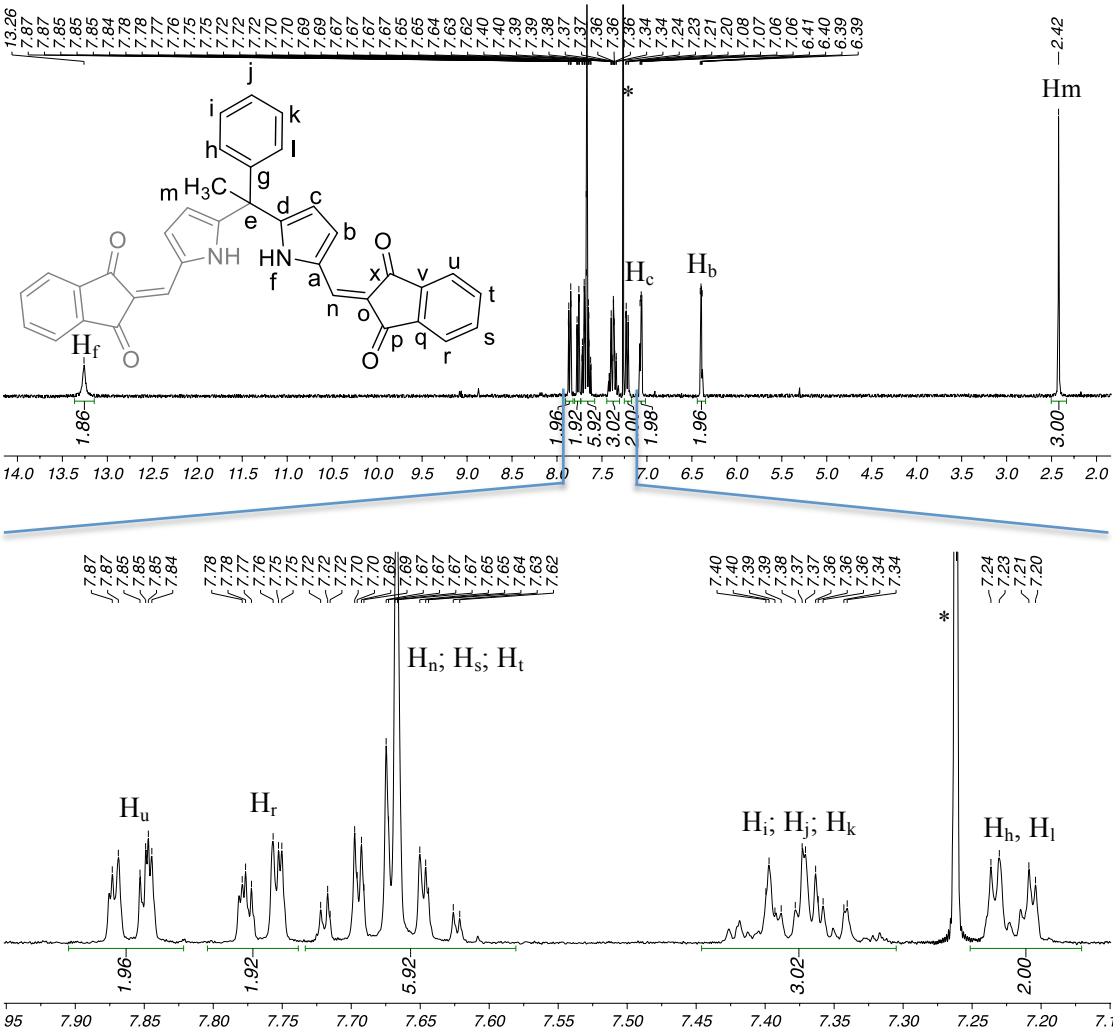

Figure 2.10: ^{1}H-NMR spectrum of compound **2.19** in $CDCl_3$, * stands for $CHCl_3$.

Further confirmation of this structure was obtained by the ^{13}C-NMR spectrum (Fig. 2.11) where the singlets at δ 192.0 and 190.7 ppm are attributed to the ketone C=O carbons C_p and C_x. Also the signals due the aromatic protons of the indane-1,3-dione moieties are located at δ 141.09 (C_q), 140.08 (C_v), 134.6 (C_s), 134.3 (C_t), 122.6 (C_r) and 122.4 (C_u) ppm. The signal previously attributed to C_n is now found at δ 132.7 ppm. The remaining signals are attributed to the DPM framework and have similar shifts to the ones encountered in the starting material.

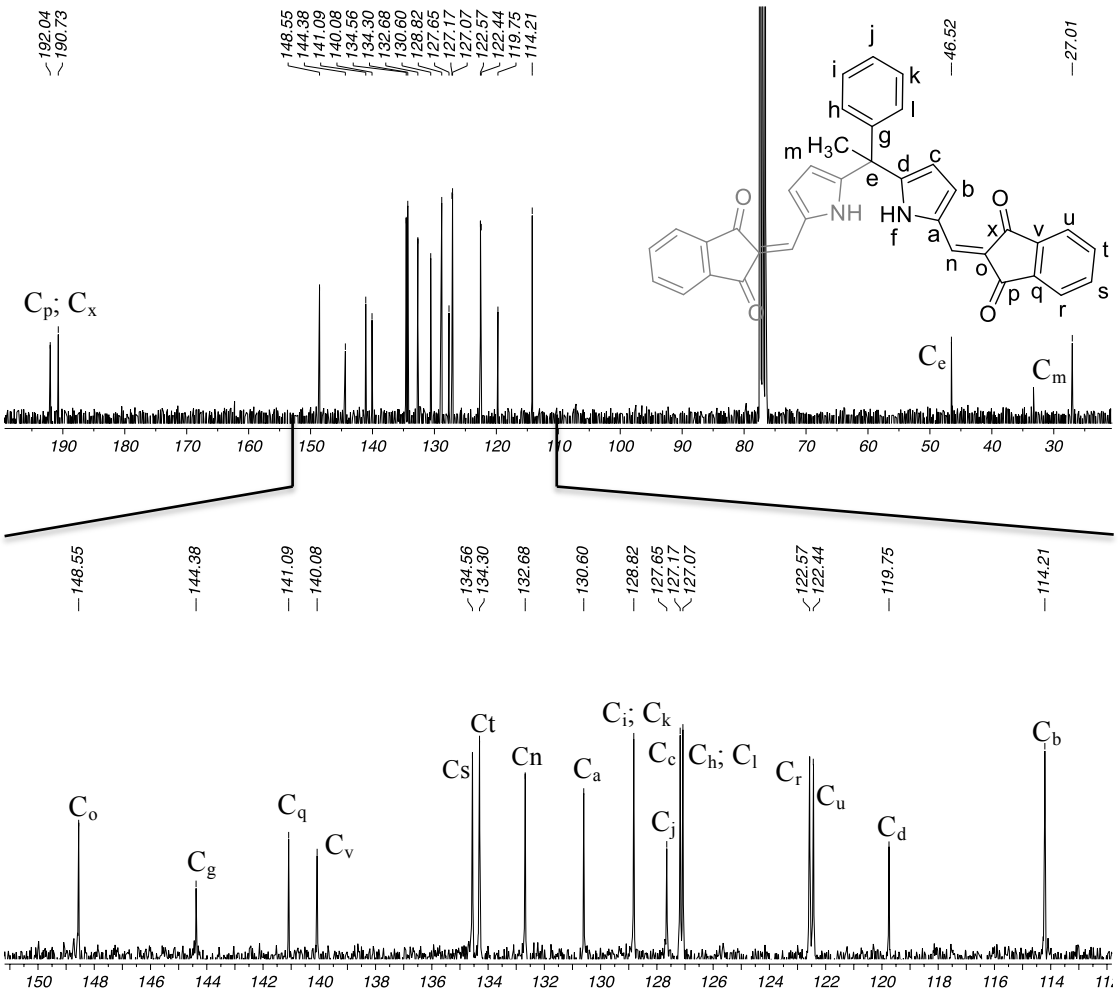

Figure 2.11: ^{13}C-NMR spectrum of compound **2.19** in $CDCl_3$, * stands for $CHCl_3$.

^{1}H-NMR data are reported for compound **2.20** is demonstrated in the next figure. As it is possible to note, all the signals of **2.20** are easily recognized in the spectrum and the major differences for the starting material are similar to the previous ones (Figure 2.12).

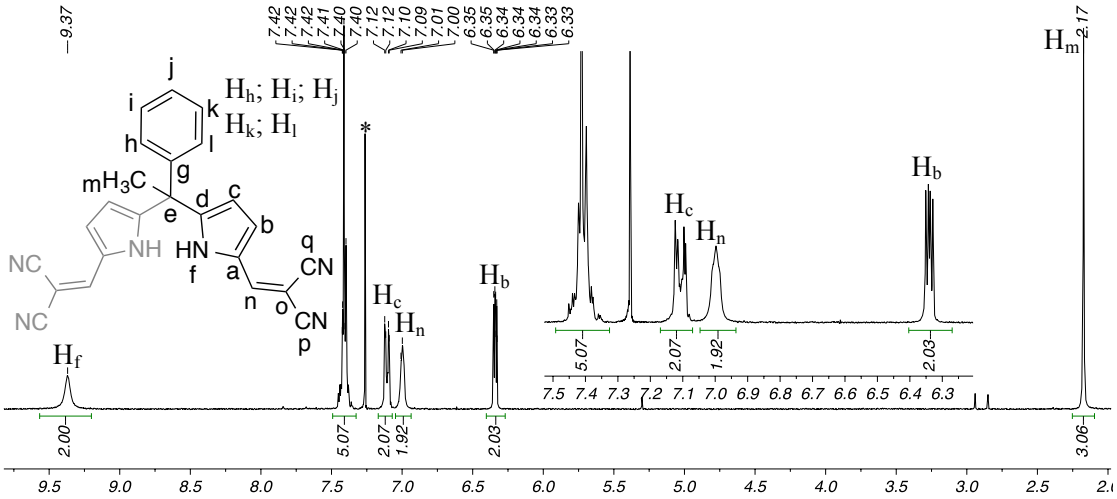

Figure 2.12: ^{1}H-NMR spectrum of compound **2.20** in $CDCl_3$,* stands for $CHCl_3$.

The success achieved with the initial bipyrrolic compound **2.16**, which was in turn synthesized in a single attempt, proved to be short lived as indicated above. For instance, further reaction with a different Knoevenagel nucleophile indane-1,3-dione proved a lack of generality in the procedure and a discrepancy in the yields. The solubility problems on the bipyrrolic synthon and the difference in the nucleophiles reactivity may be the cause for this inconsistency.

For the remaining DPM **2.18**-**2.20**, this methodology showed to destabilize dipyrromethane **2.13**, when more reactive nucleophiles are used (*e.g.* malononitrile) yielding complex bluish mixtures, which failed to exhibit any features of a typical functionalized DPM. This behavior can be associated with the fairly ease in the oxidation of these compound into dipyrromethenes. However compound **2.18** was isolated in a relatively low yield by crystallization from the reactional media being the only viable procedure to obtain the desired compounds from this starting material. Nevertheless characterization by NMR spectroscopy and mass spectrometry indicates the final product from this reaction is a dipyrromethene (**2.18**), an oxidized form of DPM. This is in fact in accordance with our previous assumptions.

More interestingly, DPM **2.14** undergoes Knoevenagel reaction in very good yields and the products proved to be very stable in the solid state (**2.19** and **2.20**). The effortless manner on how these reactions run with this DPM, indeed shows that this synthon can be a subject of more studies on its reactivity in the α-positions.

2.2.3. Acyclic precursors: Anion binding studies

2.2.3.1. General considerations

The design of acyclic oligopyrrolic anion receptors is a thriving segment in anion receptor development. A big impetus for this work arose from the natural product prodigiosin (**2.21**, Figure 2.13). Prodigiosin and its derivatives have been studied extensively for their promising immunosuppressive and anticancer activity [29-32].

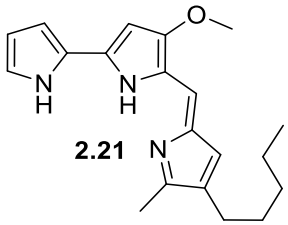

Figure 2.13: Prodigiosin structure.

Prodigiosins are believed, in part, to mediate their anticancer action via the promotion of H^+/Cl^- transport. This is believed to lead to cell apoptosis by neutralization of acidic compartments and acidification of the cytoplasm [33,34]. The resulting disruptions in natural anion transport lead to apoptosis, or so-called programmed cell death. Numerous analogues of prodigiosin have been developed and are recognized for their anion-binding properties [35].

Multiple other acyclic oligopyrrolic receptors have been reported by Sessler *et al.* These include the dipyrrolylquinoxalines (depicted in the introduction, Figure 1.27), which incorporate chromogenic quinoxaline unit for sensing upon interaction with anions [36].

A common strategy for making the pyrrolic NH a better hydrogen-bond donor (through an increase in its inherent acidity) is to functionalize the *β*-position of the pyrroles with electron withdrawing groups, while the *α*-positions are normally functionalized with further binding sites. This strategy has been pursued with pyridine-2,6-dicarboxamide system functionalized with two pyrroles bearing ester groups (**2.22**-**2.24**) and acyclic pyrrolic anion-binding systems developed by Gale *et al.* (**2.25**-**2.26**) (Figure 2.14) [37,38].

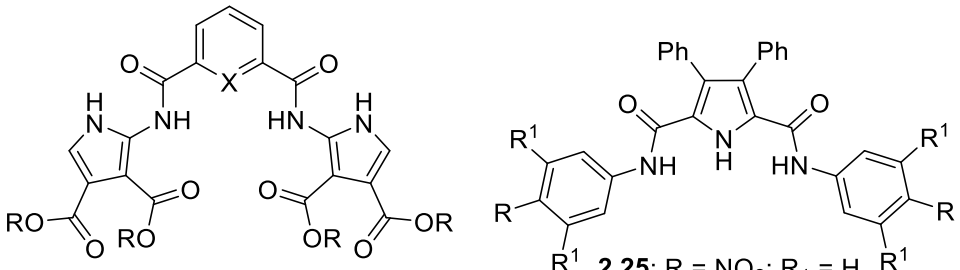

2.22; R = CH_2CH_3; X = N
2.23; R = $CH_2CH_2CH(CH_3)_2$; X = N
2.24; R = CH_2CH_3; X = CH

2.25; R = NO_2; R_1 = H
2.26; R = H; R_1 = NO_2

Figure 2.14: Acyclic pyrrole-based anion-binding receptors.

One interesting segment of this area is the chromogenic anion sensing in which a compound (chemosensor) differently changes its color in the presence of different anions [39,40].

Current analitycal techniques are not very suitable for fast detection protocols [41,42]. Consequently, it is important to develop methods allowing straightforward analyte detection. In this regard, colorimetric sensors offer the advantage of providing information with minimal equipment, allowing the so-called "naked-eye" detection. There are numerous examples of colorimetric probes for anionic species [23,43-47]. Common drawbacks of these systems are that they often require complicated synthesis and their design is not flexible, therefore every analyte requires its own probe design.

Some examples using the push-pull approach on the *β*-position of pyrrolic moieties have been used in the literature, giving rise to the expected colorimetric effect [26,48]. This effect is illustrated in the next figure where a set of calix[4]pyrroles bearing push-pull moieties in the *β*-positions (**2.27** and **2.29**) and a DPM bearing substitutions in the *α*-position (**2.28**) show enhanced chromogenic effect [25].

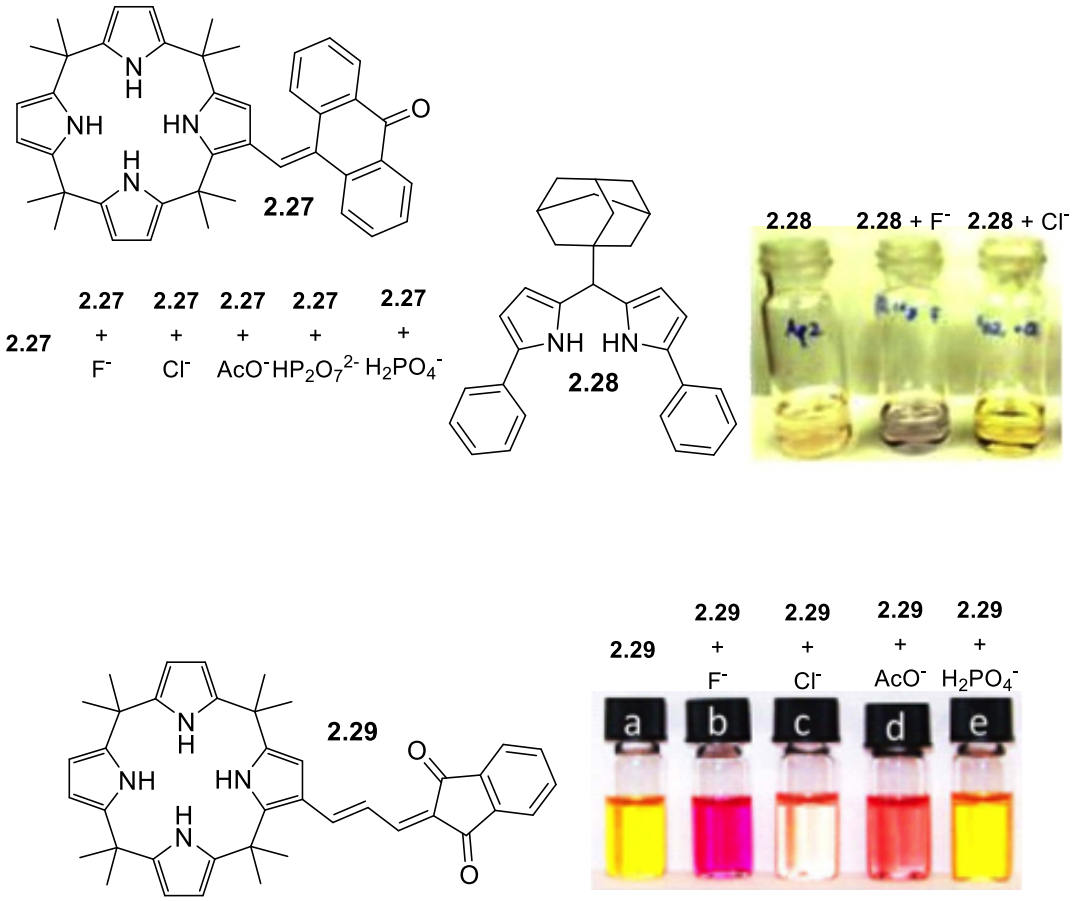

Figure 2.15: Chromogenic compounds **2.27**-**2.29**.

While, these studies showed the versatility of several chromogenic compounds bearing pyrrole moieties functionalized on both β and α-position, compounds **2.16**, **2.17**, **2.19** and **2.20** were synthesized with the same premises using for this end the substitutions at the α-positions. This concept of using push-pull moieties in the α-positions of the dipyrrolic compounds showed the increased binding affinities and the corresponding colorimetric capabilities towards different anions.

2.2.3.2. Methods used to analyze the binding properties

The interaction between compounds and anions can be studied through different techniques, such as UV-Vis or/and fluorescence spectroscopy, nuclear magnetic resonance (NMR) or isothermal titration calorimetry (ITC). The choice amongst these techniques to study the anion binding capability is strongly dependent of the compounds chemical-physical proprieties. Nevertheless, the most commonly technique used is UV-Vis and/or

fluorescence spectroscopy, since it is only necessary a measurable change in the UV-Vis (or fluorescence) spectrum of the free compound associated with the complex formation.

The simplest equilibrium that can be establish between the host (compound) and the guest (anion) can be resumed by the equation 2.1.

$$H + G \leftrightarrows HG \qquad K_a = \frac{[HG]}{[H][G]} \ (eq.2.1)$$

Where [H], [G], [HG] and K_a correspond to the host, guest and the host:guest equilibrium concentration and affinity constant, respectively. The practical methodologies developed to calculate the affinity constant include the addition of small aliquots of a guest stock solution to a solution of host and measuring the optical properties of the resulting solution. During this study UV-Vis titrations were undertaken.

The UV-Vis spectrophotometric titration is a very sensitive technique that allows detection at very low concentrations. It has, however, some limitations: the host and the complex must be UV-Vis active and they must absorb at different wavelengths. This technique (UV-Vis spectroscopy) also admits the determination of the stoichiometry of the complex HG by the application of the Job method. Nevertheless the last, shows many limitations, particularly when dealing with stoichiometries higher than 1:1 HG [49].

The anion binding tests were followed by UV-Vis spectroscopy using DMSO as solvent and carried out at 22 °C, with several anions such as fluoride, chloride, bromide, acetate, dihydrogen phosphate, nitrate and nitrite as their tetrabutylammonium salt form. The determination of the affinity constants were achieved with non-linear regression (2:1, 1:1 and 1:2 Host:Guest complex) based on equilibrium equations and Lambert-Beer law equations (2.2) (2.3) and (2.4):

Non-linear regression for the 2:1 (Host:Guest) complex (K_a units are given in M^{-2})

$$\frac{\Delta A}{l} = \frac{[H].K_{11}.\Delta\epsilon_{11}.[G] + K_{11}.K_{21}.\Delta\epsilon_{21}.[H][G]}{1 + K_{11}.[G] + K_{11}.K_{21}.[G][H]} \ (eq.2.2)$$

Non-linear regression for the 1:1 (Host:Guest) complex (K_a units are given in M^{-1})

$$\frac{\Delta A}{l} = \frac{[H].K.\Delta\epsilon.[G]}{1 + K.[G]} \ (eq.2.3)$$

Non-linear regression for the 1:2 (Host:Guest) complex (K_a units are given in M^{-2})

$$\frac{\Delta A}{l} = \frac{[H].K_{11}.\Delta\epsilon_{11}.[G] + K_{11}.K_{12}.\Delta\epsilon_{12}.[G]^2}{1 + K_{11}.[G] + K_{11}.K_{12}.[G]^2} \quad (eq.2.4)$$

Here, ΔA is the absorbance variation, l the path length the, K_a the affinity constant (K_{11} and K_{12} are the partial affinity constants, the global affinity constant are given by the product K_a=K_{11}*K_{12}), Δε is the molar absorptivity coefficient, [H] the concentration of the host (chemosensor) and [G] the concentration of guest (anion).

The binding properties of compounds **2.16**, **2.17**, **2.19** and **2.20** can be studied through different techniques, however the technique of choice by convenience was the UV-Vis spectroscopy, in DMSO and carried out at 22 °C, with several anions such as fluoride, chloride, bromide, acetate, dihydrogen phosphate, nitrate and nitrite as their tetrabutylamonium salts.

2.2.3.3. Results and discussion

These new compounds display a strong UV-Vis spectrum, showing the maximum of absorbance at 505 and 517 nm for compound **2.16** and **2.17**, respectively while the DPM based compounds show their maxima at 465 and 409 nm for compound **2.19** and **2.20** respectively (Figure 2.16). The interaction between these compounds with different anions was studied by UV-Vis tracking the corresponding perturbation in each sensor.

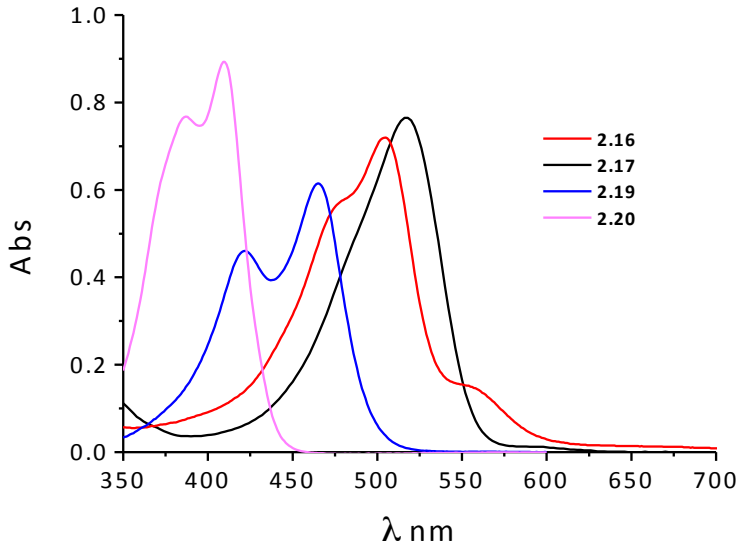

Figure 2.16: UV-Vis spectrum of compound **2.16**, **2.17**, **2.19** and **2.20**.

The perturbation in UV-Vis spectra caused by the addition of anions was recorded and the graphics of ΔAbs *vs* anion concentration were plotted and treated with a standard 1:1 non-linear equation. This treatment leads to a poor fit of the experimental data and higher residual values. In fact, the presence of more than one isosbestic point and the shape of the curves point to a more complex stoichiometry rather than a 1:1 stoichiometry.

In order to better understand the interaction processes we decided to apply the tree possible equations describing the formation of 2:1, 1:1 and 1:2 complex stoichiometry (see figure 2.17 and 2.18).

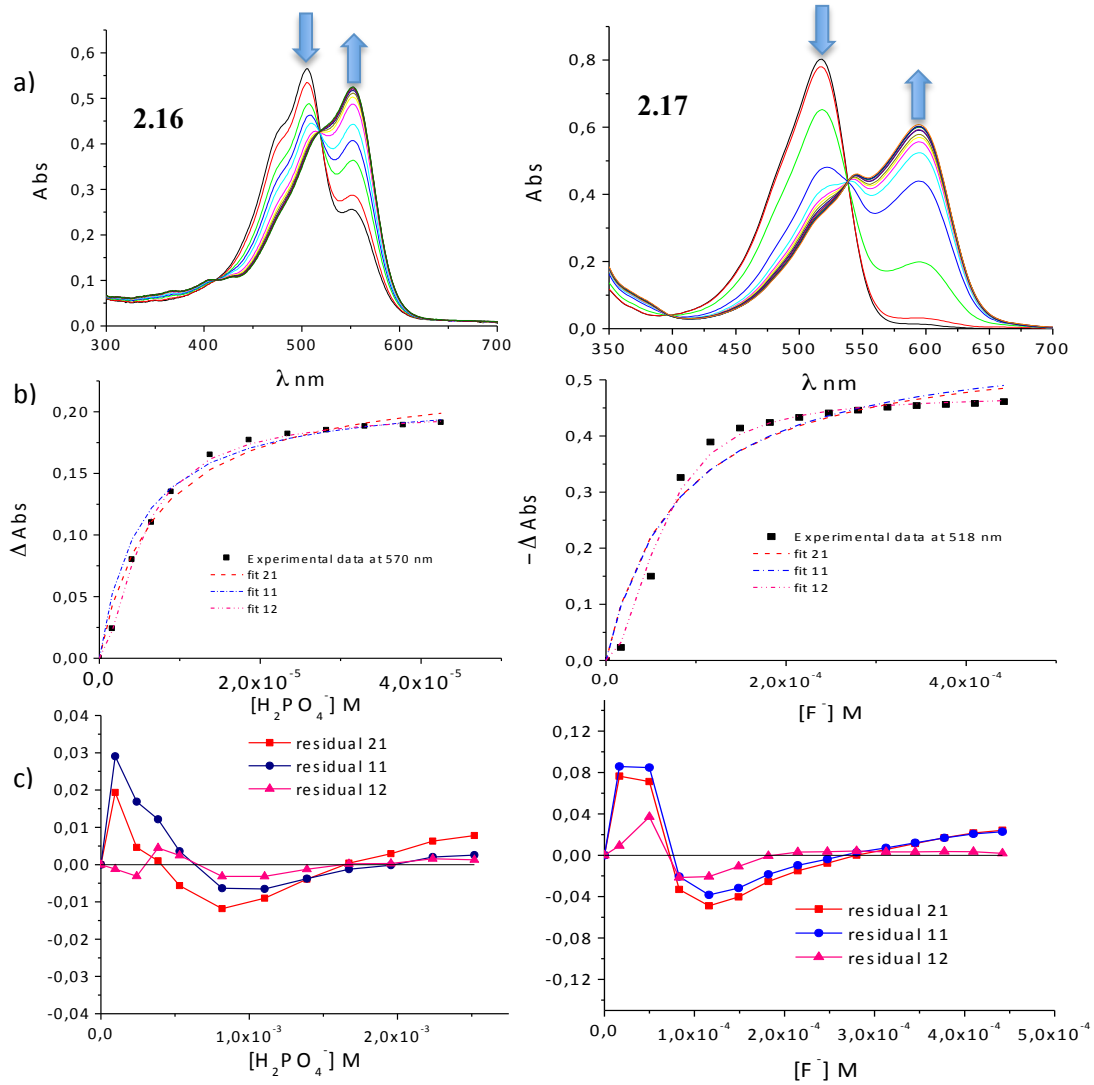

Figure 2.17: a) Titration examples of **2.16** with dihydrogen phosphate and **2.17** with fluoride anions in DMSO; b) Experimental data and fit titration for **2.16** and **2.17**; c) Residuals obtained in the treatment applied to the experimental fit.

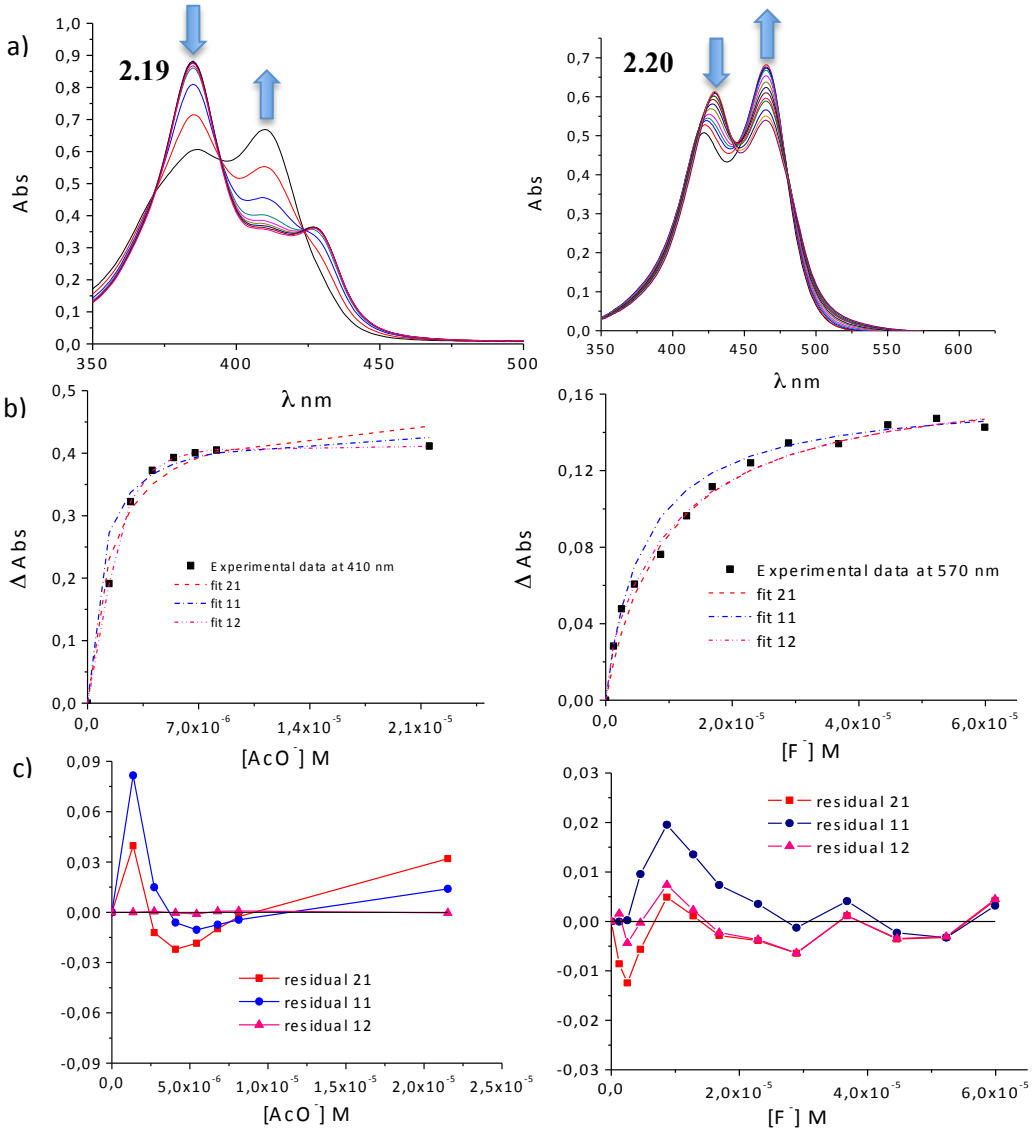

Figure 2.18: a) Titration examples of **2.19** with acetate and **2.20** with fluoride anions in DMSO; b) Experimental data and fit titration for **2.19** and **2.20**; c) Residuals obtained in the treatment applied to the experimental fit.

As can be observed, the best fit in these experimental data were obtained for the stoichiometry 1:2 (Host:Guest). In order to verify this behavior in a structural perspective we performed ^{1}H-NMR titrations with compound **2.20** and fluoride anion.

When the complex is formed a change of the chemical shift of the receptor protons is observed, because, in the complex, the magnetic field around the nucleus is not equivalent to the field in the uncomplexed host. The chemical shift of a proton will be the

average signal from the free host and from the host associated with the guest, provided that the exchange is fast on the NMR timescale.

Upon addition of the guest to a solution of receptor **2.20**, the pyrrolic (H_a, figure 2.19) protons shifted about δ 6.5 ppm downfield, which is the typical behavior of a proton involved in a hydrogen bond interaction. The signal belonging to the *β*-pyrrolic protons H_c had an upfield movement while the H_b had a downfield movement. These protons were not directly involved in the hydrogen bond but its change in chemical shift was a consequence of the binding process up to 0.5 eq. of anion. At the same time the data provided from the NMR clearly shows a loss of resolution with an increase broadening of all the signals in the spectra with increasing additions of fluoride anion. These results allowed us to assume that two phenomena were occurring simultaneously: hydrogen bonding (once the NH start to move to higher ppm) and deprotonation (once the peaks broadening occur at 0.5 equivalents of anion).

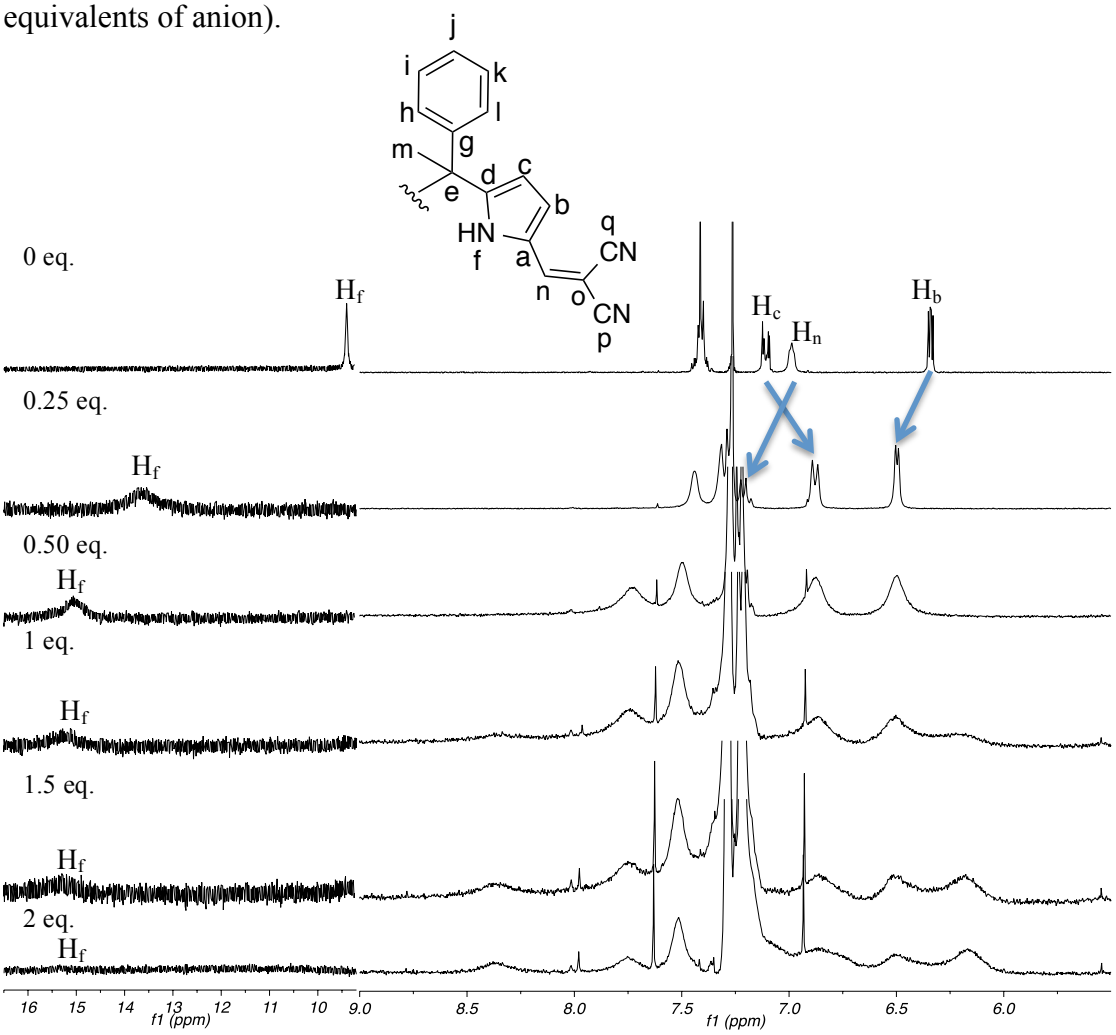

Figure 2.19: ^{1}H NMR titration of compound **2.20** in $CDCl_3$ with fluoride anion.

After the treatment of all experimental data, we were able to obtain the affinity constants for all the sensors (table 2.4).

Table 2.4: Affinity constants ($K = K_{11} \times K_{12}$, M^{-2}) at 22 °C for compounds **2.16**, **2.17**, **2.19** and **2.20**.

	2.16	2.17	2.19	2.20
F^-	7.39×10^9	3.96×10^8	2.81×10^8	3.19×10^9
AcO^-	1.42×10^8	2.16×10^8	1.43×10^8	6.77×10^8
$H_2PO_4^-$	1.50×10^7	5.88×10^6	-	5.21×10^7
$K AcO^-/H_2PO_4^-$	9.5	36.7		13.0

Comparing our sensors, it is clear that the presence of the cyano groups increase the affinity to the studied anions. It is also interesting to note that the selectivity for the acetate anion when compared with $H_2PO_4^-$ dramatically increases in the sensor **2.17** bearing the indane-1,3-dione moieties. With compound **2.17** the affinity constant ratio $K AcO^-/H_2PO_4^-$ is 36.7 and in the case of compound **2.19** the addition of $H_2PO_4^-$ anion do not causes any perturbation in the UV-Vis spectrum.

Dichloromethane solutions of sensors show the early anticipated naked-eye detection with the changing coloration after the addition of fluoride or acetate, dihydrogen phosphate and, to a lesser extent, chloride anions (Figure 2.20). No color changes are observed after the addition of bromide, nitrate, and nitrite anions. The color changes observed are thus directly related with the values of the affinity constants.

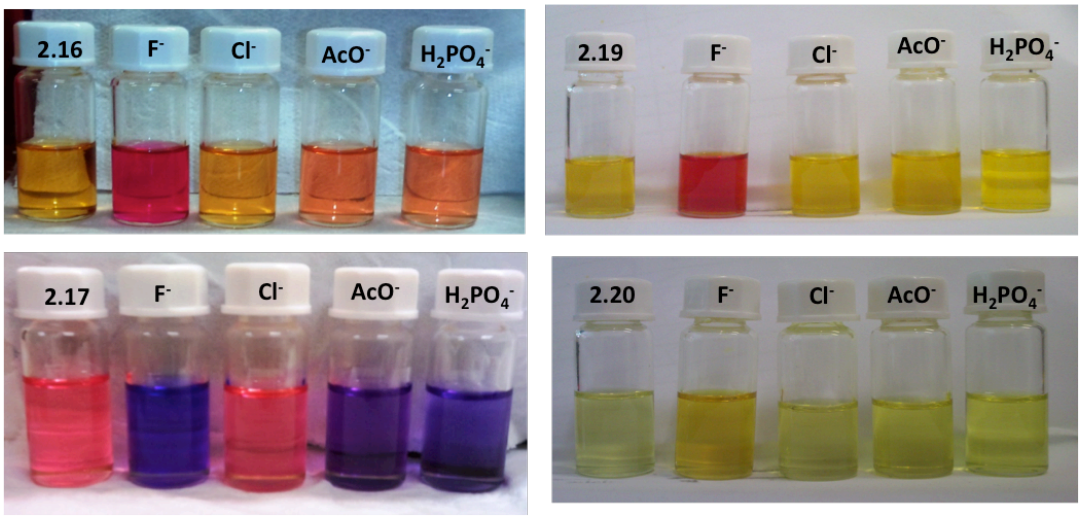

Figure 2.20: Changes in the coloration of sensors in CH_2Cl_2, upon anion addition.

In conclusion highly chromogenic sensors can be obtained from the reaction between bipyrrole units and active methylene compounds in moderate to good yields. These new sensors showed high affinity constants for fluoride, acetate and dihydrogen phosphate anions. It is also important to note that sensor **2.17** exhibited an affinity constant ratio $KAcO^-/H_2PO_4^-$ of 36.7.

2.3. Experimental

2.3.1. General

All reactions, unless otherwise stated, were routinely carried out under nitrogen atmosphere. Organic extracts were dried over anhydrous Na_2SO_4 and evaporated, after filtration, using a Buchi rotary evaporator. Tetrahydrofuran (THF) and toluene solvents were used dried over sodium. Anhydrous dichloromethane was freshly distilled from calcium hydride; DMF was stored over 4 Å molecular sieves. Pyrrole, phosphoryl chloride and thionyl chloride were all distilled immediately prior to use. Experiments were monitored using TLC analysis performed on Merck Kieselgel 60 F254 silica gel or, aluminum oxide 150 F 254 neutral (type T) 0.2 mm coated plastic plates with fluorescent indicator and developed with iodine vapour and vanillin solution when necessary, whilst column chromatography employing silica gel 60 (0.040-0.063 or 230-400 mesh), supplied by E. Merck Co.

^{1}H-NMR (300 MHz) and ^{13}C-NMR (75 MHz) spectra were recorded on a Brucker AC 300 or 500 instruments. Chemical shifts are reported as δ-values in ppm relative to TMS. UV-

Vis spectra were recorded on a Shimadzu spectrophotometer. The mass analyses were conducted in a MALDITOF/ TOF 4800 Applied Biosystems spectrometer.

Deuterated chloroform for NMR spectra was used as it is. Other solvents used in reactions were used as they were from the different brands. The solvents used in this work were purchased from different brands like Fluka, Merck, and Acros.

2.3.2. Experimental procedures

Synthesis of 2,2'-bipyrrole intermediate ***1.35***

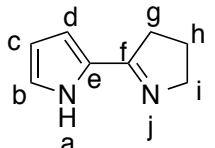

1.35

Chemical Formula: $C_8H_{10}N_2$
Exact Mass: 134.08

A round bottom flask containing freshly distilled pyrrole (25 mL, 36 mmol), pyrrolidin-2-one (12.8 mL, 168 mmol) and 1,2-dichloroethane (200 mL) was cooled to 0 °C and equipped with an addition funnel containing $POCl_3$ (26.2 mL, 279 mmol) and a magnetic stirring bar. $POCl_3$ was added dropwise over 1 h. At the end of the addition, the reaction medium was allowed to warm up to room temperature and stirred vigorously for 2 hours. The reaction mixture was then quenched with an aqueous solution of KOH (10 M). After neutralization the mixture was extracted with CH_2Cl_2 (3x100 mL). The combined organic phases were washed with H_2O (100 mL) and dried over anhydrous Na_2SO_4. Concentration under vacuum and further crystallization from $CHCl_3$ yielded the desired product as a white powder (14.4 g, η = 60%).

^{1}H-NMR (300 MHz, $CDCl_3$) δ 6.93 (dd, J = 10.4, 5.2 Hz, 1H, α-pyrrolic H_b), 6.54 (dd, J = 3.6, 1.4 Hz, 1H, β-pyrrolic H_d), 6.27 – 6.19 (m, 1H, β-pyrrolic H_c), 4.09 – 3.93 (m, 2H, H_i), 2.90 (m, 2H, H_g), 2.09 – 1.93 (m, 2H, H_h).
^{13}C-NMR (75 MHz, $CDCl_3$) δ 166.3 (C_e), 127.6 (C2), 122.0 (C4), 113.2 (C3), 109.2 (C6), 60.3 (C9), 34.9 (C7), 22.6 (C8).
ESI (TOF MS): m/z = 135.1 $[M+H]^+$

*Synthesis of 2,2'-bipyrrole **1.36***

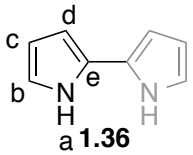

1.36

Chemical Formula: $C_8H_8N_2$
Exact Mass: 132.07

In a 250 mL round bottom flask equipped with a condenser and a stirring, **1.35** (3.0 g, 22 mmol) was dissolved in *p*-cymene (80 mL) followed by the addition of Pd (5%) charcoal (1.5 g). The reaction mixture was allowed to heat until reflux, and was left to react during 3 h. Meanwhile, the reaction was monitored by TLC. After cooling, the reaction mixture was filtrated and purified by column chromatography on silica gel, using petroleum ether-dichloromethane (1:1) as eluent, giving **1.36** as a light green solid (0.8 g, η = 30%).

^{1}H NMR (300 MHz, $CDCl_3$) δ 8.24 (s, 2H, NH, H_a), 6.77 (dd, J = 2.6, 1.6 Hz, 2H, α-pyrrolic H_b), 6.26-6.20 (m, 4H, β-pyrrolic H_c and H_b).
^{13}C NMR (75 MHz, $CDCl_3$) δ 125.9 (α-pyrrolic C_e), 117.6 (α-pyrrolic C_b), 109.4 (β-pyrrolic C_d), 103.5 (β-pyrrolic C_c).
ESI (TOF MS): m/z = 133.0 $[M+H]^+$

*General procedure for the preparation of dipyrromethanes **2.6-2.9***

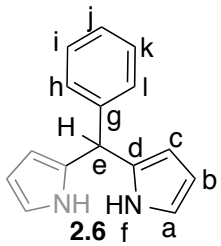

2.6

Chemical Formula: $C_{15}H_{14}N_2$
Exact Mass: 222.12

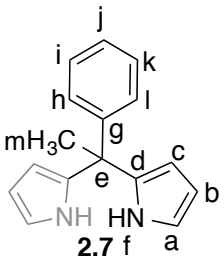

2.7

Chemical Formula: $C_{16}H_{16}N_2$
Exact Mass: 236.13

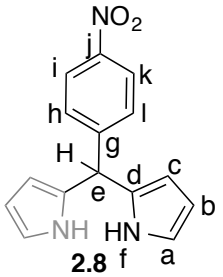

2.8

Chemical Formula: $C_{15}H_{13}N_3O_2$
Exact Mass: 267.10

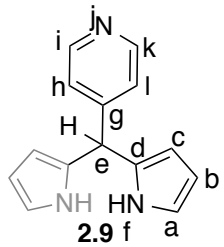

2.9

Chemical Formula: $C_{14}H_{13}N_3$
Exact Mass: 223.11

To 100 mL of 0.18 M aqueous HCl, pyrrole (3 eq. or 6 eq.) was added, followed by the addition of the appropriate aldehydes - (1 eq., 2 g). The reaction mixture was stirred at rt and the reaction progress was monitored by TLC. After the required time for each aldehyde/ketone (4h for aldehyde **2.1**, 4h for ketone **2.2**, 2h for aldehyde **2.3** and 6h for aldehyde **2.4**), the precipitated, which often sticks to the walls of the flask and the stirring bar and might hamper the stirring, was filtered off and washed with water and petroleum ether to afford aryl-DPM **2.6-2.9,** in 82, 76, 95 and 42%, respectively.

*dipyrromethane **2.6***

^{1}H NMR (300 MHz, $CDCl_3$) δ 7.93 (s, 2H, NH_f), 7.38 – 7.18 (m, 5H, phenyl H_h, H_i, H_j, H_k, H_l), 6.70 (dd, J = 2.7, 1.6 Hz, 2H, β-pyrrolic H_c), 6.16 (dd, J = 6.0, 2.7 Hz, 2H, β-pyrrolic H_b), 5.92 (dd, J = 3.4, 2.5 Hz, 2H, α-pyrrolic H_a), 5.48 (s, 1H, *meso* H_e).

^{13}C NMR (75 MHz, $CDCl_3$) δ 142.0 (C_g), 132.5 (C_j), 128.6 (C_h and C_l), 128.3 (C_i and C_k) 127.0 (C_d), 117.2 (C_a), 108.4 (C_d), 107.2, (C_b), 43.9 (C_e).

HRMS (ESI): *m/z* calculated for $C_{15}H_{15}N_2$ = 223.1229 $[M+H]^+$ found 223.1221

*dipyrromethane **2.7***

^{1}H NMR (300 MHz, $CDCl_3$) δ 7.77 (s, 2H, NH_f), 7.33 – 7.19 (m, 3H, *p*- and *o*-phenyl H_j, H_h and H_l), 7.15 – 7.09 (m, 2H, *m*-phenyl H_i and H_k), 6.67 (dd, J = 2.7, 1.6 Hz, 2H, β-pyrrolic H_c), 6.17 (dd, J = 3.3, 2.7 Hz, 2H, β-pyrrolic H_b), 5.97 (dd, J = 3.4, 2.7, 1H, α-pyrrolic H_a), 2.05 (s, 3H, CH_3, H_m).

^{13}C NMR (75 MHz, $CDCl_3$) δ 147.2 (C_g), 137.4 (C_j), 128.1 (C_h and C_l), 126.7 (C_i and C_k), 116.9 (C_a), 108.2 (C_d), 106.2 (C_b), 44.7 (C_e), 28.8 (C_m).

ESI (TOF MS): *m/z* = 259.0 $[M+Na]^+$

*dipyrromethane **2.8***

^{1}H NMR (300 MHz, $CDCl_3$) δ 8.21 – 8.14 (m, 2H, *o*-phenyl H_h and H_l), 8.01 (s, 2H, NH_f), 7.41 – 7.33 (m, 2H, *m*-phenyl H_i and H_k), 6.75 (dd, J = 2.7, 1.6 Hz, 2H, β-pyrrolic H_c), 6.18 (dd, J = 6.0, 2.8 Hz, 2H, β-pyrrolic H_b), 5.91 – 5.83 (m, 2H, α-pyrrolic H_a), 5.58 (s, 1H, *meso* H_e).

^{13}C NMR (75 MHz, $CDCl_3$) δ 149.6 (C_j), 146.9 (C_g), 130.8 (C_d), 129.2 (C_h and C_l), 123.9 (C_i and C_k), 118.0 (C_a), 108.8 (C_c), 107.8 (C_b), 43.8 (C_e).

HRMS (FAB+): *m/z* calculated for $C_{15}H_{14}N_3O_2$ = 268.1080 $[M+H]^+$, found = 268.1081
Melting Point: 158.0 ºC

*dipyrromethane **2.9***

^{1}H NMR (300 MHz, $CDCl_3$) δ 8.56 – 8.47 (m, 2H, *o*-pyridyl H_h and H_l), 8.08 (s, 2H, NH_f), 7.18 – 7.09 (m, 2H, *m*-pyridyl H_i and H_k), 6.74 (dd, J = 2.6, 1.5 Hz, 2H β-pyrrolic H_c), 6.17 (dd, J = 3.4, 2.7 Hz, 2H, β-pyrrolic H_b), 5.90 (dd, J = 3.4, 2.4, Hz, 2H, α-pyrrolic H_a), 5.46 (s, 1H, *meso* H_e).
^{13}C NMR (75 MHz, $CDCl_3$) δ 151.2 (C_g), 149.9 (C_h and C_l), 130.6 (C_d), 123.6 (Ci and Ck), 117.9 (C_a), 108.6 (C_c), 107.70 (C_b), 43.4 (C_e).
ESI (TOF MS): *m/z* = 223.1 $[M+H]^+$
Melting Point: 144.7 ºC

*Synthesis of dipyrromethane **2.10***

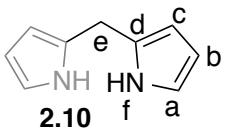

2.10

Chemical Formula: $C_9H_{10}N_2$
Exact Mass: 146.08

A suspension of paraformaldehyde (**2.5**, 0.43 g, 14.4 mmol) in pyrrole (25 mL, 360 mmol) was placed in a 100 mL two-necked round-bottomed flask equipped with an internal thermometer and a water condenser in the reflux position. The solution was heated to 65 °C, and then the heat source was removed and TFA (0.11 mL, 0.14 mmol) was added immediately. A sharp increase in the temperature of the solution was observed up to 80 ºC and the solution rapidly became clear and dark. After 5 min the reaction was quenched with a 0.1 M solution of NaOH and the product was purified by evaporation of the pyrrole followed by silica gel chromatography using CH_2Cl_2/hexane (1:1) with 1% NEt_3. Recrystallization from ethanol/hexane 1:1) furnished **2.10** (0.85 g, 40%) as colorless crystals.

^{1}H NMR (300 MHz, $CDCl_3$) δ 7.79 (s, 2H, NH_f), 6.63 (q, J = 2.3 Hz, 2H, β-pyrrolic H_c), 6.15 (q, J = 2.9 Hz, 2H, β-pyrrolic H_b), 6.03 (s, 2H, α-pyrrolic H_a), 3.95 (s, 2H, *meso* H_e).
^{13}C NMR (75 MHz, $CDCl_3$) δ 129.1 (C_d), 117.3 (C_a), 108.3 (C_c), 106.4 (C_b), 26.3 (C_e).
ESI (TOF MS): *m/z* = 185.1 $[M+K]^+$

Melting Point: 76.7 ºC

Synthesis of bipyrrole ***2.11***

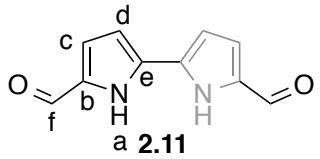

Chemical Formula: $C_{10}H_8N_2O_2$
Exact Mass: 188.06

In a sealed round bottom flask containing **1.36** (1 g, 7.56 mmol), and purged with N_2, dried DMF (4.6 mL, 58.451 mmol) was added with a syringe. After this the mixture was cooled to 0 °C and $POCl_3$ (2.17 mL, 23.90 mmol) was added dropwise over 15 min. At the end of the addition, the reaction medium was heated to 60 ºC for 1 hour. Later, an aqueous solution of NaOAc (3 M) was added to the mixture with a syringe and the mixture was maintained for 2 hours at 80 ºC. After completion of these tasks, the mixture was filtrated and the yellow-green solid obtained was dried in vacuum and used without further purification (1.3 g, η = 84%).

^{1}H NMR (300 MHz, $CDCl_3$) δ 11.89 (s, 2H, NH_a), 9.31 (s, 2H, CHO, H_f), 6.76 (dd, J = 3.9, 2.3 Hz, 2H, β-pyrrolic H_c), 6.46 (dd, J = 3.9, 2.4 Hz, 2H, β-pyrrolic H_d).
^{13}C NMR (75 MHz, $CDCl_3$) δ 178.1 (CHO, C_f), 132.9 (C_b), 131.2 (C_e), 121.3 (C_d), 109.5 (C_c).
ESI (TOF MS): m/z = 189.1 $[M+H]^+$
Melting Point: > 350 ºC

Synthesis of bipyrrole ***2.12***

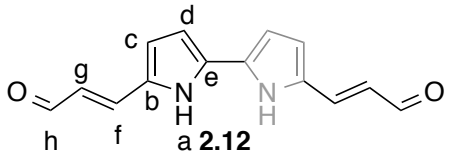

Chemical Formula: $C_{14}H_{12}N_2O_2$
Exact Mass: 240.09

In a sealed round bottom flask containing **1.36** (1 g, 7.56 mmol, and purged with N_2, 3-(dimethylamino)acrylaldehyde (1.57 g, 15.9 mmol) dissolved in dichloroethane (10 mL) was added with a syringe. After this the mixture was cooled to 0 °C and $POCl_3$ (2.17 mL, 23.9 mmol) was added dropwise over 15 min. At the end of the addition, the reaction was allowed to react at rt during 4 h. Later, an aqueous solution of NaOH (3 M) was added to the mixture with a syringe and maintained for 6 hours at rt. After completion of these tasks,

the mixture was filtrated and the reddish solid obtained was recrystallized in ethanol, dried in vacuum and used without further purification (1.2 g, η = 82%).

^{1}H NMR (300 MHz, DMSO) δ 11.74 (s, 2H, NH_a), 9.50 (d, J = 8.0 Hz, 2H, CHO, H_h), 7.45 (d, J = 15.6 Hz, 2H, H_f), 6.78 (d, J = 1.9 Hz, 4H, β-pyrrolic H_c and H_d), 6.60 (dd, J = 15.6, 8.0 Hz, 2H, H_g).

^{13}C NMR (75 MHz, DMSO) δ 193.0 (CHO, C_h), 141.6 (C_g), 138.2 (C_b), 129.6 (C_f), 122.1 (C_e), 118.7 (C_d), 109.5 (C_c).

ESI (TOF MS): m/z = 274.3 $[M+Na]^+$

Melting Point: > 350 ºC

*General procedure for the synthesis of dipyrromethanes **2.13-2.15***

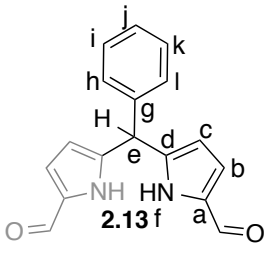

Chemical Formula: $C_{17}H_{14}N_2O_2$
Exact Mass: 278.11

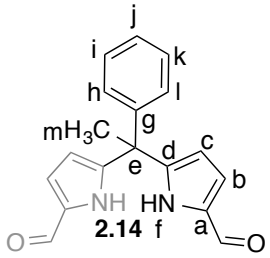

Chemical Formula: $C_{18}H_{16}N_2O_2$
Exact Mass: 292.12

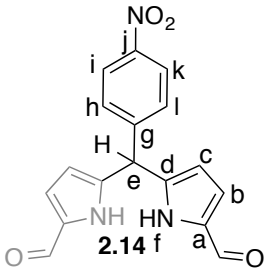

Chemical Formula: $C_{17}H_{13}N_3O_4$
Exact Mass: 323.09

Dimethylformamide (6.1 mmol) was added to a 100 mL round-bottomed flask, cooled to 0 ºC, and flushed with nitrogen for 5 min. $POCl_3$ (5.0 mmol) was added dropwise over 15 min with stirring. Dry dichloromethane (10 mL) was then added, and the mixture was stirred at room temperature for 15 min. The mixture was cooled again to 0 ºC, the correspond aryl-DPM **2.6-2.8** were added (3.25 mmol) in dichloromethane (20 mL) dropwise over 30 minutes. After this addition the mixture was allowed to react at room temperature during 1 h. Before finishing the reaction the mixture was warmed to 40 ºC for 15 min and then allowed to cool to room temperature. A saturated sodium carbonate (50 mL) was added, and the reaction was stirred vigorously at room temperature for 12 h. The mixture was extracted with ethyl acetate (3x100 mL), and the combined organic layers were dried over Na_2SO_4, filtered, and evaporated. The crude compound was subjected to silica gel column chromatography and eluted with petroleum ether/ethyl acetate (70:30),

which afforded pure 1,9-diformyl-DPM **2.13**, **2.14** and **2.15** as light-brown solids in 60, 65 and 63% yield, respectively.

*dipyrromethane **2.13***

^{1}H NMR (300 MHz, $CDCl_3$) δ 10.57 (s, 2H, NH_f), 9.19 (s, 2H, CHO, H_n), 7.47 – 7.21 (m, 6H, phenyl H_h, H_i, H_j, H_k and H_l), 6.86 (dd, J = 3.9, 2.4 Hz, 2H, β-pyrrolic H_c), 6.06 (dd, J = 3.9, 2.4, 2H, β-pyrrolic H_b), 5.58 (s, 1H, *meso* H_e).

^{13}C NMR (75 MHz, $CDCl_3$) δ 179.0 (CHO, C_n), 141.6 (C_a), 139.1 (C_g), 132.6 (C_j), 129.0 (C_h and C_l), 128.4 (C_i and C_k), 127.7 (C_c), 122.3 (C_d), 111.6 (C_b), 44.4 (C_e).

ESI (TOF MS): m/z = 279.1 $[M+H]+$

Melting Point: 118.3 ºC

*dipyrromethane **2.14***

^{1}H NMR (300 MHz, $CDCl_3$) δ 9.80 (s, 2H, NH_f), 9.57 (s, 2H, CHO, H_n) 7.37 – 7.23 (m, 3H, *p*- and *o*-phenyl H_j, H_h and H_l), 7.14 – 7.05 (m, 2H, *m*-phenyl H_i and H_k), 6.89 (dd, J = 3.9, 2.4 Hz, 2H, β-pyrrolic H_c), 6.14 (dd, J = 3.9, 2.6 Hz, 2H, β-pyrrolic H_b), 2.12 (s, 3H, *meso*-CH_3, H_m).

^{13}C NMR (75 MHz, $CDCl_3$) δ 179.0 (CHO, C_n), 145.5 (C_a), 144.4 (G_g), 132.6 (C_j), 128.7 (C_h and C_l), 127.6 (C_c), 127.1 (C_i and C_k), 121.8 (C_d), 110.4 (C_b), 45.5 (C_e), 28.4 (C_m).

ESI (TOF MS): m/z = 331.1 $[M+K]^+$

Melting Point: > 223.4 ºC

*dipyrromethane 2**.15***

^{1}H NMR (300 MHz, $CDCl_3$) δ 10.73 (s, 2H, NH_f), 9.24 (s, 2H, CHO, H_n), 8.26 – 8.15 (m, 2H, *o*-phenyl H_h and H_l), 7.70 – 7.58 (m, 2H, *m*-phenyl H_i and H_k), 6.92 (dd, J = 3.9, 2.5 Hz, 2H, β-pyrrolic H_c), 5.99 (dd, J = 4.0, 2.5 Hz, 2H, β-pyrrolic H_b), 5.71 (s, 1H, H_e).

^{13}C NMR (126 MHz, $CDCl_3$) δ 179.9 (CHO, C_n), 149.2 (C_j), 147.7 (C_a), 143.5 (C_j), 132.5 (C_i and C_k), 127.6 (C_c), 123.5 (C_h and C_l), 122.4 (C_d), 111.7 (C_b), 73.9 (C_e).

ESI (TOF MS): m/z = 362.1 $[M+K]^+$

Melting Point: > 137.8 ºC

*General procedure for the preparation of bipyrroles **2.16** and **2.17***

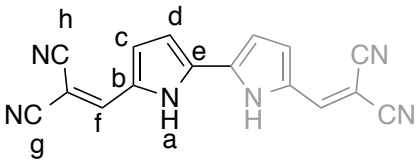

Chemical Formula: $C_{16}H_8N_6$
Exact Mass: 284.08

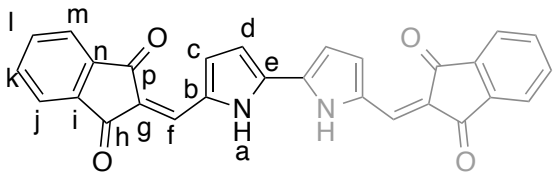

Chemical Formula: $C_{28}H_{16}N_2O_4$
Exact Mass: 444.11

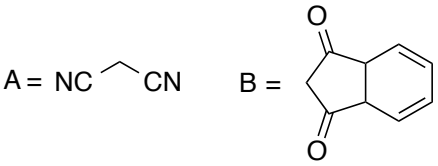

To a stirred solution of **2.11** (50 mg, 0.26 mmol) in DMSO (3 mL), a catalytic amount of NEt_3, A or B (3 eq.) and 4A molecular sieves were added. The reaction was left at 80 ºC for 12 h and was followed by TLC. After stirring for the required time, the reaction was allowed to cool to room temperature and after this chloroform was added to the mixture. After 1 h the precipitate was filtered and the brown solid was characterized without further purification (yield = 76%). Compound **2.17** synthesized according the same procedure changing the NEt_3 for piperidine and purification over silica gel afforded a yield of 16%.

*bipyrrole **2.16***

^{1}H NMR (300 MHz, DMSO-d_6) δ 12.76 (s, 2H, NH_a), 7.82 (s, 2H, H_f), 7.54 – 7.45 (d, J = 4.5, 2H, β-pyrrolic H_d), 7.06 (d, J = 4.4 Hz, 2H, β-pyrrolic H_c).

^{13}C NMR (75 MHz, DMSO-d_6) δ 145.5 (C_f), 131.8 (C_b), 128.3 (C_e), 119.4 (C_d), 115.6 (C_g), 115.0 (C_h), 113.3 (C_c).

HRMS (ESI): *m/z* calculated for $C_{16}H_9N_6$ = 285.0883 $[M+H]^+$ found 285.0872

ESI (TOF MS): *m/z* = 307.0 $[M+Na]^+$

Melting Point: > 350 ºC

*bipyrrole **2.17***

^{1}H NMR (300 MHz, DMSO-d_6) δ 13.41 (d, J = 1.5 Hz, 2H, NH_a), 7.98 – 7.88 (m, 8H, H_j H_k H_l H_m), 7.78 (s, 2H, H_f), 7.31 (d, J = 2.9 Hz, 2H, β-pyrrolic H_d), 6.93 (d, J = 4.1 Hz, 2H, β-pyrrolic H_c).

HRMS (ESI): *m/z* calculated for $C_{28}H_{17}N_2O_4$ = 445.1182 $[M+H]^+$ found 445.1178

ESI (TOF MS): *m/z* = 445.1 $[M+H]^+$

Melting Point: > 350 ºC

Synthesis of dipyrromethanes ***2.18***

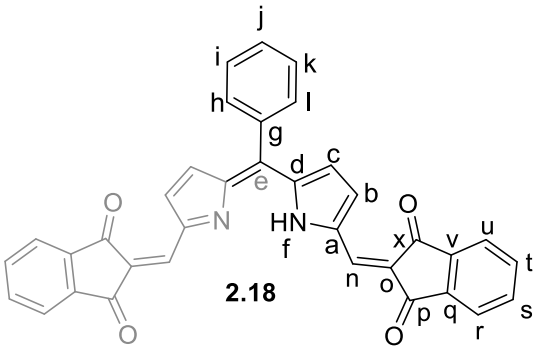

Chemical Formula: $C_{35}H_{20}N_2O_4$
Exact Mass: 532.14

To stirred solution of indane-1,3-dione (3 eq.) in $CHCl_3$ (3 mL), a catalytic amount of NEt_3 and diformyl-DPM **2.13** (0.10 mmol) were added in the presence of 4A molecular sieves. The reaction was left at rt until complete consumption of the starting material. After stirring for the required time, the reaction was evaporated under vacuum and the dark residues re-dissolved in $CHCl_3$ and a few drops of hexane. The yellowish products were filtered providing **2.18** (yield = 32%)

^{1}H NMR (300 MHz, DMSO-d_6) δ 13.23 (s, 2H, H_f), 7.88 (m, 8H, H_r, H_s H_t and H_u), 7.73 (s, 2H, H_n), 7.53 – 7.28 (m, 7H, phenyl H_h, H_i, H_j, H_k, H_l and β-pyrrolic, H_c), 6.50 (d, J = 3.1 Hz, 2H, β-pyrrolic H_b), 5.77 (s, 1H, H_e).

^{13}C NMR (75 MHz, DMSO-d_6) δ 191.6 (C_p), 190.6 (C_x), 147.9 (C_o), 140.7 (C_q), 139.6 (C_v), 138.2 (C_s), 135.5 (C_t) 135.3 (C_n), 132.4 (C_a), 129.6 (C_i and C_k), 128.7 (C_j), 128.5 (C_c), 126.6 (C_h and C_l), 122.7 (C_r), 122.5 (C_u), 121.7 (C_d), 113.6 (C_b), 74.1 (C_e).

HRMS (ESI): *m/z* calculated for $C_{35}H_{21}N_2O_4$ = 533.1495 $[M+H]^+$ found 533.1486

ESI (TOF MS): *m/z* = 533.2 $[M+H]^+$

Melting Point: 229.8 ºC

*Synthesis of dipyrromethanes **2.19-2.20***

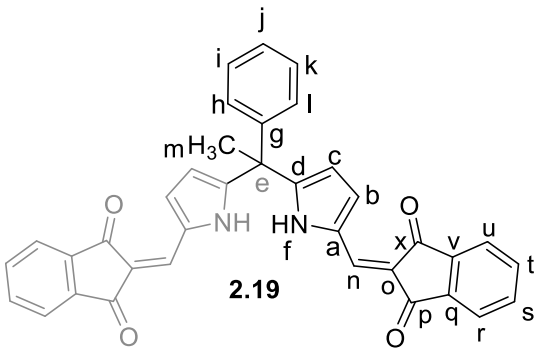

Chemical Formula: $C_{36}H_{24}N_2O_4$
Exact Mass: 548.17

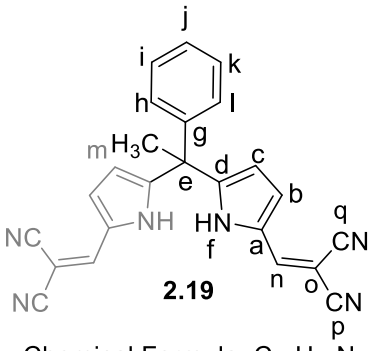

Chemical Formula: $C_{24}H_{16}N_6$
Exact Mass: 388.14

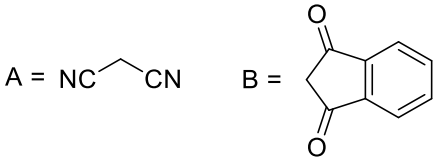

To stired solution of A or B (3 eq.) in $CHCl_3$ (3 mL), a catalytic amount of NEt_3 and diformyl-DPM **2.14** (30 mg, 0.10 mmol) were added in the presence of 4Å molecular sieves. The reaction was left at rt until complete consumption of the starting material. After stirring for the required time, the reaction was evaporated under vacuum and the dark residues purified by flash silica gel chromatography (eluent: dichloromethane) The yellowish/orange fractions were collected and crystalized in mixtures of $CHCl_3$/ hexane providing **2.19** (yield = 58%) and **2.20** (yield = 70%).

*dipyrromethane **2.19***

^{1}H NMR (300 MHz, $CDCl_3$) δ 13.26 (s, 1H, NH_f), 7.87 – 7.84 (m, 2H, H_u), 7.78 – 7.75 (m, 2H, H_r), 7.72 – 7.62 (m, 6H, H_n, H_s and H_t), 7.46 – 7.31 (m, 3H, H_h, H_l, and H_k), 7.24 – 7.20 (m, 2H, H_i and H_j), 7.07 (dd, J = 4.0, 2.1 Hz, 2H, β-pyrrolic H_c), 6.40 (dd, J = 4.0, 2.4 Hz, 2H, β-pyrrolic H_b), 2.42 (s, 3H, *meso* H, H_m).

^{13}C NMR (75 MHz, $CDCl_3$) δ 192.0 (C_p), 190.7 (C_x), 148.6 (C_o), 141.1 (C_q), 140.1 (C_v), 134.6 (C_s), 134.3 (C_t), 132.7 (C_n), 130.6 (C_a), 128.8 (C_i, C_k), 127.7 (C_j), 127.2 (C_c), 127.1 (C_h and C_l), 122.6 (C_r), 122.4 (C_u), 119.8 (C_d), 114.2 (C_b), 46.5 (C_e), 27.01 (C_m).

HRMS (ESI): *m/z* calculated for $C_{36}H_{25}N_2O_4$ = 549.1808 $[M+H]^+$ found 549.1803

ESI (TOF MS): *m/z* = 571.2 $[M+Na]^+$

Melting Point: 271.7 ºC

dipyrromethane ***2.20***

^{1}H NMR (300 MHz, $CDCl_3$) δ 9.37 (s, 2H, Hf), 7.44 – 7.37 (m, 5H, phenyl H_h, H_i, H_j, H_k and H_l), 7.15 – 7.07 (m, 2H, β-pyrrolic H_c), 7.03 – 6.97 (m, 2H, H_n), 6.44 – 6.04 (m, 2H, β-pyrrolic H_b), 2.17 (s, 3H, CH_3, H_m).

^{13}C NMR (75 MHz, $CDCl_3$) δ 147.7, 145.4, 142.2 (C_g), 129.5, 128.6 (C_p), 126.7 (C_q), 126.6, 125.7, 115.6, 114.3 (C_d), 112.1 (C_b) 46.0 (C_e), 27.3 (C_m).

HRMS (ESI): *m/z* calculated for $C_{24}H_{17}N_6$ = 389.1509 $[M+H]^+$ found 389.1505

ESI (TOF MS): *m/z* = 411.1 $[M+Na]^+$

Melting Point: 188.2 ºC

2.3.3. UV-Vis binding studies

Obtaining association constants by UV-Vis titration experiments involves titration of a solution of host with a specific guest and recording a UV-Vis spectrum after each addition. Anion was added by micropipete in a solution with a concentration two orders of magnitude higher than the host concentration previously prepared. The solution was manually stirred and the spectrum recorded again. This process was repeated until a titration data set was recorded. The instrument used was a UV-Vis - Shimadzu spectrophotometer.

After the data from the titration experiment have been acquired, curve-fitting equations are employed to determine the association constant. This was possible using different a set of equilibrium equations and the following approaches:

An equilibrium where two different species interact each other in a 1:1 fashion can be illustrated by the following equation:

$$H + G \overset{K_{11}}{\rightleftharpoons} HG$$

$$K_{11} = \frac{[HG]}{[H][G]} \qquad (2.1)$$

Where K_{11} is the affinity constant (mol^{-1} dm^3 (M^{-1})), H the host and G the guest or in this specific case the anion. Considering that the absorptivity of all species are within the limits of linearity comprehended in Lambert-Beer law a set of distinct molar absorptivity is chosen maintaining the wavelength constant.

Using the Lambert-Beer law and considering that the initial concentration of Host is represented by $[H]_T$, the initial absorbance is interpreted by equation 2.5.

$$Abs_0 = \varepsilon_0 l[H]_T \qquad (2.5)$$

Aware that the absorbance of a solution at a certain wavelength is the average sum of the absorbance contributions of all species in solution is implicit that, in any point of the equilibrium the absorbance is given by equation 2.6.

$$Abs = \varepsilon_H l[H] + \varepsilon_G l[G] + \varepsilon_{11} l[HG] \qquad (2.6)$$

Where [G] e [H] match the anion and sensor concentration in the equilibrium and [HG] is corresponding to the concentration of the complex H:G, also in the equilibrium. Therefore, the mass balance of the species present in solution can be described by the following equations:

$$[H]_T = [H] + [HG] \qquad (2.7)$$
$$[G]_T = [A] + [HG] \qquad (2.8)$$

Here, $[G]_T$ matches to the total concentration of anion in the equilibrium. Combination of equation 2.6 with equations 2.7 and 2.8 it is possible to rewrite them in function of the absorptivity for the total concentrations of anion.

$$Abs = \varepsilon_s l[H]_T + \varepsilon_A l[G]_T + \Delta\varepsilon_{11} l[HG] \qquad (2.9)$$

Were $\Delta\varepsilon_{11} = \varepsilon_{11} - \varepsilon_H - \varepsilon_G$. In practical terms when the studied anions don't show any absorbance in the studied wavelengths the component associated with the anion concentration is eliminated in equation 2.9, since its irrelevance. This approach gives us equation 2.10.

$$Abs = \varepsilon_s l[H]_T + \Delta\varepsilon_{11} l[HG] \qquad (2.10)$$

The last equation can additionally be altered, eliminating the [HG] component applying equation (2.10), obtaining equation (2.11).

$$Abs = K_{11}\Delta\varepsilon_{11} l[H][G] + \varepsilon_s l[H]_T \qquad (2.11)$$

Since the variation of absorbance translates the formation of the complex the last equation can be further simplified obtaining 2.12.

$$\Delta Abs = K_{11}\Delta\varepsilon_{11} l [H][G] \quad (2.12)$$

Finally combing this equation with the mass balance of the sensor, results in equation 2.13, admitting the possibility to calculate the value of K_{11}.

$$\frac{\Delta Abs}{l} = \frac{[S]_T \, K_{11} \, \Delta\varepsilon_{11} \, [A]}{1 + K_{11}[A]} \quad (2.13)$$

From the experimental perspective after acquisition of all spectrum from the different additions of anion a constant wavelength is selected and the values of the absorbances are plotted against the concentration of anion. To this experimental plot equation 2.13 is adjusted to the plot using the least square method obtaining the value of K_{11}. This means that the overall solution minimizes the sum of the squares of the errors made in the results of the equation. The square sum difference between the theoretical curve given by the adjustment and the experimental data acquired are the residuals or χ^2.

2.4. References

1. Arsenault GP, Bullock E and Macdonald SF. *J. Am. Chem. Soc*. 1960; **82**: 4384-4389.

2. Taniguchi M, Balakumar A, Fan DZ, McDowell BE and Lindsey JS. *J. Porphyrins Phthalocyanines* 2005; **9**: 554-574.

3. Taniguchi M, Fan DZ and Lindsey JS. *Abstr. Pap. Am. Chem. S.* 2005; **230**: U3417-U3417.

4. Harmjanz M and Scott MJ. *Chem. Soc. Rev.* 2000: 397-398.

5. Cho WS, Kim HJ, Littler BJ, Miller MA, Lee CH and Lindsey JS. *J. Org. Chem.* 1999; **64**: 7890-7901.

6. Gryko D and Lindsey JS. *J. Org. Chem.* 2000; **65**: 2249-2252.

7. Terazono Y, North EJ, Moore AL, Moore TA and Gust D. *Org. Lett.* 2012; **14**: 1776-1779.

8. Boens N, Leen V and Dehaen W. *Chem. Soc. Rev.* 2012; **41**: 1130-1172.

9. Kamkaew A, Lim SH, Lee HB, Kiew LV, Chung LY and Burgess K. *Chem. Soc. Rev.* 2013; **42**: 77-88.

10. Ulrich G, Ziessel R and Harriman A. *Angew. Chem. Int. Ed.* 2008; **47**: 1184-1201.

11. Lee C-H and S. Lindsey J. *Tetrahedron* 1994; **50**: 11427-11440.

12. Gryko DT, Gryko D and Lee CH. *Chem. Soc. Rev.* 2012; **41**: 3780-3789.

13. Rohand T, Dolusic E, Ngo TH, Maes W and Dehaen W. *Arkivoc* 2007: 307-324.

14. Rapoport H and Castagno.N. *J. Am. Chem. Soc.* 1962; **84**: 2178-2181.

15. Rapoport H, Castagno.N and Holden KG. *J. Org. Chem.* 1964; **29**: 883-885.

16. Rapoport H and Holden KG. *J. Am. Chem. Soc.* 1962; **84**: 635-642.

17. Littler BJ, Miller MA, Hung CH, Wagner RW, O'Shea DF, Boyle PD and Lindsey JS. *J. Org. Chem.* 1999; **64**: 1391-1396.

18. Davis JT, Gale PA, Okunola OA, Prados P, Iglesias-Sanchez JC, Torroba T and Quesada R. *Nat. Chem.* 2009; **1**: 138-144.

19. Moore SJ, Haynes CJE, Gonzalez J, Sutton JL, Brooks SJ, Light ME, Herniman J, Langley GJ, Soto-Cerrato V, Perez-Tomas R, Marques I, Costa PJ, Felix V and Gale PA. *Chem. Sci.* 2013; **4**: 103-117.

20. Moore SJ, Wenzel M, Light ME, Morley R, Bradberry SJ, Gomez-Iglesias P, Soto-Cerrato V, Perez-Tomas R and Gale PA. *Chem. Sci.* 2012; **3**: 2501-2509.

21. Busschaert N, Kirby IL, Young S, Coles SJ, Horton PN, Light ME and Gale PA. *Angew. Chem. Int. Ed.* 2012; **51**: 4426-4430.

22. Gale PA, Busschaert N, Haynes CJE, Karagiannidis LE and Kirby IL. *Angew. Chem. Int. Ed.* 2014; **43**: 205-241.

23. Suksai C and Tuntulani T. *Top. Curr. Chem.* 2005; **255**: 163-198.

24. Suksai C and Tuntulani T. *Chem. Soc. Rev.* 2003; **32**: 192-202.

25. Aleskovic M, Basaric N, Halasz I, Liang X, Qin WW and Mlinaric-Majerski K. *Tetrahedron* 2013; **69**: 1725-1734.

26. Farinha ASF, Tome AC and Cavaleiro JAS. *Tetrahedron Lett.* 2010; **51**: 2184-2187.

27. Wong MW, Xie HF and Kwa ST. J. *Mol. Model.* 2013; **19**: 205-213.

28. Dehaen W, Gale PA, Garcia-Garrido SE, Kostermans M and Light ME. *New J. Chem.* 2007; **31**: 691-696.

29. Campas C, Dalmau M, Montaner B, Barragan M, Bellosillo B, Colomer D, Pons G, Perez-Tomas R and Gil J. *Leukemia* 2003; **17**: 746-750.

30. Diaz-Ruiz C, Montaner B and Perez-Tomas R. *Histol. Histopathol.* 2001; **16**: 415-421.

31. Liu P, Wang YY, Qi X, Gu QQ, Geng MY and Li J. *Plos One* 2013; **8**.

32. Han SB, Kim HM, Kim YH, Lee CW, Jang ES, Son KH, Kim SU and Kim YK. *Int. J. Immunopharmacol.* 1998; **20**: 1-13.

33. Perez-Tomas R and Vinas M. *Curr. Med. Chem.* 2010; **17**: 2222-2231.

34. Pandey R, Chander R and Sainis KB. *Curr. Pharm. Des.* 2009; **15**: 732-741.

35. Gale PA. Acc. Chem. Res. 2011; 44: 216-226.

36. Anzenbacher P, Try AC, Miyaji H, Jursikova K, Lynch VM, Marquez M and Sessler JL. *J. Am. Chem. Soc.* 2000; **122**: 10268-10272.

37. Sessler JL, Barkey NM, Pantos GD and Lynch VM. *New J. Chem.* 2007; **31**: 646-654.

38. Gale PA. *Chem. Commun.* 2005: 3761-3772.

39. de Silva AP, Gunaratne HQN, Gunnlaugsson T, Huxley AJM, McCoy CP, Rademacher JT and Rice TE. *Chem. Rev.* 1997; **97**: 1515-1566.

40. Gale PA, Garcia-Garrido SE and Garric J. *Chem. Soc. Rev.* 2008; **37**: 151-190.

41. Welz B and Sperling M. Atomic Absorption Spectrometry; Wiley- VCH: Weinheim, 1999

42. Taylor HE. Inductively coupled plasma- mass spectrometry: practices and techniques; Academic Press: San Diego, 2000

43. Anzenbacher P, Palacios MA, Jursikova K and Marquez M. *Org. Lett.* 2005; **7**: 5027-5030.

44. Gunnlaugsson T, Kruger PE, Jensen P, Tierney J, Ali HDP and Hussey GM. *J. Org. Chem.* 2005; **70**: 10875-10878.

45. Ali HDP, Kruger PE and Gunnlaugsson T. *New J. Chem.* 2008; **32**: 1153-1161.

46. Basurto S, Riant O, Moreno D, Rojo J and Torroba T. *J. Org. Chem.* 2007; **72**: 4673-4688.

47. Suksai C and Tuntulani T. *Angew. Chem. Int. Ed.* 2003; **32**: 192-202.

48. Nishiyabu R and Anzenbacher P. *J. Am. Chem. Soc.* 2005; **127**: 8270-8271.

49. Connors KA. Binding Constants, The Measurement of Molecular Complex Stability; Wiley & Sons: New York, 1987

3 Diels-Alder Reactions on Bipyrroles and Sapphyrins

3. Diels-Alder Reactions on Bipyrroles and Sapphyrins

3.1. Overview

The Diels-Alder (D-A) reaction is an important cycloaddition reaction in organic chemistry. It is named for its primary developers, the German chemists Otto Diels and Kurt Alder, who received the Nobel Prize in chemistry in 1950 for their work. At the time the reaction involved the cycloaddition of a conjugated diene **3.1** with an alkene **3.2** furnishing a compound containing a six-membered ring **3.3**. This reaction occurred in a single step, with a cyclic flow of electrons and typically the diene **3.1** and dienophile **3.2** are mixed in equimolar proportions (Scheme 3.1) [1-3].

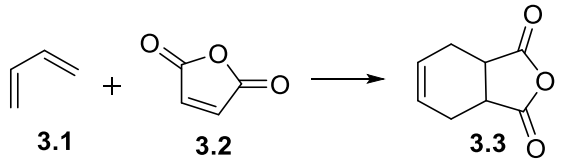

Scheme 3.1

This reaction may be executed under relatively simple reaction conditions by heating together the two components, diene and dienophile, in non-polar solvents, followed by evaporation, which leads usually to products in high yields. Many aspects of this reaction have been developed over the last 50 years of evolution in organic chemistry. All these developments involved the use of Lewis acid catalysis, very high pressures, temperatures and/or the inverse electron demand version and also have been highlighted recently in several reviews [4-6].

In general, D-A reactions are concerted cycloadditions, although other mechanisms have also been proposed. There are not many heterocycles that undergo cycloaddition reactions and usually, for these reactions to succeed, special activation of the heterocyclic compound or a very reactive dienophile is necessary [7-9]. Most of the problems arise from the fact that, in the course of the reaction, the aromaticity of the heterocyclic ring is damaged. Nevertheless, if the reaction is accomplished, a D-A adduct can be one of the key intermediates to obtain several key natural products [10,11].

Until now, expanded porphyrins attracted much attention because of their structural and functional features and unique metal-coordination properties. However there are only a few reports on their chemical transformation by D-A reactions. Nevertheless, the first

report of a D-A reaction in an expanded porphyrin was achieved by Osuka and co-workers in 2004 (Fig. 3.2) [12]. This reaction was accomplished by reacting *meso*-pentafluorphenyl [26]hexaphyrin and benzosultine **3.6** in benzene at reflux for 24 h under nitrogen atmosphere. After addition of DDQ, at rt the reaction was stirred for more 12 h. Further separation by column chromatography provided adducts **3.4** and **3.5** in 55 and 46% yield, respectively.

In the same work, using similar reactional conditions and **3.7**, these researchers were able to obtain an anthracene bridged hexaphyrin **3.8** (Fig. 3.2). Interestingly the D-A reaction occurs selectively at the inner C-C double bond to provide novel aromatic ring-fused hexaphyrin.

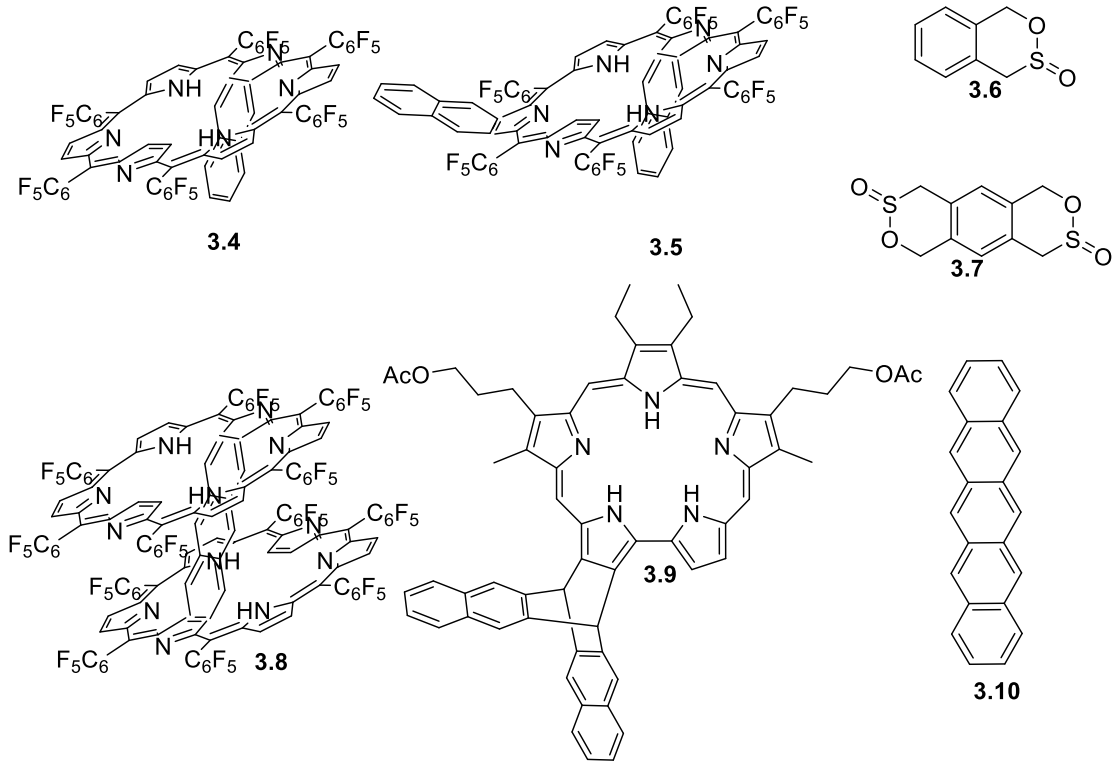

Figure 3.1: Expanded macrocycles used in Diels-Alder reactions.

Latter in 2005 Tomé *et al.* attempted a D-A reaction between sapphyrin and pentacene trying to reproduce a chemistry studied for corroles and phorphyrin derivatives (fig. 3.1) [13-16]. However, when the reaction between [22]sapphyrin and pentacene **3.10** was carried out, some differences were observed when compared to what is found in the case of corroles [17]. Instead of the dehydrogenated compounds derived from [4+2] mono- and bisadducts, as well as [4+4] cycloadducts observed for corroles, sapphyrins originated

mainly [4+2] monoadducts **3.9**, highlighting the reactivity differences between these two analogues.

The work, developed in this area show that D-A reactions can be a method to chemically transform expanded porphyrins, but unfortunately the instability normally shown by these macrocycles to high temperatures makes the D-A reactional conditions prohibitive for this end. Other approach to obtain new expanded porphyrin derivatives with D-A reactions is the use of these methods in the building blocks before the synthesis of the macrocycles. Here most of these precursors can be stabilized with electron withdrawing groups and used with harsher methods in organic synthesis. To note that D-A is a widespread methodology used over the last years in heterocyclic aza-dienes like pyrrole, pyrazoles, imidazoles and so on [18]. Unfortunately, its use in units comprising more than one pyrrole is still a subject of further development.

3.1.1. Diels-Alder reactions with bipyrrolic precursors: experimental results

In order to achieve our objectives, we first attempted to make the reaction with dimethyl acetylenedicarboxylate (DMAD) and the α-free bipyrrole **1.36** in toluene at reflux for 1 h. Unfortunately, the active α positions of the bipyrrolic unit, as expected, were the preferred site of reaction, and instead of obtaining the D-A adduct **3.12** Michael additions have occurred at each α-free position of the bipyrrolic unit leading to compound **3.11** in 23% yield (Scheme 3.2).

Latter we found that this reaction was possible to be performed at rt during 30 minutes in THF with improved yields. Here the better solubilization of the α-free bipyrrole **1.36** and the less extreme conditions originated an increased yield (η = 67 %).

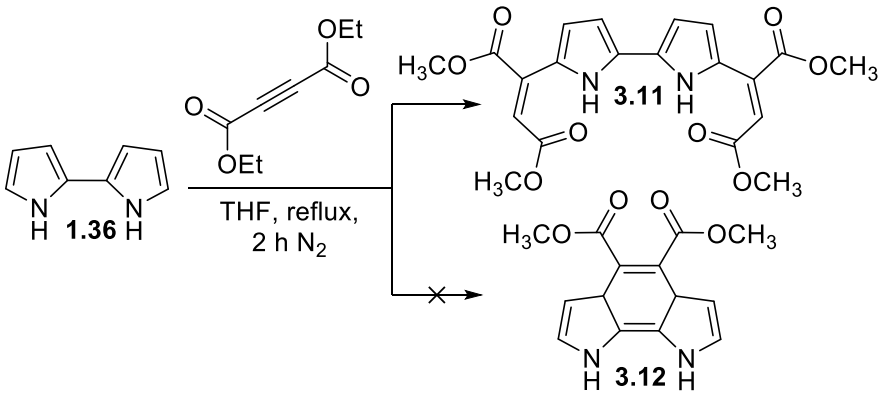

Scheme 3.2

The characterization of compound **3.11** was supported by ^{1}H and ^{13}C-NMR (Fig. 3.2 and 3.3, respectively). In Fig. 3.2 the presence of two singlets due to the methyl groups in the aliphatic zone of the spectra (δ 3.92 and 3.85 ppm, respectively) both integrating for 6 protons and the disappearance of the signal attributed to the *α*-pyrrolic protons at around δ 6.77 ppm (for compound **1.36**) shows the presence of a Michael addition adduct instead of the D-A adduct, as expected. Also the *β*-pyrrolic signal previously seen as a multiplet in compound **1.36** is now seen as two doublet of doublets at δ 6.85 and 6.65 ppm, each one integrating for 2 protons, respectively (Fig. 3.2). The NH protons can also be found in this spectrum and are displayed as a broad singlet at δ 13.16 ppm.

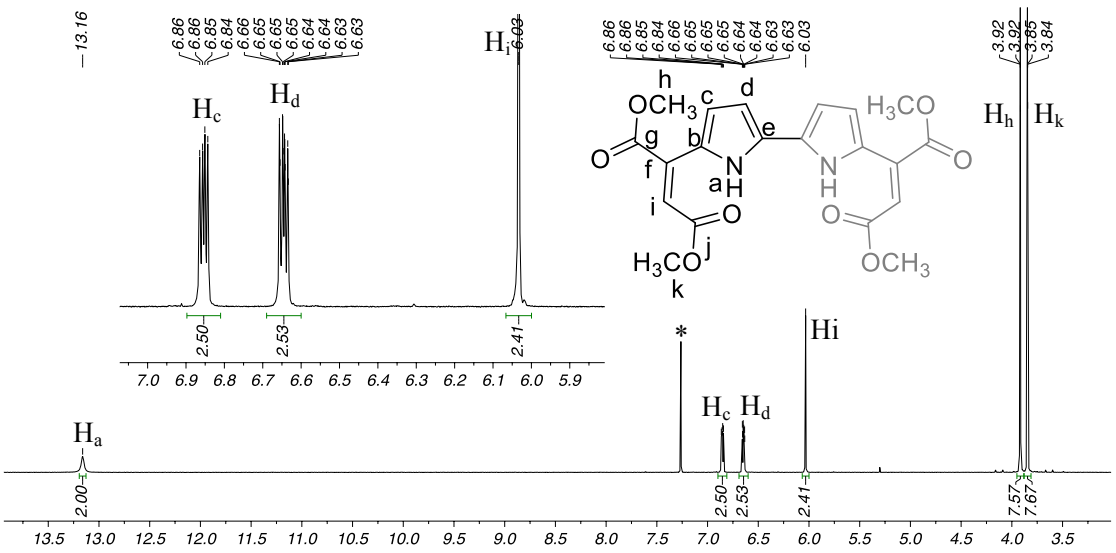

Figure 3.2: ^{1}H-NMR spectrum of compound **3.11** in $CDCl_3$, * stands for $CHCl_3$.

The presence of the methyl groups at δ 52.9 and 52.4 ppm along with the carbonyl groups at δ 169.2 and 167.9 ppm of the DMAD moieties in the ^{13}C-NMR show, without any reasonable doubt, that the Michael adduct **3.11** was synthesized instead of the desired product **3.12**. Also the carbons included in the double bonds of these moieties are depicted at δ 127.2 and 109.8 ppm as expected for this compound. The rest of the signals are due the *β*-pyrrolic carbons and are displayed at a reasonable shifting when compared to the starting material **1.36** (Fig. 3.3).

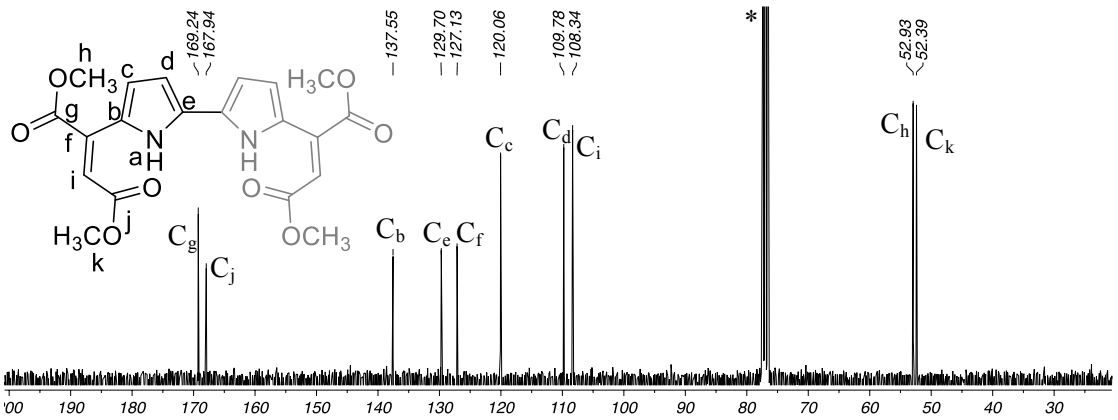

Figure 3.3: ^{13}C-NMR spectrum of compound **3.11** in $CDCl_3$, * stands for $CHCl_3$.

With these preliminary results we concluded that the *α*-positions had to be protected before attempting any functionalization in precursor **1.36** and therefore compound **2.11** was used in the same conditions previously described (Scheme 3.3).

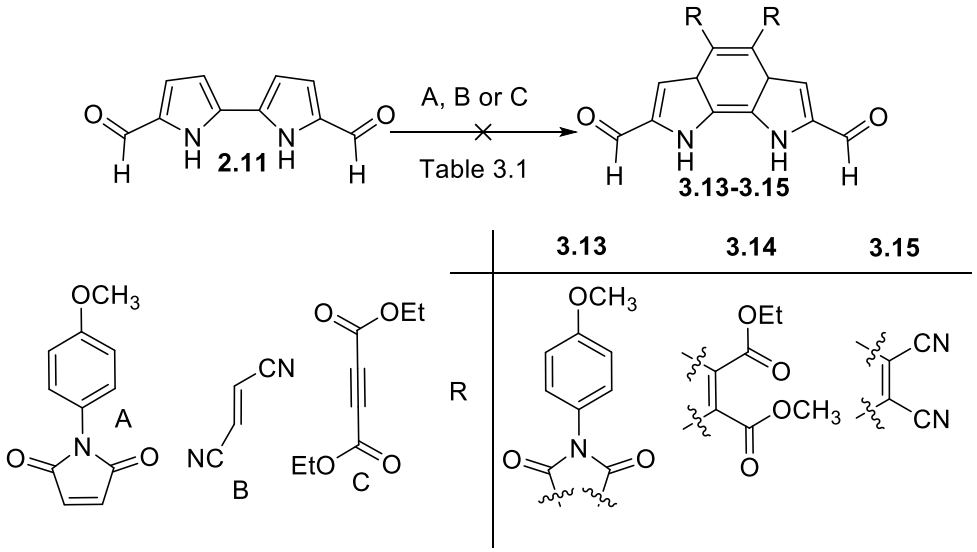

Conditions exemplified in table 3.1.

Scheme 3.3

Henceforward, several D-A reactions with several combinations of conditions (temperature, solvents, and dienophiles A-C) and even under MW irradiation were attempted without success (Table 3.1).

Table 3.1: Conditions used in the D-A attempts on precursor **2.11**.

dienophile	solvent	Temperature ºC	Time h
A	THF	Reflux	24
A	*o*-Diclorobenzene	140-180	48
A	Trichlorobenzene	200	48
B	Toluene	reflux	48
C	Toluene	Reflux	48
C	Toluene	MW*	2h
C	*o*-Diclorobenzene	140-180	48

*Microwave conditions:

Intriguingly, when subjected to a D-A reaction **2.11** shows a remarkable stability. This is shown by its stability at 150 ºC during 24 h, and decomposition far above this temperature (*e.g.* 200 ºC, during 24 h) when exposed to long times of reaction. Furthermore, a reaction with viable products was not achieved with the conditions described in table 3.1.

Nevertheless while attempting the reactions in MW the appearance of a new much less polar spot in the TLC led us to the synthesis of **3.16** instead of **3.14**. This showed that a *cis* configuration of the bipyrrolic compound **2.11** was possible, yet it has preferred to react in much more reactive sites as it is the NH groups. This compound was latter achieved 76% using a procedure where the presence of a catalyst amount of NEt_3 in THF allowed us to obtain a much higher yield. In analogy and having in mind possible cyclization with these units, the same was performed in **2.12** obtaining from there, compound **3.17** (Scheme 3.4).

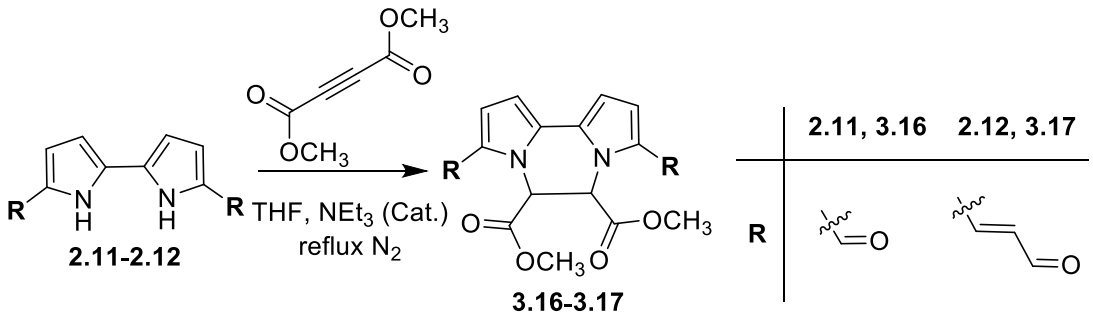

Scheme 3.4

From the ^{1}H-NMR data (Fig. 3.4) it can be observed that all the signals of the bipyrrolic unit remain in the spectra almost at the same shift as the starting material. The

new signals due to the DMAD moieties are shown as singlets, one at high field for the methyl ester function (δ 3.72 (for **3.16**) and δ 3.73 pmm (for **3.17**)) and another signal at down field due to the protons at the carbons bonded to the nitrogens (δ 6.76 (for **3.16**) and δ 5.88 ppm (for **3.17**)). Here in compound **3.17** is possible to note a differentiation between the pyrrolic protons H_c and H_d, whilst in the starting material they combined in the same signal.

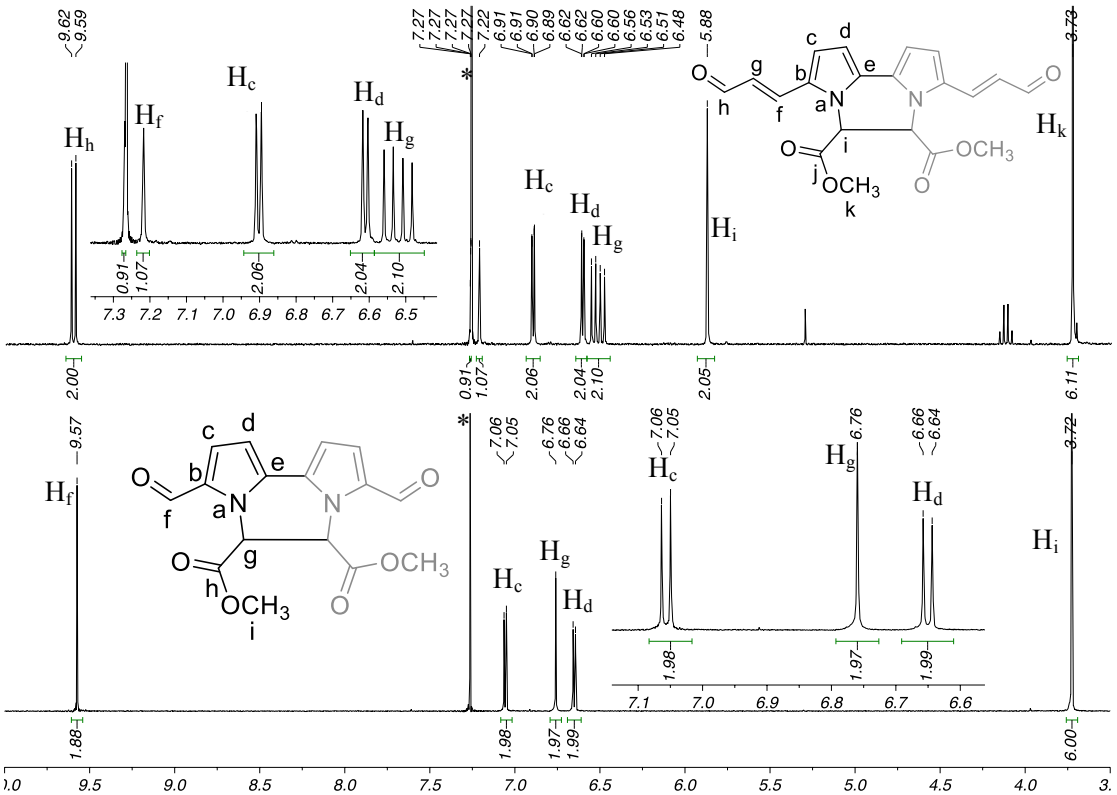

Figure 3.4: ^{1}H-NMR spectra of compounds **3.16** and **3.17** in $CDCl_3$, * stands for $CHCl_3$.

For the ^{13}C-NMR spectra of compound **3.16** is possible to assign all the signals for its structure. The signal related to the carbonyl groups of the DMAD moiety is shown at δ 167.6 ppm the methyl ester appear at the aliphatic area of the spectra at δ 53.7 ppm and also the protons of the carbon bonded the nitrogen atom is displayed at δ 57.1 ppm. The remaining signals are related to the aromatic carbons of the bipyrrolic unit and the aldehyde function appears shifted downfield at δ 179.8 ppm. Also compound **3.17** has its structure fully attributed in the ^{13}C-NMR and the resemblances between **3.16** and **3.17** are highlighted in figure 3.5. Here again it's possible to note all the signals endorsed to the bipyrrolic structure and the spacer between the aldehyde functions and the bipyrrolic backbone.

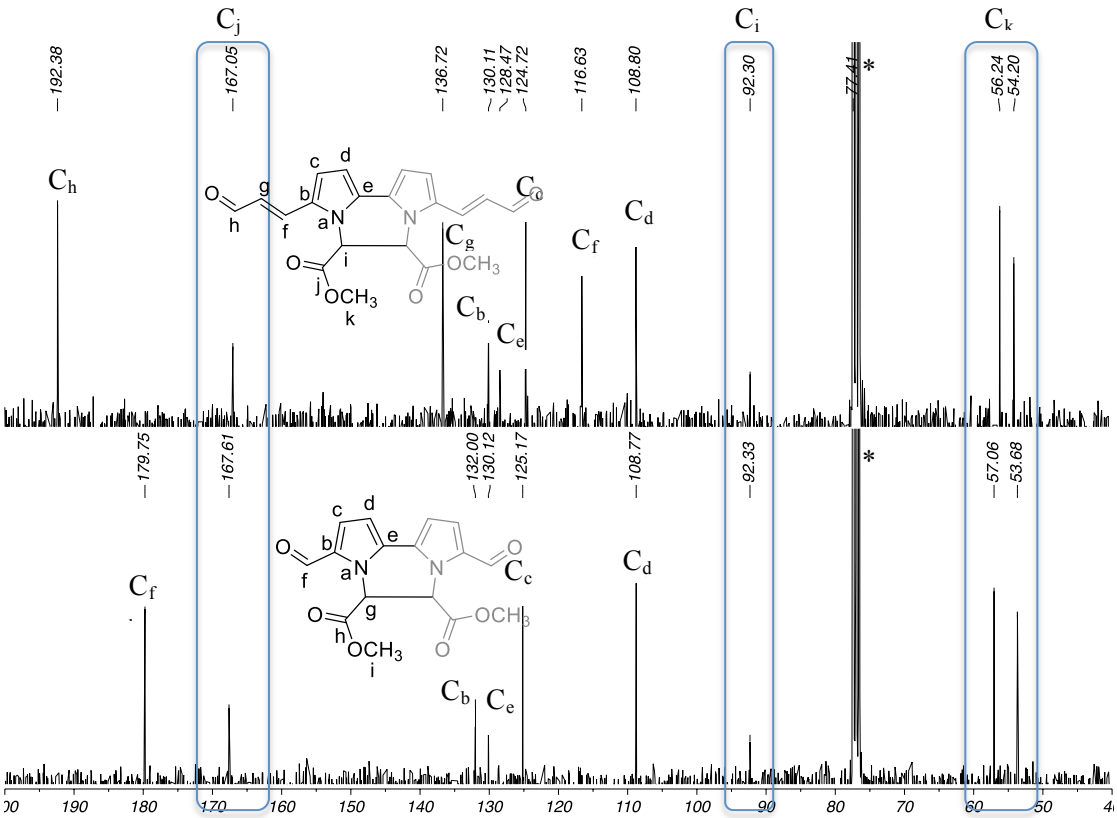

Figure 3.5: ^{13}C-NMR spectrum of compound **3.16** and **3.17** in $CDCl_3$, * stands for $CHCl_3$.

Like all reactions, D-A reactions are conditioned to the used reagents and their substituents. The way these substituents can affect the rate of the reaction may be rationalized with the aid of the Frontier Molecular Orbital (FMO) theory. This theory was developed during a study of the role of orbital symmetry in pericyclic reactions by Woodward and Hoffmann [19] and, independently, by Fukui [20]. Later, Houk contributed significantly to the understanding of the reactivity and selectivity of these processes [21]. This means that there are several pre-requisites that need to be achieved in order to have a successful D-A reaction. The FMO theory states that a reaction between two compounds is controlled by the efficiency with which the molecular orbitals of the individual reaction partners interact [22,23]. The interaction is most efficient for those orbitals that overlap best and are closest in energy. The FMO theory further assumes that the reactivity is completely determined by interactions of the electrons that are highest in energy of one of the reaction partners (i.e. those in the Highest Occupied Molecular Orbital, the HOMO) with the Lowest Unoccupied Molecular Orbital (LUMO) of the other partner. Applied to the D-A reactions, two modes of interaction are possible: the reaction can be controlled by the interaction of the HOMO of the diene and the LUMO of the dienophile (normal

electron demand), or by the interaction between the LUMO of the diene and the HOMO of the dienophile (inverse electron demand). In the former case, a reduction of the diene-HOMO dienophile-LUMO energy gap can be fulfilled by either raising the energy of the HOMO of the diene by introducing electron donating substituents or lowering the energy of the dienophile-LUMO by the introduction of electron withdrawing substituents.

Experiments have suggested that there are no intermediates along the reaction coordination. In other words, the D-A reaction is a concerted reaction. All bond formation occurs in one smooth process involving the π electrons from the diene and dienophile. This means that the diene must add across only one face of the dienophile because it is impossible for the two ends of the diene to simultaneously approach an alkene from opposite faces [24-27].

Also, it is also evident that the diene must adopt the so-called *cis* conformation in order to react with a dienophile in this way, despite the fact that this conformation is more sterically constrained than the preferred *trans* conformer. Dienes that cannot adopt this conformation cannot undergo D-A reaction [28,29].

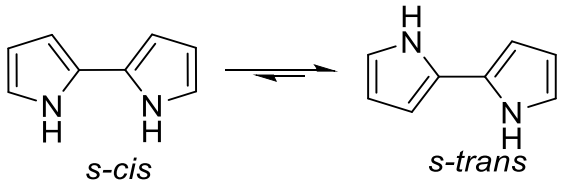

Figure 3.6: Diene conformations.

Overlap between the highest occupied MO of the diene (HOMO) and the lowest unoccupied MO of the dienophile (LUMO) is thermally allowed in the D-A reaction, provided the orbitals are of similar energy. Normally electron-withdrawing groups on the dienophile facilitate the reaction, since this will lower the energy of the LUMO. Good dienophiles often bear one or two of the following substituents: CHO, COR, COOR, CN, C=C, Ph, or halogen. On the other hand the diene component should be as electron-rich as possible. Here two possible reasons for the ineffectiveness of these attempts can be recognized. The presence of electronegative aldehyde groups in **2.11** probably removed the diene capability of this precursor, blocking the desired outcome.

Regarding the deactivation problems that the substituents in *α*-positions may cause, we established some methodologies to surpass these problems, altering the electroatractive character of the aldehyde groups to a different functional group like: a) reduction of the

aldehyde group to an alcohol with $NaBH_4$ or b) attempting the acetal or thioacetal formation, reacting **2.11** with ethylene glycol (EG) or propane-1,3-dithiol (PD), respectively (Fig. 3.7).

Other methodology requires the use of an electron rich dienophile (c) forcing an inverse demand D-A reaction (figure 3.7). This alternative scenario for the reaction is favored by an electron-poor diene, which might be the case.

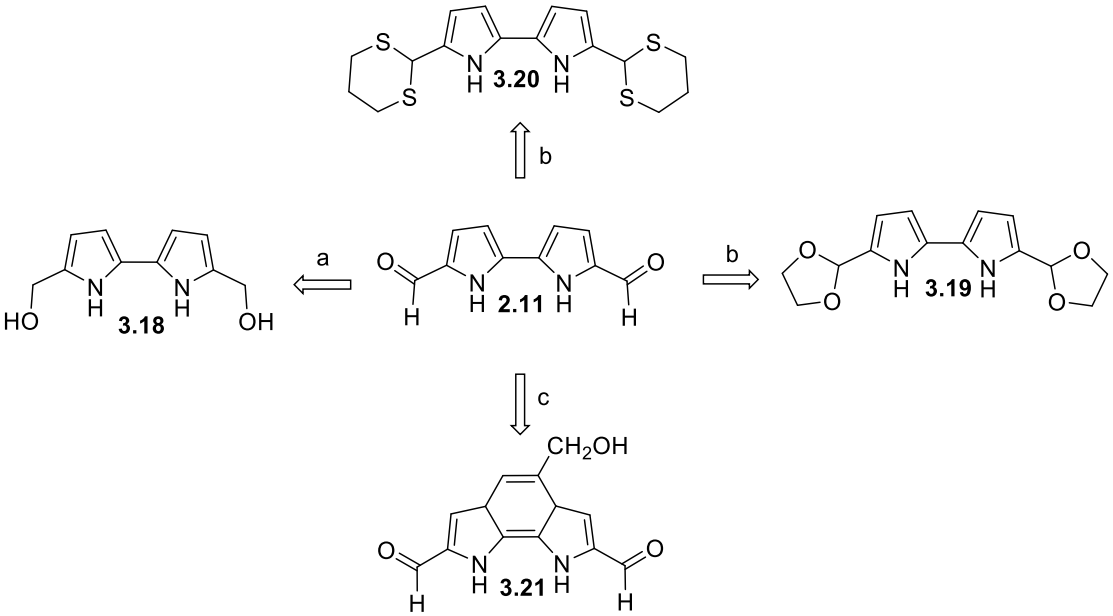

Figure 3.7: Bipyrrole activation attempts (a and b) and Inverse Demand Diels-Alder reaction (c).

Transformation of the formyl groups of **2.11** to provide the requisite alcohol functionalities in **3.18** was accomplished in a one-step reaction, by reduction of **2.11** with $NaBH_4$ in THF in 1 hour reaction under inert atmosphere (Scheme 3.5).

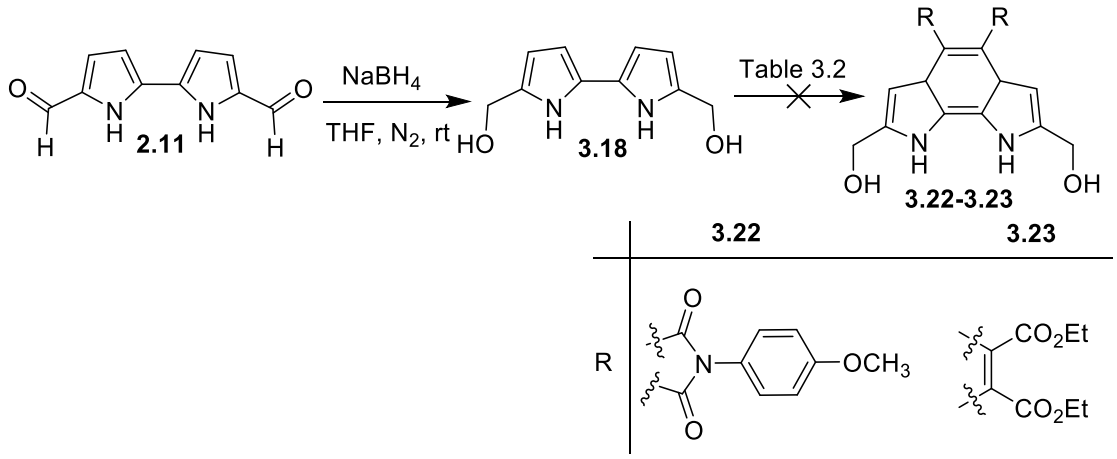

conditions illustrated in table 3.2.

Scheme 3.5

Moreover, despite the high yields obtained in the above reduction reaction with bipyrrole **2.11**, this intermediate proved unsuitable for further elaboration to the corresponding benzobipyrrolic compound. The reason is mainly attributed to its high instability even at room temperature preventing a reaction type (D-A), which normally requires by temperature (Scheme 3.5).

When it is used as starting material in the D-A reactions only degradation of the starting material was observed even at rt (Table 3.2).

Table 3.2: D-A conditions used with compound **3.21**.

Dienophile	Solvent	Temperature	Time
A	THF	rt	12h
A	Toluene	reflux	3h
A	THF	reflux	6h
C	THF	rt	12h
C	THF	reflux	6h
C	Toluene	reflux	3h

^{1}H-NMR exemplified in figure 3.8, clearly show about loss of the aldehyde functions of **2.11** (δ 9.46 ppm) and the presence of a new signal displayed as a singlet with an integration of four, due the two new CH_2 groups (δ 4.43 ppm, H_g). Also in compound **3.18** the signals attributed to the *β*-pyrrolic positions (δ 6.04 and 5.95 ppm, H_c and H_d) are

less shifted than in compound **2.11** (δ 7.04 and 6.70 ppm) probably due the less electronegative surroundings these protons have in this structure.

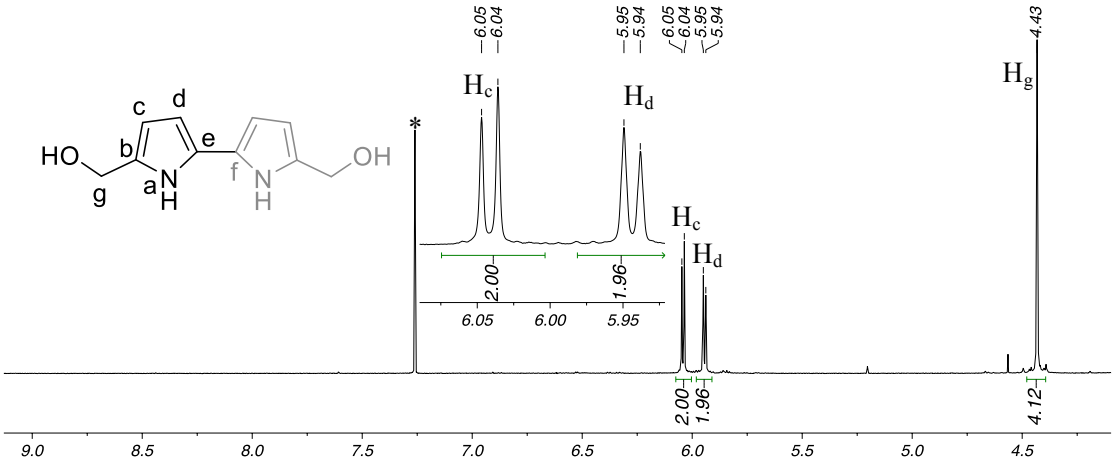

Figure 3.8: ^{1}H-NMR spectrum of compound **3.18** in $CDCl_3$, * stands for $CHCl_3$.

Also the acetalization or thioacetalization with ethylene glycol (EG) and propane-1,3-dithiol (PD), respectively, were unsuccessful using well established methodologies reported in the literature (Scheme 3.6) [30,31].

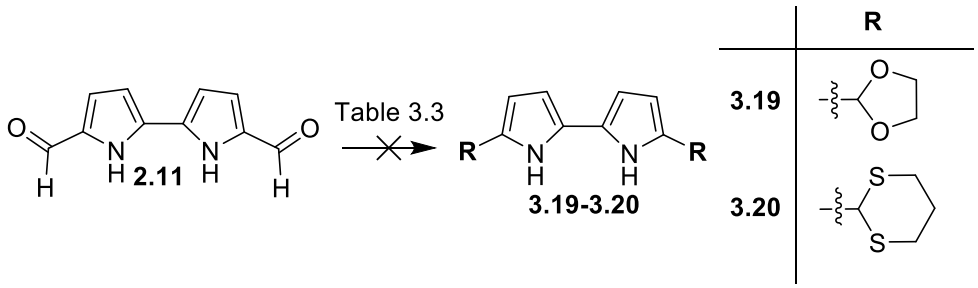

Scheme 3.6

The products obtained from these attempts displayed a bluish color and were insoluble even in highly polar solvents (*e.g.* DMSO or DMF). The acidic media used in these reactions decomposed the starting material and explain the lack of results by these methods (table 3.3). In fact, also a thioacetalization process using Lewis acid catalysis resulted only in polymerization of compound **2.11** (Table 3.3) [32].

Table 3.3: Conditions and methods used in acetalization or thioacetalization reactions.

Acetal	Solvent	Temperature	Catalyst	Time
EG	Toluene	reflux	*p*-TsOH	6 h
PD	CH_2Cl_2	rt	$BF_3.OEt_2$	3 h
PD	CH_2Cl_2	rt	I_2	30 min.

Undeniably, we required a versatile strategy, which would ideally be tolerant to a diverse range of substituents and considerably simplistic in terms of synthetic steps. After a considerable effort, an alternative scenario such as the inverse demand D-A reaction was tried but unfortunately no practical results were achieved (Scheme 3.7) [33,34].

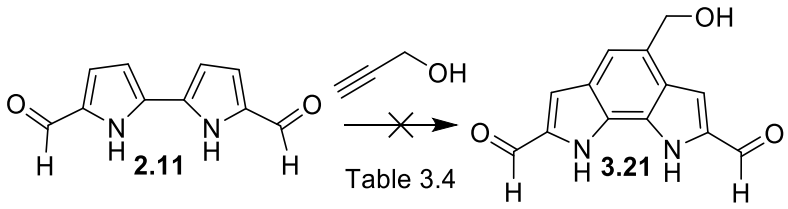

Scheme 3.7

The conditions used for these reactions are similar to the ones used previously in D-A reactions. The use of less temperature is associated with the boiling point of the used dienophile (propargyl alcohol, PA), which is around 102 ºC (Table 3.4). Note that in entries 3 and 4 of the table 3.4, propargyl alcohol (PA) was used as a solvent of the reaction. Any attempts using a sealed tube and a higher temperature than the PA boiling poit led to its polymerization.

Table 3.4: Conditions and methods used in the Inverse Demand D-A reactions with **2.11**.

Dienophile	Solvent	Temperature ºC	Time h
PA	Toluene	rt	48
PA	Toluene	reflux	48
PA	PA	rt	48
PA	PA	reflux	48

The lack of success with these methods prompted an investigation into different strategies. Here, encouraged by our success at achieving Knoevenagel condensations, we focused our attention on applying these methodologies to the corresponding dipyrrolic

substrates already presented. Although, the chemistry presented above provided some dipyrrolic intermediates, for subsequent access to expanded porphyrins, it lacked generality and proved inefficient to access the benzobypirrolic units. Moreover, the difomyl-bipyrrolic intermediate employed **2.11**, was generally inert to the exposed conditions and the formyl groups and their electroactractive capability proved to weaken their availability to undergo in D-A reactions. Furthermore all attempts to make this unit more reactive showed to be ineffective as well, from which several other problems arise, such as the instability of the key intermediates for D-A reaction with **3.18** and the difficulties in the isolation of protected intermediates. On the contrary, Michael additions to these units proved to be highly efficient reactions regarding the easy accessibility to compounds such as **3.19** and **3.20** and the high yields accomplished. Other strategy like the inverse demand D-A was also ineffective. Mechanistically, both the D-A approaches require a *cis* conformation diene to tolerate the cyclization step and formation of the products. While this *cis* conformation showed to be possible in Michael addition reactions it may be the limiting step when the dienophyles approach the diene. Additionally, another important pre-requisite is the HOMO-LUMO energies, which have to be similar in order to allow a complete flow of electrons from the donor to the acceptor.

3.2. Diels-Alder reactions with sapphyrins

Sapphyrins containing in their periphery was the first expanded porphyrin to be reported in the literature and remains among the most extensively studied. Much of the interest in this macrocycle reflects its ability to bind anions, a phenomenon that has been examined in solution and in the solid state by a wide range of experimental techniques.

Considerable effort has been devoted since the nineties to modifying the classic Rothemund synthesis of porphyrins to obtain novel porphyrinoid systems (namely the expanded porphyrin chemistry), and some of these systems and attempts regarding the historical point of view or importance related to their applications has been discussed in the introduction of the present thesis. Nevertheless several contributions considering the synthesis of sapphyrins have been made over the last 20 years rising significantly its availability.

One groundbreaking contribution was made by Lindsey and co-workers while optimizing the synthesis of *N*-confused porphyrin obtained in a remarkable 40% yield, also

obtained tetraphenylsapphyrin with a direct condensation of pyrrole and benzaldehyde gave a yield of 1.2% of tetraphenylsapphyrin **1.89** (figure 3.9) [35,36]. Almost at the same time, Chandrasekar and co-workers have also reported the use of dipyrromethanes as potential precursors in the direct synthesis of sapphyrin exposing 5-phenyldipyrromethane to one equivalent of trifluoracetic acid, followed by oxidation with chloranil, giving rise to sapphyrin **1.89** in yields of up to 11% [37].

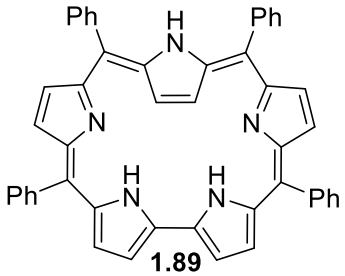

1.89

Figure 3.9: Tetraphenylsapphyrin synthesized by Lindsay and Chendraseker methodologies.

Although other products, such as porphyrins and *N*-confused porphyrins, complement the formation of **1.89**, the method could provide an attractive alternative of producing sapphyrins from dipyrromethanes, which are readily available in multigram scales.

While efforts targeting the synthesis of *meso*-substituted sapphyrins have been made, improved syntheses of *β*-substituted sapphyrins continued to be developed.

In 1999, Richter and Lash reported the use of $FeCl_3$ in the oxidation step of a [4+1] sapphyrin synthesis [38]. Condensation of the linear tetrapyrrole **1.56** with pyrroledialdehyde **3.22** followed by oxidation with 0.1 M aqueous $FeCl_3$ solution give sapphyrin **3.23** in 50% yield. Compared to the 36% yield obtained when DDQ was used as the oxidant, this increase was considered significant (Scheme 3.8).

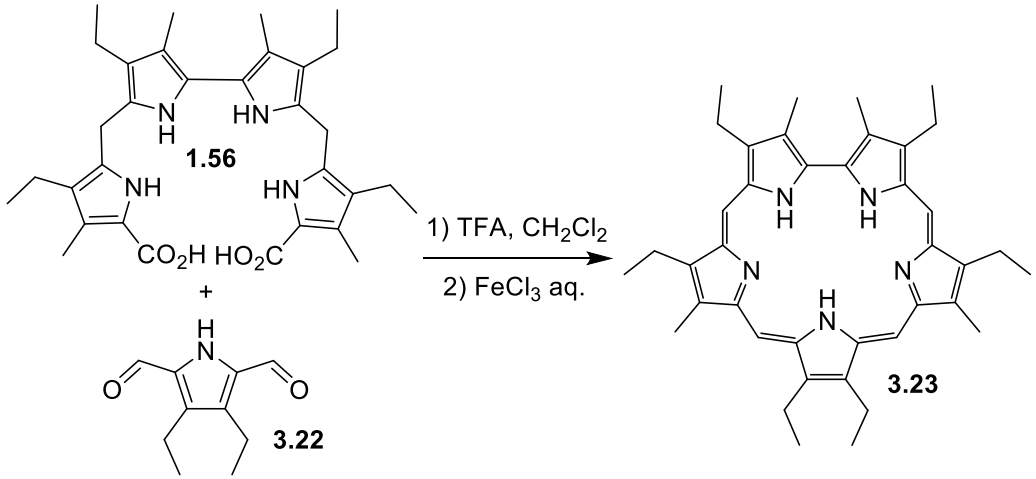

Scheme 3.8

Also, Sessler and co-workers in an attempt to increase the yields at which sapphyrins were obtained, reported a methodology that does not require the use of a preformed bipyrrolic moiety, allowing sapphyrins **3.29-3.31** to be obtained in yields ranging from 28 to 34% (scheme 3.9). The condensation reaction was executed mixing tripyrranedialdehyde **3.24** with two equivalents of pyrroles **1.20**, **3.25** and **3.26** under acidic conditions, followed by oxidation with DDQ. As expected from such a reaction sequence, the corresponding porphyrins were also isolated in approximately 10% yield.

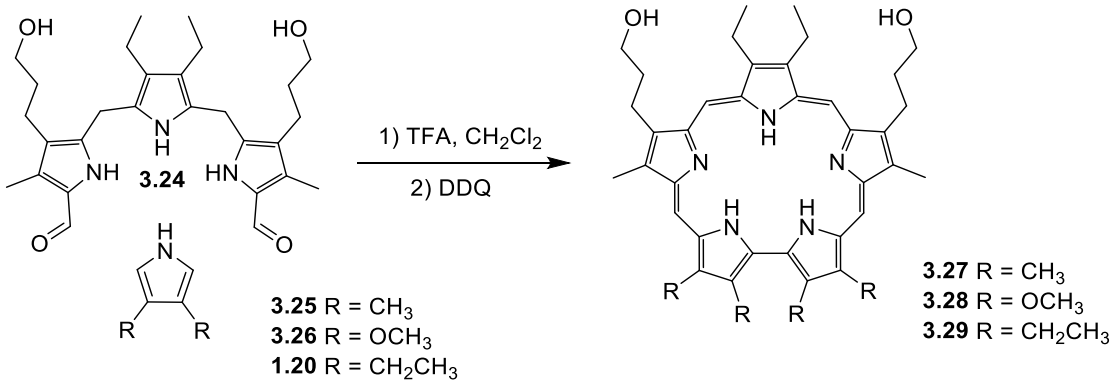

Scheme 3.9

While the overall yield of sapphyrin is somewhat higher for the more classic 3+2 synthesis than for this new 3+1+1 procedure, this latter approach obviates the need to prepare bipyrrole and is in this way three steps shorter. As such, it provides a fine complement to the existing methods. It also allows for the synthesis of sapphyrins that contain various symmetric bipyrrolic subunits that are not currently used as sapphyrin **3.28**.

From a structural standpoint, sapphyrins also adopt an analogy to the contracted porphyrin analogues, corroles, since both contain a bipyrrolic subunit. Since it was shown that corroles and sapphyrins could participate in D-A reactions as shown in overview section 3.1. From this perspective in the next section several approaches in order to obtain novel expanded porphyrins regarding the sapphyrin type and functionalization through D-A reactions was studied.

3.2.1. Diels-Alder reactions with sapphyrins: experimental results

Initially, we sought to access these benzosapphyrins analogues through our original D-A strategy. Therefore, we now required efficient routes towards the synthesis of sapphyrin **3.31** (scheme 3.10). While the above methodologies show some interesting systems towards the synthesis of these precursors, the choice set on the condensation methodology previously described by Tomé *et al.*[39]. This sapphyrin is readily available from the condensation reaction between tripyrromethane **3.30** (kindly provided by Professor Jonathan Sessler, Austin University) and the previously synthesized bipyrrole **2.11**. This reaction is thus maintained stirring during 24 h in the presence of air allowing the oxidation of the macrocycle while the reaction is occurring. After neutralization with a few drops of NEt_3 is possible to verify a change in the coloration of the mixture changing from dark brown to a greenish solution. Further evaporation and purification over neutral alumina and silica gel provides compound **3.31** in about 18% yield.

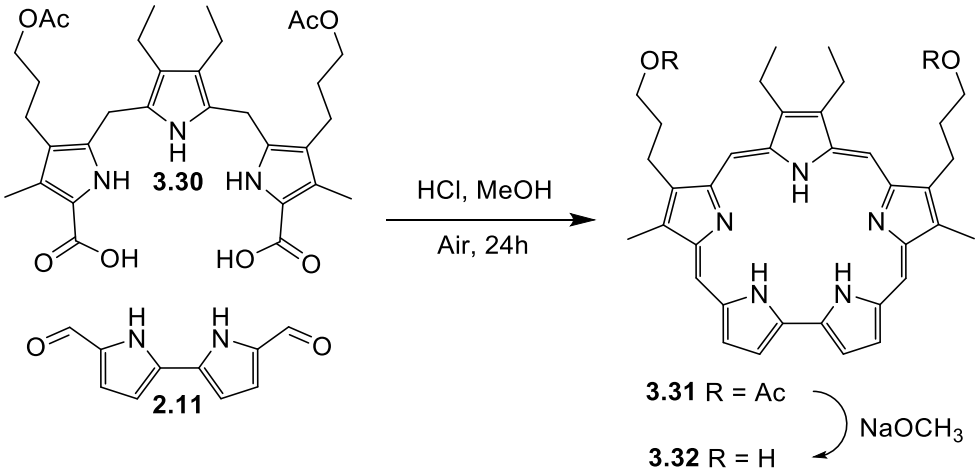

Scheme 3.10

The structure of compound **3.31** was deduced from their 1D and 2D NMR spectra (COSY and HSQC). The ^{1}H NMR spectrum of compound **3.31** (Figure 3.10) protons of

the alkyl groups on the periphery of the sapphyrin. This spectrum contains two singlets and 2 doublets correlated between themselves at higher frequency values (δ 11.63, 11.52, 10.55 and 10.25 ppm) corresponding to the four *meso*-H (H_e and H_j) and the signals due the resonances from the *β*-pyrrolic protons existent in the bipyrrolic moiety (H_b and H_c).

A closer analysis of the aliphatic region indicates the existence of several aliphatic protons at δ 3.30, 4.36 and 4.67–4.83 ppm, which are attributed to the surrounding CH_2 and CH_3 protons, and in this case is possible to attribute them as a quintet for protons H_p, a singlet for protons H_t and a multiplet at δ 4.83-4.67 ppm, comprehending protons H_m, H_o and H_p, respectively. It is also possible to find a sharp singlet at δ 2.30 ppm attributed to the acetates in **3.31** structure. Finally the signal endorsed to H_n resonance in the ^{1}H-NMR spectra without the addition of TFA is overlapped with the acetate signal, nevertheless this signal is clearly displayed when this spectra is acquired in acidic media (b, figure 3.10, expansion) integrating for four protons and recognized as a triplet at δ 2.32 ppm. These findings are consistent with the anticipated structure **3.31**.

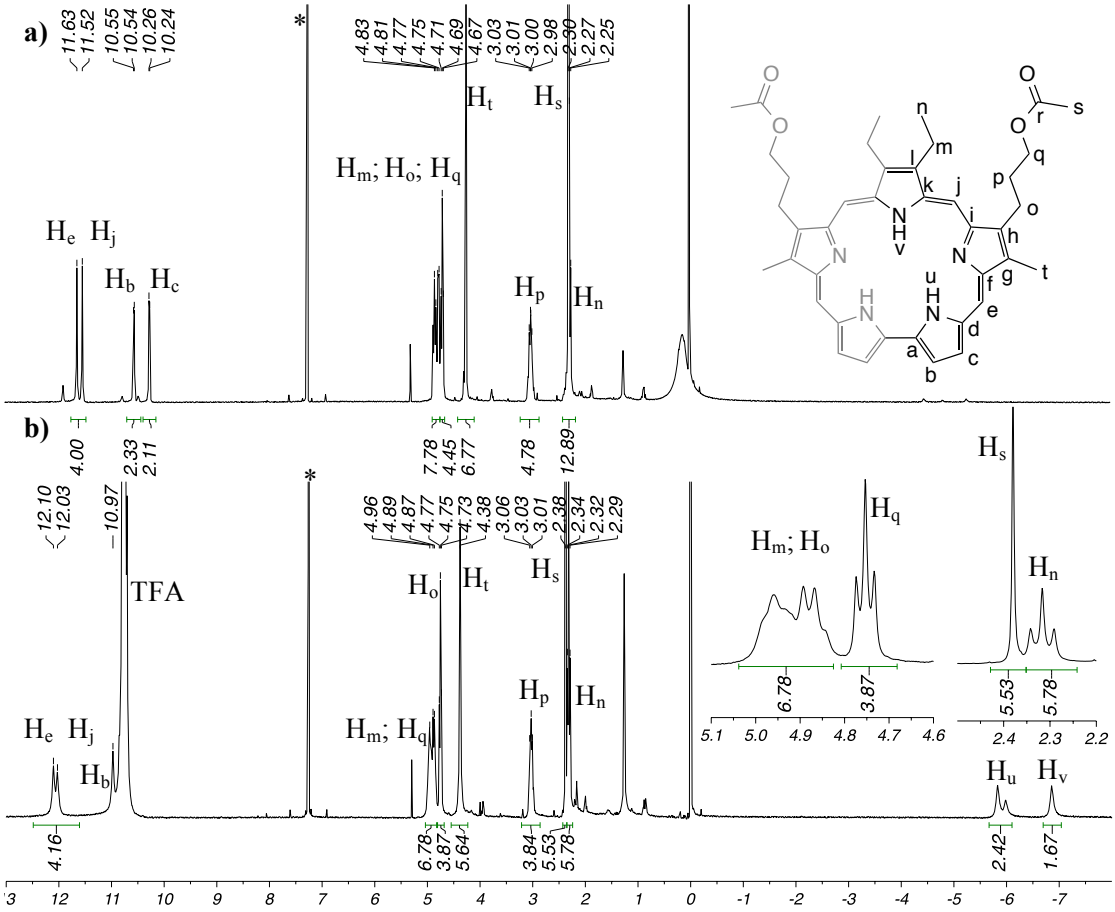

Figure 3.10: a) ^{1}H-NMR spectrum of compound **3.31** in $CDCl_3$, * stands for $CHCl_3$; b) ^{1}H-NMR spectrum of compound **3.31** in $CDCl_3$/TFA (5%), * stands for $CHCl_3$.

While the synthesis of sapphyrin **3.31** was achieved the deprotection of the acetate groups were also done (compound **3.32**, η = 88%) using sodium metoxide in a solution of CH_2Cl_2:MeOH (2:1) at reflux during 24 h. The characterization of this compound is presented in the next figure and clearly shows the disappearance of the acetate signal at δ 2.30 ppm (sharp singlet).

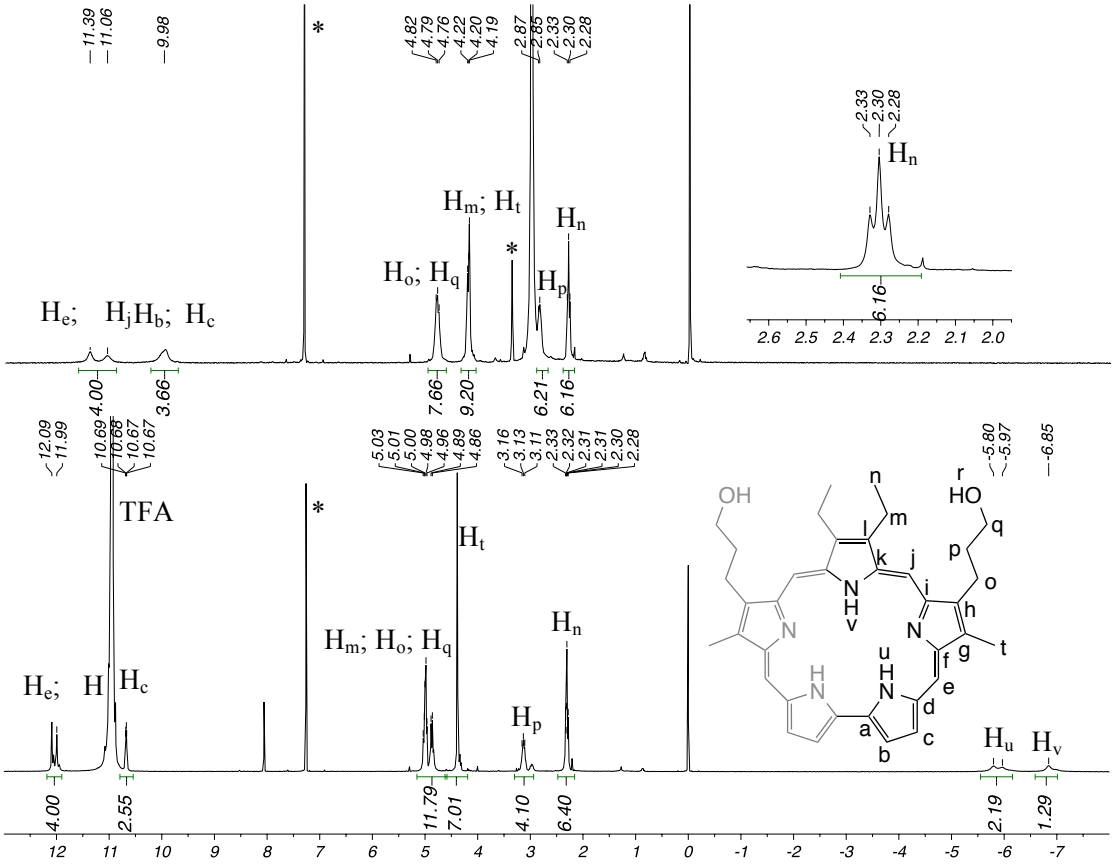

Figure 3.11: a) ^{1}H-NMR spectrum of compound **3.32** in $CDCl_3$/Methanol-d_4 (10%), * stands for $CHCl_3$ and Methanol; b) ^{1}H-NMR spectrum of compound **3.32** in $CDCl_3$/TFA (10%), * stands for $CHCl_3$.

Here again the inner NH protons don't appear in the spectra when this is acquired in $CDCl_3$/MeOD-d_4. Still, analysis using $CDCl_3$ and a few drops of TFA in the NMR tube shows clearly the presence of the NH inner protons at higher fields (δ -5.99 and -6.85 ppm). This compound was not subject to further investigation.

Using the same methodology, attempts in the synthesis of higher expanded sapphyrin type compounds, which could give us insights about the increased π conjugation and a new synthon for D-A reactions. For these reasons attempts with bipyrrole **2.12** using the same condensation conditions used in the synthesis of **3.31** were made in order to obtain compound **3.33**.

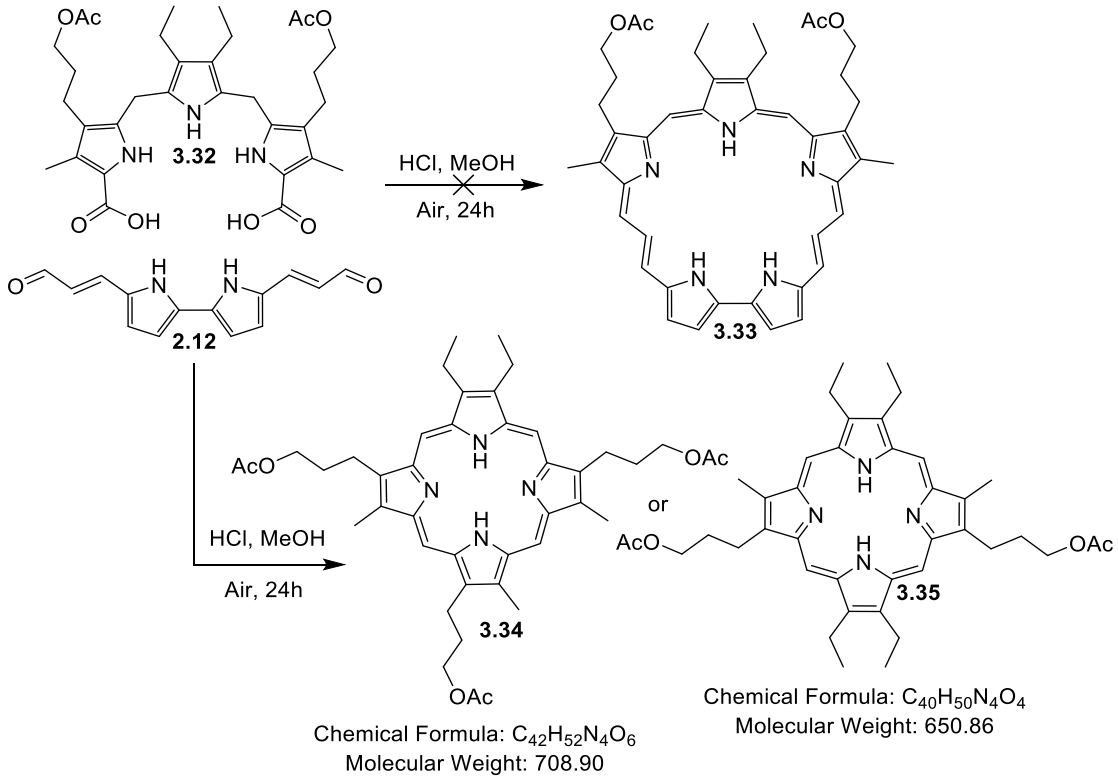

Scheme 3.11

After the neutralization step it became clear that the reaction was not displaying the same coloration as the one achieved in the synthesis of **3.31**. In fact, further analysis showed that the major fraction of this reaction exposed a reddish coloration and UV-Vis absorption spectra shows a distinct profile from the one found for sapphyrin **3.31** with a blue shifted Soret band at and four Q bands at (Fig. 3.12).

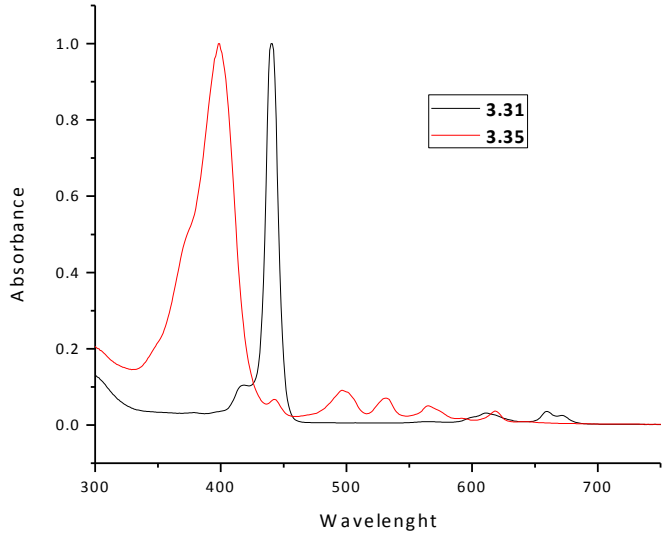

Figure 3.12: UV-Vis spectrum of compounds **3.31** and **3.34**.

Additional studies into the spectroscopic features of this compound showed the absence of the signals due to the *β*-protons and the presence of a single signal at higher fields attributed to the inner NH protons (δ -3.76 ppm against δ -6.22 and -7.15 ppm for compound **3.31**) along with the signals located at low field between δ 10.01 and 10.10 ppm normally attributed to protons positioned at the *meso* positions of the macrocycle, shows a profile with more similarities to a porphyrin ^{1}H-NMR than the expected product **3.33** (Figure 3.13).

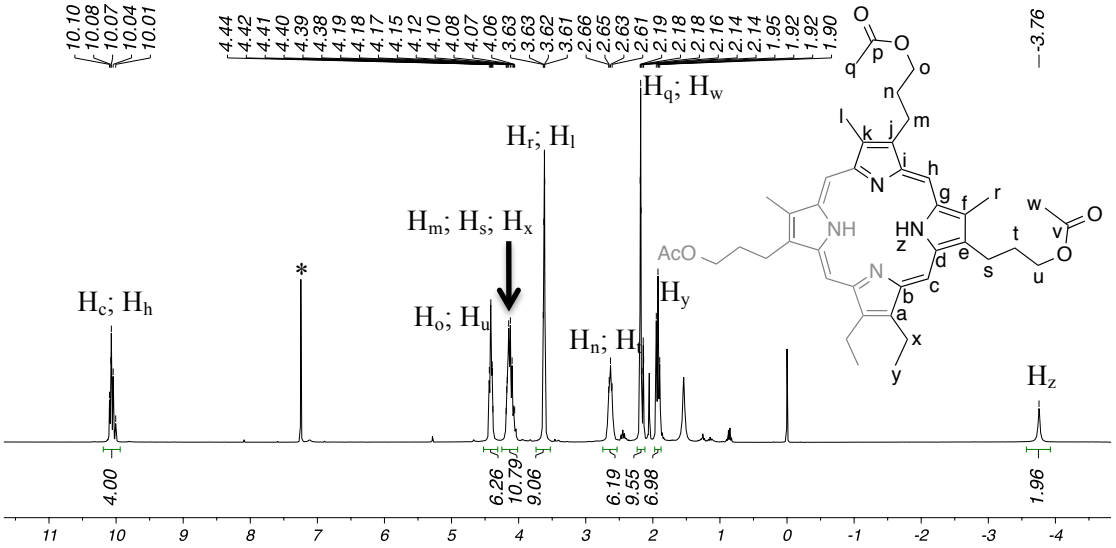

Figure 3.13: ^{1}H-NMR spectrum of compound **3.34** in $CDCl_3$, * stands for $CHCl_3$.

Knowing in advance about the absence of *β*-pyrrolic protons in this structure we concluded that some type of scrambling happened during this synthesis, an occurrence already reported in literature by Dolphin and co-workers when attempting the synthesis of pentaphyrins, in which depending on the acid used in the condensation reaction a rearrangement between the precursors provide the synthesis of porphyrins [40].

With these initial suppositions, we can predict that only the pyrroles from the tripyrromethane derivative participated in the condensation reaction producing a porphyrin and by exclusion only two arrangements can be the result from this reaction **3.34** or **3.35**. Mass analysis of the major fraction showed porphyrin **3.34** (*m/z* = 709.4 $[M+H]^+$) as the major product of this reaction. Further analysis of ^{1}H-NMR of compound **3.34** concerning its aliphatic area is possible to note several resemblances to **3.31** structure. In fact, a closer look shows exactly an increment of three protons in the signals attributed to the *β*-CH_3 (δ 3.63 ppm, H_l and H_r) and the acetate groups (δ 2.14-2.19 ppm a multiplet corresponding to H_q and H_w) both signals integrating for nine protons, while the signals due the CH_2 groups of the acetyloxypropyl substituents, show an increment of two protons at δ 4.06-4.19 ppm (H_o and H_u) and at δ 4.38-4.44 ppm (H_m, H_s and H_x). The remaining signals were attributed unambiguously and are in accordance with the proposed structure. Final confirmation of structure **3.34** was achieved by x-ray diffraction where a crystal structure provided the confirmation of **3.34**, beyond reasonable doubt (figure 3.15).

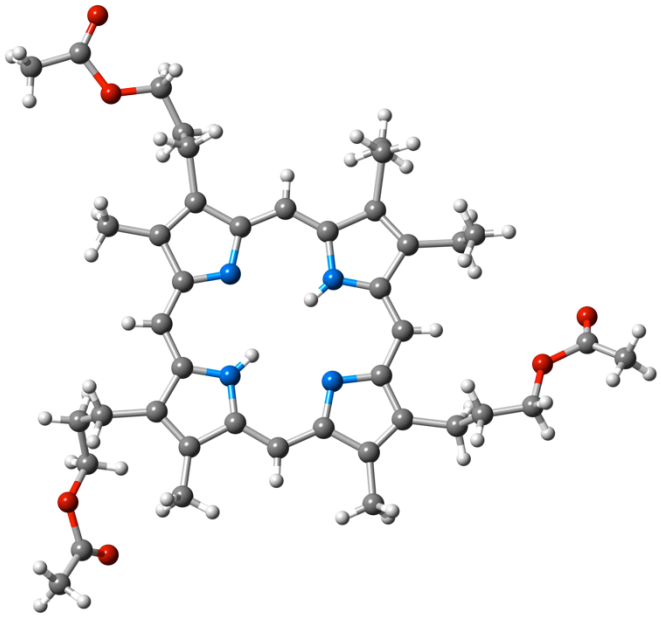

Figure 3.14: Crystal structure of compound **3.34** obtained in CH_2Cl_2/MeOH solvent mixture.

Reaction attempts using compound **3.29** alone in the same conditions used in the synthesis of **3.34**, with DDQ oxidation have been tried in order to see the extent of these reactions and increase the yield of **3.35**. Interestingly these attempts did not allowed us to corroborate the presence of compound **3.35** and only complex mixtures were possible to be perceived over TLC analysis. In fact the complexity inherent to these kind of reactions can be demonstrated by these attempts, where the presence of bipyrrol **2.12** in the reactional media leads to the synthesis of porphyrin **3.35**, nevertheless its absence did not yield the same result when **3.32** alone is exposed to the same conditions. Unfortunately, to date, all attempts to self-condense this intermediate (**2.12**), with **3.32** and catalytic HCl in chloroform, initially at room temperature in the presence of air and then in CH_2Cl_2 in catalytic trifluoroacetic acid proceeded by DDQ, failed to yield the desired products, let alone the porphyrin **3.34**, and therefore this route was abandoned.

Following our studies on D-A reactions on sapphyrins macrocycles, **3.31** was first reacted with DMAD in toluene at reflux for 6 h (Scheme 3.12). The outcome from this reaction was rather easy to isolate through preparative TLC using EA as eluent, although the structure from the major fraction isolated was rather unexpected, evaluating by the spectroscopic analysis obtained from it.

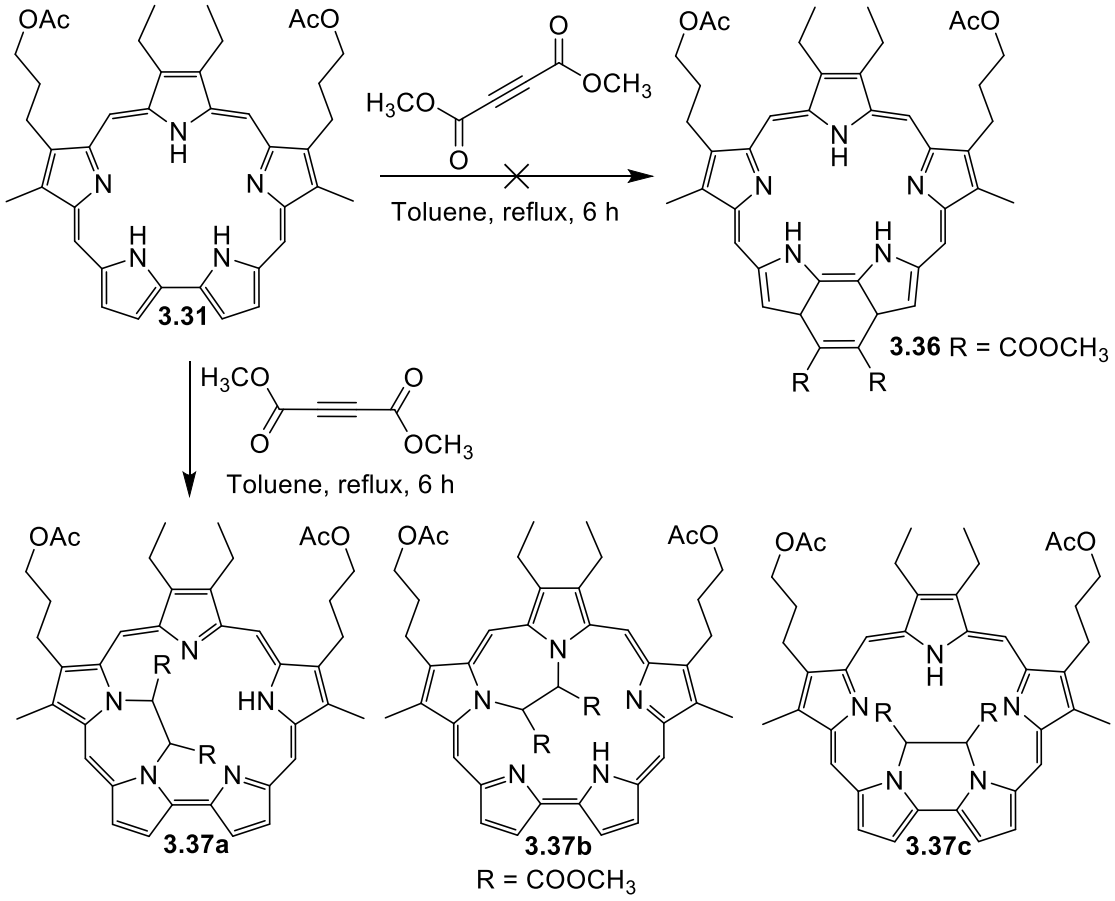

Scheme 3.12

Initial analysis by ^{1}H-NMR spectroscopy showed a loss of symmetry evaluating by the rather unusual split of the signal attributed to the *β*-pyrrolic protons and the signal attributed to *β*-CH_2 which are now seen as doublets each one integrating for one proton at δ 10.49, 10.29, 10.01, 9.77 ppm with a coupling constants of J = 4.6 and 4.3 Hz, and two singlets integrating for 3 protons individually at δ 4.21 and 3.78 ppm (H_t and $H_{t'}$). Also the signals attributed to the *meso*-H experienced the same behavior, giving place to a set of two singlets at δ 11.19 and 10.99 ppm integrating for one proton each and a doublet at δ 10.79 ppm integrating for two protons.

In fact these initial findings showed that the expected D-A reaction did not occurred and instead the reaction has occurred in such a way in which the molecule loss its symmetry, judging by the ^{1}H-NMR illustrated in the next figure.

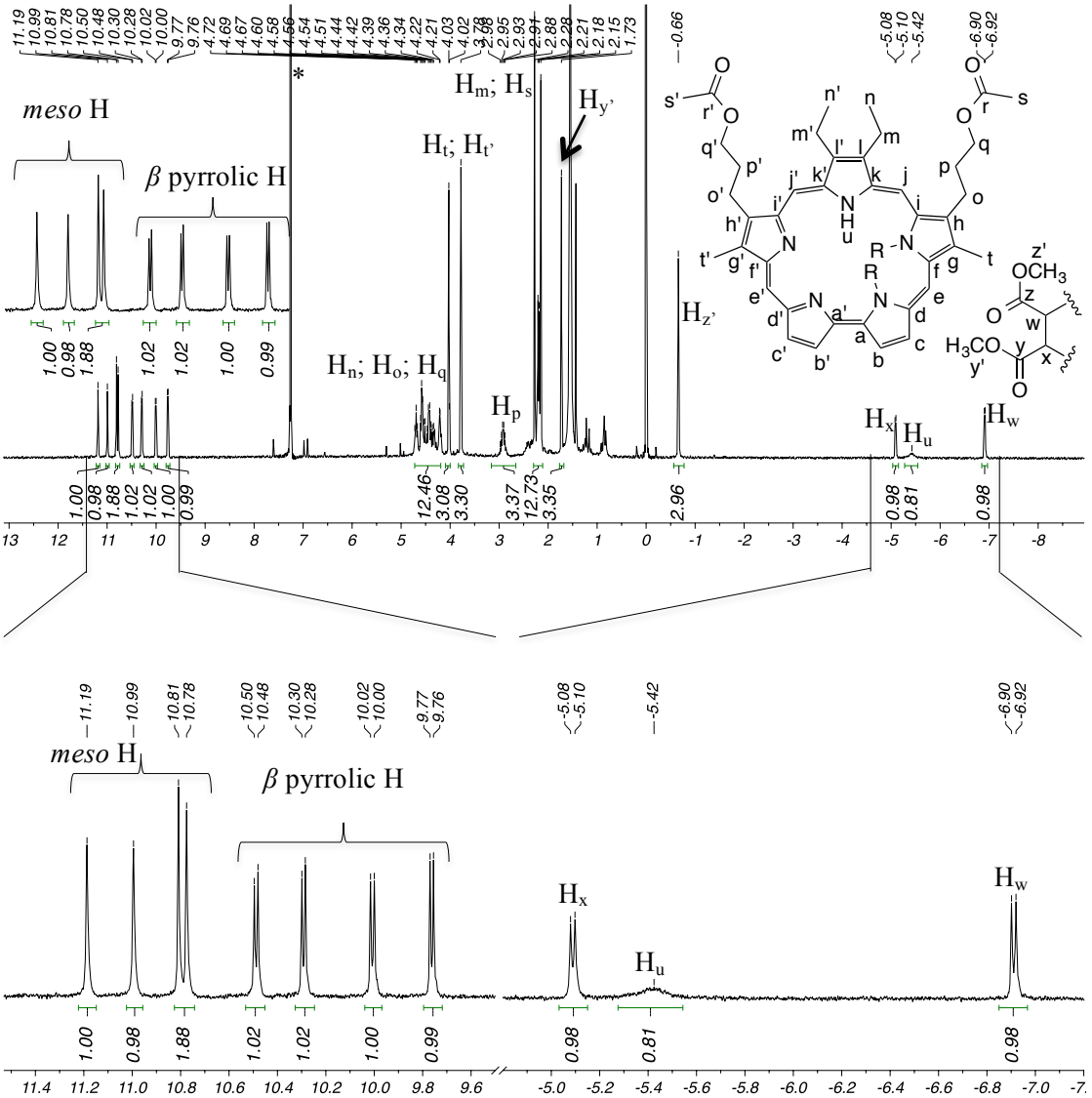

Figure 3.15: ^{1}H-NMR spectrum of compound **3.37** in $CDCl_3$ * stands for $CHCl_3$.

Interestingly, a closer insight to the ^{1}H-NMR spectra of this compound showed a new set of signals highly shielded at δ -0.66 ppm, a singlet integrating for 3 protons and two doublets at δ -5.09 and -6.91 ppm integrating for one proton each. Considering the coupling constants of the latter signals which couple with each other (J = 5.5) and the higher field location show a signal pattern usual when a substitution occurs in the inner space of the macrocycle. Furthermore only one NH proton can be distinguished in this region of the spectra. These findings were further supported with bidimensional spectroscopic techniques (HSQC and HMBC, Figures 3.16 and 3.17).

HSQC (Figure 3.16) analysis show that the signals at higher fields δ -0.66, -5.09 and -6.91 ppm correlate with carbons $C_{z'}$, C_x and C_w (δ 47.4, 51.5 and 47.8 ppm,

respectively) located in the aliphatic area of the spectra. These findings are consistent with the impression that the reaction occurred in the inner NH sites of the molecule.

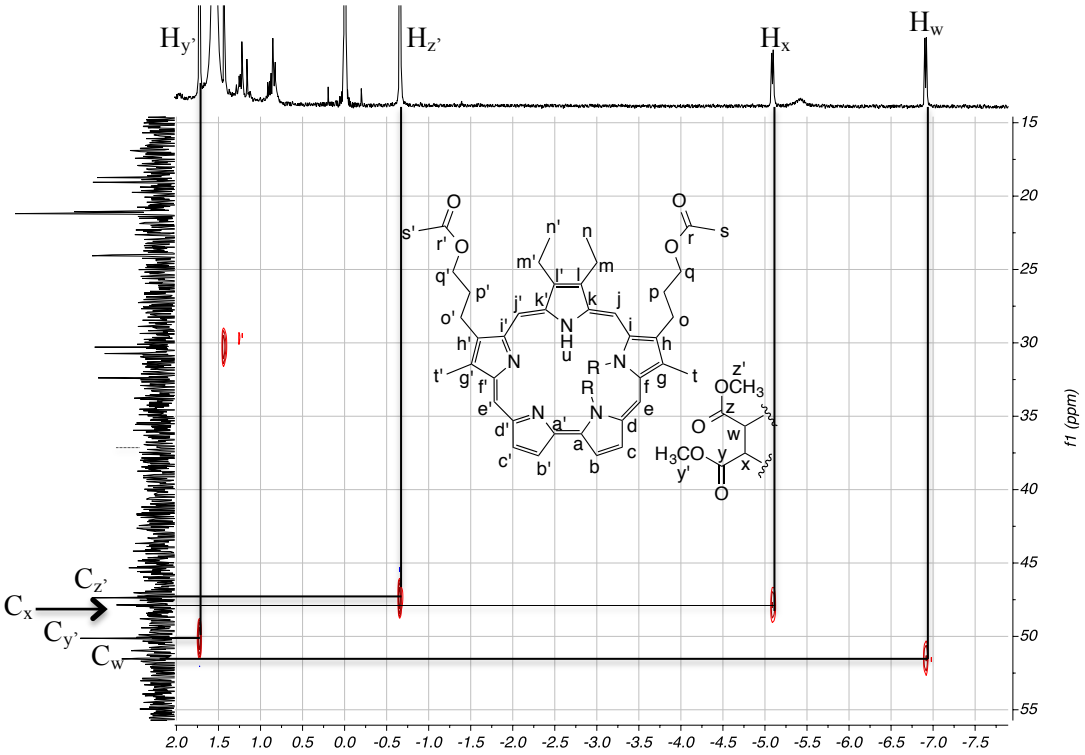

Figure 3.16: HSQC spectrum of compound **3.37** in $CDCl_3$.

Further analysis from the HMBC (Figure 3.16) spectrum it was also possible to confirm the close proximity between H_w (δ - 6.91 ppm), H_x (δ -5.09 ppm), $H_{z'}$ (-0.66 ppm) and $H_{y'}$ (δ 3.99 ppm).

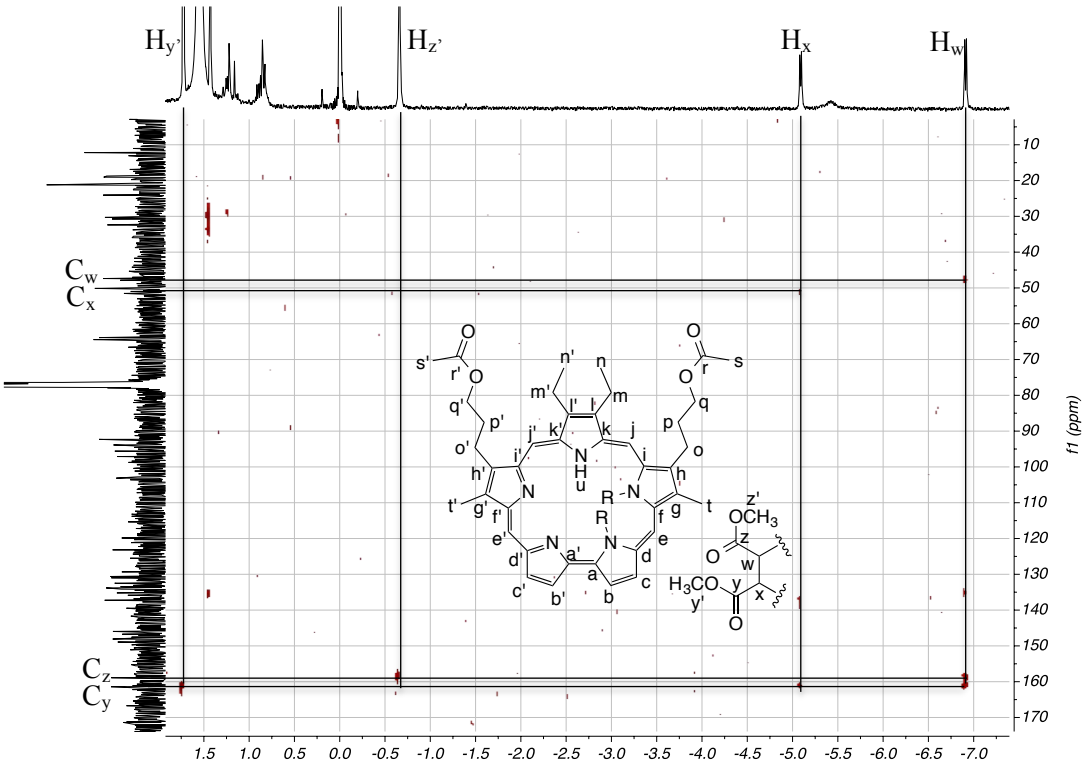

Figure 3.17: HMBC spectra of compound **3.37** in $CDCl_3$.

Here the long distance correlations between $H_{z'}$ (δ 10.51 ppm) and $H_{y'}$ (δ 3.88 ppm) with quaternary carbons C_z (δ 158.9 ppm) and C_y (δ 161.0 ppm) were also correlated (Figure 3.18).

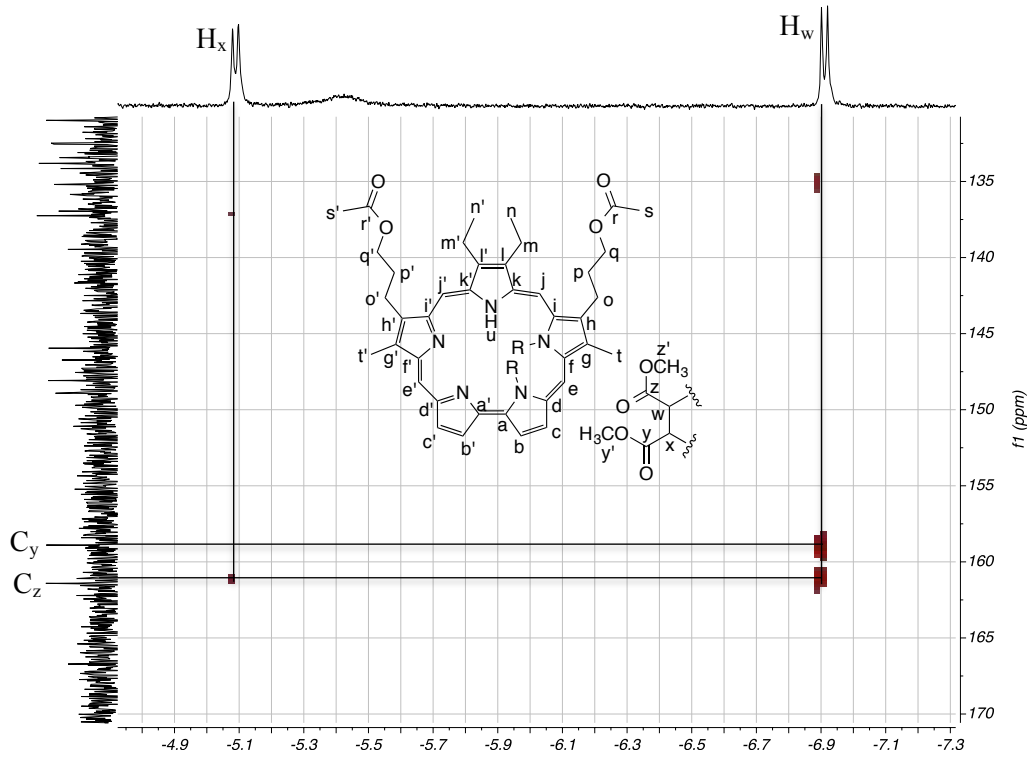

Figure 3.18: HSQC spectrum of compound **3.37** in $CDCl_3$.

The HSQC and HMBC spectra of compound **3.37** allowed the assignment of almost all the carbon resonances with exception for the signals due the *meso* and *β*-pyrrolic carbons. In spite of having sets of four signals for each one, a specific attribution is complicated since there is no absolute certain about the isomer obtained from this reaction.

Our efforts in this kind of reactions and having a prior access to bipyrrolic precursor **2.12** encouraged us to attempt the synthesis of sapphyrin derivative **3.37c** from the reaction of bipyrrole **2.12** and tripyrromethane **3.32** (Scheme 3.13). This possibility would allow us to exclude a possible enantiomer and try to understand if the previous reaction was taking place in one of the nitrogens located in the bipyrrolic moiety, excluding a possible enantiomer from the previous reaction.

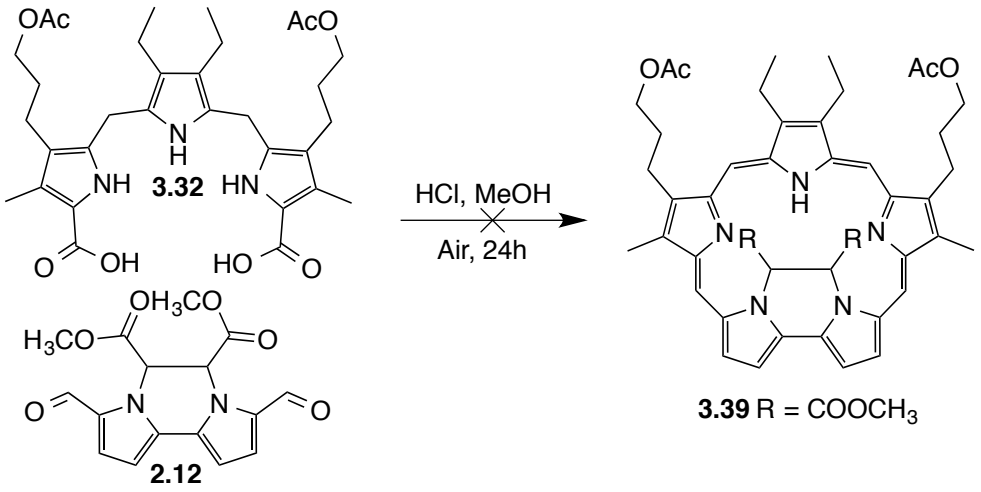

Scheme 3.13

This reaction was attempted in the same conditions as the previous nevertheless the possible product obtained showed low stability at rt complicating its purification and full characterization. The reason of this instability might be related with the obligatory steric hindrance introduced by the DMAD fraction of bipyrrole **2.12**. This provides an extra constrain in the sapphyrin framework not stabilizing it.

The chemistry presented above summarizes our attempts at another route towards obtaining the elusive benzosapphyrin derivative by means of a D-A, albeit, in this instance via reaction of DMAD with macrocycle **3.31**, instead of the first approach demonstrated in section 3.1. Accordingly, derivative **2.12** was also subject of ciclization reactions with **3.32** allowing a synthon for posterior functionalization through D-A, however, the result from this reaction revealed to be a scrambling product from the reaction of tripyrromethane **3.32** with the product of its own decomposition mediated by acidic media. Interestingly, when exposed to D-A reaction conditions **3.31**, the DMAD moiety reacted inside the macrocycles core furnishing. These findings are supported by the high field signals presented in the ^{1}H-NMR spectra attributed to the substitution pattern involved in this reaction, showing that the signals attributed to the DMAD moiety is surrounded by a strong diamagnetic ring (**3.37**). While it was not possible to determine which isomer we obtained from this reaction, attempts in the synthesis of isomer **3.37c** by rational synthesis were performed without the expected success (**3.38**). In fact the chemistry presented above show the unpredictability of expanded porphyrins when attempts are made to synthesize them or when they are subject of reactions their revealing a vast amount of possibilities, which are not taken into account when synthesizing their tetrapyrrolic counterparts.

3.3. Anion binding studies

Anion binding studies of sapphyrins **3.31** and **3.37,** in their protonated forms, were performed in order to inquire if the DMAD moiety in **3.37** induces a decrease in anion binding affinity. Sapphyrins interacts with anions in their core when their inner NH are protonated, for this reason both **3.31.HCl** and **3.37.HCl** were prepared performing a simple work-up with an HCl solution 0.1M. Stock solution of compounds **3.31.HCl** and **3.37.HCl** were prepared and anion binding studies were performed in a mixture of $CHCl_3$:MeOH (95:5) as solvent at 25 °C.

The perturbation caused by the addition of fluoride anion to **3.31.HCl** was followed by UV-Vis spectroscopy and, as expected, variations were observed in the Soret and Q bands (Figure 3.18a). When the same procedure was applied to **3.37.HCl**, the variations on the Soret and Q bands were very soft leading to a small variation from the anion free compound (Figure 3.18b). Trough Jobs method it was possible to confirm the 1:1 stoichiometry for the formation of sapphyrin:anion complex. The plot of ΔAbsorbance *vs* anion concentration at 440 nm were done and a non-linear equation were applied obtaining the affinity constants of $2.5x10^5$ and $3.5x10^3$ M^{-1}, for compound **3.31.HCl** and **3.37.HCl**, respectively. The treatment and procedures used in these tests are explained in section two of this thesis. Equations and methodologies are used accordingly.

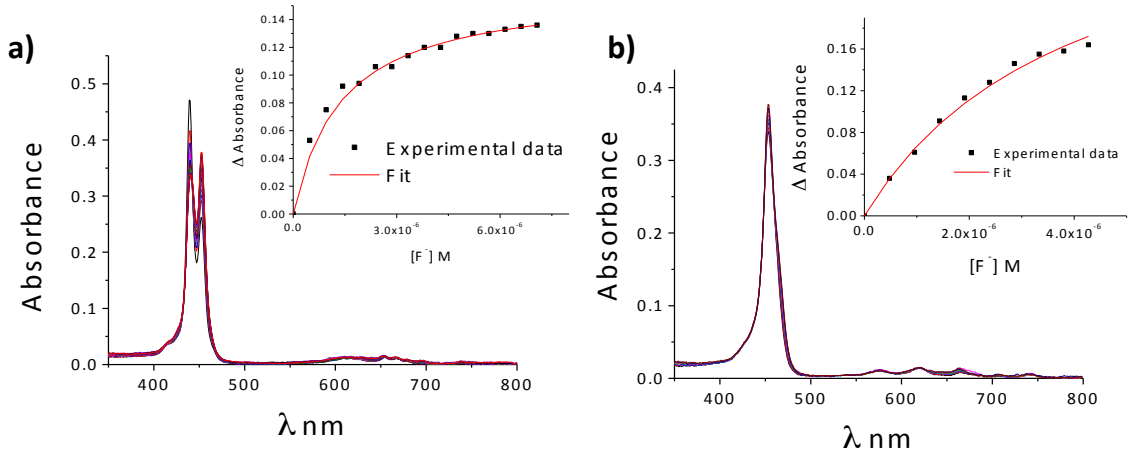

Figure 3.18: Absorption titration of a) Saphyrin **3.31.HCl**, b) Saphyrin **3.37.HCl** with fluoride anion*; insets:* fit of the experimental data at 440 nm with a 1:1 non-linear regression.

These anion binding results confirm that adduct **3.37.HCl** has a dramatic decrease in the affinity constant and thereby, present an extra obstruction in is core, when compared

with **3.31**.HCl. These findings in concordance with the NMR characterization of this adduct discussed in detail previously.

3.4. Experimental data

3.4.1. Experimental procedures

*Preparation of bipyrrole **3.11***

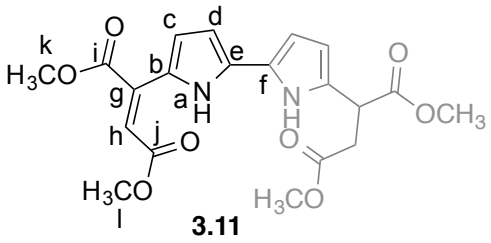

3.11

Chemical Formula: $C_{20}H_{22}N_2O_8$
Exact Mass: 418.14

To a stirred solution of **1.36** (100 mg, 0.756 mmol) in THF (3 mL), dimethyl acetylenedicarboxylate (414 µL, 4.54 mmol) was added. The reaction was left at rt for 30 min. and was monitored by TLC. After stirring for the required time, the solvent was evaporated under vacuum, and the residue was purified by column chromatography on silica gel with petroleum ether and dichloromethane (1:1) (203 mg, yield = 67 %).

^{1}H NMR (300 MHz, $CDCl_3$) δ 13.16 (s, 2H, NH_a), 6.85 (dd, J = 4.1, 2.3 Hz, 2H, β-pyrrolic H_c)), 6.65 (dd, J = 4.0, 2.5 Hz, 2H, β-pyrrolic H_d), 6.03 (s, 2H, H_j), 3.92 (s, 6H, OCH_3, H_h), 3.85 (s, 6H, OCH_3, H_k).
^{13}C NMR (75 MHz, $CDCl_3$) δ 169.3 (C_g), 167.9 (C_j), 137.56 (C_b), 129.72 (Ce), 127.2 (C_f), 120.1 (β-pyrrolic C_c), 109.8 (β-pyrrolic C_d), 108.3 (C_i), 52.9 (C_h), 52.4 (C_k).

*Preparation of bipyrrole **3.19***

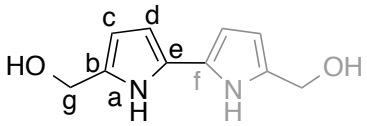

Chemical Formula: $C_{10}H_{12}N_2O_2$
Exact Mass: 192.09

To a stirred solution of compound **2.11** (100 mg, 0.531 mmol) in dried THF, was added 120 mg of $NaBH_4$ (3.19 mmol). The mixture was allowed to react at rt during one hour. The mixture was then quenched with distilled water (20 mL), and extracted with ethyl

acetate (3 x 25 mL). The combined organic extracts were dried over Na_2SO_4 and further evaporation of the solvents furnished a white solid. Purification by crystallization with a mixture of CH_2Cl_2 /hexane furnished **3.19** (90 mg) in 61% yield.

^{1}H NMR (300 MHz, $CDCl_3$) δ 6.03 (dd, J = 4.1, 2.3 Hz, 2H, β-pyrrolic H_c), 5.93 (dd, J = 4.0, 2.5 Hz, 2H, β-pyrrolic H_d), 4.41 (s, 4H, H_g).

*General procedure used in the preparation of bipyrrole **3.19** and **3.20***

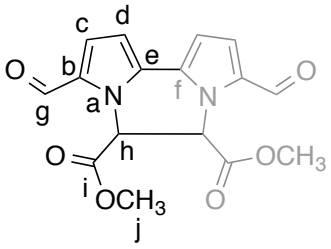

3.19
Chemical Formula: $C_{16}H_{14}N_2O_6$
Exact Mass: 330.09

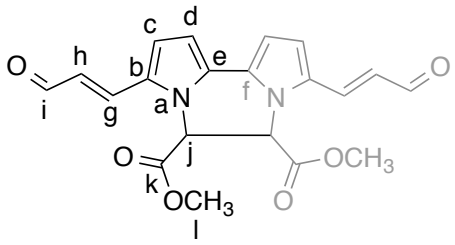

3.20
Chemical Formula: $C_{20}H_{18}N_2O_6$
Exact Mass: 382.12

To a stirred solution of the corresponding diformyl-bipyrrole (500 mg, 1.51 mmol (**2.11**) and 1.30 mmol (**2.12**)) in THF (20 mL), dimethyl acetylenedicarboxylate (1.29 mL, 9.06 mmol) and a catalytic amount of NEt_3 were added. The reaction was left refluxing for 6 h and was monotorized by TLC. After stirring for the required time, the solvent was evaporated in vacuum. A mixture of petroleum ether and dichloromethane (1:1) was added to the brown residue and after 1 h the desired compound was filtrated and washed with petroleum ether. The yellow solid corresponding to **3.19** was then dried in vacuum and used without further purification (yield = 76%). The solid corresponding to **3.20** was further chromatographed over flash silica gel, furnishing a reddish powder corresponding to **3.20** in 63% yield.

*Bipyrrole **3.19***

^{1}H NMR (300 MHz, $CDCl_3$) δ 9.57 (s, 2H, CHO, H_g), 7.06 (d, J = 4.2 Hz, 2H, β-pyrrolic H_c), 6.76 (s, 2H, H_h), 6.65 (d, J = 4.2 Hz, 2H, β-pyrrolic H_d), 3.72 (s, 6H, H_j).

^{13}C NMR (75 MHz, $CDCl_3$) δ 179.8 (CHO, C_f), 167.6 (C_h), 132.0 (α-pyrrolic C_b), 130.1 (α-pyrrolic C_e), 125.2 (β-pyrrolic C_c), 108.8 (β-pyrrolic C_d), 57.1 (C_g), 53.7 (C_i).

HRMS (ESI) m/z: calculated for $[M+H]^+$ = 331.0924, found 331.0936.

Melting Point: 237.3 ºC

Bipyrrole ***3.20***

^{1}H NMR (300 MHz, $CDCl_3$) δ 9.60 (d, J = 7.5 Hz, 2H, C<u>H</u>O, H_i), 6.90 (dd, J = 4.1, 0.5 Hz, 2H, β-pyrrolic H_d), 6.61 (dd, J = 4.2, 0.5 Hz, 2H, β-pyrrolic H_c), 6.52 (dd, J = 15.5, 7.6 Hz, 2H,x), 5.88 (s, 2H,x), 3.73 (s, 6H, H_l).

^{13}C NMR (75 MHz, $CDCl_3$) δ 192.4 (CHO, C_h), 167.1 (C_j), 136.7 (C_g), 130.1 (α-pyrrolic C_b), 128.5 (α-pyrrolic, C_e), 124.7 (β-pyrrolic, C_c), 116.6 (C_f), 108.8 (β-pyrrolic C_d), 56.2 (C_j), 54.2 (C_k).

Melting Point: 288.7 ºC

Preparation of [22]sapphyrin ***3.31***

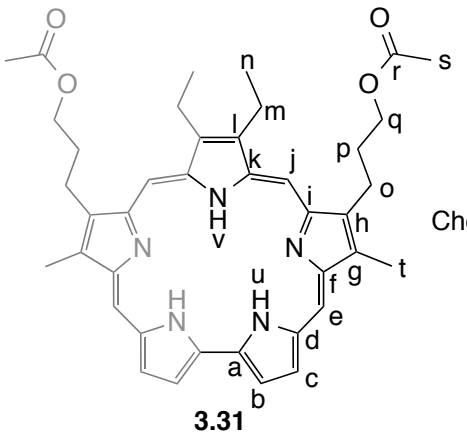

3.31

Chemical Formula: $C_{40}H_{45}N_5O_4$
Exact Mass: 659.34715

Conc. HCl (0.075 mL) was added dropwise to a stirred solution of the tripyrromethane dicarboxylic acid **3.30** (0.59 g, 1.1 mmol) and bipyrrole **2.11** (0.188 mg, 1.1 mmol) in MeOH (1 L) at room temperature. The reaction was monitored by TLC and deemed complete after 24 h. The solution was neutralized with NEt_3 and concentrated to a few milliliters under reduced pressure. The crude mixture was purified by passing through a plug of neutral alumina using CH_2Cl_2/MeOH (95:5) as eluent. Sapphyrin **3.31** was then purified by column chromatography (silica gel) using THF/petroleum ether (1:1) as eluent. Sapphyrin **3.31** was crystallized from $CHCl_3$/ethanol, yielding blue crystals (130 mg, 18% yield).

^{1}H NMR (300 MHz, $CDCl_3$) δ 11.57 (2s, 4H, *meso*-H), 10.39 (2s, 4H, β-pyrrolic), 4.99 – 4.57 (m, 12H, H_q, H_m and H_o), 4.23 (s, 6H, H_t), 3.14 – 2.94 (m, 4H, H_p), 2.28 (d, J = 7.4 Hz, 12H, H_s, H_n).

^{1}H NMR (300 MHz, $CDCl_3$/TFA 10%) δ 12.06 (2s, 4H, *meso*-H), 10.97 (s, 2H, β-pyrrolic), 5.09 – 4.82 (m, 8H, H_q and H_m), 4.75 (t, J = 6.1 Hz, 4H, H_o), 4.38 (s, 6H, H_t), 3.03 (t, J = 7.8 Hz, 4H, H_p), 2.38 (s, 6H, H_s), 2.32 (t, J = 7.6 Hz, 6H, H_n), -5.91 (d, J = 46.1 Hz, 3H, NH_u), -6.86 (s, 2H, NH_v).

^{13}C NMR (126 MHz, $CDCl_3$/TFA 10%) δ 175.4 (C_r), 144.54-132.0 (quaternary C), 130.7 (β-pyrrolic C), 123.3 (β-pyrrolic C), 113.0 (*meso*-H), 110.7 (*meso*-H), 65.7 (H_o), 31.7 (C_p), 24.1 (C_q), 21.1 (C_m), 21.1 (C_s), 18.3 (C_n), 12.9 (C_t).

HRMS (ESI+) m/z: calculated for $C_{40}H_{46}N_5O_4$ $[M+H]^+$ = 660.3550, found 660.3581.

Melting Point: > 350.0 ºC

Preparation of [22]sapphyrin ***3.32***

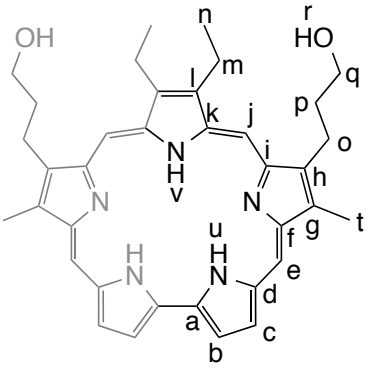

Chemical Formula: $C_{36}H_{41}N_5O_2$
Exact Mass: 575.33

3.32

NaOMe (50 eq. 0.23 mmol, 0.12 mg) was added to a stirred solution of the sapphyrin **3.31** (30 mg, 0.04 mmol) in CH_2Cl_2/MeOH (2:1, 10 mL) at room temperature, and afterwards taken it into reflux. The reaction was monitored by TLC and deemed complete after 24 h. The crude mixture was purified by passing through a plug of neutral alumina using CH_2Cl_2/MeOH (90:10) as eluent. Sapphyrin **3.32** was crystallized from $CHCl_3$/acetone, yielding blue crystals (21.1 mg, 88% yield).

^{1}H NMR (300 MHz, $CDCl_3$/Methanol-d_4 10%) δ 11.23 (2s, 4H, *meso*-H_e and H_j), 9.98 (s, 4H, β-pyrrolic H), 4.92 – 4.66 (m, 8H, H_m and H_q), 4.36 – 4.05 (m, 10H, H_o and H_t), 2.86 (d, J = 6.9 Hz, 6H, H_p), 2.30 (t, J = 7.5 Hz, 6H, H_n).

^{13}C NMR (75 MHz, $CDCl_3$/Methanol-d_4 10%) δ 143.9-129.9 (quaternary C), 127.8 (*β*-pyrrolic C), 121.6 (*β*-pyrrolic C), 98.4 (*meso*-C), 90.5 (*meso*-C), 61.5 (C_o), 36.1 (C_p), 23.9 (C_q), 20.9 (H_m), 18.8 (C_n), 12.7 (C_t).

^{1}H NMR (300 MHz, $CDCl_3$/TFA 10%) *δ* 12.04 (2s, 4H, *meso*-H), 10.68 (d, *J* = 4.7, 2H, *β*-pyrrolic), 5.00 (dt, *J* = 11.7, 6.1 Hz, 8H, H_m and H_q), 4.87 (d, *J* = 7.6 Hz, 4H, H_o and H_t), 4.38 (d, *J* = 2.8 Hz, 6H, H_o and H_t), 3.13 (t, *J* = 7.8 Hz, 4H, Hn), 2.31 (t, *J* = 8.7 Hz, 6H, H_n), -5.88 (d, *J* = 50.9 Hz, 2H, H_u), -6.85 (s, 1H, H_v).

^{13}C NMR (126 MHz, $CDCl_3$/TFA 10%) *δ* 141.7-133.4 (quaternary C), 132.2 (*β*-pyrrolic C), 125.2 (*β*-pyrrolic C), 102.1 (*meso*-C), 90.0 (*meso*-C), 52.0 (C_o) 36.2 (C_p), 23.4 (C_q), 20.2 (H_m), 18.65 (C_n), 12.4 (C_t).

HRMS (ESI+)*m/z*: calculated for $C_{36}H_{42}N_5O_2$ $[M+H]^+$ = 576.3333, found 576.3326.

Melting Point: > 350.0 ºC

*Synthesis of porphyrin **3.35***

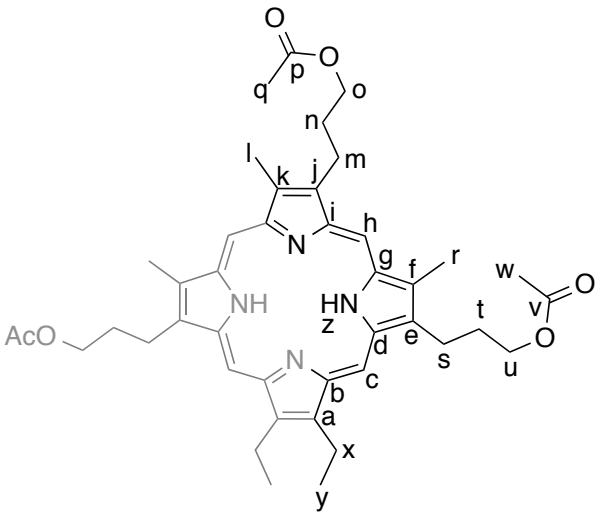

Chemical Formula: $C_{42}H_{52}N_4O_6$
Exact Mass: 708.39

3.35

Conc. HCl (0.075 mL) was added dropwise to a stirred solution of the tripyrromethane dicarboxylic acid **3.30** (0.591 mg, 1.10 mmol) and **2.12** (420 mg, 1.10 mmol) in MeOH (1 L) at room temperature. The reaction was monitored by TLC and deemed complete after 24 h. The solution was neutralized with Net_3 and concentrated to a few millilitres under reduced pressure. The crude mixture was purified by passing through a plug of neutral alumina using CH_2Cl_2 as eluent. Porphyrin **3.37** was next purified by preparative TLC using EA/petroleum ether (2:1) and crystallized from CH_2Cl_2/ethanol, yielding reddish crystals (23.2 mg, 3 % yield).

^{1}H NMR (300 MHz, $CDCl_3$) δ 10.19 – 9.94 (m, 4H, *meso* H_c and H_h), 4.52 – 4.31 (m, 6H, H_o, H_u), 4.25 – 4.02 (m, 12H, H_m, H_s and H_x), 3.74 – 3.53 (m, 9H, β-CH_3, H_r, H_l), 2.63 (t, J = 6.6 Hz, 6H, H_n and H_t), 2.23 – 2.12 (m, 9H, H_q and H_w), 1.92 (t, J = 7.6 Hz, 6H, H_y), -3.76 (s, 2H, NH_z).

^{13}C NMR (75 MHz, $CDCl_3$) δ 171.3 (C_v, C_p), 141.34-135.8 (quaternary C), 96.7 (*meso* C), 96.4 (*meso* C), 95.94 (*meso* C), 64.1 (H_o and H_u), 31.8 (C_n and C_t), 22.8 (H_m and H_s), 21.1 (C_q, C_w), 19.8 (C_x), 18.52 (C_y), 11.8 (x), 11.7 (C_r and C_l).

MALDI-TOF: *m/z* 709.4 $[M+H]^+$

HRMS (ESI+)*m/z*: calculated for $C_{42}H_{53}N_4O_6$ $[M+H]^+$ = 709.3959, found 709.3958.

Melting Point: > 350.0 ºC

Synthesis of [22]sapphyrin adduct ***3.37***

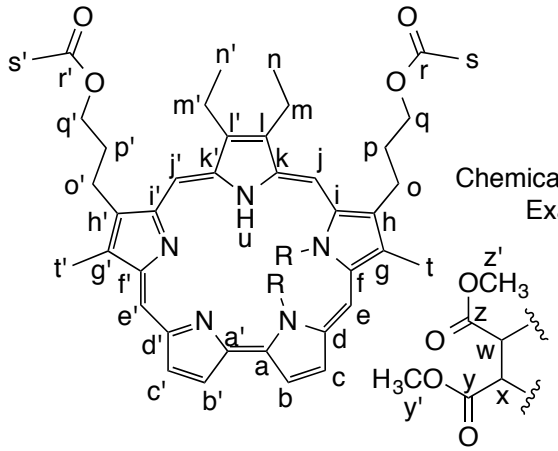

A solution of sapphyrin (20.0 mg, 0.03 mmol) and (21.0 mg, 0.15 μmol, 5 equiv) in toluene (2 mL) was stirred for 12 h at reflux under a nitrogen atmosphere. The reaction mixture was directly evaporated and adduct **3.35** was purified by preparative TLC using EA as the eluent, followed by crystallization from ethanol/hexane (5.1 mg, 21 % yield).

^{1}H NMR (300 MHz, $CDCl_3$) δ 11.19 (s, 1H, *meso*-H), 10.99 (s, 1H, *meso*-H), 10.79 (d, J = 10.0 Hz, 2H, *meso*-H), 10.49 (d, J = 4.6 Hz, 1H, β-pyrrolic H), 10.29 (d, J = 4.3 Hz, 1H, β-pyrrolic H), 10.01 (d, J = 4.6 Hz, 1H, β-pyrrolic H), 9.76 (d, J = 4.3 Hz, 1H, β-pyrrolic H), 4.72 – 4.19 (m, 12H, H_m, H_o and H_x), 4.03 (s, 3H, β-CH_3, H_t), 3.78 (s, 3H, β-CH_3, $H_{t'}$), 2.93 (dt, J = 14.0, 7.2 Hz, 4H, H_p), 2.30 – 2.11 (m, 12H, H_q, H_n, $H_{n'}$, H_s and $H_{s'}$), 1.73 (s,

3H, $H_{y'}$), -0.66 (s, 3H, $H_{z'}$), -5.09 (d, J = 5.5 Hz, 1H, H_x), -5.42 (s, 1H, NH_u), -6.91 (d, J = 5.5 Hz, 1H, H_w).

^{13}C NMR (75 MHz, $CDCl_3$) δ 171.4 (C_r and $C_{r'}$), 161.4 (C_y), 158.9 (C_z), 152.1-135.2 (quaternary C), 134.2 (β-pyrrolic H), 133.8-131.0 (quaternary C), 129.3 (β-pyrrolic C), 123.2 (β-pyrrolic C), 119.9 (β-pyrrolic C), 103.13 (*meso*-C), 97.1 (*meso*-C), 95.6 (*meso*-C), 93.9 (*meso*-C), 64.4 (H_q and $H_{q'}$), 51.5 (C_w), 50.1 ($H_{y'}$), 47.8 (C_x), 47.4 ($H_{z'}$), 32.4 (H_p and $H_{p'}$), 24.1 (H_m and $H_{m'}$) 21.1 (H_s and $H_{s'}$), 18.7 (H_n and $H_{n'}$), 12.2 (H_t and $H_{t'}$).

HRMS (ESI+)*m/z*: calculated for $C_{46}H_{52}N_5O_8$ $[M+H]^+$ = 802.3810, found 802.3795.

Melting Point: > 350.0 ºC

3.5. References

1. Sauer J and Sustmann R. *Angew. Chem. Int. Ed.* 1980; **19**: 779-807.
2. Kagan HB and Riant O. *Chem. Rev.* 1992; **92**: 1007-1019.
3. Pindur U, Lutz G and Otto C. *Chem. Rev.* 1993; **93**: 741-761.
4. Juhl M and Tanner D. *Chem. Soc. Rev.* 2009; **38**: 2983-2992.
5. Merino P, Marques-Lopez E, Tejero T and Herrera RP. *Synthesis-Stuttgart* 2010: 1-26.
6. Nair V, Menon RS, Biju AT and Abhilash KG. *Chem. Soc. Rev.* 2012; **41**: 1050-1059.
7. Jacobi PA, Touchette KM and Selnick HG. *J. Org. Chem.* 1992; **57**: 6305-6313.
8. Grieco PA, Zelle RE, Lis R and Finn J. *J. Am. Chem. Soc.* 1983; **105**: 1403-1404.
9. Hsu CT, Wang NY, Latimer LH and Sih CJ. *J. Am. Chem. Soc.* 1983; **105**: 593-601.
10. Klein LL. *J. Am. Chem. Soc.* 1985; **107**: 2573-2574.
11. Li Y and Houk KN. *J. Am. Chem. Soc.* 1993; **115**: 7478-7485.
12. Hata H, Shinokubo H and Osuka A. *Angew. Chem. Int. Ed.* 2005; **44**: 932-935.
13. Tome JPC, Cho DG, Sessler JL, Neves MGPMS, Tome AC, Silva AMS and Cavaleiro JAS. *Tetrahedron Lett.* 2006; **47**: 3131-3134.
14. Silva AMG, Tome AC, Neves MGPMS and Calvaleiro JAS. *Tetrahedron Lett.* 2000; **41**: 3065-3068.
15. Vale LSHP, Barata JFB, Neves MGPMS, Faustino MAF, Tome AC, Silva AMS, Paz FAA and Cavaleiro JAS. *Tetrahedron Lett.* 2007; **48**: 8904-8908.
16. Barata JFB, Neves MGPMS, Tome AC and Cavaleiro JAS. *J. Porphyrins Phthalocyanines* 2009; **13**: 415-418.
17. Barata JFB, Silva AMG, Faustino MAF, Neves MGPMS, Tome AC, Silva AMS and Cavaleiro JAS. *Synlett* 2004: 1291-1293.
18. Boger DL. *Chem. Rev.* 1986; **86**: 781-793.
19. Woodward RB and Hoffmann R. *Angew. Chem. Int. Ed.* 1969; **8**: 781-853.
20. Fukui K. *Acc. Chem. Res.* 1971; **4**: 57-64.
21. Houk KN. *Acc. Chem. Res.* 1975; **8**: 361-369.
22. Li Y and Evans JNS. *J. Am. Chem. Soc.* 1995; **117**: 7756-7759.
23. Dannenberg JJ. *Chem. Rev.* 1999; **99**: 1225-1241.

24. Houk KN, Li Y and Evanseck JD. *Angew. Chem. Int. Ed.* 1992; **31**: 682-708.

25. McCabe JR and Eckert CA. *Acc. Chem. Res.* 1974; **7**: 251-257.

26. Asano T and Le Noble WJ. *Chem. Rev.* 1978; **78**: 407-489.

27. Van Eldik R, Asano T and Le Noble WJ. *Chem. Rev.* 1989; **89**: 549-688.

28. Sauer J. *Angew. Chem. Int. Ed.* 1967; **6**: 16-33.

29. Nicolaou KC, Snyder SA, Montagnon T and Vassilikogiannakis G. *Angew. Chem. Int. Ed.* 2002; **41**: 1668-1698.

30. Wuts PGM and Greene TW. *Greene's Protective Groups in Organic Synthesis, 4th Edition*; John Wiley & Sons, Inc., 2006

31. Kim JH, Coric I, Vellalath S and List B. *Angew. Chem. Int. Ed.* 2013; **52**: 4474-4477.

32. Firouzabadi H, Iranpoor N and Hazarkhani H. *J. Org. Chem.* 2001; **66**: 7527-7529.

33. Knall AC and Slugovc C. *Angew. Chem. Int. Ed.* 2013; **42**: 5131-5142.

34. Jiang XX and Wang R. *Chem. Rev.* 2013; **113**: 5515-5546.

35. Geier GR, Ciringh Y, Li FR, Haynes DM and Lindsey JS. *Org. Lett.* 2000; **2**: 1745-1748.

36. Geier GR and Lindsey JS. *J. Org. Chem.* 1999; **64**: 1596-1603.

37. Narayanan SJ, Sridevi B, Srinivasan A, Chandrashekar TK and Roy R. *Tetrahedron Lett.* 1998; **39**: 7389-7392.

38. Richter DT and Lash TD. *Tetrahedron Lett.* 1999; **40**: 6735-6738.

39. Tome JPC, Cho DG, Sessler JL, Neves MGPMS, Tome AC, Silva AMS and Cavaleiro JAS. *Tetrahedron Lett.* 2006; **47**: 3131-3134.

40. Dansodanquah RE, Xie LY and Dolphin D. *Heterocycles* 1995; **41**: 2553-2564.

4. Nucleophilic substitution reactions on *meso*-pentafluorophenyl expanded porphyrins

4. Nucleophilic substitution reactions on *meso*-pentafluorophenyl expanded porphyrins

4.1. *meso*-Pentafluorophenyl pentaphyrins: overview

Pentaphyrins(1.1.1.1.1) that bear five pyrroles regularly connected through *meso*-carbons, contain a structural addition of a pyrrole and a *meso*-carbon to the planar porphyrin skeleton. Regarding this subject, *β*-alkylated pentaphyrins **1.63**, **4.1**, doubly *N*-confused mono-oxygenated and di-oxigenated pentaphyrins **4.2** and **4.3**, respectively, were shown to be non-fused macrocycles [1-3]. However, *meso*-aryl substituted pentaphyrin **1.101**, formed from a modified Rothemund-Lindsey protocol, was forced to take an *N*-fused conformation with two inverted pyrroles, because of severe steric congestion [4]. The reaction mechanism is until now unknown, yet the removal of one *meso*-pentafluorophenyl substituents from **1.101** to 5,10,15,20-tetrakispentafluorophenyl [22]pentaphyrin (**4.4**) led to a drastic conformational change from a *N*-fused macrocycle to a non-fused yet planar pentaphyrin with an inverted pyrrole (**4.4**) [5]. In fact, regular *meso*-substituted pentafluorophenyl pentaphyrins are only known as *N*-fused species [6]. The ones that do not display this feature have enough structural modifications in order to adjust its conformation in such a way where the macrocycle does not require *N*-fusion to stabilize itself. These examples are depicted in the next figure, where **4.2** and **4.3** are doubly *N*-confused (two pyrroles of the structure contain bonds at *β*-position and *α*-position maintaining its conjugation).

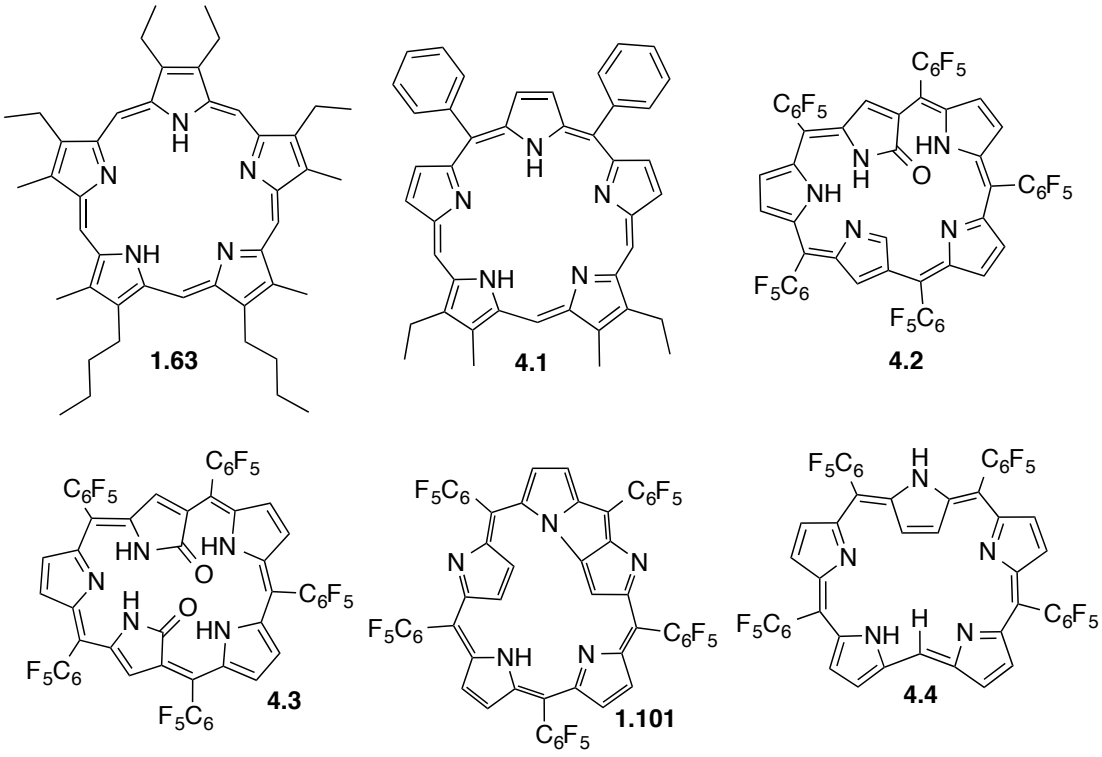

Figure 4.1: Pentaphyrin structures.

The behaviour that these macrocycles display and their structural appearance is highly dependent of the substituents that they have around the macrocycle, being completely regular (NH pointing to the interior of the macrocycle) when there are no substituents in the *meso*-positions (*e.g.* **1.63**), one or two pyrroles may suffer inversion when the *meso*-positions are partially substituted (*e.g.* **4.4**), or they may suffer *N*-fusion when these positions are fully substituted by pentafluorophenyl motifs (*e.g.* **1.101**). *N*-confusion, in the other hand is synthetically achieved using building blocks containing already the *N*-confused motifs (**4.2** and **4.3**) [7]. One interesting example of the last two classes of pentaphyrins is compound **1.104** (Scheme 1.18) which contains a single *N*-confused site, nevertheless further oxidation followed by rearrangement makes it a mixed *N*-confused and doubly *N*-fused macrocycle (compounds **1.105** and **1.106**) [3].

During the synthesis of compound **1.101** under modified Linsey-Rothemund conditions, namely, the acid catalyzed condensation of pentafluorobenzaldehyde and unsubstituted pyrrole, followed by oxidation with DDQ, along with **1.101** it is possible to additionally obtain, *meso*-pentafluorophenyl porphyrin (12%), *meso*-pentafluorophenyl [26]hexaphyrin (20%), and other higher analogues of *meso*-pentafluorophenyl type [4].

An interesting feature of *N*-fused pentaphyrin **1.101** is that it can exist in two stable oxidation states, namely **1.100** and **1.101** that contain 24 and 22 peripheric π-electrons, respectively. Conveniently, the two species are readily interconverted by means of oxidation with DDQ or by reduction with sodium borohydride (Scheme 4.1). This behavior occurs in all the expanded products obtained from the Linsey-Rothemund methodology discussed previously [8].

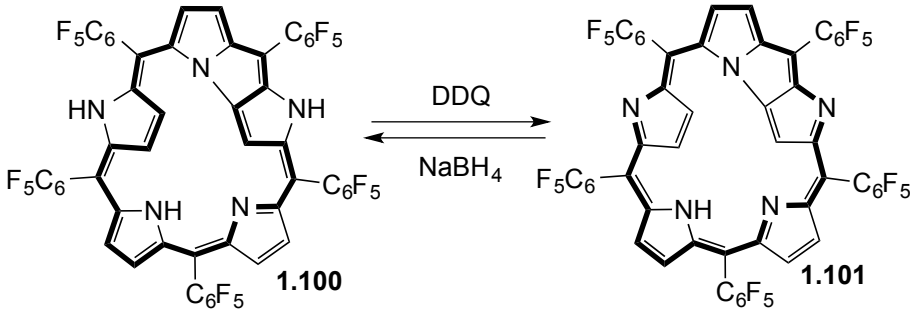

Scheme 4.1

Concerning the definition of expanded porphyrins as already referred in the introduction section of this thesis, macrocycles that contain pyrrole subunits linked together either directly or through one or more spacer atoms in such a manner that the internal ring pathway (strong black delineation in scheme 4.1 in macrocycles **1.100** and **1.101**) contains a minimum of 17 atoms. This can also be extended to the number of π electrons present in the macrocycle. Along the shortest conjugation pathway it is possible to count 24 and 22 π electrons showing the oxidation states of **1.100** and **1.101**, respectively [9].

Most of the interest of regular *meso*-substituted *N*-fused pentaphyrins until now has been drifted to the structural diversity of which macrocycle can display a distinct metallation chemistry and several aromatic characteristics are discussed and studied over DFT calculations [10-15]. Among them, phosphorous and rhodium complexes of compounds **1.100** and **1.101** have been developed by Osuka and coworkers showing in each case the structural diversity of these macrocycles providing macrocycles **4.5**, **4.6** and **4.7**, respectively [12,14]. Recently Suzuki and co-workers were able to add a new derivative to the family of pentaphyrins reacting **1.101** with NBS, obtaining an unprecedented skeletal recombination acquiring **4.8** [16].

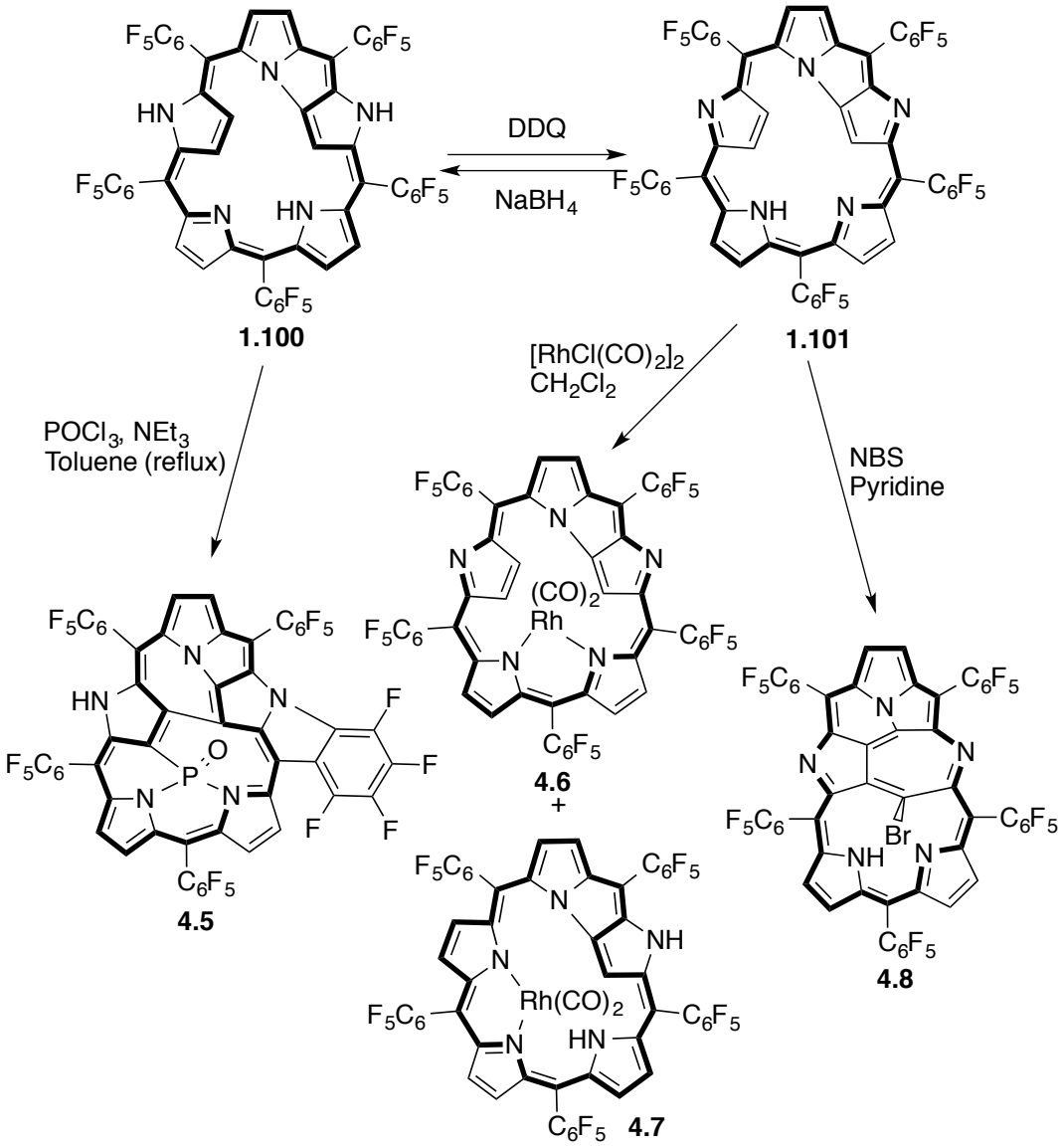

Scheme 4.2

Subsequently, not much has been developed and only derivatives with one or no substitution in the *meso*-positions of these macrocycles have found interest in biomedical fields (figure 4.2) [17-22].

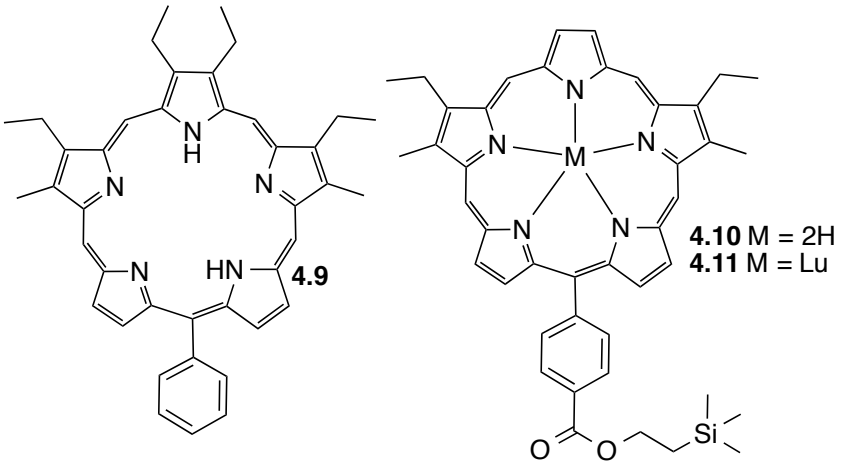

Figure 4.2: Pentaphyrins used in biomedical studies.

Most of the biomedical studies with compounds presented in figure 4.2 were achieved by Commuzzi *et al.,* where pentaphyrins **4.9** and **4.10** showed anti-tumor activity against several cancer cell lines and effective antibacterial activity against *gram*-positive bacteria*,* respectively [19,21]. Latter these authors, discovered that the 1:1 complex of **4.10** with Lu(III) giving **4.11**, significantly increases the cellular uptake, and reactive oxidative species production against four cancer cell lines. This study displayed that metal complexation was a useful strategy to potentiate these compounds as PDT drug agents [22]. These examples combine a photosensitizer (PS), light and oxygen leading to the formation of cytotoxic species (singlet oxygen and free radicals) that can destroy those microorganisms or cancer cells. This can also be an effective concept in the photodecontamination of drinking and wastewater samples under solar radiation. Several studies already reported in literature show that cationic tetrapyrrolic macrocycles, can be very effective agents against bacteria strains that are resistant to antibiotics. Having in mind the red-shifted absorption of expanded macrocycles we focused in the functionalization of expanded porphyrins with moieties, which would allow us to obtain final cationic compounds to apply as agents in aPDT.

4.2. *meso*-Pentafluorophenyl *N*-fused pentaphyrins: experimental results

Synthetically, expanded porphyrins of *meso* aryl type are achieved in one pot reaction, where pyrrole reacts with pentafluorobenzaldehyde in presence of $BF_3.OEt_2$. The reactants are dissolved in CH_2Cl_2 in a concentration of about 67 mM, and the use of

CH_2Cl_2 is of high importance, since attempts made with $CHCl_3$ leads to a decrease in the overall yield of the desired macrocycles. Purification over a short pad of neutral alumina followed by silica flash chromatography leads to pure **1.101**.

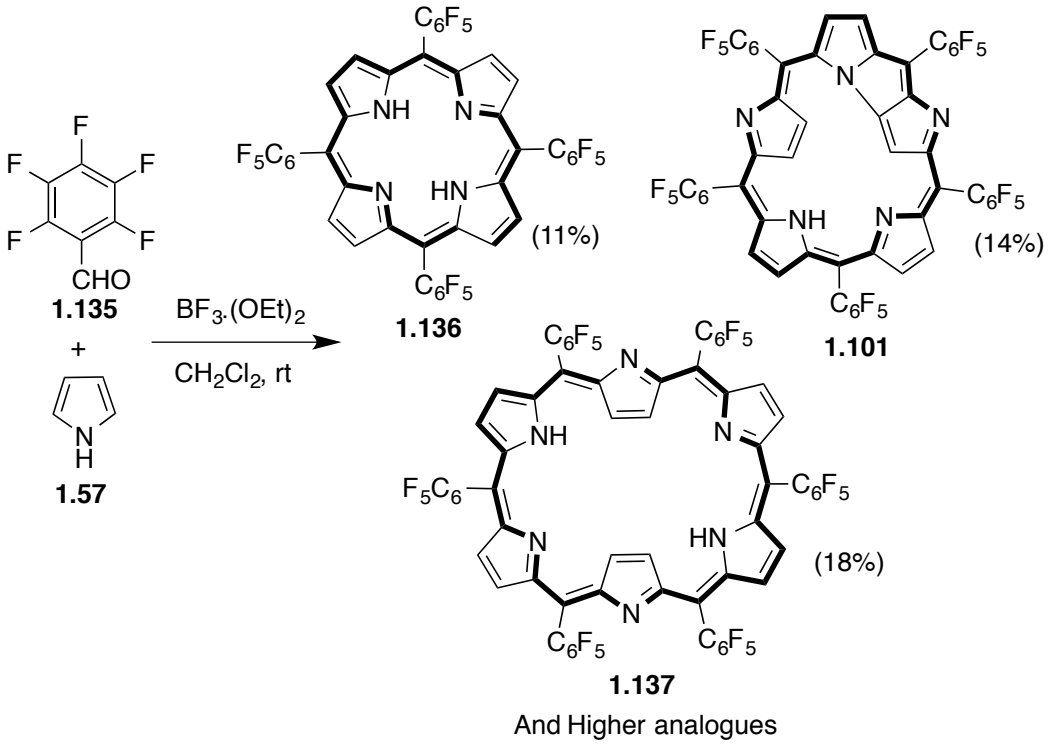

Scheme 4.3

The structure of **1.101** can be drawn with a 22 π aromatic circuit (Scheme 4.3). In support of this, the ^{1}H-NMR spectrum of **1.101** (Figure 4.3) showed the aromatic ring current effect: a set of *β*-H (H_l and H_m) atoms of the inverted pyrrole ring, the inner N($H_{c'}$), and inner H_b signals of the fused ring appeared at δ 2.19, 1.70, 1.18, and -2.30 ppm, respectively, while the peripheral *β*-H have resonances around δ 9.2 - 8.3 ppm.

On the other side, the ^{1}H-NMR spectrum of **1.100** shows three sets of *β*-H atoms intercorrelated between them at δ 8.20-8.10, 6.20-5.86 and 5.85-5.57 ppm. The correspondences are examined in the expansion of the ^{1}H-NMR of compound **1.100** (Figure 4.3 c)). It is also possible to find the NH protons at δ 6.59, 6.72, and 13.68 ppm (corresponding to H_z, $H_{b'}$, and $H_{d'}$). The reason why the third signal appears extremely low field shifted is probably because he is within the range for a hydrogen bonding interaction. When a solution of **1.101** in CH_2Cl_2 was treated with $NaBH_4$ the red solution changed to

brown and afforded **1.100**, quantitatively. In turn, **1.100** can oxidized to **1.101** by treatment with DDQ [11, 12].

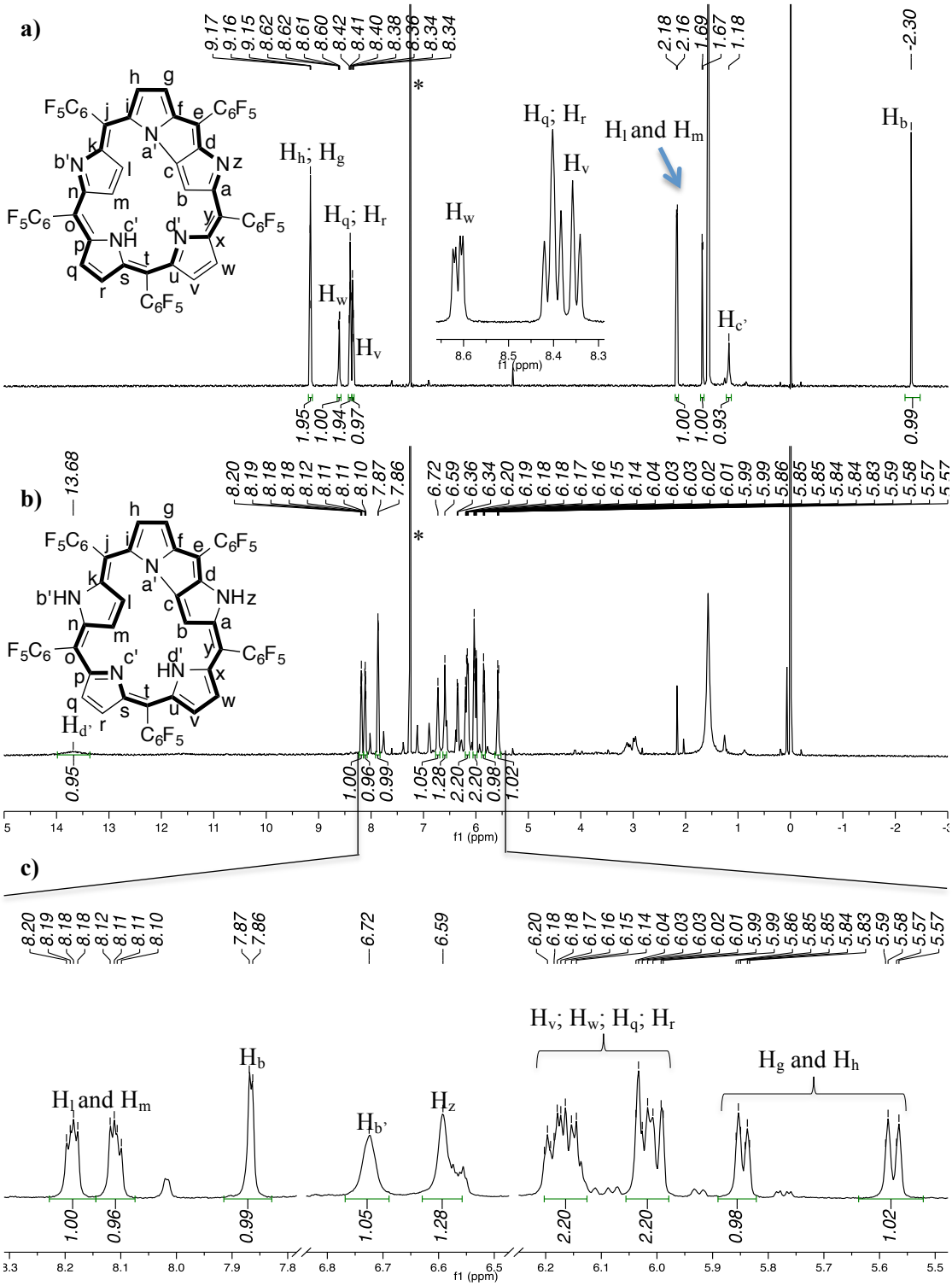

Figure 4.3: a) ^{1}H-NMR spectrum of compound **1.101** in $CDCl_3$ * stands for $CDCl_3$; b) ^{1}H-NMR spectrum of compound **1.100** in $CDCl_3$ * stands for $CDCl_3$; c) expansion of the ^{1}H-NMR spectrum of compound **1.100.**

The absorption spectra of these compounds show broad bands with λ_{max} at 433, 499 and 764 nm for compound **1.101** and λ_{max} at 458 and 552 nm, for compound **1.100**, which presumably reflects the distortion from planarity and the extended π system of these compounds (Figure 4.4).

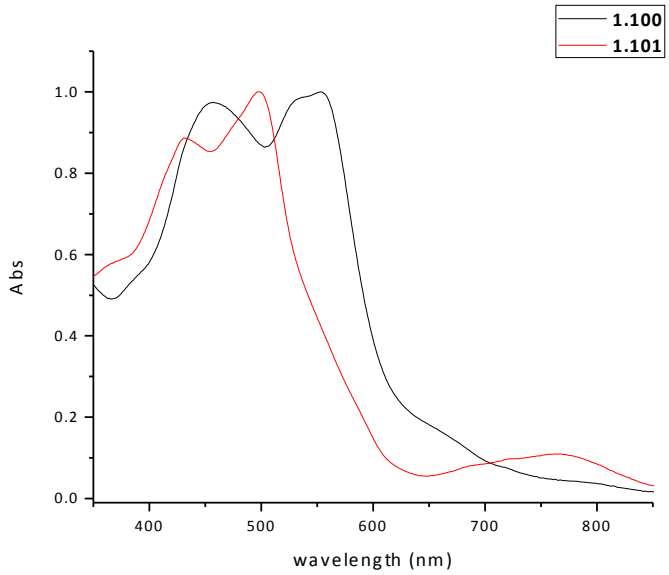

Figure 4.4: UV-Vis spectra of compounds **1.100** and **1.101** in CH_2Cl_2.

These compounds, we examined the nucleophilic substitution reactions at the *para*-fluorine atoms in the *meso*-pentafluorophenyl substituents in **1.101**, since the analogous reactions have been demonstrated in *meso*-tetrakispentafluorophenyl substituted porphyrins. Initial attempts in reacting compound **1.101** with 4-mecaptopyridine (5 eq.) with basic conditions led to a complex mixture of compounds from where **4.11** was isolated along with other less substituted homologues, after a complicated purification process. Additional attempts in the presence of higher amounts of diethylamine (DEA) and an increase from 5 to 7.5 equivalents of 4-mercaptopyridine gave rise to the formation of product **4.11** at room temperature in moderate yields (54%) along with higher substituted analogues.

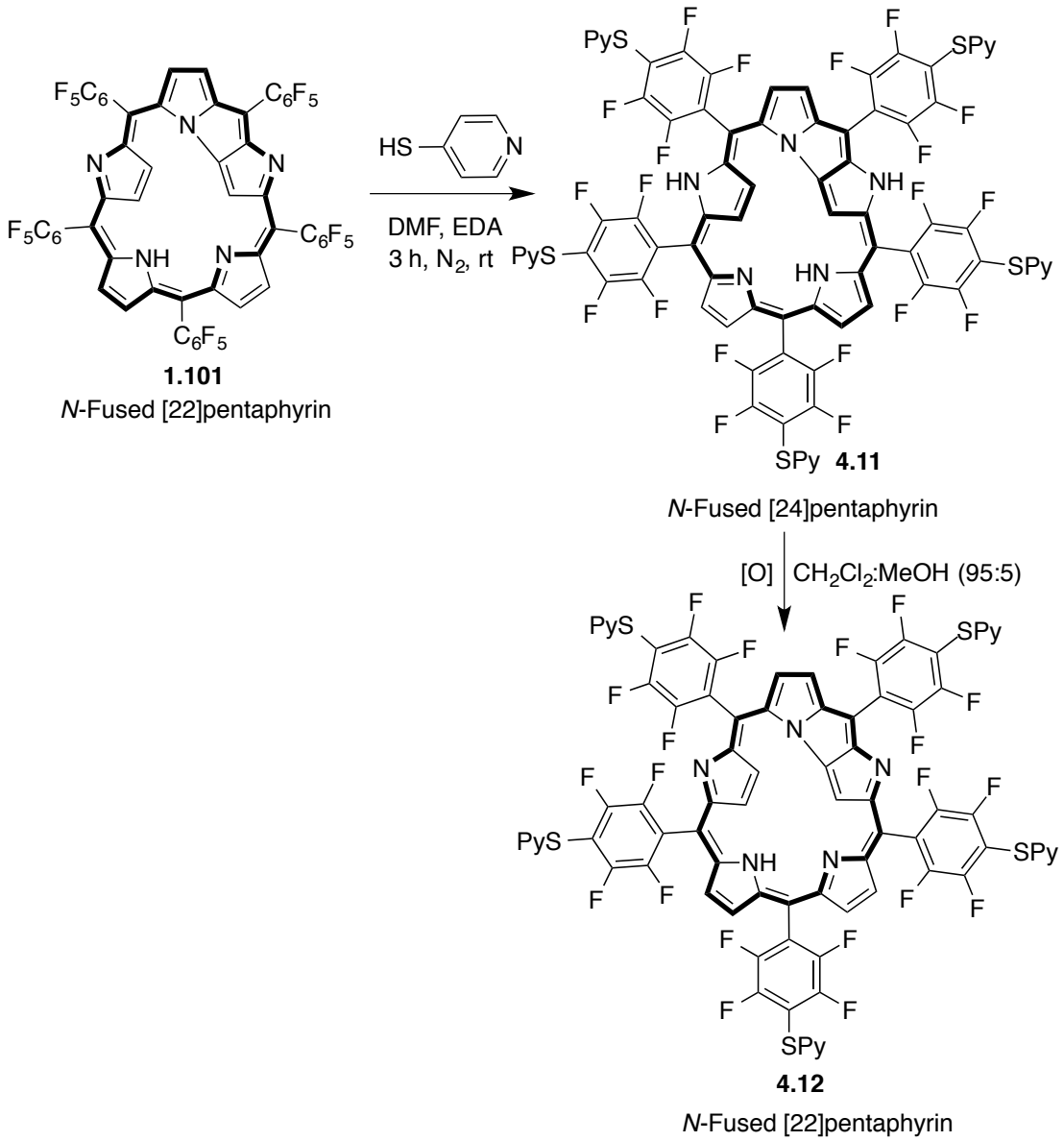

1.101
N-Fused [22]pentaphyrin

4.11
N-Fused [24]pentaphyrin

4.12
N-Fused [22]pentaphyrin

Scheme 4.4

Initial control of the reaction by analytical TLC showed that the anticipated nucleophilic substitution was accomplished, nevertheless the distinct red coloration of **1.101** changed to a brown color more similar to the one of compound **1.100**. Also a change in π electronic system was suggested from its absorption spectrum (λ_{max} = 488 nm, Figure 4.5) that was substantially altered from that of **1.101** but is similar to that of *N*-fused [24]pentaphyrin (**1.100**).

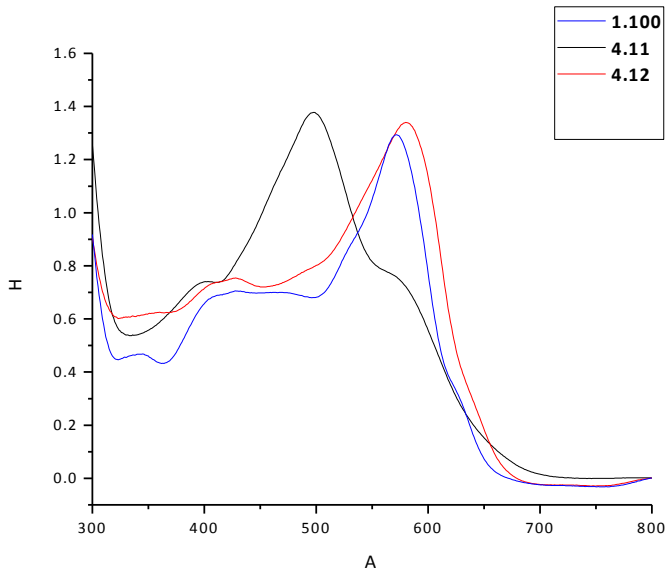

Figure 4.5: UV-Vis spectrum of compounds **1.100**, **4.11** and **4.12** in DMF.

To better understand the behavior of the last experience, macrocycle **1.101** was left stirring in basic conditions and the same reduction behavior is observed even with different bases (*e.g.* NEt_3 or DIPEA). A reduction of this nature has already been reported in other expanded macrocycles indicating that the amine can act as a reducing agent towards *N*-Fused [22]Pentaphyrin **1.101** [23].

Treatment of **4.11** with an excess amount of DDQ (10 eq.) gave rise to the formation of a reddish compound attributed to its oxidized analogue, nevertheless the product of this reaction became highly insoluble and its increased polarity hampered any type of purification. Further studies into the oxidation process of this compound led us to attempt different oxidation reagents as manganese dioxide (MnO_2). Here the reaction proceeded efficiently, reacting 75 eq. of MnO_2 with compound **4.11** during 6 hours at rt. Additional reactions decreasing the equivalent amounts of DDQ to 1.1 equivalents, also provided compound **4.12** in less time of reaction (1 h) and similar yields. In fact, the failed initial attempts of oxidation with an excess amount of DDQ are eventually associated with side reactions in the pyridine moiety and in this specific case being DDQ a strong oxidizing agent the formation of *N*-oxide compounds type would have the insolubility and polarity characteristics observed for the initial products obtained from these attempts. On the other hand, using MnO_2, even in higher amounts (300 eq.) specifically reduces the macrocycle avoiding any side products.

Figure 4.5 shows the ^{1}H-NMR spectra of both compounds and their major differences. As expected from a macrocycle bearing 24 π electrons in its shortest conjugations pathway much weaker or no aromatic character is expected for a reduced form of *N*-fused pentaphyrin. For this reason compound **4.11** has no high field protons being the protons related to the macrocycles allocated at lower fields (Figure 4.6). The ^{1}H-NMR spectrum of compound **4.11** is characterized by a general shift of all signals to lower fields. Moreover, the signals attributed to the pyridine moiety are located at lower field as two unresolved signals integrating each one for 10 protons endorsed to the *meta* ($H_{g'}$) and *ortho* ($H_{f'}$) positions of these penta substituted compounds. The remaining signals were attributed based on the previous attributions.

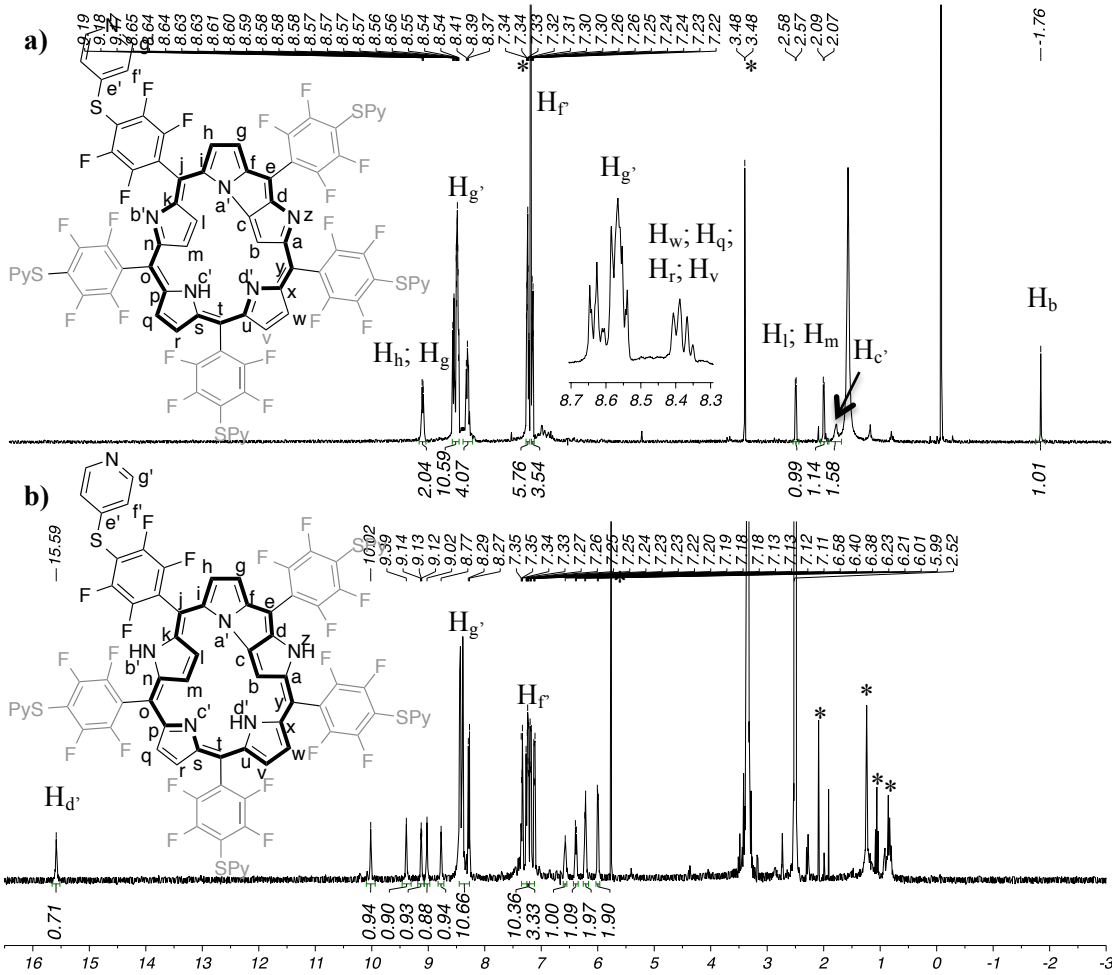

Figure 4.6: a) ^{1}H-NMR spectrum of compound **4.12** in $CDCl_3$ * stands for $CHCl_3$ and solvent impurities; b) ^{1}H-NMR spectrum of compound **4.11** in DMSO * stands for solvent impurities

On the contrary, from ^{1}H-NMR spectra of compound **4.12** is evident the aromatic character considering the inner CH_b, $NH_{c'}$ and the remaining internal β-H protons (H_l and

H_m) which appear at higher fields around δ -1.76, 1.87, 2.08 and 2.57 ppm, respectively. These chemical shifts are in accordance with **1.101**. The remaining signals are presented at the aromatic region of the spectra, particularly, the signals due to the pyridine moiety of molecule **4.12** ($CDCl_3$), which despite being acquired in a different solvent from compound **4.11** (DMSO-*d*$_6$) are located almost in an identical chemical shift (δ 8.65-8.54 relative to $H_{g'}$ and δ 7.34-7.22 ppm relative to $H_{f'}$ integrating both for 10 protons). In sum, these signals show some closeness with the signals displayed by compound **1.101**, inferring their similarities.

Cationization reactions of compounds **4.11** and **4.12** led to an interesting observation. In the previous pages, was discussed the ability of basic media to reduce compound **1.100** and consequently the final product of the previous reaction led to **4.11**. For our surprise, similar reduction occurred when **4.12** was reacted with CH_3I in DMF for 3 hour at 40 ºC leading to compound **4.13** (Scheme 4.5).

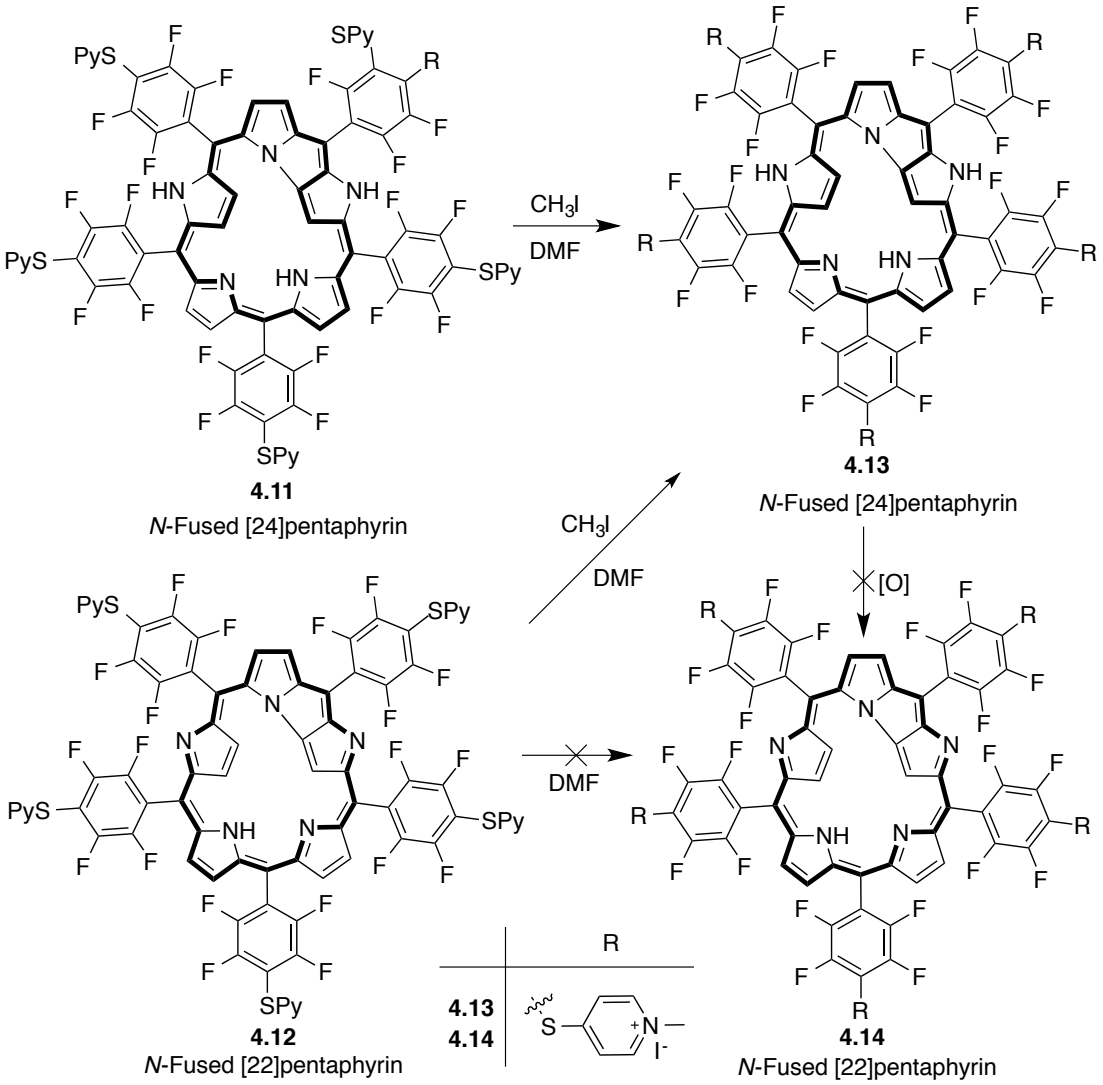

Scheme 4.5

Several attempts were made in order to characterize compound **4.13** by NMR spectroscopy, nevertheless, clear characterization by this technique proved to be impossible to obtain. In fact, whilst the HRMS shows the parent ions peaks at *m/z* = 1063.9724 $[M+2I^-]^{2+}$ (calculated for: $C_{85}H_{47}F_{20}I_3N_{10}S_5$, 1063.9662) and the UV-Vis spectra is in accordance with a reduced for of *N*-fused pentaphyrin with λ_{max} at 503 nm (Figure 4.7), not much can be developed around this final product without further characterization details.

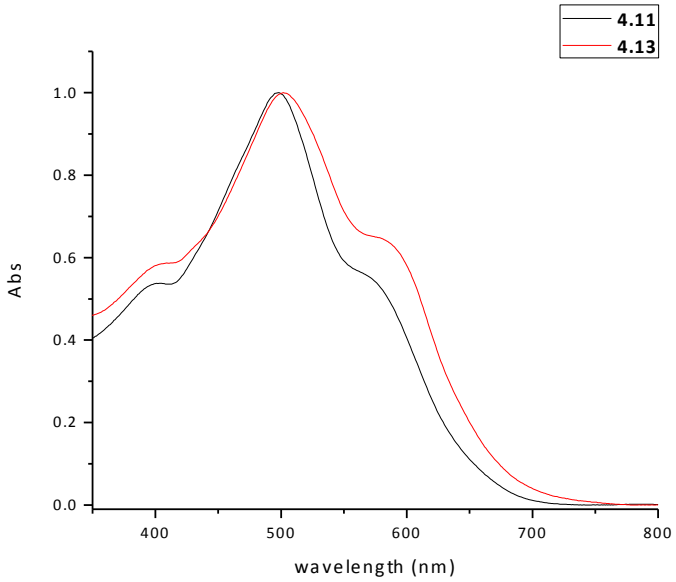

Figure 4.7: UV-Vis spectrum of compounds **4.11** and **4.13** in DMF.

These compounds are in fact a specific class of expanded porphyrins where their characteristics proved rather complicated to work with. Their stability and reactivity is diminished when compared to tetrapyrrolic analogues and consequently isolation of the products also prooved to be rather complex. This unquestionably, is consistent with the number of publications around this family of macrocycles which compared to other analogues is fairly low.

4.3. *meso*-Hexakis(pentafluorophenyl) hexaphyrins (1.1.1.1.1.1).

4.3.1. meso-Hexakis(pentafluorophenyl) hexaphyrins (1.1.1.1.1.1): overview

Over the last several decades, considerable efforts have been devoted to develop efficient artificial receptors capable of detect, remove and transport targeted guests and new aPDT and PDT agents [24-28]. Among these, *meso*-hexakis(pentafluorophenyl) [26]hexaphyrin that was first reported by our group is possible to obtain as much as 20% yield [29-31]. In fact, newer methodologies using dipyrromethanes and tripyrromethanes with variable temperatures and acids (Methanesulfonic acid (MSA) and Boron trifluoride etherate ($BF_3.(OEt)_2$) allow the synthesis of this macrocycle in up to 25% along with higher homologues [32]. Further investigations into the synthesis of derivatives of this kind, acid-catalyzed reactions of different 5-(aryl)dipyrromethane with pentafluorobenzaldehyde

allowed the preparation of a variety of "mixed" *meso*-aryl [26]hexaphyrins with different substituents at the *meso*-positions (Scheme 4.6) [30].

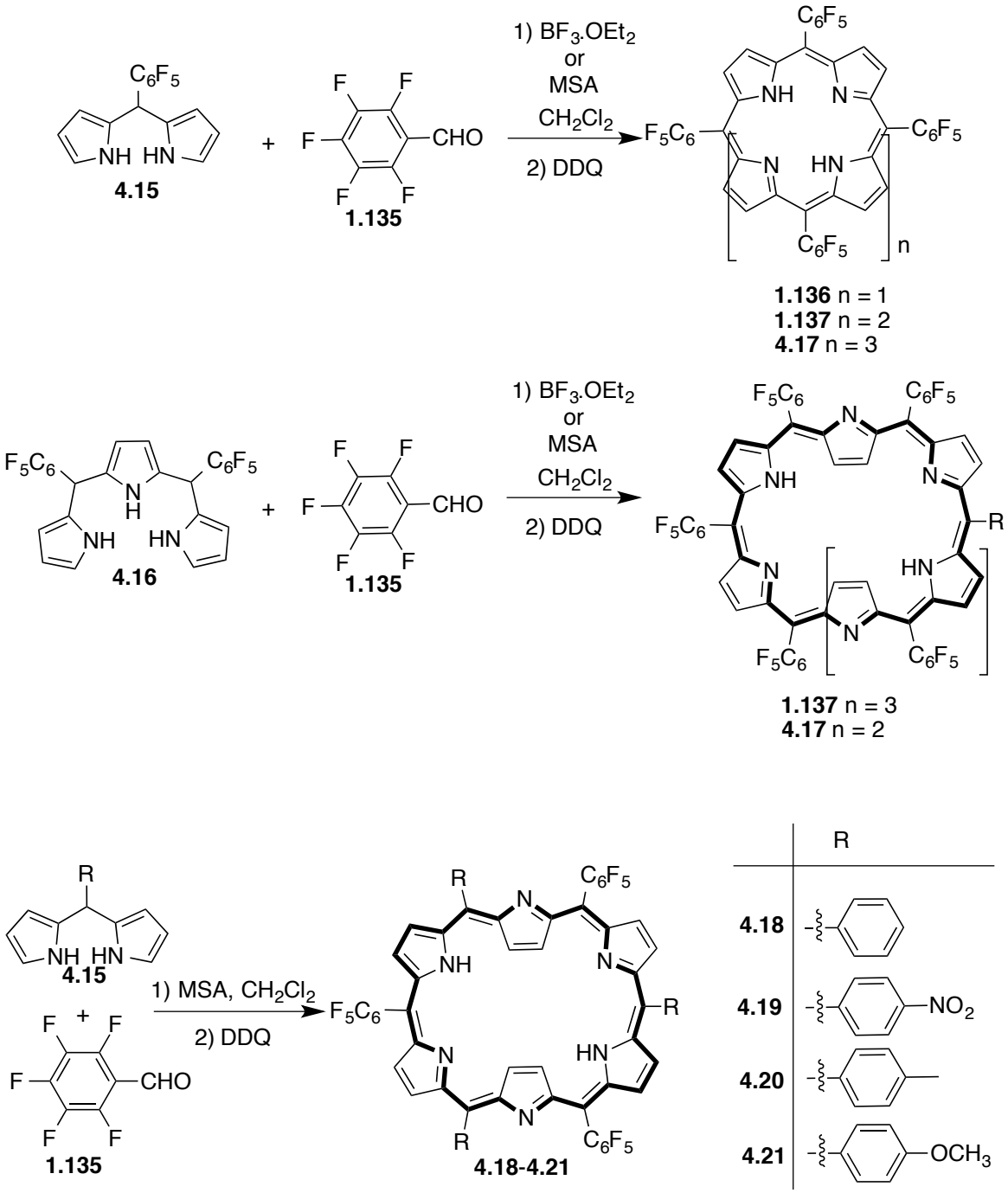

Scheme 4.6

More recently, attention has been turning towards β-substituted meso-hexakis(pentafluorophenyl) [26] and [28]hexaphyrins where the major variations in their

structures have prompt investigations towards their conformational variations upon addition of different acids (Scheme 4.7) [33,34].

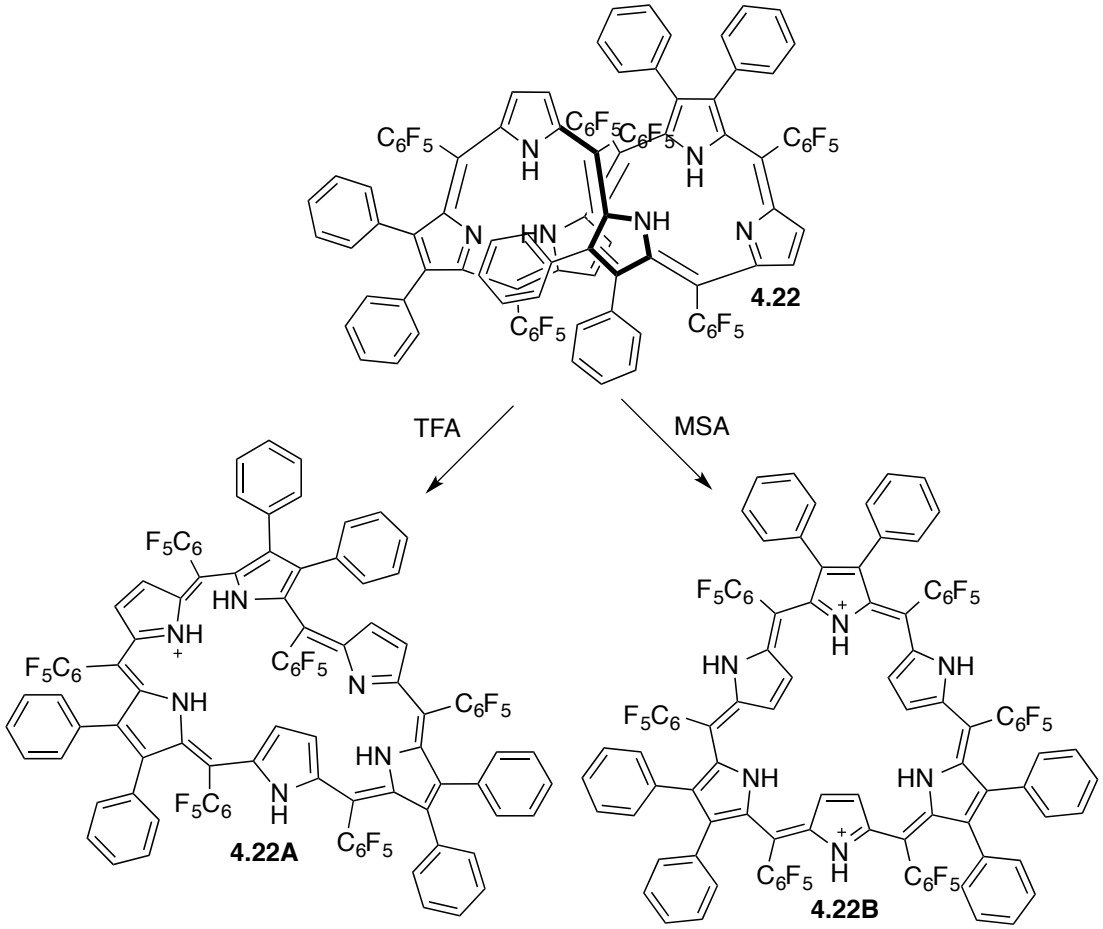

Scheme 4.7

In fact, protonation studies of *β*-substituted *meso*-hexakis(pentafluorophenyl) [28]hexaphyrins **4.22** triggered conformational changes, whereas protonation with trifluoroacetic acid led to the formation of monoprotonated Mobius aromatic species **4.22A** while protonation with methanesulfonic acid led to the formation of diprotonated triangular antiaromatic species **4.22B** [34]. In spite of the structural resemblances and their obvious aromaticity differences, *meso*-hexakis(pentafluorophenyl)[26]hexaphyrins and *meso*-hexakis(pentafluorophenyl)[28]hexaphyrins have completely different characteristics, and these have been a theme of extensive research [35-38].

These attributes makes *meso*-hexakis(pentafluorophenyl)[26]hexaphyrin an interesting compound. The large structural diversity outcome from metallation and functionalizations, strong aromaticity resulting from 26 π electrons, the unique rectangular shape with two inverted pyrroles with the nitrogens pointing outward and its sharp Soret-

like band observed at 568 nm in CH_2Cl_2 makes this compound an interesting platform to use in photodynamic therapy [39-41]. Not much has been developed in terms of straightaway applications with these compounds nevertheless, it is reported the detection of silver cations by near infrared fluorescent *meso*-hexakis(pentafluorophenyl)[26]hexaphyrins [42] and its deprotonation upon the addition of excess amounts of tetrabutylamonium fluoride [43].

On the other hand, knowing in advance that expanded porphyrins are capable of chelating anionic substrates, *meso*-hexakis(pentafluorophenyl)[28]hexaphyrin bearing a non-planar structure and the extra two nitrogen protons in the macrocycle can be explored to detect potential environment harmful anionic species and their removal from contaminated environments [44,45]. In these applications, it would be very important to construct a *meso*-hexakis(pentafluorophenyl)[26]hexaphyrin or *meso*-hexakis(pentafluorophenyl)[28]hexaphyrin chromophores and make them soluble in a wide range of solvents depending on the respective uses. For example for many biological applications including photodynamic therapy and for supramolecular interactions and recognition entities, water soluble properties are very important. These last assumptions led to, in analogy with *N*-fused Pentaphyrins, explore the substitutions of the fluorine atoms in the *para* positions of these macrocycles with a wide variety of groups.

4.3.2. meso-Hexakis(pentafluorophenyl) Hexaphyrins (1.1.1.1.1.1): experimental results

The starting materials considered in the following section were synthesized as demonstrated in the previous section. *Meso*-hexakis(pentafluorophenyl) [26]hexaphyrin **1.137** is obtained from the condensation reaction of pyrrole and pentafluorobenzaldehyde with $BF_3.OEt_2$ in 18% yield. The reduction/oxidation properties previously described for *N*-fused [22]pentaphyrins also are displayed by these macrocycles where *meso*-hexakis(pentafluorophenyl)[26]hexaphyrin **1.137** can be easily reduced in the same manner by $NaBH_4$ almost quantitatively into **1.138** (Scheme 4.8).

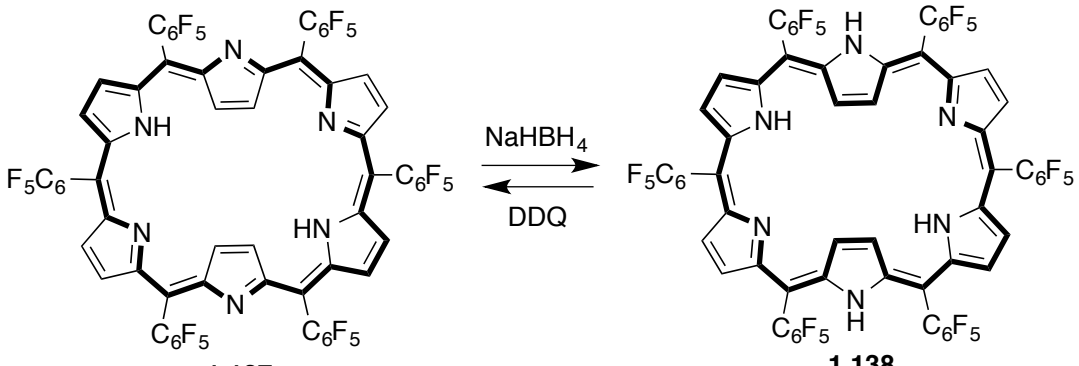

Scheme 4.8

The characterization obtained for these compounds especially by ^{1}H-NMR is rather simplistic than the previous analogues mainly because the higher degree of symmetry presented by compounds **1.137** and **1.138**. Both compounds show, in their mass spectra (MALDI), the same molecular ions at *m/z* 1462, (in the ESI-MS the $[M+H]^+$ is observed allowing the differentiation of compounds **1.137** and **1.138** through mass spectrometry) which correspond to molecules formed from six pyrroles and six pentafluorobenzaldehyde units. This might be associated with reduction processes during the analisys.^{1}H-NMR spectra of these compounds show that compound **1.137** has aromatic features and therefore, signals at δ -2.00 and -2.43 are observed and attributed to the signals (singlets) in the inner core of compound **1.137** (NH_q and the pyrrolic H_b and H_c). The remaining two doublets (J = 5.0 Hz) integrating for four protons each are assigned to the remaining pyrrolic protons of the molecule (Figure 4.8 a)). On the other side, the ^{1}H-NMR spectrum of compound **1.138** is significantly different from the previous one, with resonances at δ 2.54 (4H, s, H_b and H_c), 4.40 (br s, NH_q and H_r), 7.64 (4H, d, J = 4.7 Hz) and 7.73 ppm (4H, d, J = 4.7 Hz) (Figure 4.9 b)).

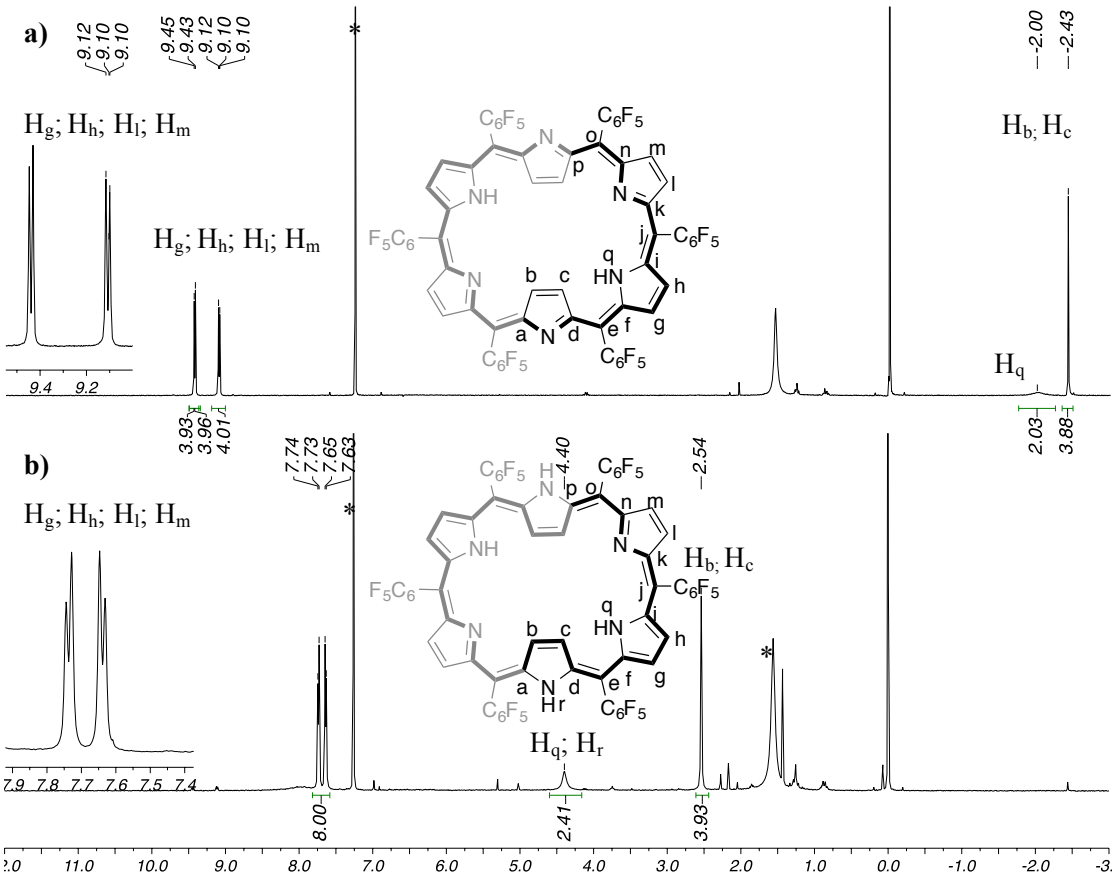

Figure 4.8: a) ^{1}H-NMR spectrum of compound **1.137** in $CDCl_3$, * stands for $CHCl_3$; b) ^{1}H-NMR spectrum of compound **1.138** in $CDCl_3$, * stands for $CHCl_3$ and solvent impurities.

One interesting observation made in compound **1.138** is the ^{1}H-NMR spectrum achieved in DMSO-d_6, where the signals not only display different chemical shifts as the multiplicity also appears in a different manner. For this reason, full characterization by NMR spectroscopy was acquired for compound **1.138** in both DMSO-d_6 and $CDCl_3$. In the next figure (Figure 4.9) is possible to note the main differences between a ^{1}H-NMR of **1.138** acquired in $CDCl_3$ and DMSO-d_6.

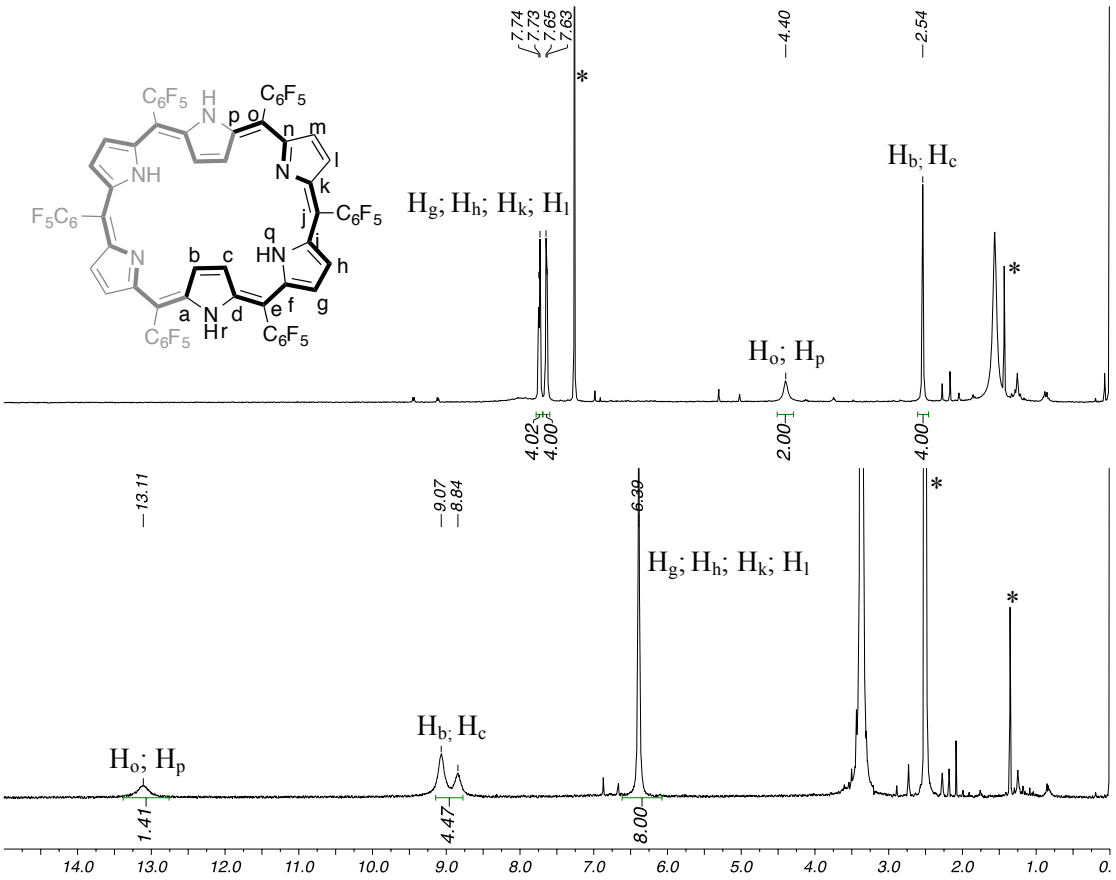

Figure 4.9: a) ^{1}H-NMR spectrum of compound **1.138** in $CDCl_3$, * stands for $CHCl_3$ and solvent impurities; b) ^{1}H-NMR spectrum of compound **1.138** in DMSO-d_6, * stands for DMSO and solvent impurities.

This differentiation is not only due to solvent interactions but also due strong structural variations. In fact **1.138** exist in solution in rapid inter-conversion conformations. When these conformational inter-conversions are fast on the ^{1}H-NMR time scale, we observe an averaged ^{1}H-NMR spectrum of a mixture of such isomers and for this reason changing the solvent might show a completely different averaged ^{1}H-NMR changing the contributions of these rapid interconverted conformations. The attribution was consequently supported by bi-dimensional techniques, where is possible to find the signals due to the *β*-protons at δ 9.07 and 6.39 ppm correlated with carbons at δ 120.8, 128.7 and 131.1 ppm, consequently being attributed based also on the integration of the signal. Moreover, the singlet at δ 6.39 ppm correlate with two different carbons shows that these are the signals on the periphery of the macrocycle (C_l, C_m). On the contrary, the signal at *δ* 13.11 ppm does not have correlation in the HSQC and therefore is attributed to the NH signals of **1.138** (H_p and H_o) (Figure 4.10).

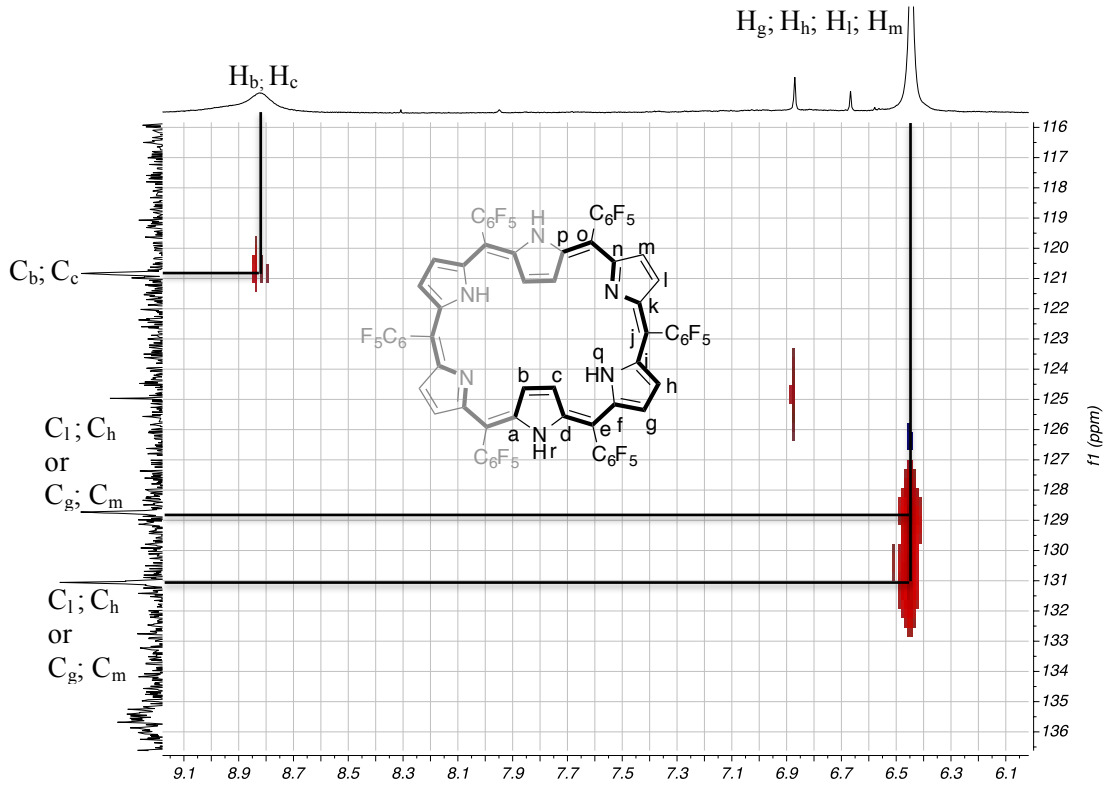

Figure 4.10: HSQC of compound **1.138** in DMSO-d_6.

4.3.3. meso-Hexakis(pentafluorophenyl) Hexaphyrins thiopyridyl derivatives: experimental results

Investigation over the nucleophilic substitution reactions at the *para*-fluorine atoms in the *meso*-pentafluorophenyl substituents of **1.137** was achieved with a similar methodology used in previous compounds. In fact the major difference lays in the equivalent amounts of 4-mercaptopyridine used in the reaction, which changed from 7.5 eq. up to 9 eq. (Scheme 4.9). After purification of this compound it was possible to note a slight increase in the yield of the reaction when compared with the smaller analogs *N*-fused pentaphyrins (64% *vs* 54%). This increase may be associated with reactivity of two rather different macrocycles or their own stability towards basic media. The substitution regioselectivity was always quite high only at the *para*-fluorine of all the six *meso*-pentafluorophenyl groups.

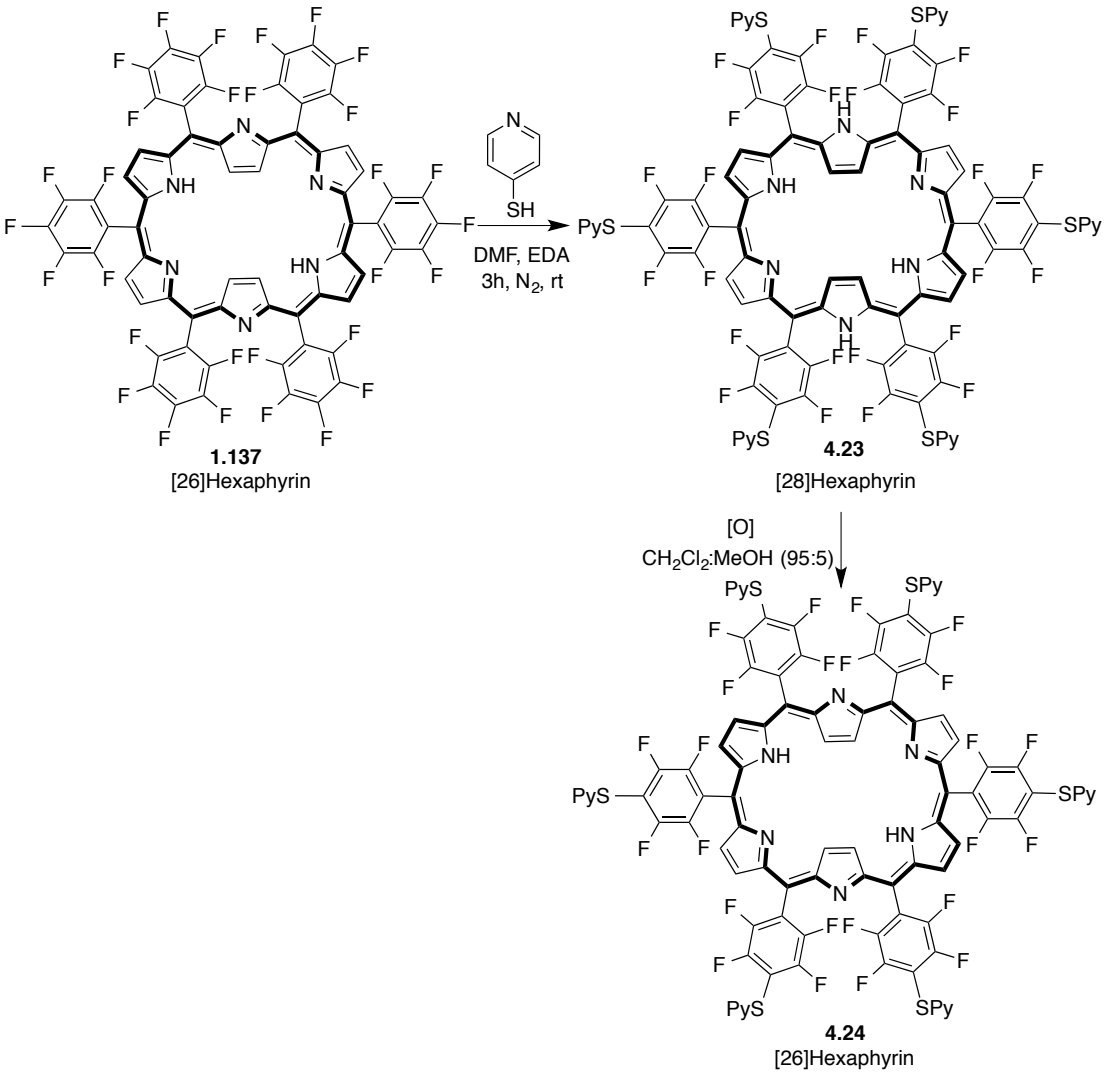

Scheme 4.9

As described for the *N*-fused pentaphyrin, a change in π-electronic system was also observed in this case, suggesting from its absorption spectrum (from λ_{max} = 565 and 711 nm to λ_{max} = 605 and 773 nm, figure 4.11a) a reduction reaction, giving rise to **4.23**. However, using trivial oxidizing agents like DDQ (1.1 eq.) or MnO_2 (50 eq.) is possible to oxidize **4.23** to **4.24** easily, judging by the hypsochromic shift showed in the UV-Vis, where the maxima absorptions located at λ_{max} = 605 and 773 nm changes to λ_{max} = 575 and 718 nm (Figure 4.11b). The UV-Vis profiles of compounds **4.23** and **4.24** compared to the non substituted counterparts **1.137** and **1.138**, are in good accordance, however is possible to note a slight bathocromic effect when comparing **1.137** with **4.23** and **1.138** with **4.24**,

showing that the substitutions in the *para* positions of the *meso*-pentafluorophenyl moieties causes a generalized red-shift in compounds **4.23** and **4.24** (Figure 4.11c).

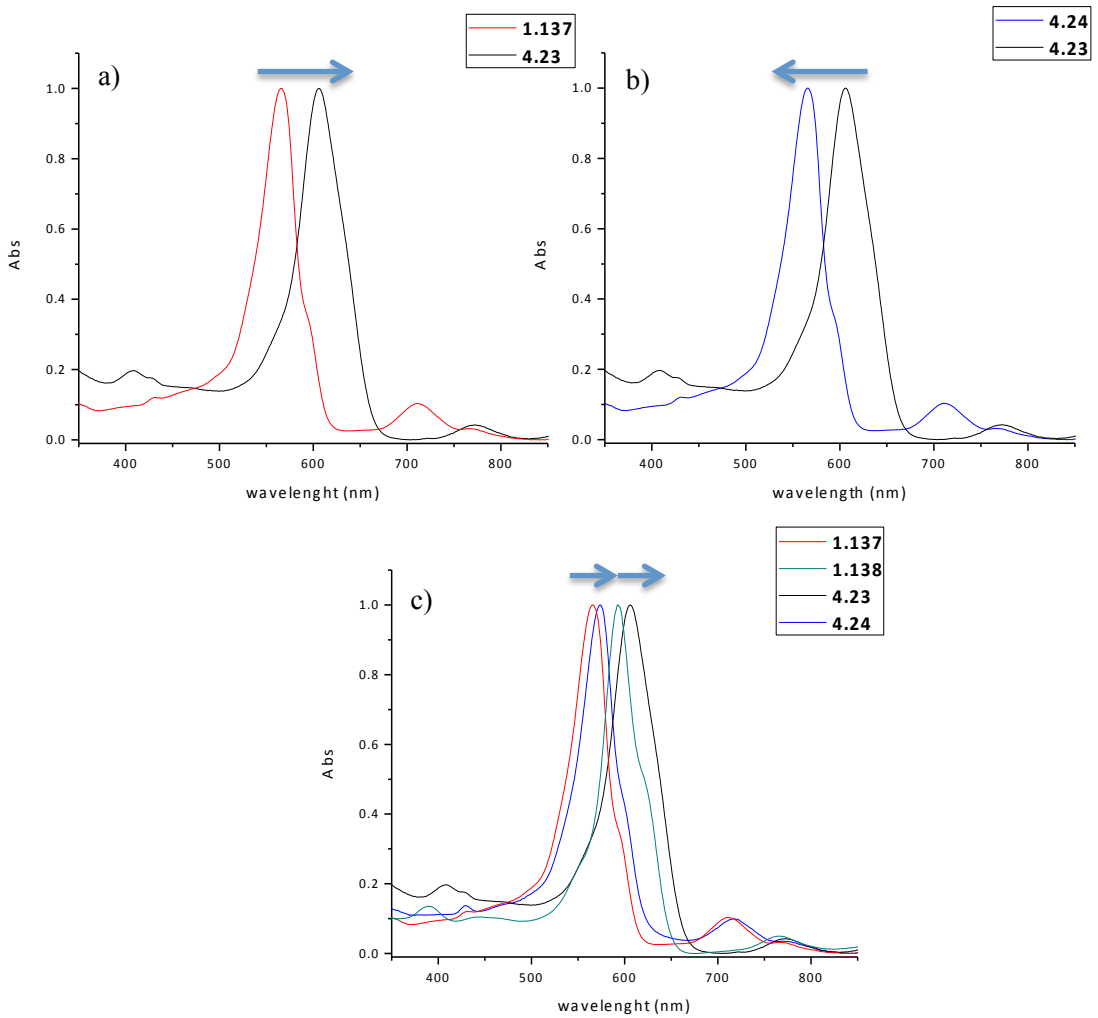

Figure 4.11: a) Absorption spectrum of compounds **1.137**, and **4.23** highlighting the changes in the nucleophilic substitution reaction depicted in scheme 4.9; b) Absorption spectrum of compounds **4.23**, and **4.24** highlighting the changes in the oxidation reaction depicted in scheme 4.9; c) Combined UV-Vis spectrum of compounds **1.138**, **4.23** and **4.24**. All spectra were recorded in CH_2Cl_2.

Characterization by ^{19}F-NMR showed effectively that the substitutions occurred in the *para* positions of the *meso*-pentafluorophenyl where is possible to note the correspondent disappearance of the fluorine atoms (Figure 4.12). Here the comparison between the ^{19}F-NMR spectra of compounds **1.138** and **4.23** in DMSO allows a straightforward comparison where is possible to note the shift of the signals corresponding

to the *meta*-fluorines, which in the presence of a highly electronegative surrounding (-SPy) moves from δ -185.39 – -185.99 and -186.56 – -187.26 ppm to *δ* -155.56 and -156.75 ppm.

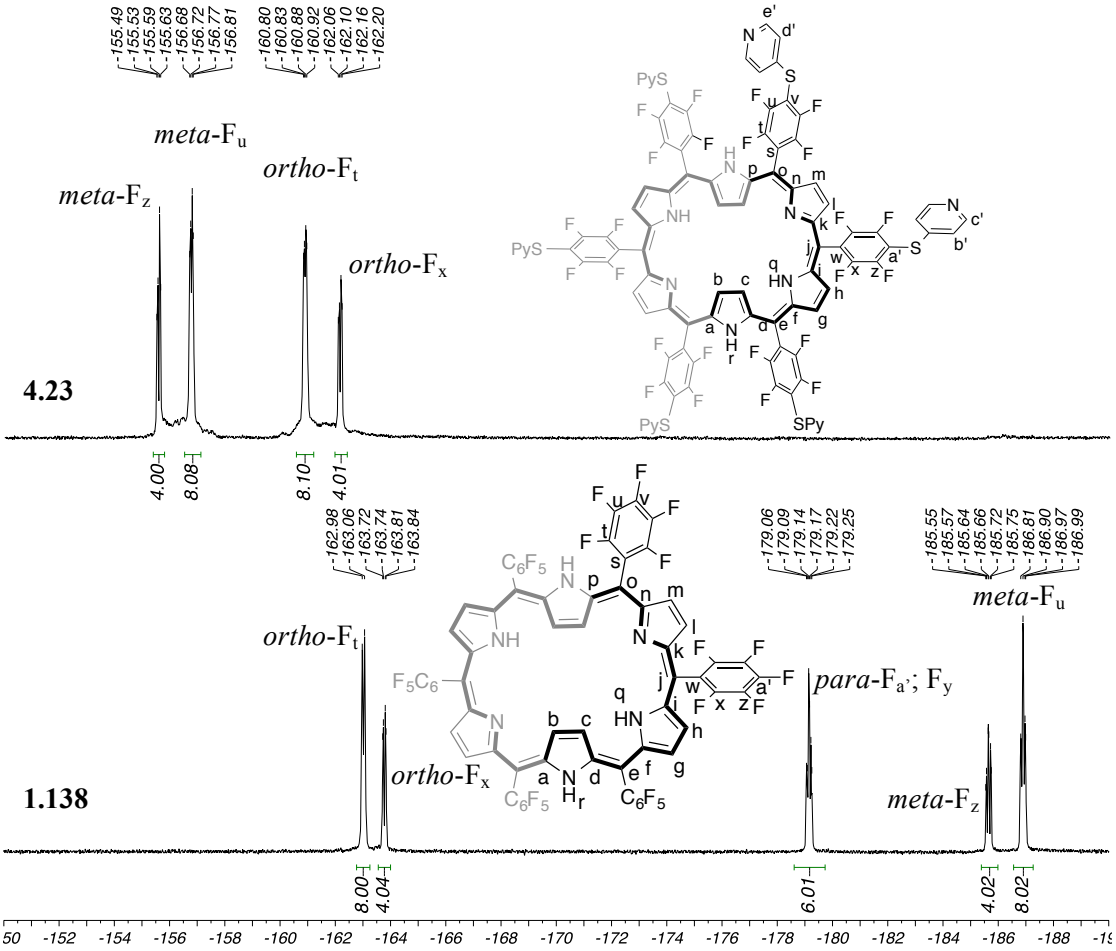

Figure 4.12: ^{19}F-NMR spectra of compounds **1.138** and **4.23** in DMSO-*d*$_6$.

Initial insights into the ^{1}H-NMR spectrum of compound **4.23** in DMSO-*d*$_6$ presented a similar profile to the one showed for compound **1.138**. The ^{1}H-NMR spectrum shows the signals corresponding to the pyridine moieties between δ 7.07 and 8.51 ppm. Here is possible to note that the signals are split into doublets corresponding to the eight protons located at the far edges of the rectangular conformation of the macrocycle resonating at δ 8.40 and 7.30 ppm interrelated with a coupling constant of J = 6 Hz ($H_{b'}$ and $H_{a'}$, respectively). The signals belonging to the protons located at the closer edges of the macrocycle are also two doublets correlated with the same coupling constant at δ 8.35 and 7.08 ppm integrating for 8 protons each (H_x and H_y, Figure 4.13). The remaining signals belong to the macrocycle are in accordance with the previous compounds.

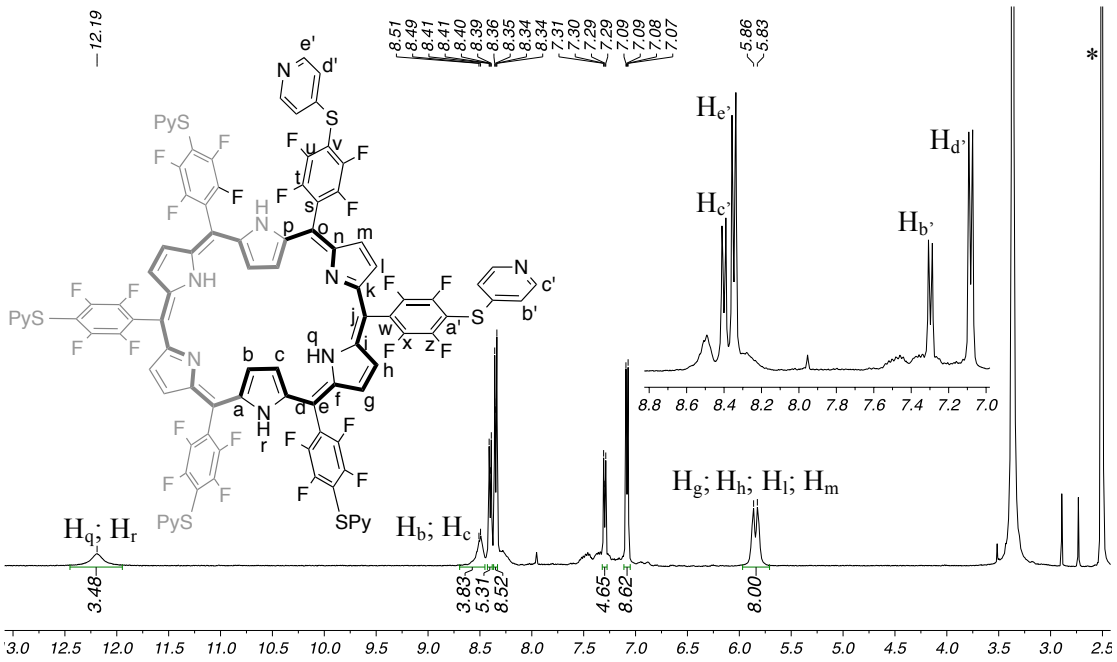

Figure 4.13: ^{1}H-NMR spectrum of compound **4.23** in DMSO-d_6, * stands for DMSO.

Oxidation of compound **4.23** by the methodologies already discussed originated compound **4.24**. The characterization of this compound was achieved either by NMR spectroscopy and positive-mode high-resolution electrospray ionization mass spectrometry (HR-ESI-MS) where the parent ion peak is found at *m/z* = 1004.5733 $[M+2H]^{2+}$ (calculated for $C_{96}H_{40}F_{24}N_{12}S_6$: 1004.0717). In spite of the many structural resemblances compound **4.24** has with compound **4.23**, the ^{1}H-NMR spectrum of **4.24** in DMSO-d_6 (Figure 4.14) does not show the same pattern as **4.23**. In fact, **4.24** has a nearly planar rectangular shape and in figure 4.14 is possible to note the almost identical pattern of this spectra with the ^{1}H-NMR spectra of **1.137** acquired in $CDCl_3$. Furthermore the signals attributed to the resonances attributed to the protons in the pyridine moieties are located at δ 8.70-8.65 ppm in the form of a multiplet integrating for 12 protons ($H_{e'}$ and $H_{c'}$), a doublet at δ 7.81 ppm integrating for 4 protons ($H_{b'}$, J = 6 Hz) and finally another doublet at δ 7.65 ppm integrating for 8 protons (J = 6 Hz).

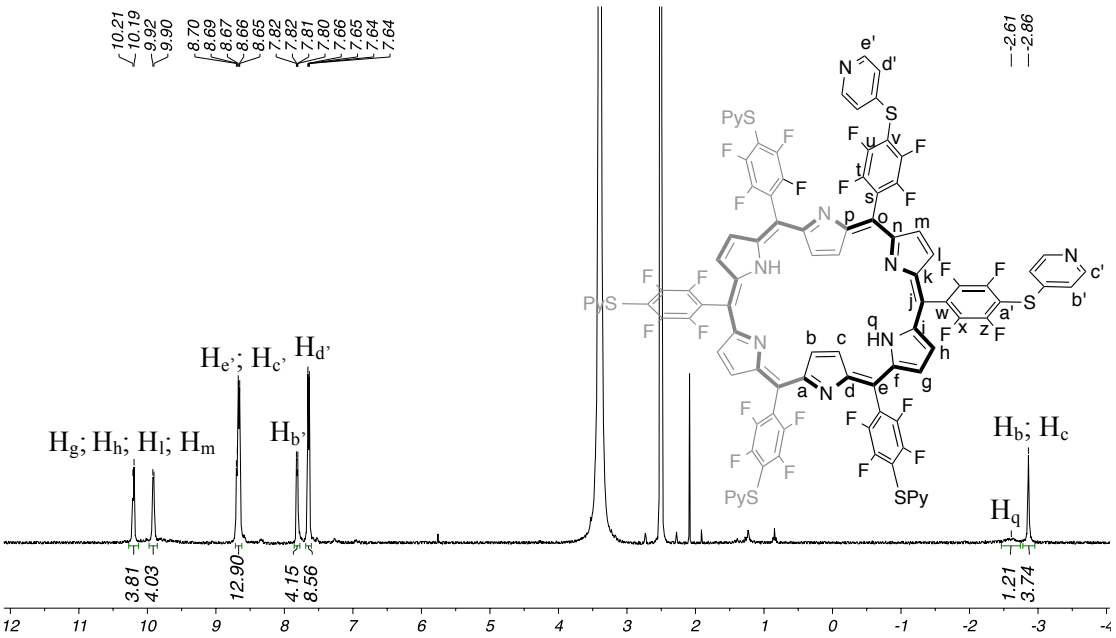

Figure 4.14: ^{1}H-NMR spectra of compound **4.24** in DMSO-d_6, * stands for DMSO-d_6.

Reaction with CH_3I of both pyridyl compounds gives raise to the reduced cationic form **4.25** as depicted in scheme 4.9 (yield = 80-86%). This same reaction was performed in compounds **1.137** and **1.138**, and in fact this no methylation reaction occurred in both compounds, however compound **1.137** was reduced to **1.138**. Note that the last reactions were done with a higher equivalent amount of CH_3I and for a longer period of time (12 h). Several reactions with compound **4.25** using different oxidants (*e.g.* MnO_2, DDQ, nitro-benzene, H_2O_2) were attempted in the pursuit of the anticipated cationic oxidized version of hexaphyrins (**4.26**), however characterization of such compounds was rather complicated since purification of cationic compounds proved complicated.

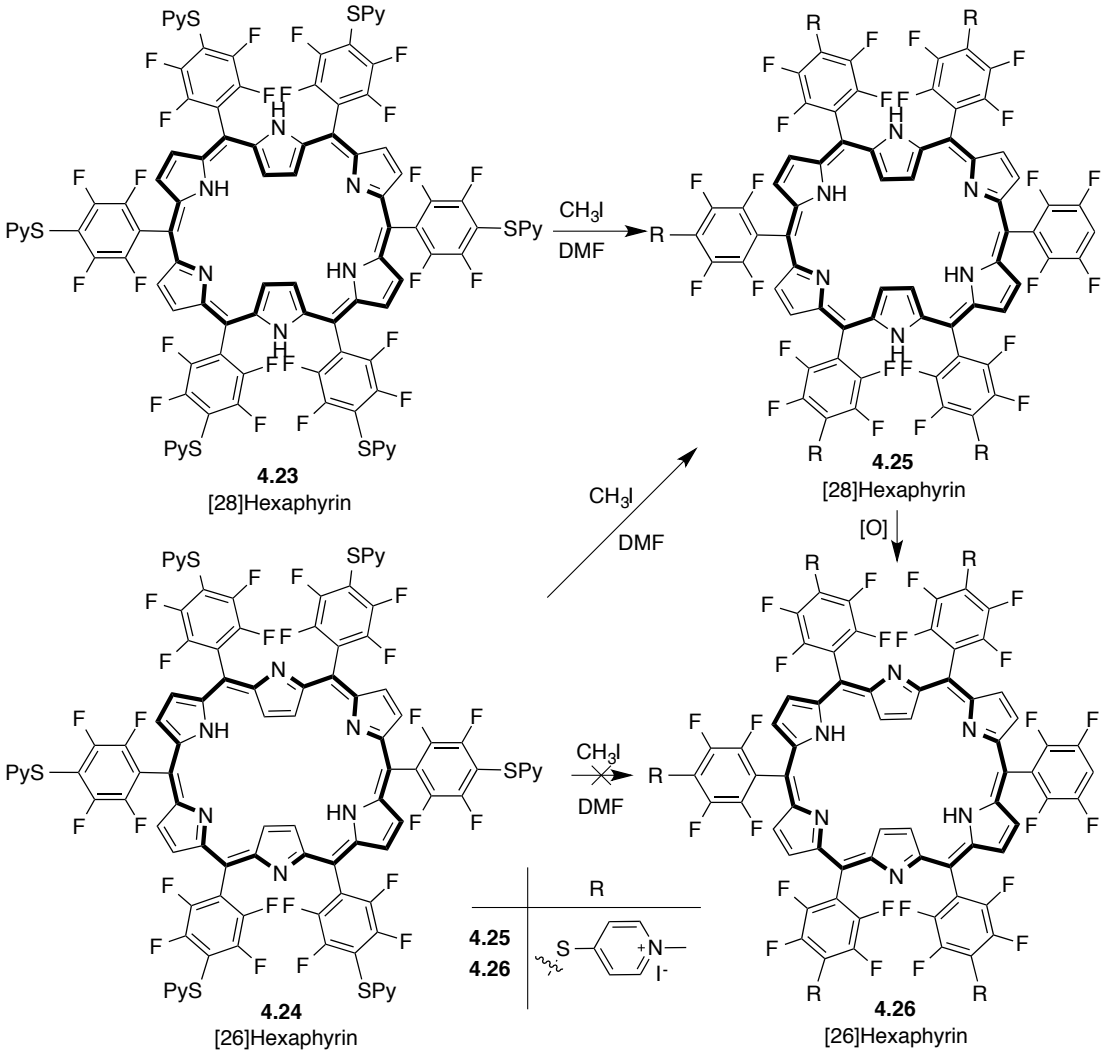

Scheme 4.10

A change in π-electronic system was observed when reacting **4.24** with CH_3I and from its absorption spectrum (from λ_{max} = 616 and 825 nm to λ_{max} = 663 nm). However, the UV-Vis spectrum of compound **4.25** is in fully accordance with a reduced form of hexaphyrins (Figure 4.15).

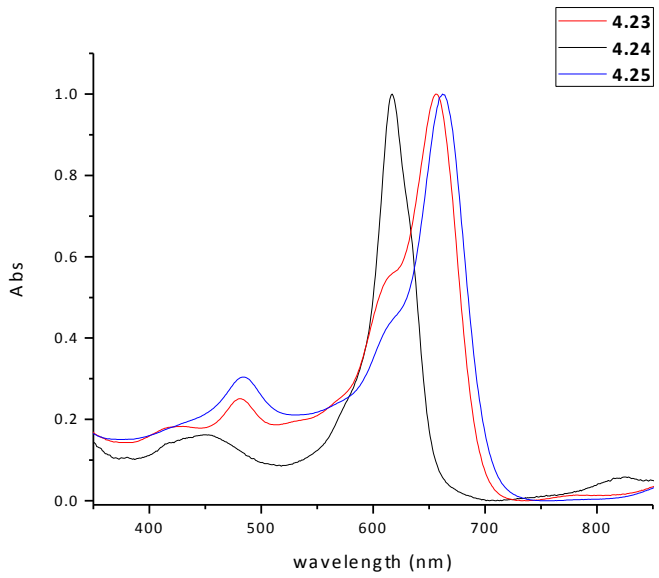

Figure 4.15: Absorption spectrum of **4.23, 4.24** and **4.25** in DMF.

^{1}H-NMR spectroscopy shows the expected introduction of the methyl groups showing their resonances as two close singlets at δ 4.25 and 4.23 ppm (Figure 4.16). These combined signals integrate to the expected 18 protons showing a fully methylated compound. Additionally, the remaining signals show a shift to lower fields when compared with the signals of compound **4.23** due the charged nitrogen in their surroundings.

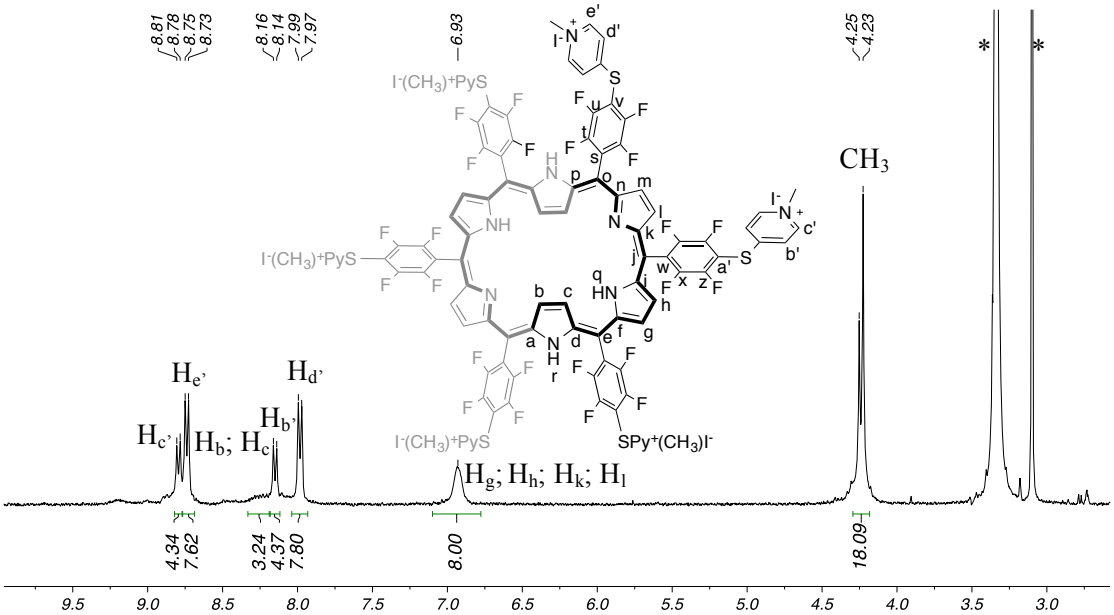

Figure 4.16: ^{1}H-NMR spectra of compound **4.25** in DMSO-d_6, * stands for DMSO and solvent impurities.

As it proved difficult to obtain a cationic oxidized derivative we sought the synthesis of other macrocycles with the same potential applications but without the oxidation/reduction behavior. Firstly we considered the insertion of zinc in macrocycle **1.137.** This would eventually protect the macrocycle from the reduction reactions. This was attempted reacting **1.137** with $Zn(OAc)_2$ in a mixture of $CHCl_3$: MeOH (7.5:2.5) in reflux for 3 h (Scheme 4.11).

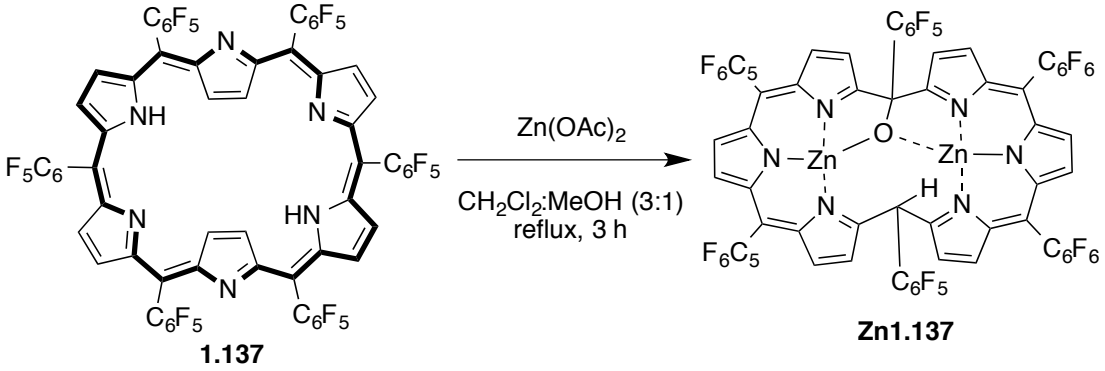

Scheme 4.11

Analysis by UV-Vis showed a bathochromic shift from λ = 566 nm to 619 nm in accordance with the appearance of a metalated compound (**Zn1.137**). Nonetheless, the UV-Vis spectrum of compound **Zn1.137** was characterized by a split of the Soret band at showing a λ_{max} at 619 and 581 nm (Figure 4.17).

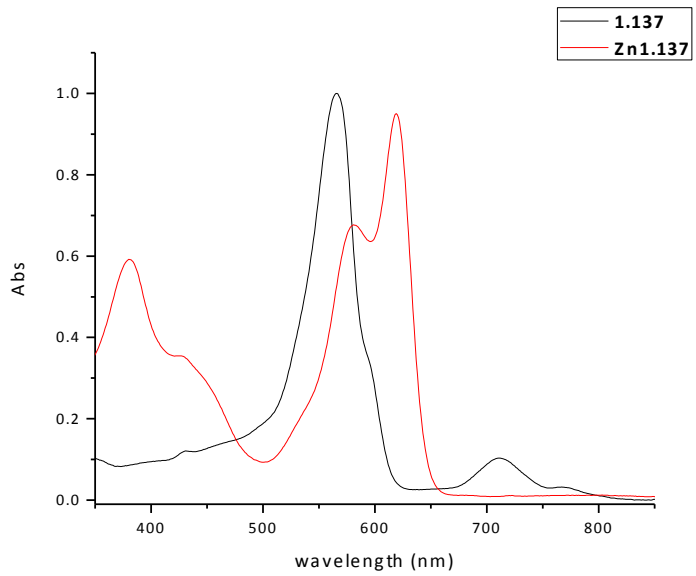

Figure 4.17: Absorption spectrum of **1.137** and **Zn1.137** in CH_2Cl_2.

This shape of the Soret band, was later associated to a rehybridization of the methene bridges, from a double bond to a simple bond, interrupting the conjugation of compound **Zn1.137**. These characteristics were already described with different metals, yet the similar UV-Vis and NMR profiles show that in fact the molecule loses its aromaticity (Figure 4.7). The ^{1}H-NMR spectrum of **Zn1.137** exhibits signals due to the pyrrolic *β*-protons in the range of *δ* 6.56-6.01 ppm and a signal due to the *meso* proton (H_o) at 10.92 ppm that has no correlation with other peaks. The lack of signals more shielded on the ^{1}H-NMR spectra is an indication of lack of aromaticity in this compound when signals due to all the *β*-protons are present in the aromatic area of the spectra.

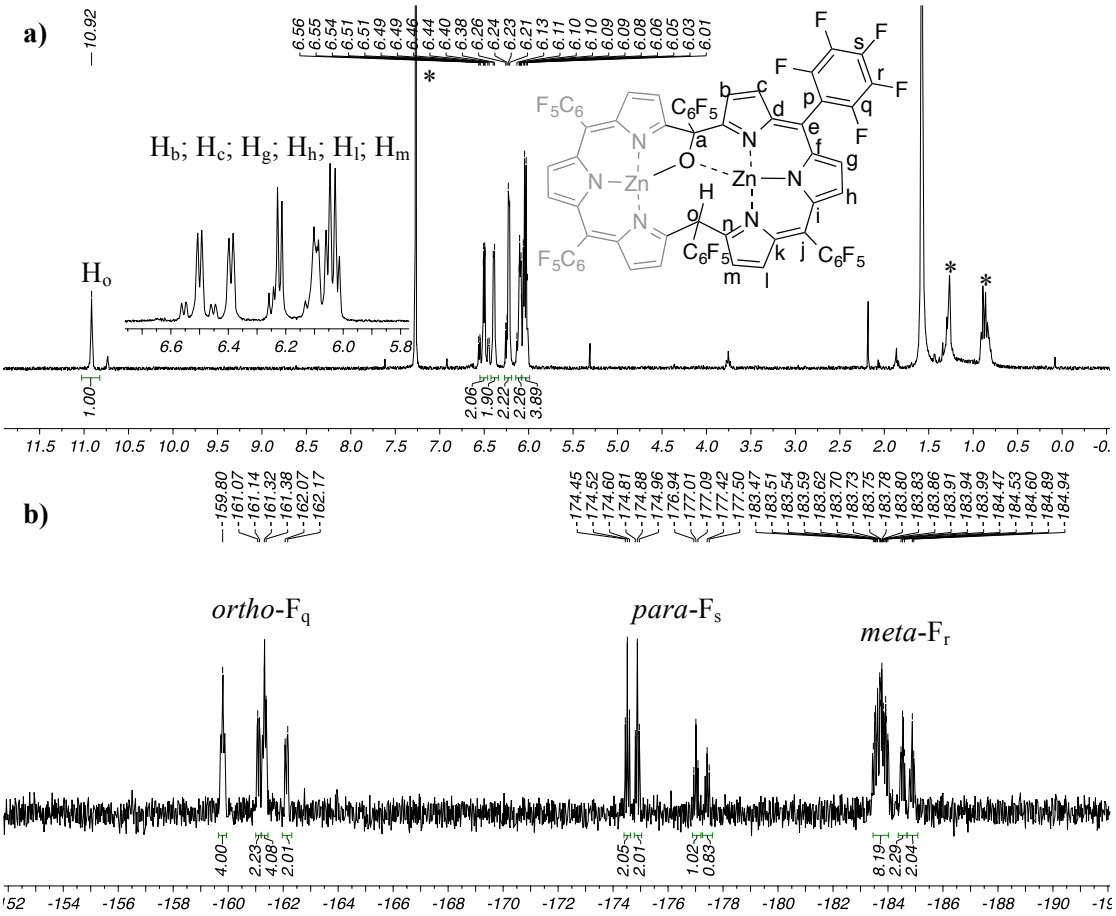

Figure 4.18: a) ^{1}H-NMR spectrum of compound **Zn1.137** in $CDCl_3$, * stands for $CHCl_3$; b) ^{19}F-NMR spectrum of compound **Zn1.137** in $CDCl_3$.

Interesting is the fact that a small change in the procedure performed in this thesis led to the synthesis of a structure without the coordinated chloride between the two zinc atoms. In fact the author of the published work used a procedure where brine was used in the work-up treatment of the reaction. Here this step was achieved differently, being the work-

up performed only with a saturated hydrogenocarbonate solution and water. This variation in the procedure removed the source of chloride and therefore MALDI(TOF) analysis gives the molecular ion minus the chloride mass *m/z* = 1602.8 [$M^{+\bullet}$] (Figure 4.7) [46].

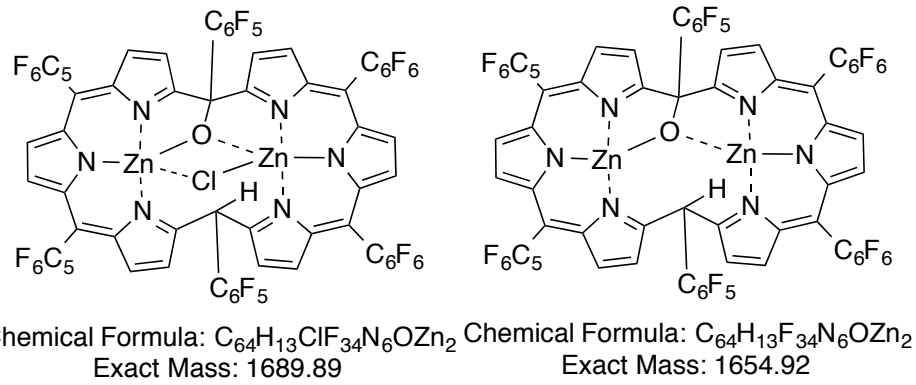

Figure 4.19: Structures of **Zn1.137.**

Other possibility explored was *N*-confused [26]hexaphyrins, which, can be synthesized from **1.137** directly under an unprecedented pyrrolic rearrangement with yields around 24%. This was achieved under aerobic conditions, adding a large excess of CuCl (I) to a solution of **1.137** in pyridine for 3 h (Scheme 4.9). After usual workup followed by chromatographic separation through a silica gel column, a reddish solid was isolated as the major product (**1.151**). Positive-mode high-resolution mass spectroscopy (HRMS) exhibited the parent ion peak at *m/z* = 1613.8972 $[M]^{+\bullet}$ (calcd for $C_{66}H_{10}Cu_2F_{30}N_6O_2Cu_2$: 1613.8941), therefore demonstrating that two oxygen atoms are incorporated in addition with two copper ions. This complex was straightforwardly demetalated to its free base **1.152**, upon treatment with an excess of TFA.

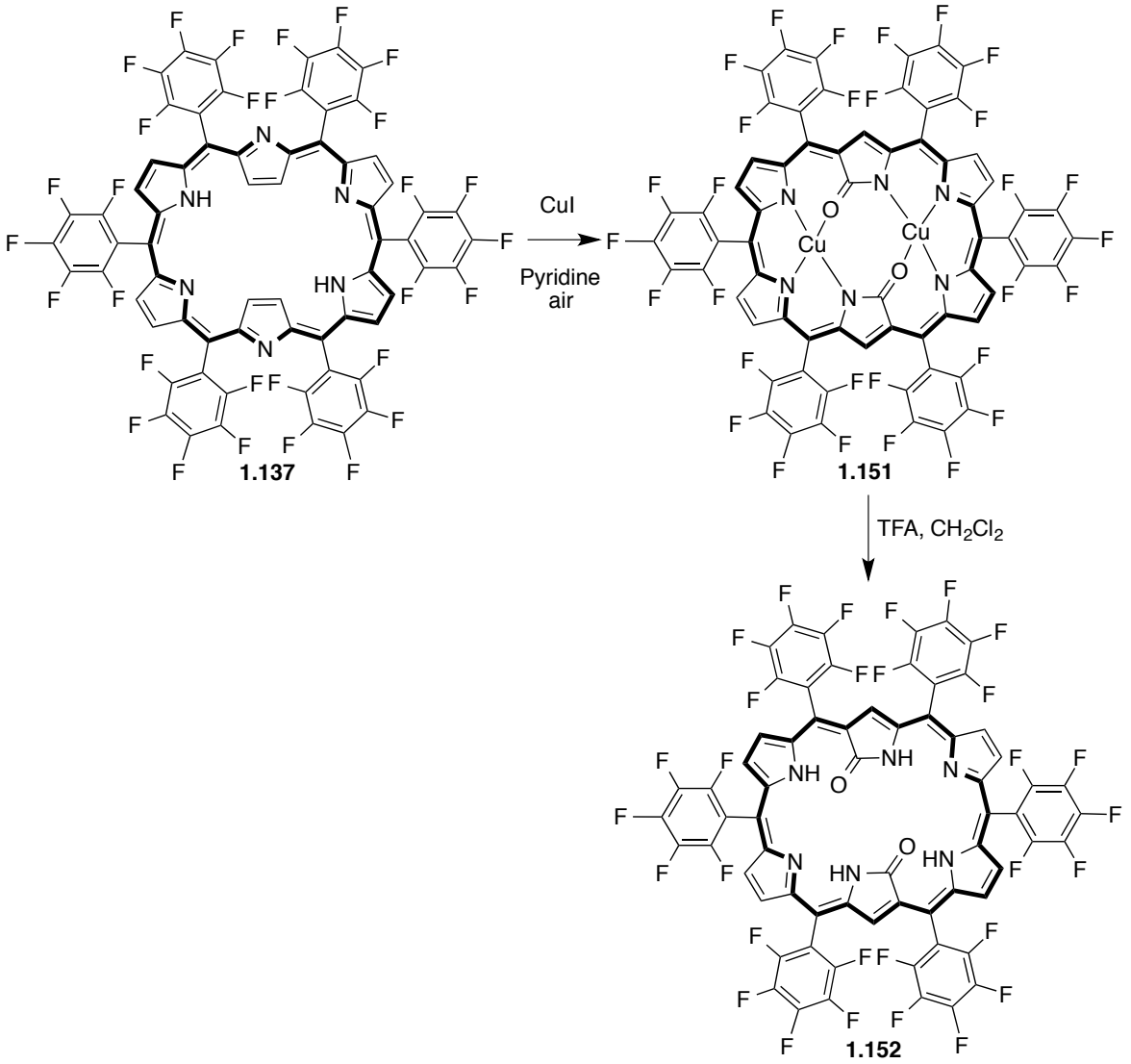

Scheme 4.12

The characterization of compound **1.152** was achieved by NMR spectroscopy and HRMS and all the data is consistent with the presented structure. The ^{1}H-NMR spectrum shows the same pattern observed for the previous structures where the inner protons of the macrocycle NH_n and NH_o are shielded and therefore at low chemical shifts displayed as singlets at δ -0.28 and -0.77 ppm. On the contrary the signals due the protons in the surrounding periphery of **1.152** present themselves at low fields, as a singlet for H_a integrating for two protons at 10.77 ppm and the β-pyrrolic protons (H_k, H_j, H_f and H_e) are the expected intercorrelated doublets at δ 9.51 (j= 5.2 Hz), 9.44 (j = 5.2 Hz), 9.23 (j = 4.8 Hz) and 9.19 (j = 4.8 Hz). Also the ^{19}F-NMR give us information about the fluorine atoms present in this molecule and here the arrangement is similar to the previous analogues.

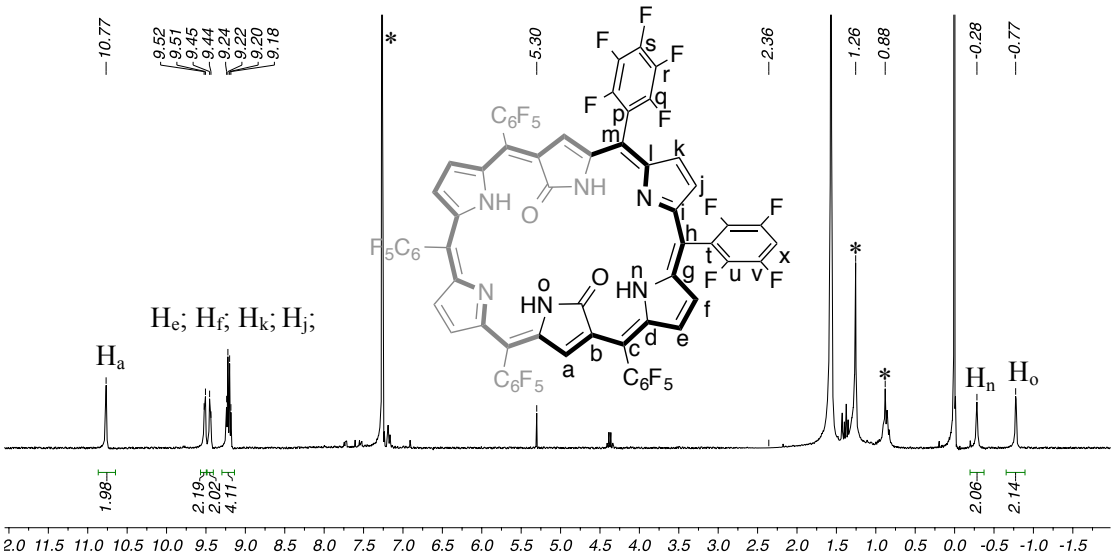

Figure 4.20: ^{1}H-NMR spectrum of compound **1.152** in $CDCl_3$ * stands for $CHCl_3$ and solvent impurities.

Supplementary characterization with ^{19}F-MMR shows exactly the same pattern as hexaphyrins with splited signals for each the *ortho* and *meta* positions integrating each one for 4F and 8F, characteristic of compounds with a rectangular shape. The remaining fluorines are located at the *para* positions and the same split of the signal is noted, hereby with half the integrations for each signal 2F and 4F (Figure 4.21).

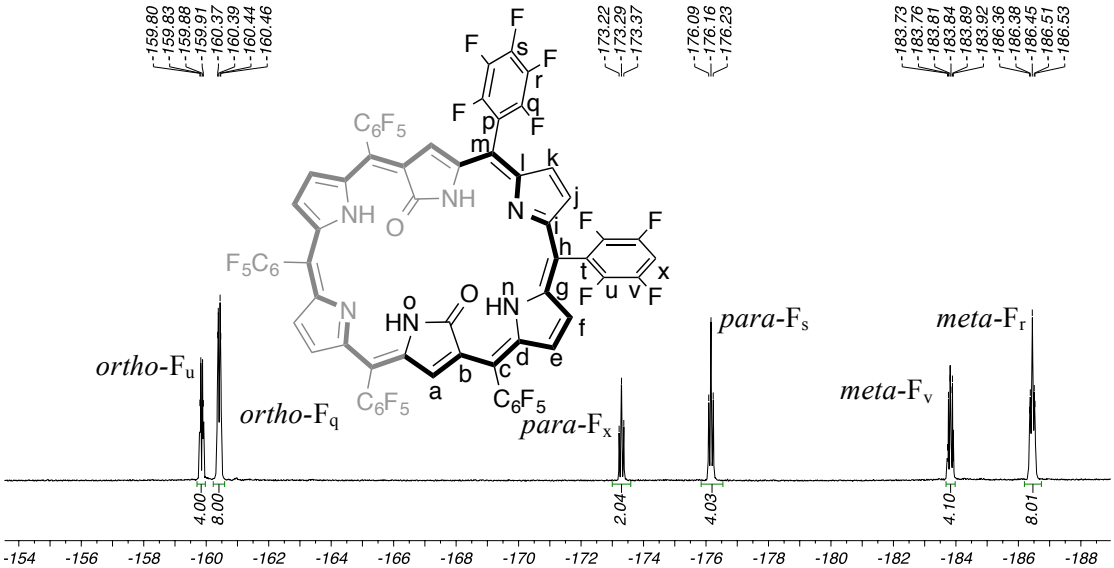

Figure 4.21: ^{19}F-NMR spectrum of compound **1.152** in $CDCl_3$.

After these synthesis the same procedures used as before were tried (EDA, 4-mercaptopyridine in DMF for 6h), however this prooved rather unsuccessful. In fact, these

macrocycles display completelly different behaviour upon the same reactional conditions and this is another example. While *N*-fused pentaphyrins proved to be unstable towards these conditions based on the yield obtained these were isolated. Hexaphyrins, on the contrary, showed to be the most reliable macrocycle displaying a high stability towards these conditions, nevertheless when the subject of reactions in basic media, macrocycle **1.152**, forms a complex mixtures resolved by analytic TLC analisys. While this compound showed to be stable in acidic media, towards basic media is the opposite (Scheme 4.13).

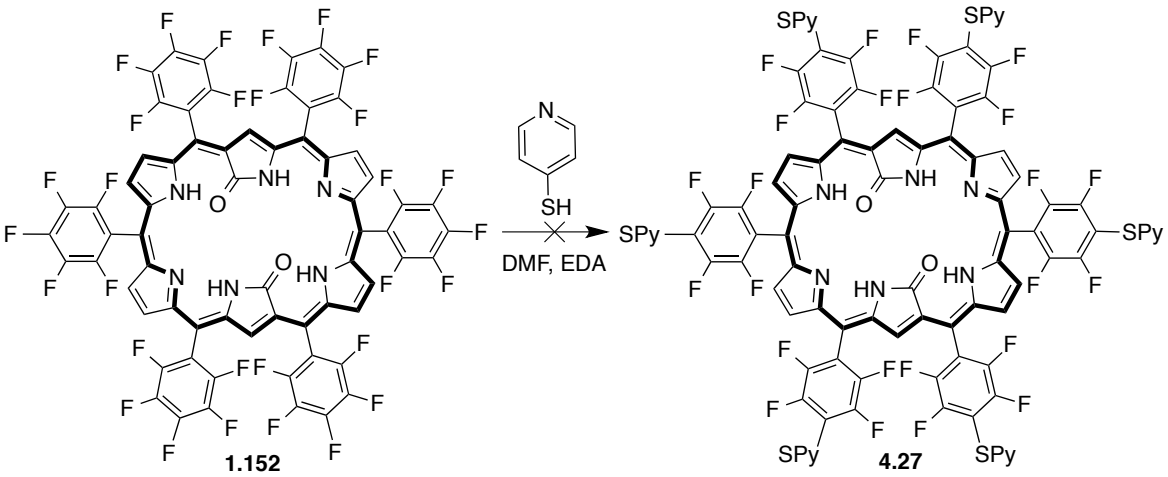

Scheme 4.13

A workaround this subject was to induce *N*-confusion in compound **4.24** avoiding the use of the basic media necessary to achieve the necessary nucleophilic substitutions. This synthesis proved to be efficient in the synthesis of *N*-confused hexaphyrins (**4.26)** from *meso* substituted [26]hexaphyrins (**4.24**) yet it cost a slight decrease in the final overall yield (18%, Scheme 4.14).

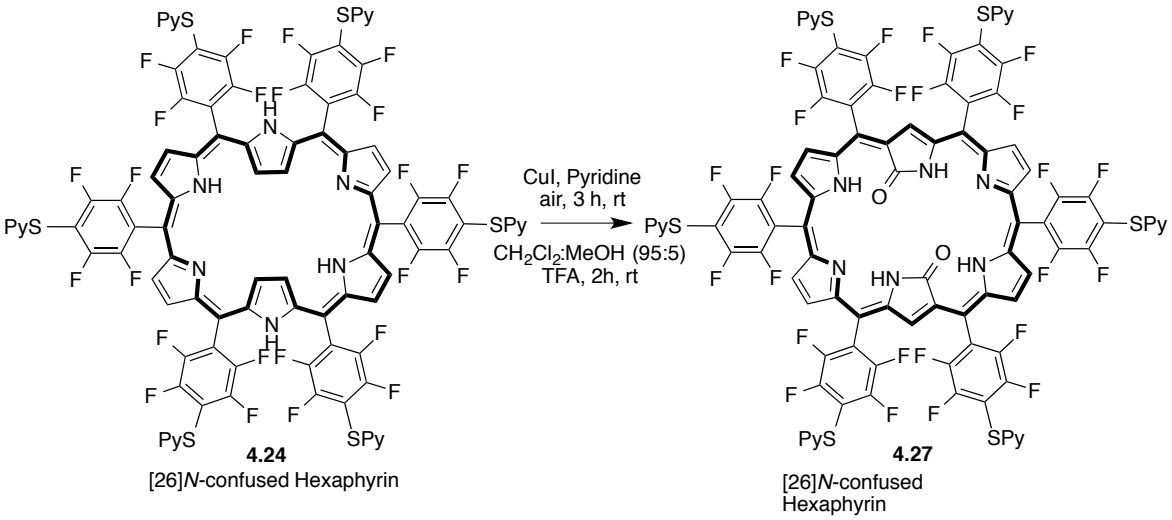

Scheme 4.14

The characterization of compound **4.27**, both by UV-Vis (Figure 4.22) and ^{1}H-NMR spectroscopy are in accordance with an *N*-confused hexaphyrin **4.24**. The UV-Vis, highlights the differences between compound **4.24** and **4.27** in terms of wavelength. The product of this reaction shows a blue-shifted Soret band at λ_{max} = 569 nm and two Q bands at λ = 724 and 798 nm. This profile clearly distinguishes compound **4.27** from **4.24**. It is also possible to note a much lighter variation between **1.152** and **4.26**, however in accordance with the previous analogues, substitutions at the *para* positions of the *meso*-pentafluorophenyl moieties of **1.152** induces a bathochromic effect in compound **4.26**, as it is possible note by the variation of the Soret band from λ_{max} = 564 nm to λ_{max} = 569 nm.

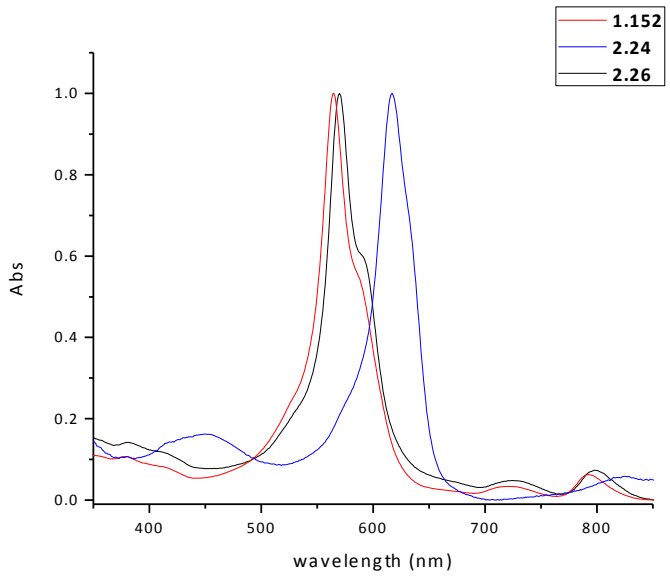

Figure 4.22: Absorption spectrum of **1.152**, **4.24** and **4.27** in DMF.

Using compound **1.152** as comparative is possible to note that the signals attributed to the *α*- and *β*-pyrrolic protons show the same profile. The major difference is located at *δ* 8.76-8.69 and 7.77 ppm where it is possible to find a multiplet and a large singlet attributed to the protons located in the pyridine moieties of compound **4.27** (figure 4.23).

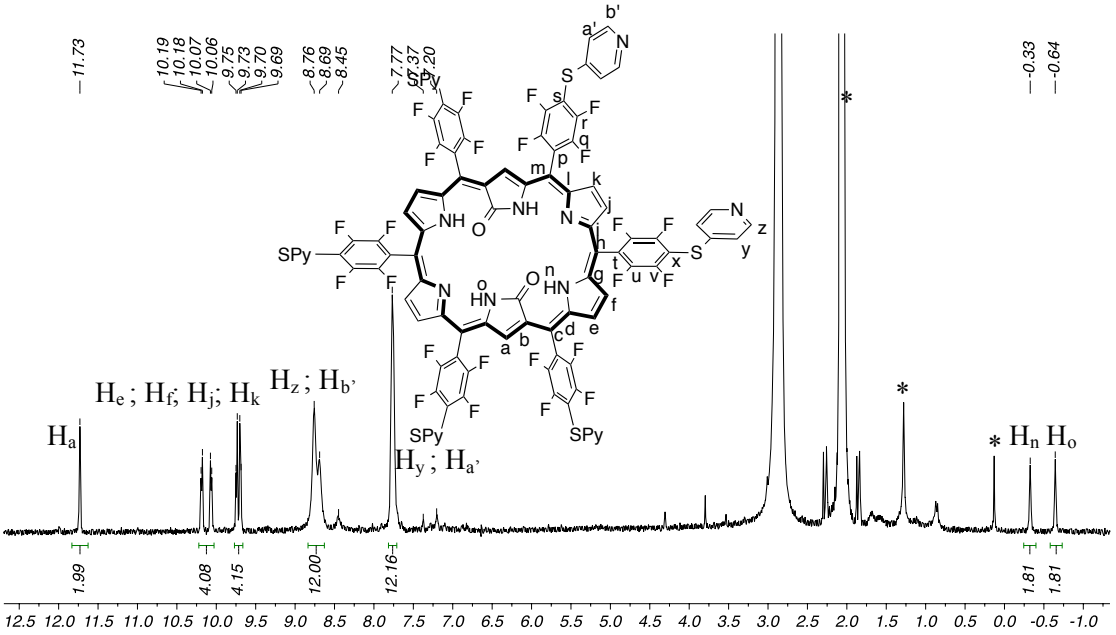

Figure 4.23: ^{1}H-NMR spectrum of compound **4.27** in acetone-d_6 * stands for acetone and solvent impurities.

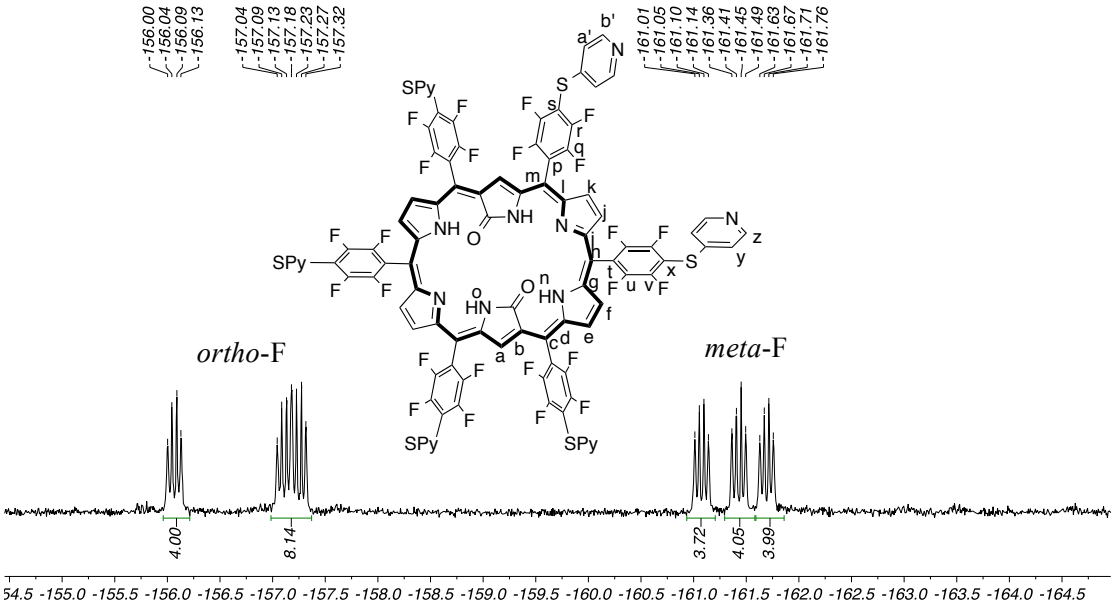

Figure 4.24: ^{19}F-NMR spectrum of compound **4.27** in acetone-d_6.

Here again, methylation reaction attempts failed to show the desired outcome. The results presented in this section show that synthetically is possible to functionalize expanded macrocycles of the *meso*-pentafluorophenyl type, namely in their *para* positions.

Synthetically, incorporating these structural modifications into *N*-fused pentaphyrins and hexaphyrins periphery proved to be a substantial challenge. The major problem arises with their oxidation/reduction behavior in basic media and their stability, which compared with other porphyrinoid compounds namely, porphyrins and phthalocyanines is diminished.

However, complete substitution of the *para* fluorines of compounds **1.101** and **1.137** were successfully achieved along with the corresponding reduction of the starting material. The use of MnO_2 showed to be efficient in their oxidation and it allowed complete oxidation of reduced version of hexaphyrins, with exception for **4.25**. In fact, MNO_2 is clearly distinguished from other oxidizing agents (*e.g.* H_2O_2, DDQ and Nitrobenzene), since it specifically oxidizes the macrocycle, diminishing the amount of side reactions (formation of compounds of the *N*-oxide type, when oxidation is attempted with **4.11** and **4.23**). In fact, the unpredictable behavior of these compounds towards reactional medias led to attempt variations of these macrocycles either by metallation (**Zn.1.137**) or by inducing *N*-confusion on compounds **1.137** or **4.24**. Metallation reactions on **1.137** proved to eliminate the aromatic character of compound **1.137**, and while there is

some interesting aspects to be further explored on this macrocycle, related to the absence of the anion coordinated to the two zincs of **Zn1.137**, it synthesis was abandoned. On the other side compound **4.24** was achieved and characterized evidencing that *N*-confusion of *para* substituted [26]hexaphyrins is possible to be induced in the same manner as in **1.152**. However its cationization showed the same exact problems as the previous attempts in order to obtain **4.13, 4.14**, and **4.26**. There is much to explore with these macrocycles with pyridine moieties, since they allow their applicability in other areas than PDI, as it is for instance catalysis. The possibility to coordinate several metals into these sites seems to be an interesting area to explore.

4.3.4. meso-Hexakis(pentafluorophenyl) hexaphyrins (1.1.1.1.1.1) ethylenediamine derivatives: experimental results

During the course of this work, we also directed some attention to the synthesis of this type of compounds with potential anion binding properties. With this end, functionalization of *meso*-pentafluorophenyl [26]hexaphyrin **1.137** with *N*-tosylethylenediamine, *N*-isopropylethylenediamine and *N*-Boc-ethylenediamine in the *para* position of the pentafluorophenyl groups were attempted. Initial reactivity studies were attempted with high amounts of the nucleophiles alone During these attempts varying the amounts of ethylenediamine A, using reflux conditions, several complex mixtures of substituted [28]hexaphyrins were obtained along with high degrees of decomposition. Further examination into these reactions, THF was used as solvent at reflux conditions, however the reaction times were long and almost no hexa substituted compound was obtained.

After several failed attempts, the use of a base and higher temperatures seemed mandatory in order to obtain the desired compound. In fact after several attempts using 50 eq. of ethylenediamines A, B or C dissolved in DMF and NEt_3, it was found that the reaction proceeded smoothly at 105 ºC. This reaction allowed a moderate yield around 42% along with less substituted analogues. However solvent change to NMP (*N*-methyl-pyrrolidinone) allowed an increase in the yield and after flash chromatography, using silica gel and CH_2Cl_2:MeOH (96:4) as eluent for **4.28** and **4.30** and CH_2Cl_2:MeOH:NEt_3 (70:28:2) as eluents for **4.29** respectively. These compounds were crystallized from CH_2Cl_2/MeOH yielding **4.28** in 69%, **4.29** in 64% and **4.30** in 75% (Scheme 4.15).

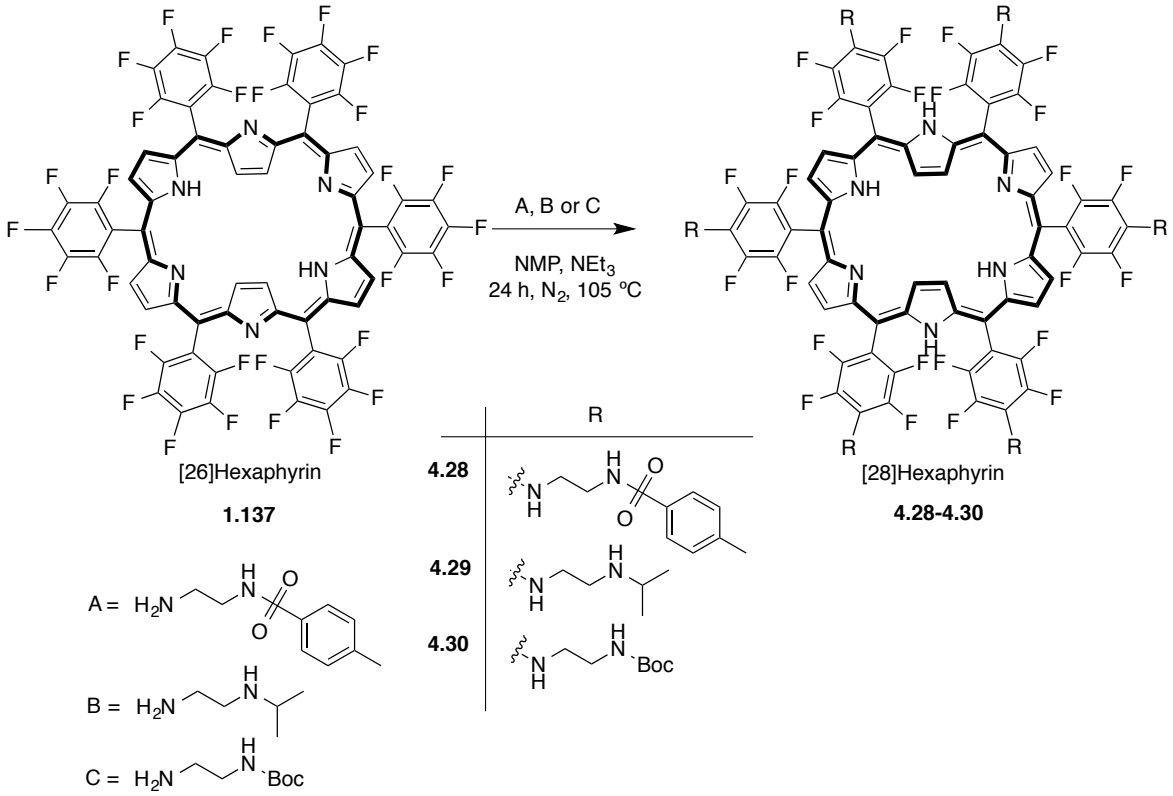

Scheme 4.15

The degree of substitution in these cases is possible to be verified by the disappearance of the resonances between δ -174.5 and -176.0 ppm, corresponding to the fluorine atoms at the *para* positions of [28]hexaphyrins **4.28**-**4.30** in the ^{19}F-NMR. Figure **4.24** highlights these differences when compared with compound **1.138**.

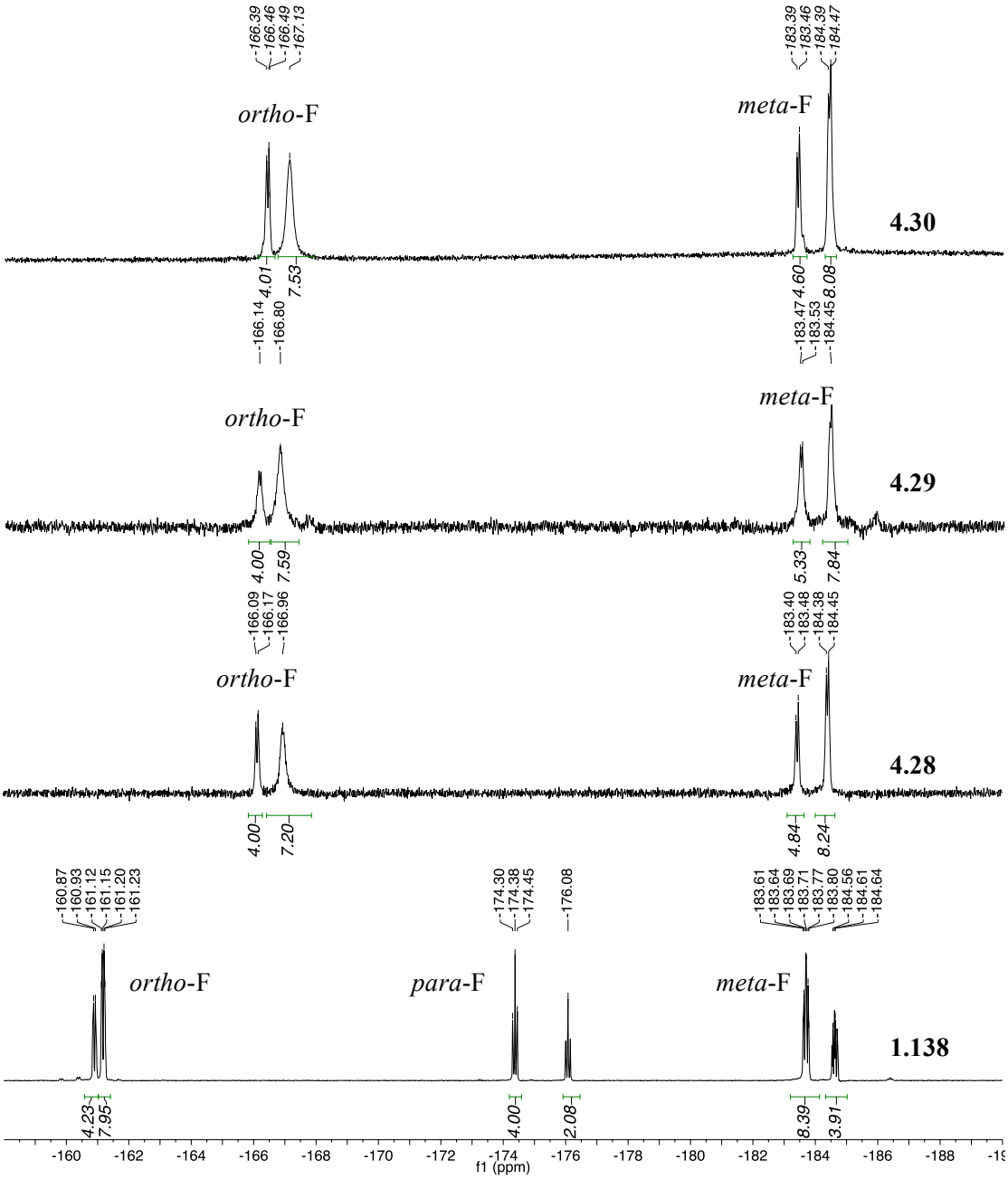

Figure 4.25: ^{19}F-NMR spectrum of compounds **1.138** and **4.28-4.30** in DMSO-d_6.

The HRMS-ESI confirm the structures, presenting for **4.28**, *m/z* = 2627.5335 ($[M+H]^+$), for **4.29** m/z = 1152.4003 ($[M+2H]^{2+}$) and for **4.30** a *m/z* = 1955.7584 ($[M+H]^+$), being consistent with the reduced form of the corresponding hexaphyrins.

In general these compounds show broad signals for most of the signals and concerning the signals around the aliphatic zone, there are similarities between compounds **4.28, 4.29** and **4.30**. These spectra show a relative intense signal at between δ 2.5 and 0.97

ppm corresponding to the CH_3 protons present in the tosyl, isopropyl and *tert*-butoxy carbamate groups of **4.28**, **4.29** and **4.30**, respectively (figure 4.26).

Closer to the solvent signals is possible to find two broad signals attributed to the outer CH_2 ($H_{a'}$ and $H_{e'}$) integrating for 12 protons. The chemical shift of this signal is very similar to the chemical shift of the deuterated solvent used in these analyses, and therefore some integration of the signals may appear overvalued.

The remaining CH_2 signals of the ethylenediamine moieties are located under the water signal of the ^{1}H-NMR spectra and were only possible to be attributed with bi-dimensional techniques. Here as an example, H-H correlation (COSY) of compound **4.28** is presented in figure 4.27 underlining the area of chemical shifts around δ 2.2 and 3.9 ppm.

In the COSY spectrum is possible to correlate all the aliphatic protons of compound **4.28**. For instance the CH_3 protons of the tosyl group correlates with the protons at the *meta*-positions of the same group. The remaining signals due to this group at the *ortho*-positions correlate with $H_{a'}$ and $H_{e'}$. Finally, $H_{a'}$ and $H_{e'}$ correlate directly with signals below the H_2O peak in the spectra showing that all the signals for this molecule indicate a correct attribution of the signals. Furthermore, the signal at δ 6.16 ppm H_z and $H_{d'}$ correlate however does not show correlation on the HSQC, thus being attributed to NH signals H_v and $H_{c'}$. Similar correlations are seen for the remaining compounds (**4.29** and **4.30**) being all the signals attributed accordingly.

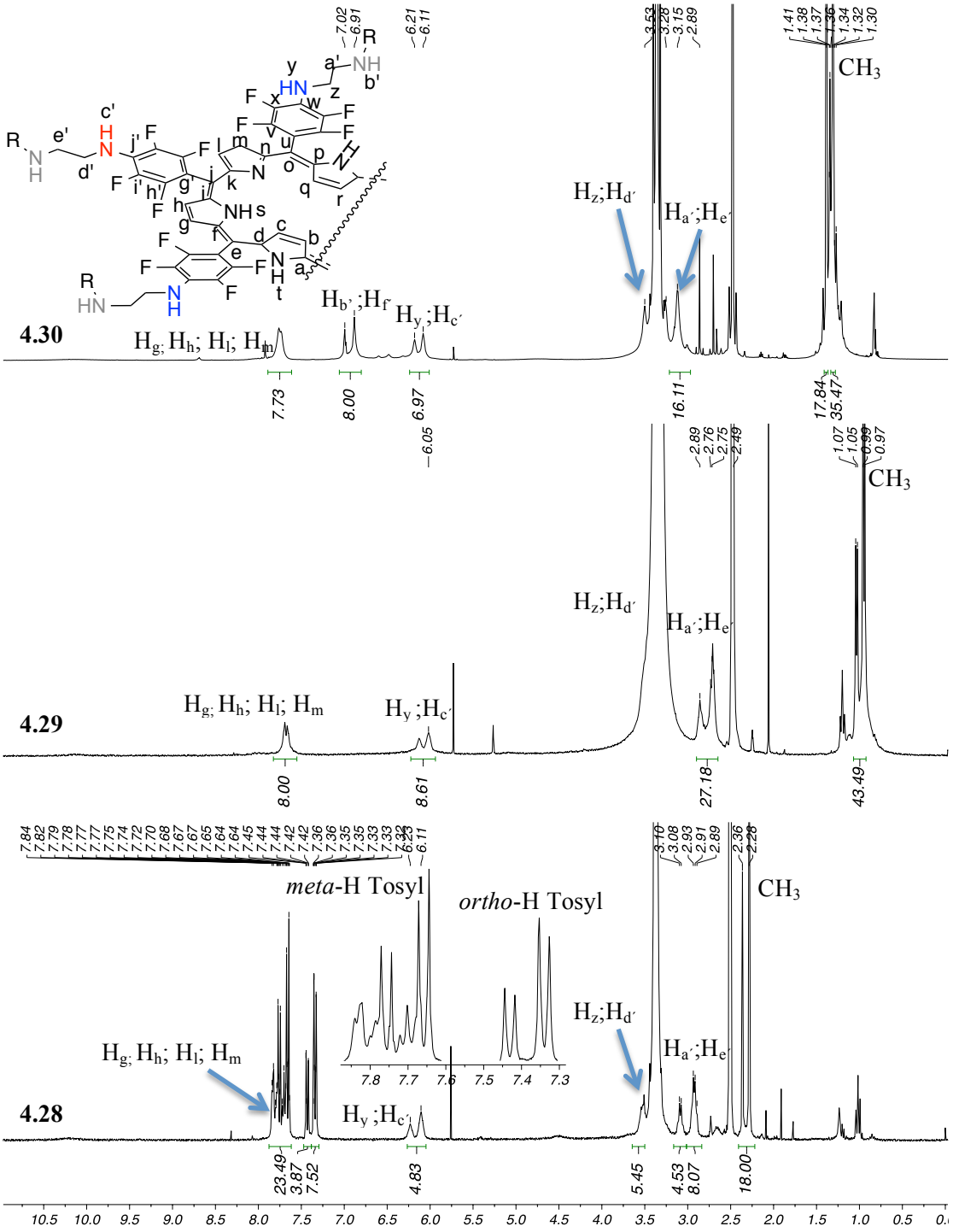

Figure 4.26: ^{1}H-NMR spectrum of compounds **4.28-4.30** in DMSO-d_6.

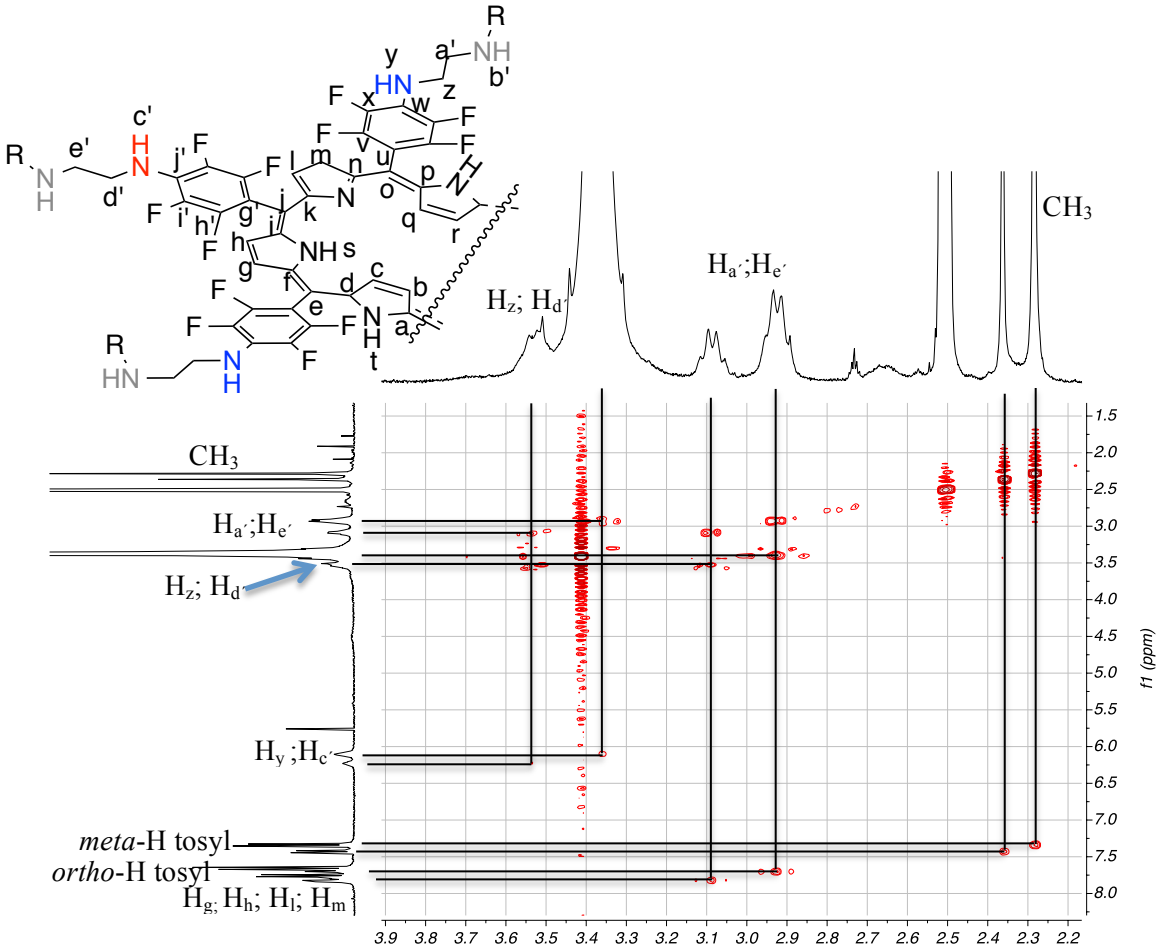

Figure 4.27: COSY spectrum of compound **4.28** in DMSO-d_6.

Subsequently, attempts in decreasing the amounts of nucleophile introduced in the reaction led to an interesting achievement. Using less than 25 equiv. of nucleophile A (*N*-tosylethylenediamine), the reaction becomes slower (48 h) and along with the desired product **4.28**, a mixture of reddish products started to appear on TLC analysis. This reaction was later, attempted with **1.137** alone with NMP and NEt_3 at 110 ºC (A, B or C) formed exclusively a red product, which is attributed to structure **1.147** (Scheme 4.16).

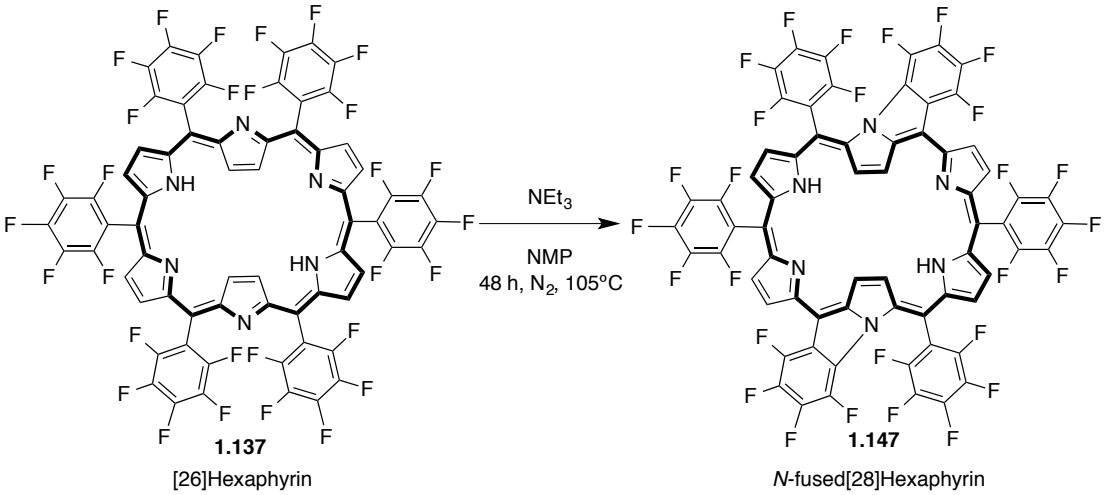

Scheme 4.16

The attribution of this structure was made based on the UV-Vis and NMR features of compound **1.147**. This compound exhibits a parent molecular ion peak at *m/z* = 1422 (calcd: *m/z* 1422) in the mass spectrum and mutually coupled two pairs of doublets at δ 6.26 and 5.46 ppm (J = 6.2 Hz), 5.37 and 4.06 ppm (J = 4.6 Hz) and finally at 5.04 and 4.53 ppm (J = 4.4 Hz) due to the pyrrolic *β*-protons in the ^{1}H-NMR spectrum (Figure 4.17).

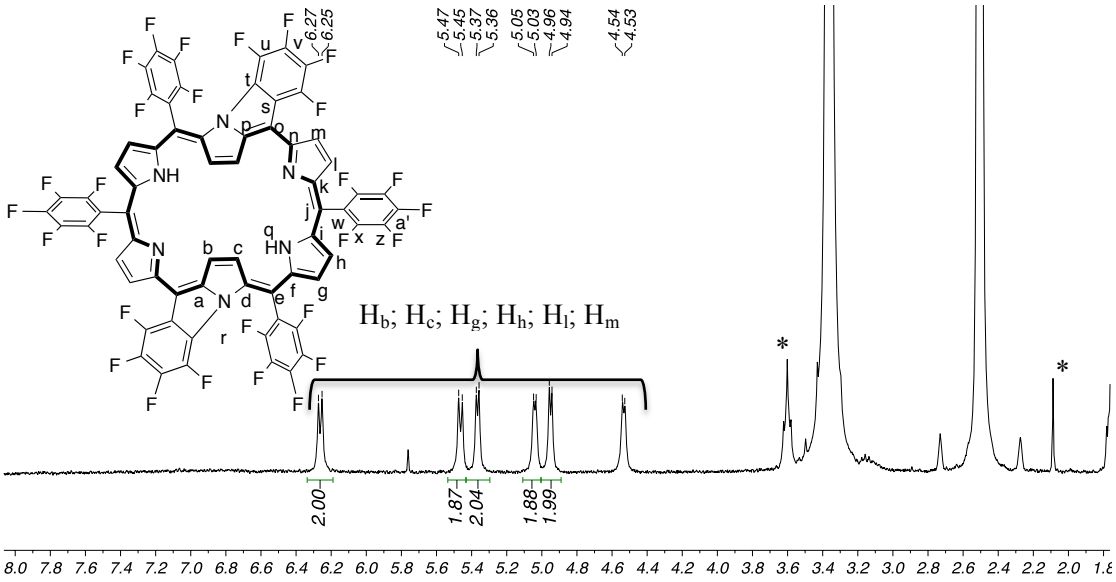

Figure 4.28: ^{1}H-NMR spectrum of compound **1.147** in DMSO-d_6, * stands for DMSO and solvent impurities.

The absorption spectra of **1.147** differ significantly from that of **1.137** and **1.138** with a much more broad Soret band with a λ_{max} = 492 nm.

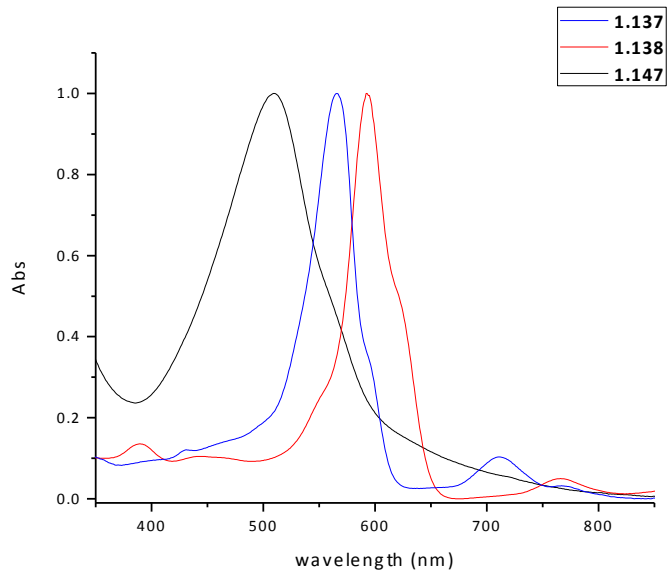

Figure 4.28: UV-Vis spectra of compounds **1.137**, **1.138** and **1.147**.

Final confirmation of some structures exhibited above, namely **4.28** and **4.30** were possible after being oxidized with MnO_2 achieving **4.31** and **4.32**, respectively (Scheme 4.18).

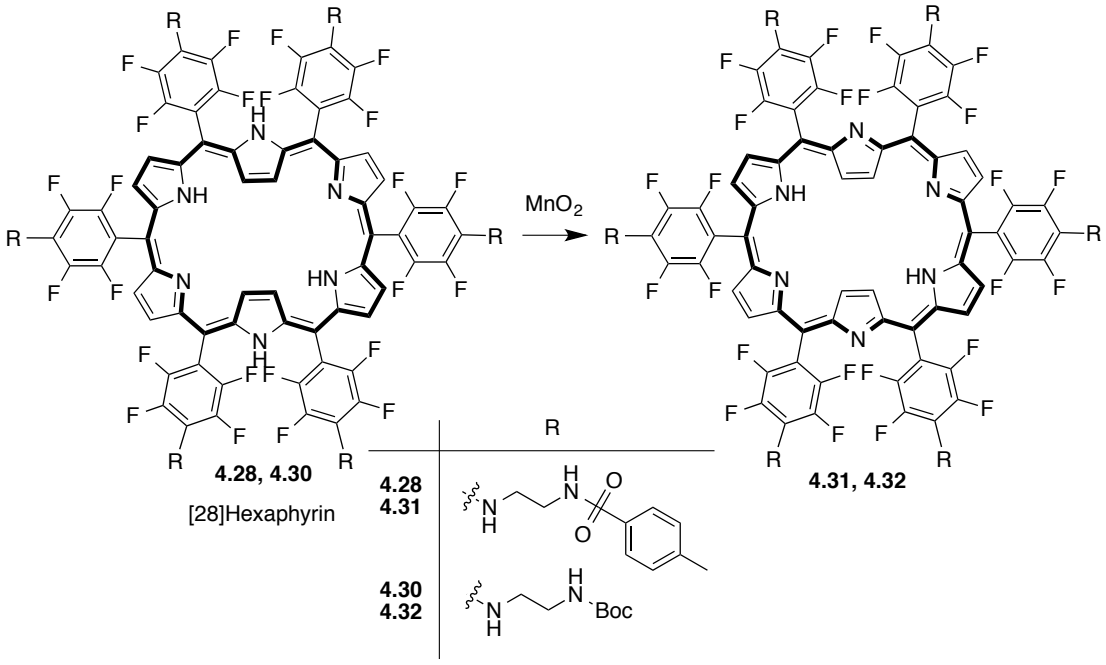

Scheme 4.17

Being aromatic compounds **4.31** and **4.32** display a nearly planar structure and therefore the ^{1}H-NMR of these compounds present much more defined signals and

multiplicities. In figure 4.29, the combined ^{1}H-NMR spectra of compounds **4.31** and **4.32** are showing clearly the desired product in a much simpler manner.

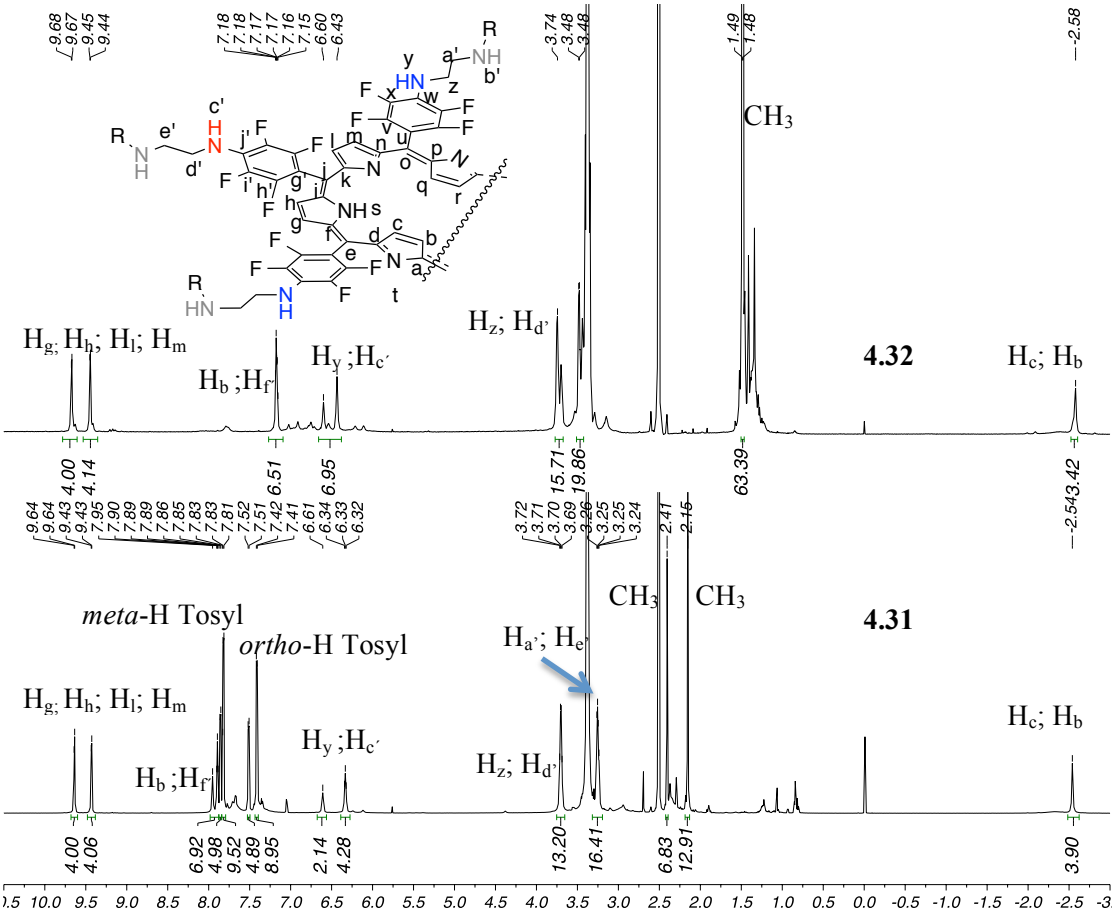

Figure 4.30: ^{1}H-NMR spectra of compounds **4.31** and **4.32** in DMSO-d_6 * stands for DMSO and solvent impurities.

The attributions were achieved using bi-dimensional techniques and based in the previous attributions, nevertheless is possible to find all the corresponding signals of compounds **4.31** and **4.32**.

Synthetically several kinds of substitutions in expanded porphyrins were made possible. While in some cases we failed to carry on the synthesis until its very end, several other possible nucleophiles can be used to range the set of necessary applications. In this case, the increase of binding sites and flexibility of the macrocycle used are of great importance when binding applications are being targeted. On the other hand, if a more static macrocycle is needed oxidation of the reduced precursors from the nucleophilic substitutions was possible using a mild oxidant as MnO_2. In fact, most of the work

developed in this thesis is around synthetic routes towards functionalization of the macrocycles. Making possible new types of reactions and understanding the reactivity of these macrocycles was definitely the limiting step of this work, namely due the unpredictability of these compounds towards different reaccional conditions. Still, these new macrocycles are in fact a potential platform for further functionalizations and these studies show a set of simple procedure towards this goal.

4.3.5. Para-substituted (meso-pentafluorophenyl)Hexaphyrins: Anion binding studies

The interaction studies of compounds **1.138**, **4.28** and **4.29** with anions were performed by UV-Vis titrations upon addition of aliquots of a stock solution of anions prepared from their tetrabutylammonium salts (Figure 4.29).

These titrations were followed by the perturbation in the UV-Vis spectra caused by the addition of fluoride, acetate and dihydrogen phosphate anions. The treatment of the experimental data with a standard non-linear curve provided the association constants in $CHCl_3$ and DMSO (Table 1). Analysis of the binding properties of **1.138** revealed a 1:1 host-guest complex in solutions**,** while compounds **4.28** and **4.29**, formed a 1:2 host-guest complexes with F^-, AcO^- and $H_2PO_4^-$, indicating that the outer periphery of macrocycles **4.28** and **4.29** is playing an active role in the association with the anions. The association constants of **1.138** in DMSO were only possible to calculate for F^- anion and the value observed was $K_a = 2.19 \times 10^3\ M^{-1}$. Attempts made with acetate and dihydrogeno phosphate anions have not shown significant perturbations in the UV-Vis spectra.

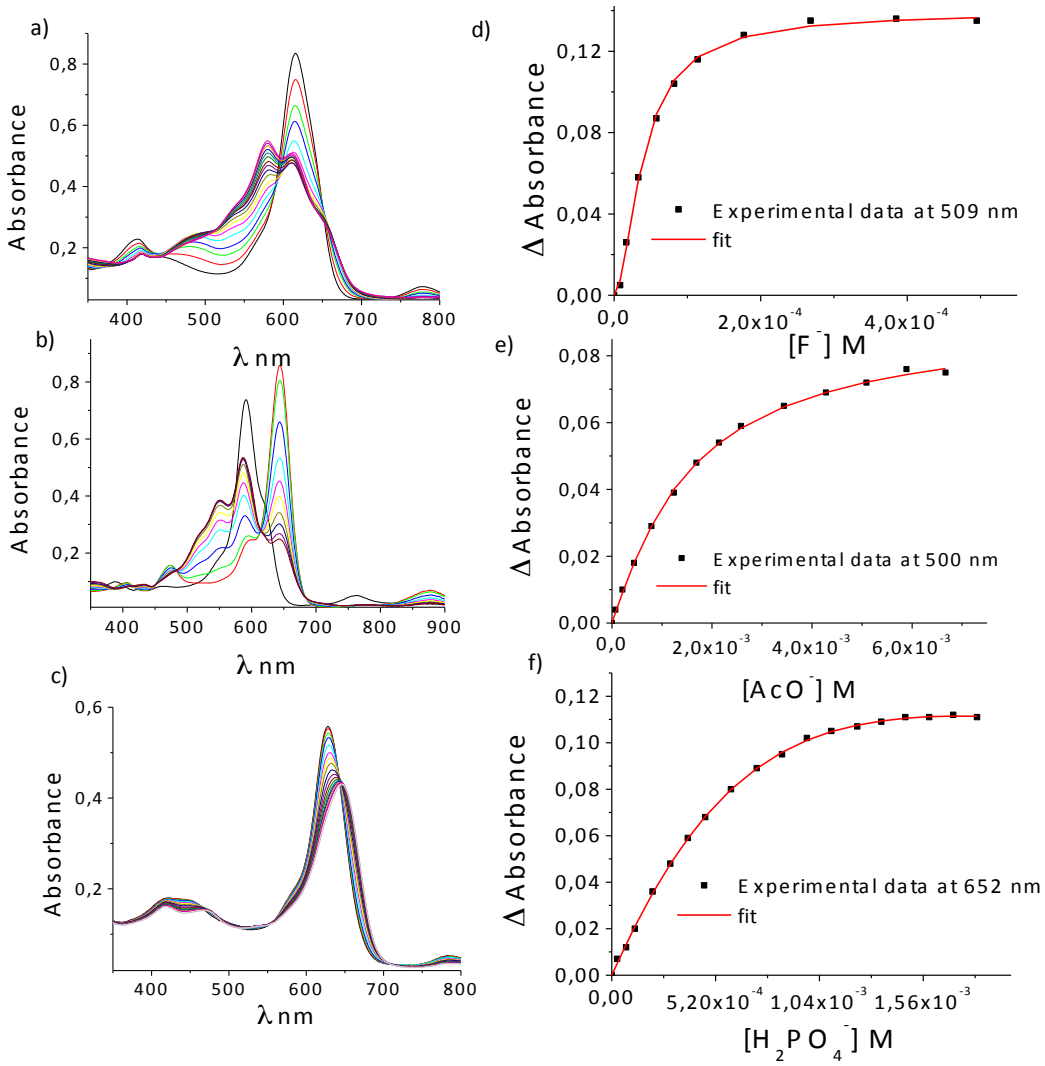

Figure 4.29: UV-Vis titration of compounds: a) **1.138** with fluoride anion in $CHCl_3$; b) **4.28** with fluoride anion in $CHCl_3$; c) **4.29** with fluoride anion in DMSO. Experimental data treatment at: d) 509 nm of compound **1.138** with fluoride anion in $CHCl_3$; e) 500 nm of compound **4.28** with acetate anion in $CHCl_3$ and; f) 652 nm of compound **4.29** with dihydrogen phosphate anion in DMSO.

Comparing chemosensors **4.28** and **4.29**, both show higher association constants in DMSO, decreasing from fluoride until dihydrogen phosphate anions ($F^->AcO^->H_2PO_4^-$). Notably, the selectivity for acetate compared with $H_2PO_4^-$ drastically increases when DMSO is used as solvent, being the best association constant ratio ($AcO^-/H_2PO_4^-$) 459.9 for chemosensor **4.29**. Other anions, such as chloride, nitrite and nitrate as their tetrabutylammonium salts did not triggered any perturbation in the UV-Vis spectra of sensors **1.138**, **4.28** and **4.29** and for this reason no results are shown for these anions (Table 4.1).

Table 4.1: Affinity constants at 22 °C for compounds **1.138, 4.28** and **4.29**.

	1.138[a,*]	**4.28**[b]		**4.29**[b]	
	$CHCl_3$	**$CHCl_3$**	**DMSO**	**$CHCl_3$**	**DMSO**
F^-	$2.32x10^4$	$1.06x10^7$	$3.94x10^{10}$	$1.32x10^7$	$4.94x10^9$
AcO^-	$1.27x10^4$	$5.31x10^5$	$4.00x10^9$	$1.63x10^5$	$2.41x10^8$
$H_2PO_4^-$	$3.16x10^3$	$2.48x10^5$	$6.51x10^7$	$3.24x10^4$	$5.24x10^5$
AcO^- /$H_2PO_4^-$	5.44	2.14	61.44	5.03	459.92

[a] These complexes are 1:1 (hexaphyrin: anion), so the *K* units are M^{-1}; [b]These complexes are 1:2 (hexaphyrin: anion), so the *K* units are M^{-2}; [*]In DMSO, *Ka* of **1** were only possible to calculate for F^- (2.19×10^3 M^{-1}).

The obtained data reveal that the increase of solvent polarity had a significant influence on the affinity behavior of receptor **4.28**. Such behavior suggests that the conformation of the molecule is influenced by the polarity of the solvent system employed and that in more polar solvents the higher acidity of the NH protons outweighs the conformational preferences of these groups.To better understand this behavior ^{1}H-NMR titrations were performed with **4.28,** both in $CDCl_3$ and DMSO-d_6. As can be observed in figure 4.31, the addition of fluoride to compound **4.28**, leads to different changes in the ^{1}H-NMR spectrum.

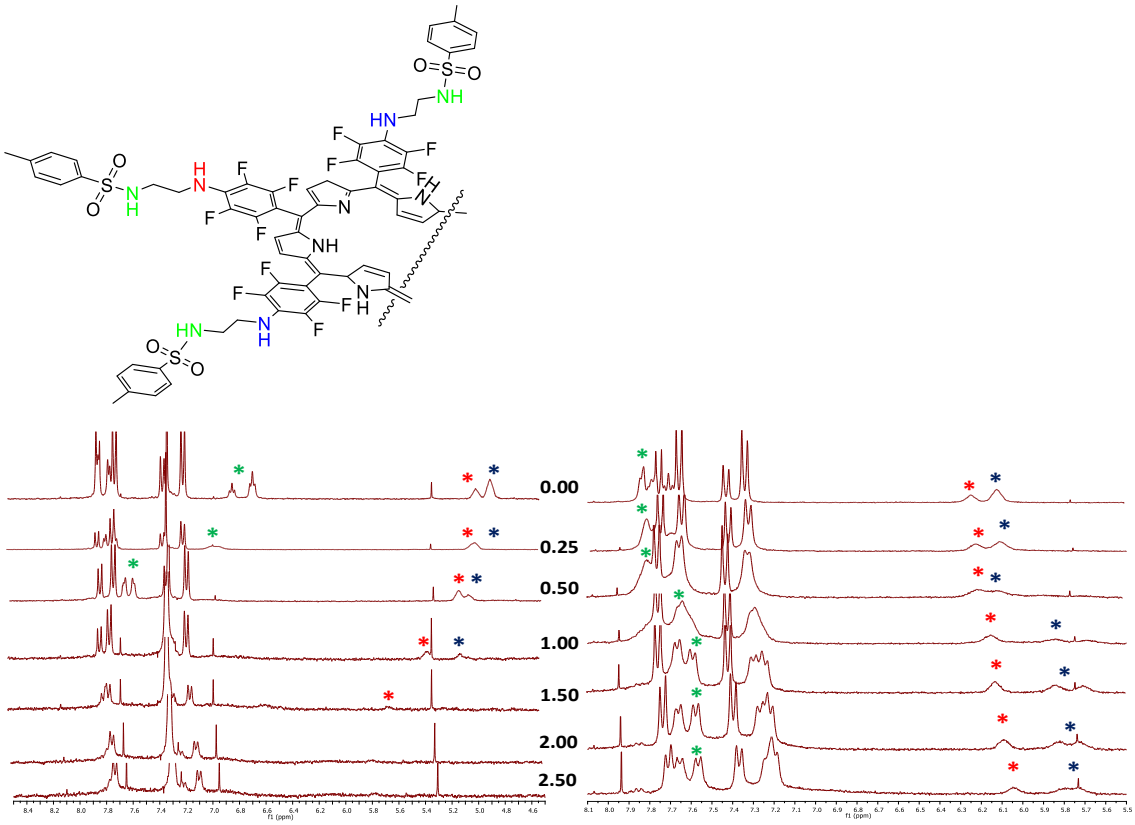

Figure 4.30: ^{1}H-NMR spectra of compound **4.28** in $CDCl_3$ (left) and DMSO (right) upon addition of F^-. Different NH Signals: *NHTs, *2 NHC_6F_4 and *4NHC_6F_4.

When the titration is performed in $CDCl_3$ the NHs closer to the tosyl groups starts disappearing at 1 equiv. of fluoride anion, this result indicat a deprotonation phenomenon. However when the same titrations were done in DMSO-d_6 negative Δδ values of theexterior NH protons show that they are sensitive to the continuous addition of fluoride. While in DMSO **4.28** shows a moderate Δδ (0.8-1.1 ppm) of the NH protons, the same studies performed in $CDCl_3$ only occur until the addition of 1 eq. of fluoride. In addition, DMSO solutions of hexaphyrins **1.138**, **4.28** and **4.29** combined with anions (F^-, AcO^- and $H_2PO_4^-$) show naked-eye color changes (Figure 4.32).

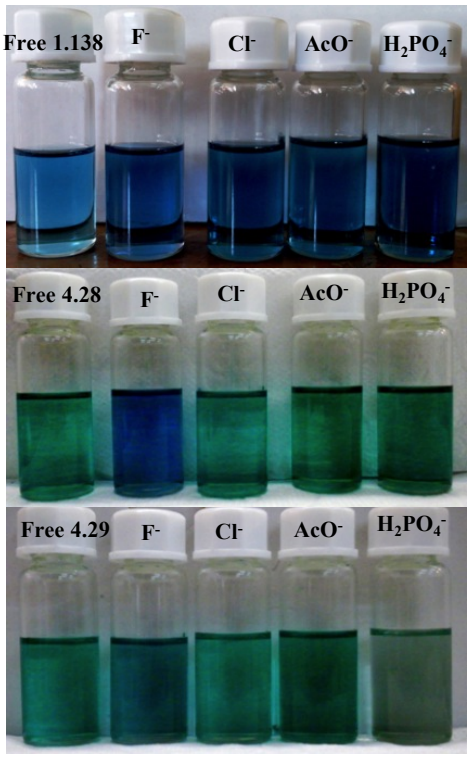

Figure 4.31: Changes in the coloration of DMSO solutions of hexaphyrins **1.138**, **4.28** and **4.29** upon addition of different anion solutions, as tetrabutylammonium salts.

No color changes are observed after the addition of bromide, nitrate, and nitrite anions, which is in concordance with the UV-Vis titrations. The color changes observed are thus directly related with the values of the affinity constants.

While the majority of work published on anion-recognition has been devoted to the study of systems operating in non-aqueous media. [28]hexaphyrins **4.28** and **4.29** are no exception since they showed no solubility in water at the working pH. A fashionable way to surpass this problem and the competition factors associated with aqueous media was the preparation of a sensor based on piezoelectric quartz crystals.

Piezoelectric sensors have proven to be versatile tools for the measurement of various processes and have found numerous applications in sensing and biodetection [47]. They are very sensitive devices to the mass deposited on its active area, robust, easy to set up and reliable when detection of certain species from aqueous media is required [48]. The measuring principle is based in the decrease or mass produces on the oscillation frequency

of the device. In these systems the magnitude of the frequency decrease is proportional to added mass [49].

The deposition of hexaphyrins **1.38**, **4.28** and **4.29** onto one face of the piezoelectric quartz crystal was performed with $CHCl_3$ solutions of the hexaphyrin derivatives and then spread by spinning at 300 rpm for 1 min. Sensors were left to dry for two days prior to use. This work was performed in collaboration with the research group of Professor Teresa Gomes, and for this reason specific experimental data are not discussed.

By adding different amounts of aqueous solution of the anion in their sodium salts, while keeping the temperature at 22 °C, an isotherm of the sensor responses (frequency decrease) vs. the anion concentration could be obtained in figure 4.33.

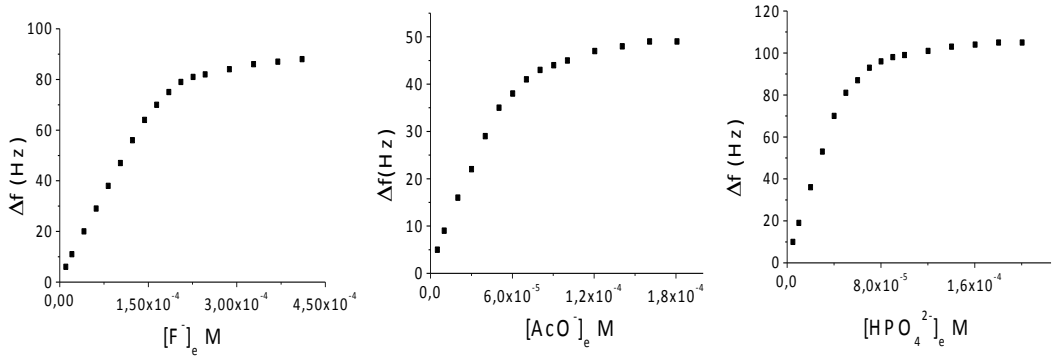

Figure 4.33: Adsorption isotherm (T=22.0 °C) of compound **1.138** (left), **4.28** (midle) and **4.29** (right) deposited onto one electrode of a piezoelectric quartz crystal, in contact with an aqueous solution of the corresponding anion as sodium salts form.

The interaction of hexaphyrin compounds with all anions was fast and reversible. Figure 4.34 shows the interaction, which can be followed by the frequency shift of the quartz crystal, when a 0.5 mL of a $5x10^{-5}$ mol L^{-1} solution of fluoride anion was injected in a constant flow of water that was passing over the coated quartz crystal face. As can be seen, the frequency was decreasing while fluoride was attaching to the hexaphyrin, and increasing while it was washed away by the water flow. The complete process including the adsorption and complete desorption last 80s.

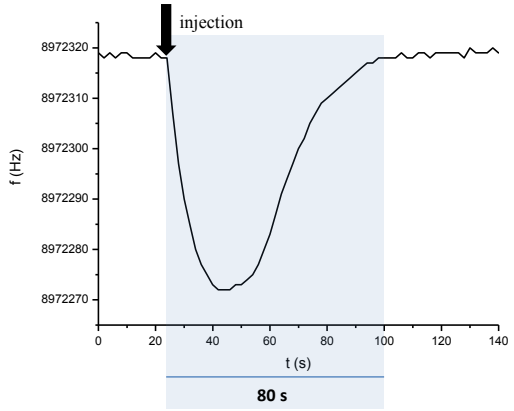

Figure 4.34: Frequency shift seen for a sensor made with **4.28**, before and after exposition to 0.5 mL of an aqueous fluoride solution at $5x10^{-5}$ mol L^{-1}.

In order to study the influence of pH on the equilibrium, experiments with fluoride anion, which have been made at pH 6.7 were repeated at pH 9.7 (the pH used in the HPO_4^{2-} experiments) and no significant differences in the results (α=0.05) were found. The sensors are not selective regarding the studied anions, however all sensors showed a remarkable stability along time, to which contributes the insolubility of [28]hexaphyrins **4.28** and **4.29** in water.

In conclusion, we sinthesized substituted *meso*-pentafluorophenyl [28]hexaphyrins and attempts were made in order to evaluate them as anion sensors. These new compounds are able to interact with several anions in solvents like $CHCl_3$ and DMSO. Antagonistically, the results demonstrate that anion complexation with hydrogen-bonding receptors in a competitive solvent is enhanced. The role of the solvent may take in this phenomenon is of high relevance either due the structure that [28]hexaphyrins may acquire when dissolved in this media and/or the possibility of participating in process of binding itself. In both cases the competitive solvent adds to the overall complexation energy and thereby strengthens binding affinity. These compounds especially compounds **4.28** and **4.29** in DMSO exhibits a pronounced constant ratio $KAcO^-/H_2PO^{4-}$, 61.44 and 459.9, respectively.

Furthermore, piezoelectric crystals coated with compounds **1.138**, **4.28** and **4.29** were successfully implemented. The deposition of these compounds is a fashionable methodology to surpass some problems encountered with chemosensors that are not soluble in aqueous media, or that can be difficult to study by other analytical method.

4.4. Experimental data

*Preparation of meso-pentakis(pentafluorophenyl)[22] N-Fused Pentaphyrin (**1.101**) and meso-hexakis(pentafluorophenyl)[26] hexaphyrin (**1.137**).*

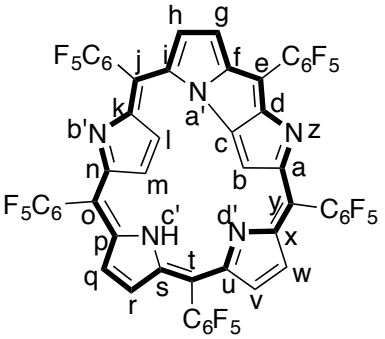

1.101

Chemical Formula: $C_{55}H_{10}F_{25}N_5$
Exact Mass: 1215.05

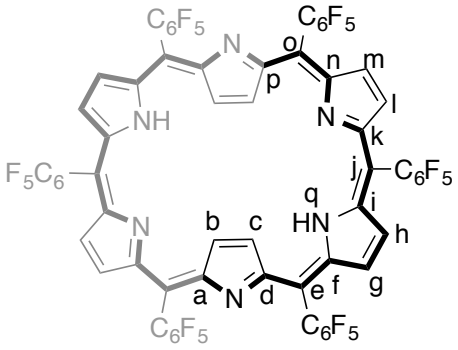

1.137

Chemical Formula: $C_{66}H_{14}F_{30}N_6$
Exact Mass: 1460.08

A solution of 2.5 M $BF_3.OEt_2$ was added to a solution of pentafluorobenzaldehyde (2.92 g, 0.02 mmol) and pyrrole (1.0 g, 0.02 mol) in CH_2Cl_2 (250 mL), and the resulting solution was stirred for 2 h under nitrogen. After adding DDQ (8.46 g, 0.037 mol), the solution was stirred for 3 h and then passed through a short alumina column to remove the DDQ. The reaction mixture was then separated by column chromatography on silica gel with a mixture of ethyl acetate:hexane (1:9) with increasing polarity until (2:8). The purple and red fractions were collected being the first compound (**1.137**) and the second (**1.101**), respectively. The solution of **1.137** and **1.101** were evaporated, and the residues recrystallized from pure hexane to give pure **1.137** (146 mg, 14%) and **1.101** (582 mg, 18%).

*meso-Pentakis(pentafluorophenyl)[22] N-fused pentaphyrin (**1.101**):*

^{1}H-NMR (300 MHz, $CDCl_3$): δ 9.16 (d, J = 1.6 Hz, 2H, H_h and H_g), 8.61 (dd, J = 4.7, 1.9 Hz, 1H, H_w), 8.40 (t, J = 5.6 Hz, 2H, H_q and H_r), 8.35 (d, J = 4.8 Hz, 1H, H_v), 2.17 (d, J = 4.5 Hz, 1H, H_l or H_m), 1.68 (d, J = 4.5 Hz, 1H, H_l or H_m), 1.18 (s, 1H, $H_{c'}$), -2.30 (s, 1H, H_b).

^{13}C-NMR (75 MHz, $CDCl_3$): δ 161.0, 160.9, 160.4, 159.7, 153.4, 152.1, 150.9, 148.1, 147.7-147.3 (m, C_6F_5), 146.8, 144.5-143.4 (m, C_6F_5), 140.8-139.9 (m, C_6F_5), 139.4-139.1 (m, C_6F_5), 137.0-136.7(m, C_6F_5), 136.2 -135.8 (m, C_6F_5), 133.8 (C_l or C_m), 133.3 (C_l or

C_m), 132.8 (C_q and C_r), 132.4, 131.5 (C_v), 129.4 (C_w), 123.3 (C_h and C_g), 122.4, 120.5, 112.7, 109.6, 100.8, 99.1, 90.0.

^{19}F-NMR (282 MHz, $CDCl_3$) δ -157.57 – -158.23 (m, 1F, *meta* -F), -158.70 – -159.05 (m, 1F, *meta* -F), -159.55 (d, *J* = 23.4 Hz, 1F, *meta* -F), -160.06 (d, *J* = 22.6 Hz 1F, *meta* -F), -160.51 (dd, *J* = 20.0, 4.9 Hz, 2F, *meta* -F), -161.16 (dd, *J* = 23.7, 5.3 Hz, 1F, *meta* -F), -161.58 (dd, *J* = 23.5, 4.7 Hz,1F, *meta* -F), -162.70 (d, *J* = 23.0 Hz,1F, *meta* -F), -163.39 (d, *J* = 23.5 Hz, 1F, *meta* -F), -172.20 (t, *J* = 21.2 Hz, 1F, *para*-F), -173.15 (t, *J* = 21.0, 1F, *para* -F), -173.45 (t, *J* = 20.9 Hz, 1F, *para* -F), -174.20 (t, *J* = 21.0 Hz 1F, *para* -F), -176.93 (t, *J* = 20.9 Hz, 1F, *para* -F), -183.20 – -183.66 (m, 4F, *ortho*-F), -184.45 (dd, *J* = 23.2, 6.6 Hz, 2F, *ortho*-F), -185.15 (td, *J* = 21.5, 7.6 Hz, 1F, *ortho*-F), -185.46 (td, *J* = 21.6, 7.9 Hz, 1F, *ortho*-F), -186.50 (tt, *J* = 22.9, 7.9 Hz, 2F, *ortho*-F).

HRMS (ESI) *m/z*: calculated for $C_{55}H_{12}F_{25}N_5$ $[M+2H]^{2+}$ = 608.5341, found 608.5334

ESI-MS: *m/z* = 1215.1 $[M+H]^+$

Melting Point: > 350 ºC

meso-hexakis(pentafluorophenyl)[26] hexaphyrin ***1.137***

^{1}H-NMR (300 MHz, $CDCl_3$) δ 9.44 (d, J = 5.0 Hz, 4H, H_g and H_h or H_K and H_l), 9.11 (d, J = 5.0 Hz, 4H, H_g and H_h or H_K and H_l), -2.00 (s, 2H, H_o), -2.43 (s, 4H, H_b and H_c).

^{19}F-NMR (282 MHz, $CDCl_3$) δ -159.85 (dd, *J* = 22.9, 8.7 Hz, 4F, *meta*-F), -160.42 (dd, *J* = 22.2, 5.9 Hz, 8F, *meta*-F), -173.29 (t, *J* = 21.2 Hz, 2F, *para*-F), -176.16 (*t*, J = 20.3 Hz, 4F, *para*-F), -183.68 – -183.98 (m, 4F, *ortho*-F), -186.19 – -186.74 (m, 8F, *ortho*-F).

HRMS (ESI) *m/z*: calculated for $C_{66}H_{16}F_{30}N_6$ $[M+2H]^{2+}$ = 731.0473, found 731.0461

ESI-MS: *m/z* = 1461.0 $[M+H]^+$

Melting Point: > 350 ºC

*Preparation of meso-hexakispentafluorophenyl N-Fused [24]Pentaphyrin (**1.100**) and meso-hexakispentafluorophenyl[28]hexaphyrin (**1.138**).*

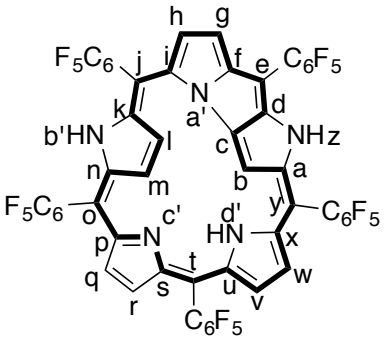

1.100

Chemical Formula: $C_{55}H_{12}F_{25}N_5$
Exact Mass: 1217.07

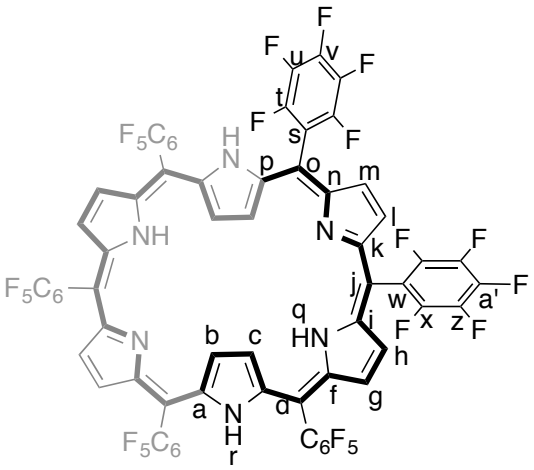

1.138

Chemical Formula: $C_{66}H_{16}F_{30}N_6$
Exact Mass: 1462.10

$NaBH_4$ (15 equiv.) was added to a solution of **1.101** (50 mg, 0.04 mmol) or **1.137** (50 mg, 0.03 mmol) in THF (10 mL) and the solution was stirred for 20 min under nitrogen. After removing the solvent, the residues were dissolved in CH_2Cl_2, and chromatographed with neutral alumina. After evaporation, the residue was recrystallized from pure hexane to give **1.100** (47 mg, 95%) and **1.138** (48 mg, 94%).

meso-pentakis(pentafluorphenyl) N-Fused [24]Pentaphyrin **1.100**

^{1}H-NMR (300 MHz, $CDCl_3$): δ 13.68 (s, 1H, $H_{d'}$), 8.15 (dd, *J* = 2.4, 3.8 Hz, 1H, H_l or H_m), 8.11 (dd, *J* = 2.4, 3.8 Hz, 1H, H_l or H_m), 7.87 (d, J = 1.9 Hz, 1H, H_b), 6.72 (s, 1H, $H_{b'}$), 6.59 (s, 1H, H_z), 6.20 – 6.14 (m, 2H, H_v and H_w or H_q and H_r), 6.04 – 5.99 (m, 2H, H_v and H_w or H_q and H_r), 5.85 (dt, *J* = 4.8, 1.2 Hz, 1H, H_g or H_h), 5.58 (dd, *J* = 5.9, 1.3 Hz, 1H, H_g or H_h).

^{13}C-NMR (126 MHz, $CDCl_3$): δ 166.4, 165.1, 154.2, 151.7, 151.6, 151.0, 150.85, 150.4, 150.3, 147.7, 146.7 - 145.6 (m, C_6F_5), 144.7-143.8 (m, C_6F_5), 142.9- 142.5(m, C_6F_5), 142.3, 142.2- 142.0 (m, C_6F_5), 141.0-140.6 (m, C_6F_5), 140.5, 140.2- 139.9 (m, C_6F_5), 139.2-138.6 (m, C_6F_5), 137.1, 137.0, 136.9-136.5 (m, C_6F_5), 136.3, 136.5, 136.3, 133.7(C_v or C_w or C_q or C_r), 133.5 (C_v or C_w or C_q or C_r), 133.3 (C_v or C_w or C_q or C_r), 129.6, 129.5,

129.0, 128.6, 128.4, 127.4, 127.0 (C_g or C_h), 126.0 (C_g or C_h), 125.0 (C_v or C_w or C_q or C_r), 124.9, 112.9, 110.6 (H_l or H_m), 108.5 (H_l or H_m), 105.0 (C_b)

^{19}F-NMR (282 MHz, $CDCl_3$) δ -160.75 – -161.83 (m, 6F, *meta*-F), -162.32 – -163.23 (m, 2F, *meta*-F), -163.59 – -164.12 (m, 2F, *meta*-F), -174.30 – -174.65 (m, 1F, *para*-F), -175.19 (t, J = 21.2 Hz, 1F, *para*-F), -176.12 – -176.38 (m, 1F, *para*-F), -176.72 (t, *J* = 20.9 Hz 1F, *para*-F), -177.15 – -177.54 (m 1F, *para*-F), -182.91– -183.32 (m, 2F, *ortho*-F), -184.10 – -185.06 (m, Hz, 8F, *ortho*-F).

HRMS (ESI) *m/z*: calculated for $C_{55}H_{13}F_{25}N_5$ $[M+2H]^{2+}$ = 609.0380, found 609.0368

Melting Point: > 350 ºC

meso-hexakis(pentafluorphenyl) [28]hexaphyrin ***1.137***

^{1}H-NMR (300 MHz, $CDCl_3$) δ 7.69 (dd, *J* = 29.3, 4.8 Hz, 8H, H_g, H_h, H_K and H_l), 4.40 (s, 2H, H_q and H_r), 2.54 (s, 4H, H_c and H_b).

^{13}C NMR (75 MHz, $CDCl_3$) δ 150.0, 147.8-147.5 (m, C_6F_5), 147.0-146.6 (m, C_6F_5), 144.5-144.2 (m, C_6F_5), 143.7-143.2 (m, C_6F_5), 140.4-138.8 (m, C_6F_5), 136.1, 135.3, 130.2 (H_g or H_h or H_k or H_l), 129.2 (H_g or H_h or H_k or H_l), 119.4 (H_o and C_p), 100.1, 96.2.

^{19}F-NMR (282 MHz, $CDCl_3$) δ -160.91 (dd, *J* = 24.1, 8.4 Hz, 4F, *meta*-F), -161.19 (dd, *J* = 23.5, 8.3 Hz, 8F, *meta*-F), -174.39 (t, *J* = 21.3 Hz, 4F, *para*-F), -176.09 (t, *J* = 20.8 Hz, 2F, *para*-F), -183.54 – -183.93 (m, 8F, *ortho*-F), -184.46 – -184.80 (m, 4F, *ortho*-F).

^{1}H-NMR (300 MHz, DMSO-d_6) δ 13.11 (s, 2H, H_o and H_p), 8.95 (d, J = 67.8 Hz, 4H, H_b and H_c), 6.39 (s, 8H, H_g; H_h; H_k; H_l).

^{13}C-NMR (75 MHz, DMSO-d_6) δ 156.3, 149.5, 147.0-146.3 (m, C_6F_5), 143.6-143.1 (m, C_6F_5), 140.0, 139.3-138.5 (m, C_6F_5), 135.8-135.3 (m, C_6F_5), 131.1, 128.3 (H_g; H_h; H_k; H_l), 125.0 (H_g; H_h; H_k; H_l), 120.8 (H_o and C_p), 105.6, 96.6.

^{19}F-NMR (282 MHz, DMSO-d_6) δ -163.02 (d, *J* = 23.8 Hz, 8F, *meta*-F), -163.78 (dd, *J* = 26.3, 7.2 Hz, 4F, *meta*-F), -179.15 (td, *J* = 22.4, 9.1 Hz, 6F, *para*-F), -185.39 – -185.99 (m, 4F, *ortho*-F), -186.56 – -187.26 (m, 8F, *ortho*-F).

HRMS (ESI) *m/z*: calculated for $C_{66}H_{18}F_{30}N_6$ $[M+2H]^{2+}$ = 732.0551, found 732.0537

Melting Point: > 350 ºC

*Preparation of N-Fused [24]Pentaphyrin **4.11** and [28]hexaphyrin **4.23***

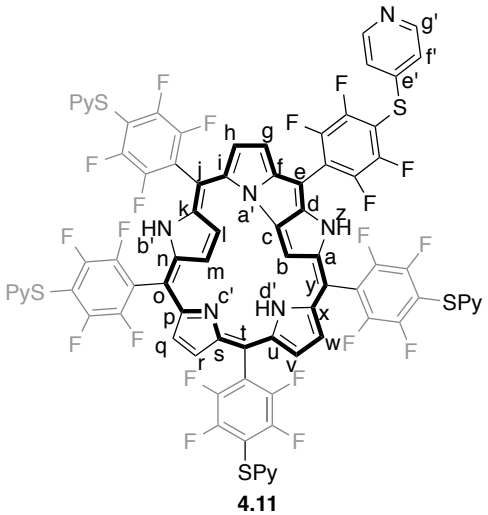

4.11

Chemical Formula: $C_{80}H_{32}F_{20}N_{10}S_5$
Exact Mass: 1672.11

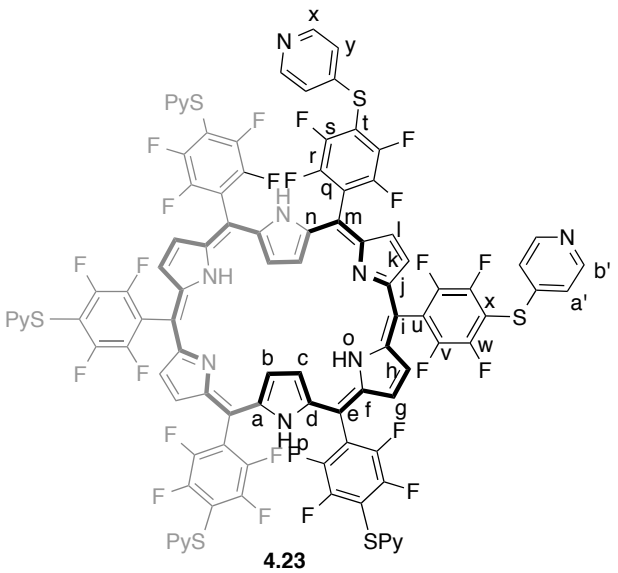

4.23

Chemical Formula: $C_{96}H_{40}F_{24}N_{12}S_6$
Exact Mass: 2008.14

4-Mercaptopyridine (7.5 or 9 equiv.) and diethylamine (6 mL) were added to a solution of **1.101** (300 mg) or **1.137** (300 mg), respectively, in dry DMF (15 mL). This mixture was kept under stirring for 6 h, under a nitrogen atmosphere, at rt. Addition of an aqueous solution of citric acid and extraction with CH_2Cl_2:MeOH (95:5) (3x100 mL) yields a residue which was subjected to flash chromatography using dichloromethane and 4% MeOH/CH_2Cl_2 as eluents. The fraction containing **4.11** or **4.23** was concentrated and crystallized from CH_2Cl_2/Ethanol.

*N-Fused [24]Pentaphyrin **4.11***

^{1}H-NMR (300 MHz, DMSO-d_6): δ 15.59 (s, 1H, $H_{d'}$), 10.02 (s, 1H, H_l or H_m), 9.39 (s, 1H, H_l or H_m), 9.15 (s, 1H, H_b), 9.07 (s, 1H, $H_{b'}$), 8.80 (s, 1H, H_z), 8.46 – 8.37 (m, 8H, $H_{g'}$), 8.32 – 8.23 (m, 2H, $H_{g'}$), 7.37 – 7.32 (m, 2H, $H_{f'}$), 7.24 (dd, J = 8.2, 4.6 Hz, 4H, $H_{f'}$), 7.21 – 7.17 (m, 2H, $H_{f'}$), 7.14 – 7.09 (m, 2H, $H_{f'}$), 6.53-6.49 (m, 1H, 1H, H_g or H_h), 6.17-6.14 (m, 1H, H_g or H_h), 6.21 (d, J = 4.3 Hz, 2H, H_v and H_w or H_q and H_r), 5.99 (d, J = 5.1 Hz, 2H, H_v and H_w or H_q and H_r).

^{13}C-NMR (126 MHz, DMSO-d_6): δ 165.4, 153.3, 152.4, 150.7, 150.0, 149.9, 149.9, 149.6, 149.1, 148.3-147.5 (m, C_6F_5), 146.5-145.7 (m, C_6F_5), 144.7, 144.7, 144.6, 144.3-143.4 (m,

C_6F_5), 142.4, 138.2, 135.3, 133.7, 132.4, 130.0-129.0 (m, C_6F_5), 120.7, 120.4, 120.3, 119.0, 115.3, 107.7, 107.2, 105.1.

^{19}F-NMR (282 MHz, DMSO-d_6): δ -155.73 – -156.03 (m, 2F, *meta*-F), -156.13 (dd, *J* = 27.2, 11.0 Hz, 1F, *meta*-F), -156.32 (dd, *J* = 27.3, 11.7 Hz, 1F, *meta*-F), -156.73 – -157.15 (m, *4F, meta*-F), -158.28 (dd, *J* = 24.3, 11.3 Hz, 1F, *meta*-F), -158.85– - 159.25 (m, 1F, *meta*-F), -159.80 (dd, *J* = 25.2, 10.6 Hz, 2F, *ortho*-F), -159.97 – -160.42 (m, 2F, *ortho*-F), -160.44 – -160.95 (m, 2F, *ortho*-F), -161.57 (dd, *J* = 27.4, 11.6 Hz, 1F, *ortho*-F), -162.19 (dd, *J* = 27.7, 11.0 Hz, 1F, *ortho*-F), -162.50 (dd, *J* = 27.0, 12.0 Hz, 1F, *ortho*-F), -162.71 (dd, *J* = 26.8, 11.6 Hz, 1F, *ortho*-F).

HRMS (ESI) *m/z*: calculated for $C_{80}H_{33}F_{20}N_{10}S_5$ $[M+H]^+$ = 1673.1174, found 1673.1188

Melting Point: > 350 ºC

[28]Hexaphyrin ***4.23***

^{1}H-NMR (300 MHz, DMSO-d_6) δ 12.19 (s, 4H,), 8.70 – 8.45 (m, 4H,), 8.43 – 8.38 (m, 4H,), 8.37 – 8.33 (m, 8H), 7.32 – 7.27 (m, 4H), 7.11 – 7.05 (m, 8H), 5.84 (d, J = 10.9 Hz, 8H,).

^{19}F-NMR (282 MHz, DMSO-d_6) δ -155.56 (dd, *J* = 27.3, 11.7 Hz, 4F, *meta*-F), -156.75 (dd, *J* = 25.9, 10.4 Hz, 8F, *meta*-F), -160.86 (dd, *J* = 23.3, 9.6 Hz, 8F, *otrho*-F), -162.13 (dd, *J* = 27.1, 11.6 Hz, 4F, *ortho*-F).

HRMS (ESI) *m/z*: calculated for $C_{96}H_{41}F24N_{12}S_6$ $[M+H]^+$ = 2009.1513, found 2009.1559

MALDI(TOF): *m/z* = 2009.7 $[M+H]^+$

Melting Point: > 350 ºC

*Preparation of N-fused [22]pentaphyrin (**4.12**) and [26]hexaphyrin (**4.24**)*

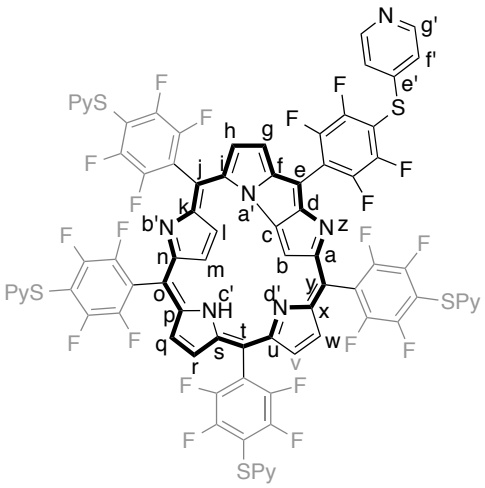

4.12

Chemical Formula: $C_{80}H_{30}F_{20}N_{10}S_5$
Exact Mass: 1670.09

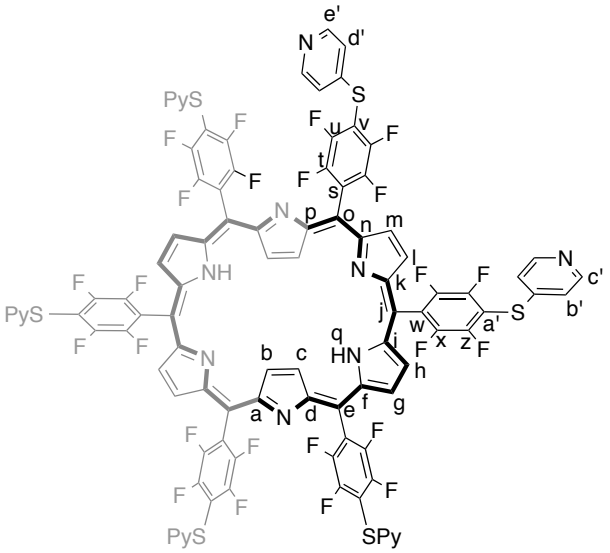

4.24

Chemical Formula: $C_{96}H_{38}F_{24}N_{12}S_6$
Exact Mass: 2006.13

Procedure 1:

DDQ (1.1 equiv) was added to a solution of **4.11** (50.0 mg, 0.04 mmol) or **4.23** (50.0, 0.03 mmol) in CH_2Cl_2:MeOH (95:5, 10 mL) and the solution was stirred for 30 min under nitrogen. After removing the solvent, the residues were redissolved again in CH_2Cl_2:MeOH (95:5), and chromatographed with neutral alumina. After evaporation, the residue was recrystallized from an ethanol:hexane mixture to yield **4.12** and **4.24**, quantitatively.

Procedure 2:

MnO_2 (75 equiv) was added to a solution of **4.11** (50.0 mg, 0.04 mmol) or **4.23** (50.0 mg, 0.03 mmol) in CH_2Cl_2:MeOH (95:5, 10 mL) and the solution was stirred for 6 h under nitrogen. After removing the solvent, the residues were redissolved again in CH_2Cl_2:MeOH (95:5), filtered and chromatographed with flash silica gel with CH_2Cl_2:MeOH (95:5) as eluent. After evaporation, the residue was recrystallized from an ethanol:hexane mixture to yield **4.12** and **4.24**, quantitatively.

N-fused [22]pentaphyrin ***4.12***

^{1}H-NMR (300 MHz, $CDCl_3$): δ 9.19 – 9.17 (m, 2H, H_h and H_g), 8.67 – 8.52 (m, 10H, Hg'), 8.42 – 8.34 (m, 4H, H_f, H_q, H_v and H_w), 7.28 – 7.20 (m, 10H, $H_{f'}$), 2.58 (d, *J* = 4.5 Hz, 1H, H_l or H_m), 2.08 (d, *J* = 4.5 Hz, 1H, H_l or H_m), 1.85 (s, 1H, $H_{c'}$), -1.76 (s, 1H, H_b).

^{13}C NMR (126 MHz, DMSO-*d*$_6$) δ 162.8, 157.1, 156.8, 156.7, 156.5, 156.5, 153.6, 150.6, 149.5, 148.9, 148.3, 147.8, 146.3-145.8 (m, C_6F_5), 144.7-144.6 (m, C_6F_5), 142.8-142.0 (m, C_6F_5), 137.2-136.8 (m, C_6F_5), 134.5, 133.5, 132.8, 132.0, 130.0, 129.1, 127.6, 127.2, 124.4, 123.2, 123.1, 123.0, 122.9, 122.1, 121.4, 120.6, 115.5, 113.1, 111.6, 109.2, 107.4, 106.2, 105.5, 103.9.

^{19}F-NMR (282 MHz, $CDCl_3$) δ -152.93 – -153.35 (m, 2F, *meta*-F), -153.79 – -153.91 (m, 2F, *meta*-F), --154.31 – -154.68 (m, 2F, *meta*-F), -155.14 (td, *J* = 25.2, 11.9 Hz, 2F, *meta*-F), -155.56 (dd, *J* = 24.9, 11.6 Hz, 1F, *meta*-F), -155.97 (dd, *J* = 25.1, 12.4 Hz, 1F, *meta*-F), -156.72 – -157.06 (m, 1H *ortho*-F), -157.55 – -158.01 (m, 1F, *ortho*-F), -158.28 (dd, *J* = 25.2, 12.9 Hz, 1F, *ortho*-F), -158.80 (dd, *J* = 24.5, 12.6 Hz, 1F, *ortho*-F), -159.35 (dd, *J* = 23.4, 11.6 Hz, 2F, *ortho*-F), -159.79 (dd, *J* = 25.4, 12.0 Hz, 1F, *ortho*-F), -160.03 (dd, *J* = 25.6, 12.0 Hz, 1F, *ortho*-F), -161.27 (dd, *J* = 24.3, 11.6 Hz, 1F, *ortho*-F), -161.91 (dd, *J* = 24.7, 12.0 Hz, 1F, *ortho*-F).

HRMS (ESI) *m/z*: calculated for $C_{80}H_{32}F_{20}N_{10}S_5$ $[M+2H]^{2+}$ =836.0511, found 836.0539

MALDI(TOF): *m/z* = 1671.7 $[M+H]^+$

Melting Point: > 350 ºC

[26]hexaphyrin ***4.24***

^{1}H NMR (300 MHz, DMSO-*d*$_6$) δ 10.20 (d, *J* = 4.9 Hz, 4H, *β* pyrrolic H), 9.91 (d, *J* = 4.9 Hz, 4H, *β* pyrrolic H), 8.68 (t, *J* = 7.2 Hz, 12H, $H_{e'}$ and $H_{c'}$), 7.86 – 7.77 (m, 4H, $H_{b'}$), 7.69 – 7.61 (m, 8H, $H_{d'}$), -2.61 (s, 2H, H_q), -2.86 (s, 4H, H_b and H_c).

^{13}C NMR (126 MHz, DMSO-*d*$_6$) δ 150.2, 149.4-148.9 (C_6F_5), 147.9, 147.1-146.9 (C_6F_5), 146.5.146.3 (C_6F_5), 146.0, 145.9, 144.9, 125.1, 123.0, 121.3, 120.9, 109.0.

^{19}F NMR (282 MHz, DMSO-*d*$_6$) δ -155.84 (dd, J = 26.8, 11.6 Hz, 4F), -157.30 (dd, J = 25.6, 10.4 Hz, 8F), -160.14 (dd, J = 24.6, 10.0 Hz, 8F), -160.71 – -161.09 (m, 4F).

HRMS (ESI) *m/z*: calculated for $C_{96}H_{40}F_{24}N_{12}S_6$ $[M+2H]^{2+}$ =1004.0714, found 1004.0717

MALDI(TOF): *m/z* = 2007.6 $[M+H]^+$

Melting Point: > 350 ºC

*Preparation of N-fused [24]pentaphyrin (**4.13**) and [28]hexaphyrin (**4.25**)*

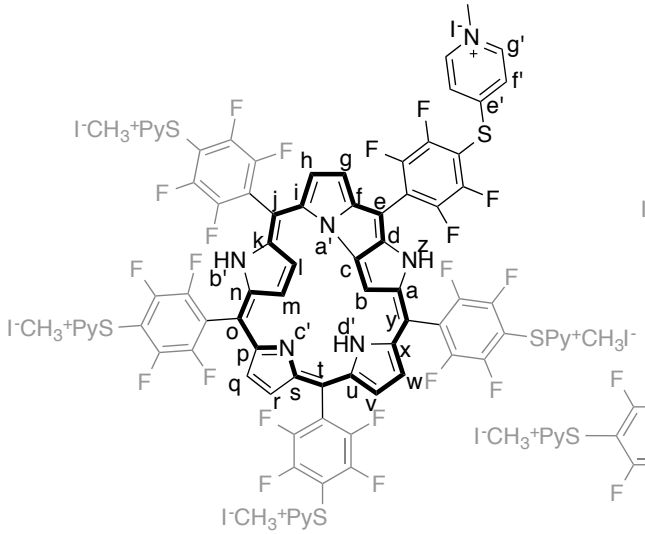

4.13

Chemical Formula: $C_{85}H_{47}F_{20}I_4N_{10}S_5^+$
Exact Mass: 2254.84

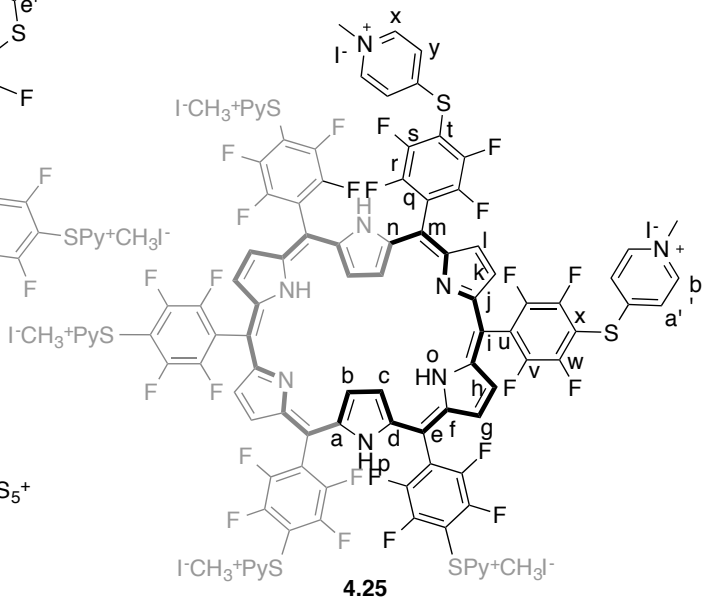

4.25

Chemical Formula: $C_{102}H_{58}F_{24}I_4N_{12}S_6^{2+}$
Exact Mass: 2605.90162

Iodomethane (30 equiv.) was added to a suspension of (75 mg of **4.11** or **4.12** or **4.22** and **4.23**) in DMF (2 mL). The reaction mixture was stirred for 6 h at 40 ºC. Afterwards, the mixture was cooled and the product precipitated with diethyl ether. The precipitate is filtered, washed with diethyl ether and afterwards retaken in acetone/methanol and re-precipitated twice, first from THF and then from acetone. The methylated compounds were filtered, washed with methanol and dried under vacuum to yield a reddish powder (**4.13**, when the reaction is done with **4.11** or **4.12**, 88%) and a bluish powder (**4.25**, when the reaction is done with **4.23** or **4.24**, 83%).

*N-fused [24]Pentaphyrin **4.13***

HRMS (ESI) *m/z*: calcd for $C_{85}H_{47}F_2O_{I3}N_{10}S_5$ $[M\text{-}2I]^{2+}$ = 1063.9696, found 1063.9724.

Melting Point: > 350 ºC

*[28]Hexaphyrin **4.25***

^{1}H NMR (300 MHz, DMSO-d_6) δ 8.77 (dd, J = 16.7, 6.7 Hz, 4H, $H_{c'}$), 8.22-8.17 (m, 8H, $H_{e'}$), 8.15 (m, 8H, $H_{b'}$, H_b and H_c), 7.98 (d, J = 6.6 Hz, 8H, $H_{d'}$), 6.93 (s, 8H, H_g, H_h, H_k, H_l), 4.24 (d, J = 7.8 Hz, 18H, CH_3).

^{13}C NMR (75 MHz, DMSO-d_6) δ 156.38, 155.93, 148.9, 148.5-148.2 (m, C_6F_5), 147.1-146.8 (m, C_6F_5), 145.6, 144.6 (Ce' and Cc'), 141.6, 139.5, 138.6, 131.7-131.3 (m, C_6F_5), 122.96 (Cb' and Cd'), 125.1, 122.9, 121.1, 120.9, 105.5, 46.9 (CH_3).

HRMS (ESI) *m/z*: calcd for $C_{102}H_{58}F_{24}I_2N_{12}S_6$ $[M-4I]^{4+}$ = 588.0229, found 588.0247.

Melting Point: > 350 ºC

*Preparation of bis zinc meso-hexakis(pentafluorophenyl) hexaphyrin type (**Zn1.137**).*

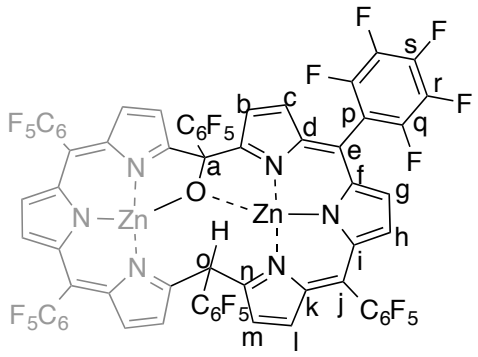

Zn1.137

Chemical Formula: $C_{66}H_{13}F_{30}N_6OZn_2$

Exact Mass: 1602.9255

Hexakis(pentafluorophenyl) [26]hexaphyrin (**1.137**) (50 mg, 0.03 mmol) was dissolved in CH_2Cl_2 (10 mL) in a 50 mL round-bottomed flask under nitrogen. Then, a solution of $Zn(OAc)_2.2H_2O$ (219 mg, 0.34 mmol, 10 equiv.) in methanol (3 mL) was added and the resulting solution was refluxed for 3 hours. Then the reaction mixture was thoroughly washed with a saturated sodium carbonate solution, water (3x50 mL) and finally the organics were dried over anhydrous Na_2SO_4. After removing the solvent, the residue was separated by column chromatography on silica gel with a 95:5 mixture of CH_2Cl_2 and methanol. The green fraction was collected and recrystallization from a mixture of CH_2Cl_2 and hexane gave **Zn1.137** (48 mg, 85%).

^{1}H NMR (300 MHz, $CDCl_3$) δ 10.92 (s, 1H, H_o), 6.50 (d, 2H, 4.9 Hz, *β* pyrrolic H), 6.39 (d, *J* = 4.6 Hz, 2H, *β* pyrrolic H), 6.24 (dd, *J* = 8.9, 4.7 Hz, 2H, *β* pyrrolic H), 6.15 – 6.08 (m, 2H, *β* pyrrolic H), 6.04 (q, *J* = 4.3 Hz, 4H, *β* pyrrolic H).

^{13}C NMR (75 MHz, $CDCl_3$) δ 168.8, 165.8, 151.3, 150.3, 148.1, 146.7, 143.6-142.1, 140.3-138.6, 137.2, 136.7, 129.6, 128.5, 126.8, 126.7, 125.7, 123.9, 112.1-110.4, 40.94 (C_o).

^{19}F NMR (282 MHz, $CDCl_3$) δ: -159.80 (t, *J* = 20.5 Hz, 4F, *meta*-F_r), -161.11 (d, *J* = 17.9 Hz, 2F, *meta*-F_r), -161.35 (d, *J* = 18.4 Hz, 4F, *meta*-F_r), -162.12 (d, *J* = 26.7 Hz, 2F, *meta*-F_r), -174.52 (t, *J* = 21.4 Hz, 2F, *para*-Fs), -174.88 (t, *J* = 21.0 Hz, 2F, *para*-F_s), -177.01 (t, *J* = 21.1 Hz, 1F, *para*-F_s), -177.46 (d, *J* = 21.2 Hz, 1F, *para*-F_s), -183.46 – -184.01 (m, 8F, *ortho*-F_q), -184.53 (t, *J* = 17.8 Hz, 2F, *ortho*-F_q), -184.91 (d, *J* = 14.2 Hz, 2F, *ortho*-F_q).

MALDI (TOF): *m/z* = 1602.8 $[M]^{+\bullet}$

Melting Point: > 350 ºC

*Preparation of doubly N-confused [26]hexaphyrin (**1.151**).*

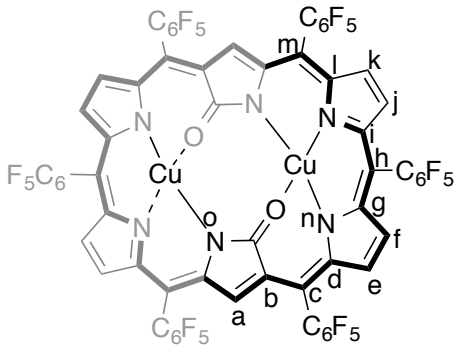

1.151

Chemical Formula: $C_{66}H_{10}Cu_2F_{30}N_6O_2$
Exact Mass: 1613.90

Compound **1.137** (400 mg, 0.27 mmol) and CuCl (2 g, 20 mmol, 75 equiv.) in pyridine (50 mL) were stirred under aerobic conditions for 3 h at room temperature. The reaction mixture was diluted with AcOEt, and the organic layer was washed sodium carbonate solution three times (3x50 mL), and dried over anhydrous Na_2SO_4. After removal of solvent, the crude product was purified by silica gel column chromatography with CH_2Cl_2/ hexane (3:7) as an eluent. The major blue fraction was collected. Recrystallization from a mixture of CH_2Cl_2/acetonitrile gave reddish solids.

HRMS (ESI+) *m/z*: calcd for $C_{66}H_{10}Cu_2F_{30}N_6O_2Cu_2$ $[M]^+$ = 1613.8941, found 1613.8972.

*Preparation of Doubly N-confused [26]hexaphyrin (**1.152**).*

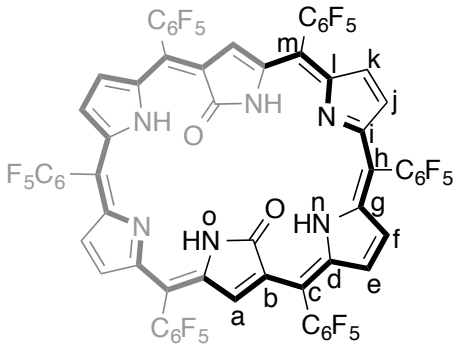

1.152
Chemical Formula: $C_{66}H_{14}F_{30}N_6O_2$
Exact Mass: 1492.0699

An excess amount of TFA (1 mL) was added to a solution of **1.151** (50 mg, 0.03 mmol) in CH_2Cl_2 (5 mL) and the resulting solution was stirred for 2 h. The reaction mixture was quenched with water. The organic layer was separated and dried over anhydrous Na_2SO_4. Recrystallization from a mixture of CH_2Cl_2/acetonitrile gave **1.152** almost quantitatively as a greenish solid (43 mg, 94%).

^{1}H-NMR (300 MHz, $CDCl_3$) δ 10.77 (s, 2H, H_a), 9.51 (d, *J* = 5.1 Hz, 2H, *β* pyrrolic protons), 9.45 (d, *J* = 5.2 Hz, 2H, *β* pyrrolic protons), 9.23 (d, *J* = 4.8 Hz, 2H, *β* pyrrolic protons), 9.19 (d, *J* = 4.8 Hz, 2H, *β* pyrrolic protons), -0.28 (s, 2H, H_o), -0.77 (s, 2H, H_n).
^{13}C-NMR (126 MHz, $CDCl_3$) *δ* 158.4, 156.9, 156.6 , 148.1-147.4 (m, C_6F_5), 146.2-145,8 (m, C_6F_5), 138.3, 137.5, 136.3, 136.2, 132.7, 130.1, 129.5, 126.8, 121.4 , 117.5-116.0, 109.6, 106.1, 105.1.
^{19}F-NMR (282 MHz, $CDCl_3$) δ -159.82 (d, *J* = 7.1 Hz, 2F, *ortho*-F_q), -159.90 (d, *J* = 7.1 Hz, 2F, *ortho*-F), -160.38 (d, *J* = 8.0 Hz, 4F, *ortho*-F), -160.45 (d, *J* = 7.7 Hz, 4F, *ortho*-F), -173.29 (dt, *J* = 39.9, 20.9 Hz, 2F, *para*-F), -176.76 (t, *J* = 20.8 Hz, 4F, *para*-F_x), -183.73– -183.92 (m, 4F, *meta*-F), -186.32 – -186.53 (m, 8F, *meta*-F)
HRMS (ESI+) *m/z*: calcd for $C_{66}H_{15}F_{30}N_6O_2$ $[M+H]^+$ = 1493.0772, found 1493.0755.
Melting Point: > 350 ºC

*Preparation of N-confused [26]hexaphyrin (**4.27**).*

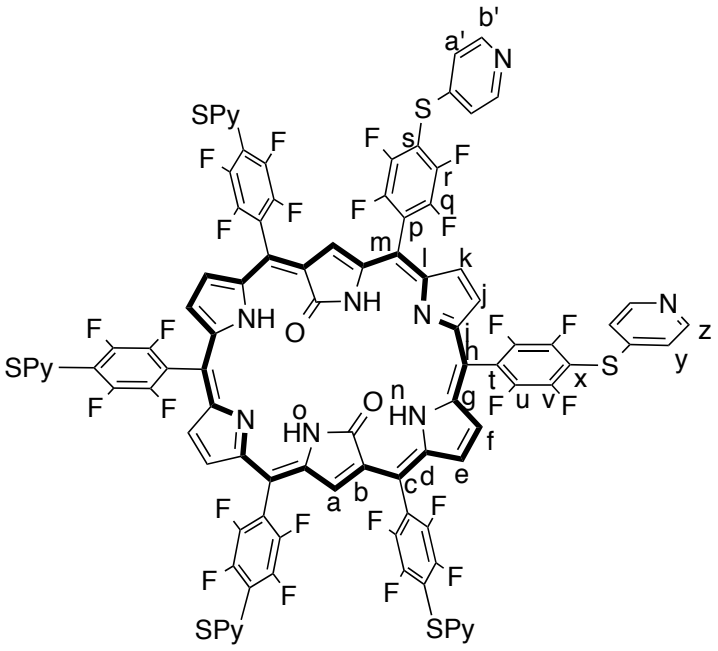

4.27
Chemical Formula: $C_{96}H_{38}F_{24}N_{12}O_2S_6$
Exact Mass: 2038.12

Compound **4.24** (350 mg, 0.174 mmol) and CuCl (1.3 g, 13.4 mmol, 75 equiv.) in pyridine (40 mL) were stirred under aerobic conditions for 3 h at room temperature. The reaction mixture was diluted with CH_2Cl_2:MeOH (95:5), and the organic layer was washed a sodium carbonate solution three times (3x50 mL), and dried over anhydrous Na_2SO_4. After removal of solvent, the crude product was purified by silica gel column chromatography with CH_2Cl_2:MeOH (95:5), as an eluent. The major blue fraction was collected. Recrystallization from a mixture of CH_2Cl_2:MeOH gave reddish solids (71 mg, 19%). After this, an excess amount of TFA (1.5 mL) was added to a solution of the previous solid (71 mg, 0.03 mmol) in 7.5 mL CH_2Cl_2:MeOH (95:5) and the resulting solution was stirred for 2 h. The reaction mixture was quenched with water, and the mixture was carefully neutralized with a sodium carbonate solution. The organic layer was then separated and dried over anhydrous Na_2SO_4. Recrystallization from a mixture of CH_2Cl_2:MeOH gave **4.26** almost quantitatively as a greenish solid (63 mg, 93%).

^{1}H NMR (300 MHz, Acetone-d_6) δ 11.73 (s, 2H, H_a), 10.18 (d, J = 5.1 Hz, 2H, β pyrrolic protons), 10.07 (d, J = 4.9 Hz, 2H, β pyrrolic protons), 8.76 – 8.45 (m, 12H, *meta*-Pyridil

H_z and $H_{b'}$), 7.77 (d, *J* = 20.7 Hz, 12H, *ortho*-Pyridil H_y and $H_{a'}$), -0.33 (s, 1H, H_o), -0.64 (s, 1H, H_n).

^{19}F NMR (282 MHz, Acetone-d_6) δ -156.00 – -156.19 (m, 4F, *ortho*-F), -157.18 (ddd, *J* = 38.7, 25.1, 11.9 Hz, 8F, *ortho*-F), -161.08 (dd, *J* = 24.4, 12.0 Hz, 4F, *meta*-F), -161.29 – -161.58 (m, 4F, *meta*-F), -161.69 (dd, J = 24.2, 12.0 Hz, 4F, *ortho*-F).

HRMS (ESI) *m/z*: calcd. for $C_{96}H_{40}F_{24}N_{12}O_2S_6$ $[M+2H]^{2+}$ = 1020.0664, found 1020.0666.

Melting Point: > 350 ºC

*General preparation of [28]hexaphyrins (**4.28-4.30**).*

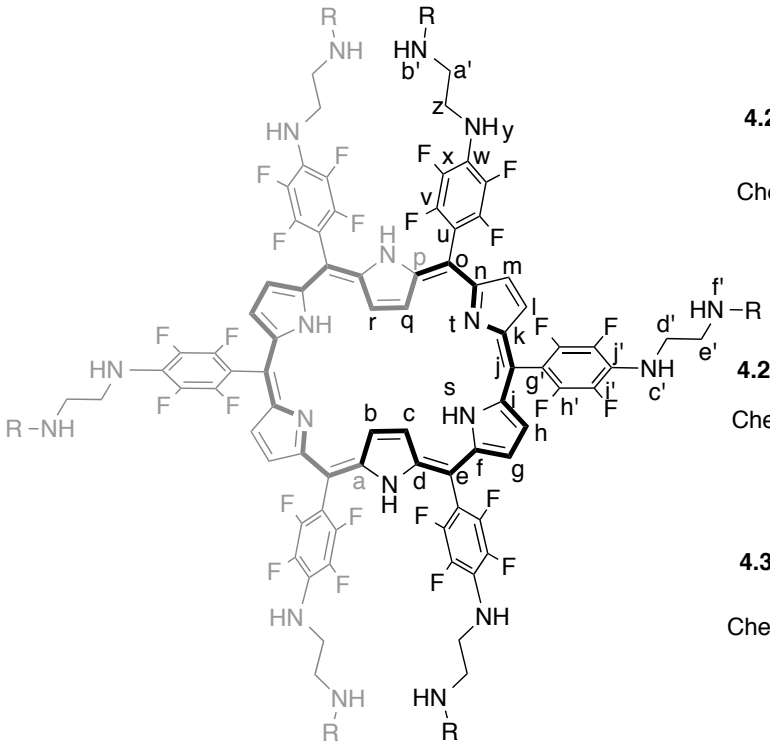

4.28 R =

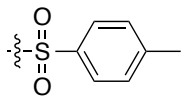

Chemical Formula: $C_{120}H_{94}F_{24}N_{18}O_{12}S_6$
Exact Mass: 2626.5240

4.29 R =

Chemical Formula: $C_{96}H_{94}F_{24}N_{18}$
Exact Mass: 1954.7526

4.30 R =

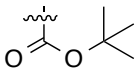

Chemical Formula: $C_{108}H_{106}F_{24}N_{18}O_{12}$
Exact Mass: 2302.7854

To a solution of **1.137** (100.0 mg, 0.068 mmol) in NMP (5 mL), *N*-tosylethylenediamine, *N*-isopropilethylenediamine or *N*-Boc-ethylenediamine (30 equiv.) and triethylamine (2 mL) were added and heated at 105 ºC. After 24 h, the reaction was cooled, quenched with a mixture of CH_2Cl_2:MeOH (95:5) and washed with a saturated solution of citric acid (50 mL) and 3x100 mL of H_2O. The organic extracts were dried over Na_2SO_4 and concentrated. The residue was chromatographed on silica gel using as eluents CH_2Cl_2:MeOH (96:4) for **4.28 and 4.30** or CH_2Cl_2/MeOH/NEt_3 (7:2.8:0.2) for **4.29** and the corresponding blue color band was collected to yield **4.28** (120 mg, 69%), **4.29** (85 mg, 64%), **4.30** (98 mg, 78%) as blue solids after recrystallization from CH_2Cl_2/MeOH.

[28]hexaphyrin ***4.28***

^{1}H-NMR (300 MHz, DMSO-d_6) δ 7.88 – 7.62 (m, 24H, *meta*-H tosyl and *β* pyrrolic protons), 7.47 – 7.38 (m, 4H, *ortho*-H tosyl), 7.38 – 7.29 (m, 8H, *ortho*-H tosyl), 6.23 (s, 2H, $H_{c'}$), 6.11 (s, 4H, H_y), 6.17 (d, J = 37.6 Hz, 4H, H_y and $H_{c'}$), 3.52 (d, J = 7.3 Hz, 4H, H_z and $H_{d'}$), 3.09 (d, J = 6.2 Hz, 4H, $H_{e'}$), 3.01 – 2.84 (overlap with water signal, 8H, $H_{a'}$), 2.32 (d, J = 23.6 Hz, 18H, CH_3).

^{13}C-NMR (75 MHz, DMSO-d_6) δ 149.70 (s), 148.49 – 146.71 (m), 145.50 – 143.28 (m), 142.73, 138.06 (ddd, J = 48.7, 27.3, 10.6 Hz), 134.96 (dd, J = 30.3, 17.9 Hz), 132.22 – 129.18 (m), 129.68, 128.35 (d, J = 12.7 Hz), 126.55, 117.18, 104.61, 96.23, 45.68 – 44.91 (m), 44.91 – 43.27 (m), 44.47 – 41.04 (m), 20.99 (d, J = 7.9 Hz).

^{19}F-NMR (282 MHz, DMSO-d_6) δ -166.13 (d, J = 20.6 Hz, 4F, *ortho*-F), -166.96 (m, 8F *ortho*-F), -183.44 (d, J = 20.5 Hz, 4F, *meta*-F), -184.41 (d, J = 20.3 Hz, 8F, *meta*-F).

HRMS (ESI+) found: 2627.5335 $[M+H]^+$; calculated for $C_{120}H_{95}F_{24}N_{18}O_{12}S_6$ (2627.5312).

Melting Point: > 350 ºC

[28]hexaphyrin ***4.29***

^{1}H-NMR (300 MHz, DMSO-d_6) δ 7.70 (d, J = 8.6 Hz, 8H, *β* pyrrolic), 6.05 (s, 8H, H_y), 6.00 (s, 4H, 2.82 $H_{c'}$), (d, J = 42.4 Hz, 12H, $H_{a'}$ and $H_{e'}$), 1.02 (dd, J = 25.7, 6.2 Hz, 36H CH_3).

^{13}C-NMR (75 MHz, DMSO-d_6): δ 178.34, 148.24 – 145.38 (m), 145.83 – 142.56 (m), 138.98 – 136.23 (m), 135.09 (dd, J = 32.5, 13.6 Hz), 130.24 – 127.08 (m), 117.35, 103.78 (dd, J = 69.8, 61.2 Hz), 63.05 – 61.75 (m), 52.01, 48.03, 46.64, 44.71, 22.56.

^{19}F-NMR (282 MHz, DMSO-d_6) δ -166.14 (s, 4F, *ortho*-F), -166.80 (s, 8F, *ortho*-F) -183.50 (d, J = 18.4 Hz, 4F, *meta*-F), -184.45 (s, 8F, 8F, *meta*-F).

HRMS (ESI)+ found: 1955.7584 $[M+H]^+$; calculated for $C_{96}H_{95}F_{24}N_{18}$ (1955.7598).

Melting Point: > 350 ºC

[28]hexaphyrin ***4.30***

^{1}H-NMR (500 MHz, DMSO-d_6) δ 7.78 (d, J = 16.4 Hz, 8H, *β* pyrrolic), 7.02 (s, 2H, $H_{f'}$), 6.01 (s, 4H, $H_{b'}$), 6.21 (s, 2H, $H_{c'}$), 6.11 (s, 4H, H_y), 3.15 (s, 12H, Hz), 1.41 (s, 18H), 1.34 (s, 56H, CH_3).

^{13}C-NMR (126 MHz, DMSO-d_6) δ 155.9, 155.8, 146.7, 144.8, 144.2, 137.7, 137.4, 135.92, 135.6, 130.2, 128.9, 128.24, 117.1, 104.2, 44.7, 44.6, 28.2, 28.1, 28.0, 27.9.

^{19}F-NMR (282 MHz, DMSO-d_6) δ -166.12 – -166.66 (m, 4F, *ortho*-F), -167.13 (s, 8F, *ortho*-F), -183.42 (d, J = 21.4 Hz, 4F, *meta*-F), -184.43 (d, J = 22.2 Hz, 4F, *meta*-F).

HRMS (ESI+) *m/z*: calculated for $C_{108}H_{108}F_{24}N_{18}O_{12}$ $[M+H]^+$ = 1152.4000, found 1152.4003.

Melting Point: > 350 ºC

Preparation of doubly N-fused [28]hexaphyrins ***1.147***

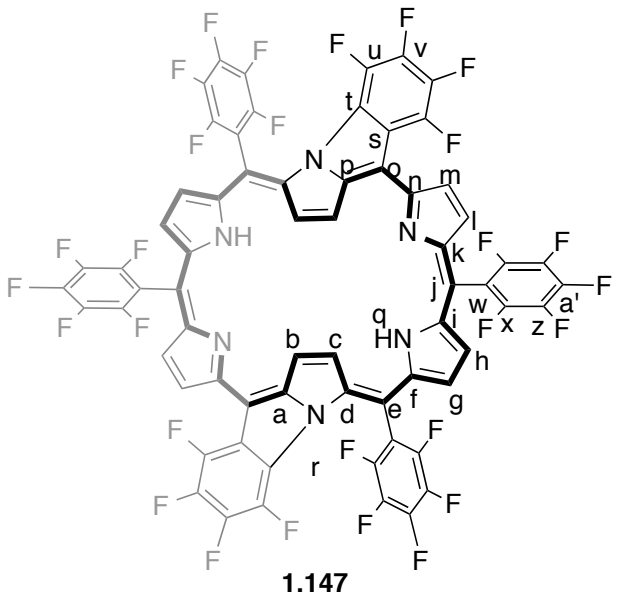

1.147

Chemical Formula: $C_{66}H_{14}F_{28}N_6$
Exact Mass: 1422.08

A solution containing **1.137** (100.0 mg, 0.068 mmol), NMP (5 mL) and triethylamine (3 mL) was heated at 110 ºC. After 24 h, the reaction was cooled, quenched with a mixture of AcOEt and washed with a saturated solution of citric acid (50 mL) and 3x100 mL of H_2O. The organic extracts were dried over Na_2SO_4 and concentrated. The residue was chromatographed on silica gel using as eluents CH_2Cl_2:hexane (1:3) the corresponding red color band was collected to yield (42 mg, 52%), as a brown solid after recrystallization from CH_2Cl_2/MeOH.

^{1}H-NMR (500 MHz, DMSO-d_6) δ 6.25 (d, 4 Hz, 2H, *β* pyrrolic protons), 5.46 (d, 4 Hz, 2H, *β* pyrrolic protons), 5.04 (d, 2H, 4 Hz, *β* pyrrolic protons), 4.95 (d, 2H, 4 Hz, *β* pyrrolic protons), 4.54 (d, 2H, 1.5 Hz, *β* pyrrolic protons)

^{13}C-NMR (75 MHz, DMSO-d_6) δ 155.01, 150.6, 143.6-142.9, 141.7, 140.4, 138.3, 137.0-136.2, 135.9, 135.0, 132.8, 129.3, 128.4, 127.5, 126.8, 124-123.2, 117.5, 117.0, 116.1, 113.0, 104.1.

MALDI(TOF): m/z = 1422.0 $[M]^{+\bullet}$

*Preparation of [26]hexaphyrins **4.31 and 4.32***

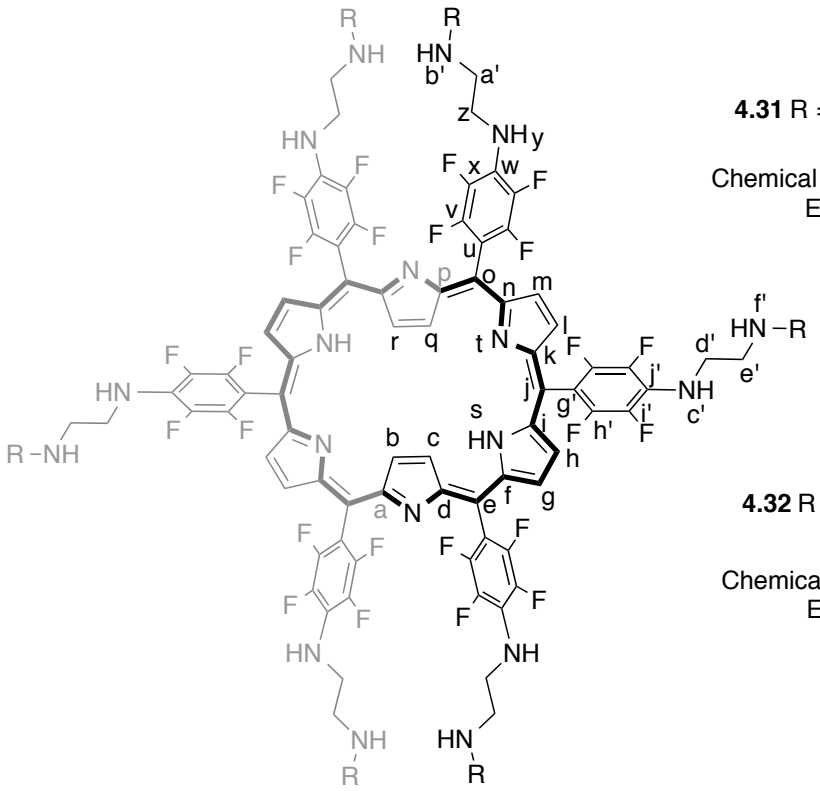

4.31 R =

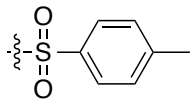

Chemical Formula: $C_{120}H_{92}F_{24}N_{18}O_{12}S_6$
Exact Mass: 2624.5083

4.32 R =

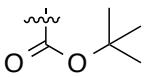

Chemical Formula: $C_{108}H_{106}F_{24}N_{18}O_{12}$
Exact Mass: 2302.7854

MnO_2 (75 equiv.) was added to a solution of **4.28** or **4.30** (50 mg) in CH_2Cl_2:MeOH (95:5, 10 mL) and the solution was stirred for 6 h under nitrogen. After removing the solvent, the residues were redissolved in again CH_2Cl_2:MeOH (95:5), filtered and chromatographed with flash silica gel with CH_2Cl_2:MeOH (95:5) as eluent. After evaporation, the residue was recrystallized from an ethanol:hexane mixture to yield **4.31** and **4.32**, almost quantitatively.

*[26]hexaphyrin **4.31***

^{1}H-NMR (700 MHz, DMSO-d_6) δ 9.64 (d, J = 4.5 Hz, 4H, *β* pyrrolic protons), 9.43 (d, J = 4.5 Hz, 4H, *β* pyrrolic protons), 7.98 – 7.88 (m, 7H, $H_{b'}$ and $H_{f'}$), 7.86 (d, J = 7.9 Hz, 4H, *meta*-H Tosyl), 7.82 (d, J = 7.9 Hz, 8H, *meta*-H Tosyl), 7.51 (d, J = 7.9 Hz, 4H, *ortho*-H

Tosyl), 7.41 (d, *J* = 7.9 Hz, 8H, *ortho*-H Tosyl), 6.61 (s, 2H, H_y or $H_{c'}$), 6.34 (d, *J* = 7.2 Hz, 4H, H_y or $H_{c'}$), 3.70 (q, *J* = 6.7 Hz, 12H, H_z and $H_{d'}$), 3.25 (dd, *J* = 12.0, 6.0 Hz, 12H, $H_{a'}$ and $H_{e'}$), 2.41 (s, 6H, CH_3), 2.15 (s, 12H, CH_3), -2.54 (s, 4H, H_c and H_b).
HRMS (ESI+) found: 2625.5216 $[M+H]^+$; calculated for $C_{120}H_{93}F_{24}N_{18}O_{12}S_6$ (2625.5155).
Melting Point: > 350 ºC

[26]hexaphyrin ***4.32***
^{1}H-NMR (700 MHz, DMSO-d_6) δ 9.67 (d, *J* = 4.4 Hz, *β* pyrrolic protons), 9.45 (d, *J* = 4.6 Hz, 4H, *β* pyrrolic protons), 7.17 (dt, *J* = 9.2, 6.0 Hz, 7H,$H_{b'}$ and $H_{f'}$), 6.52 (d, *J* = 115.7 Hz, 7H, H_y and $H_{c'}$), 3.74 (s, 12H, H_z and $H_{d'}$), 3.48 (d, *J* = 6.1 Hz, 12H, $H_{a'}$ and $H_{e'}$), 1.48 (d, *J* = 5.9 Hz, 56H, CH_3), -2.58 (s, 4H, H_c and H_b).
^{13}C-NMR (75 MHz, CDCl3) δ 170.2, 158.1, 148.71, 142.8, 138.98-136.23 (m), 131.5, 130.2, 127.7, 127.7, 120.61, 120.40, 113.66, 112.0, 106.5, 77.2, 55.6, 44.1.
HRMS (ESI+) found: 1151.39561 $[M+2H]^{2+}$; calculated for $C_{108}H_{107}F_{24}N_{18}O_{12}$ 1151.39408.
Melting Point: > 350 ºC

4.5. References

1. Burrell AK, Hemmi G, Lynch V and Sessler JL. *J. Am. Chem. Soc.* 1991; **113**: 4690-4692.

2. Bruckner C, Sternberg ED, Boyle RW and Dolphin D. *Chem. Commun.* 1997: 1689-1690.

3. Srinivasan A, Ishizuka T, Maeda H and Furuta H. *Angew. Chem. Int. Ed.* 2004; **43**: 2951-2955.

4. Shin JY, Furuta H and Osuka A. *Angew. Chem. Int. Ed.* 2001; **40**: 619-621.

5. Yoneda T, Mori H, Lee BS, Yoon MC, Kim D and Osuka A. *Chem. Commun.* 2012; **48**: 6785-6787.

6. Alonso M, Geerlings P and De Proft F. *J. Org. Chem.* 2013; **78**: 4419-4431.

7. Srinivasan A, Ishizuka T, Maeda H and Furuta H. *Angew Chem Int Ed.* 2004; **43**: 2951-2955.

8. Cha WY, Yoneda T, Lee S, Lim JM, Osuka A and Kim D. *Chem. Commun.* 2014; **50**: 548-550.

9. Sessler JL and Seidel D. *Angew. Chem. Int. Ed.* 2003; **42**: 5134-5175.

10. Alonso M, Geerlings P and De Proft F. *Phys. Chem. Chem. Phys.* 2014.

11. Shimizu S and Osuka A. *Eur. J. Inorg. Chem.* 2006: 1319-1335.

12. Mori S, Shin JY, Shimizu S, Ishikawa F, Furuta H and Osuka A. *Chem. Eur. J.* 2005; **11**: 2417-2425.

13. Park JK, Yoon ZS, Yoon MC, Kim KS, Mori S, Shin JY, Osuka A and Kim D. *J. Am. Chem. Soc.* 2008; **130**: 1824.

14. Higashino T and Osuka A. *Chem. Sci.* 2012; **3**: 103-107.

15. Suzuki M, Hoshino T and Neya S. *Org. Lett.* 2014; **16**: 327-329.

16. Suzuki M, Hoshino T and Neya S. *Org. Lett.* 2014; **16**: 327-329.

17. Comuzzi C, Cogoi S, Overhand M, Van der Marel GA, Overkleeft HS and Xodo LE. *J. Med. Chem.* 2006; **49**: 196-204.

18. Rossi G, Goi D and Comuzzi C. *J. Water Health* 2012; **10**: 390-399.

19. Rossi G, Fedele R, Comuzzi C and Goi D. *J Biotechnol* 2010; **150**: S438-S438.

20. Rapozzi V, Lombardo C, Cogoi S, Comuzzi C and Xodo L. *Chem. Med. Chem.* 2008; **3**: 565-568.

21. Comuzzi C, Cogoi S, Overhand M, Van der Marel GA, Overkleeft HS and Xodo LE. *J. Med. Chem.* 2006; **49**: 196-204.

22. Ballico M, Rapozzi V, Xodo LE and Comuzzi C. *Eur. J. Med. Chem.* 2011; **46**: 712-720.

23. Suzuki M, Shimizu S, Shin JY and Osuka A. *Tetrahedron Lett.* 2003; **44**: 4597-4601.

24. Gale PA, Garcia-Garrido SE and Garric J. *Chem. Soc. Rev.* 2008; **37**: 151-190.

25. Wenzel M, Hiscock JR and Gale PA. *Chem. Soc. Rev.* 2012; **41**: 480-520.

26. Gale PA. *Coord. Chem. Rev.* 2003; **240**: 191-221.

27. Caltagirone C and Gale PA. *Chem. Soc. Rev.* 2009; **38**: 520-563.

28. Gale PA. *Acc. Chem. Res.* 2006; **39**: 465-475.

29. Neves MGPMS, Martins RM, Tome AC, Silvestre AJD, Silva AMS, Felix V, Drew MGB and Cavaleiro JAS. *Chem. Commun.* 1999: 385-386.

30. Suzuki M and Osuka A. *Org. Lett.* 2003; **5**: 3943-3946.

31. Shin JY, Furuta H, Yoza K, Igarashi S and Osuka A. *J Am Chem Soc* 2001; **123**: 7190-7191.

32. Taniguchi R, Shimizu S, Suzuki M, Shin JY, Furuta H and Osuka A. *Tetrahedron Lett.* 2003; **44**: 2505-2507.

33. Koide T, Youfu K, Saito S and Osuka A. *Chem. Commun.* 2009: 6047-6049.

34. Ishida S, Higashino T, Mori S, Mori H, Aratani N, Tanaka T, Lim JM, Kim D and Osuka A. *Angew. Chem. Int. Ed.* 2014; **53**: 3427-3431.

35. Tanaka Y, Saito S, Mori S, Aratani N, Shinokubo H, Shibata N, Higuchi Y, Yoon ZS, Kim KS, Noh SB, Park JK, Kim D and Osuka A. *Angew. Chem. Int. Ed.* 2008; **47**: 681-684.

36. Yoon ZS, Osuka A and Kim D. *Nat. Chem.* 2009; **1**: 113-122.

37. Osuka A and Saito S. *Chem. Commun.* 2011; **47**: 4330-4339.

38. Ahn TK, Kwon JH, Kim DY, Cho DW, Jeong DH, Kim SK, Suzuki M, Shimizu S, Osuka A and Kim D. *J. Am. Chem. Soc.* 2005; **127**: 12856-12861.

39. Shimizu S, Anand VG, Taniguchi R, Furukawa K, Kato T, Yokoyama T and Osuka A. *J. Am. Chem. Soc.* 2004; **126**: 12280-12281.

40. Mori S and Osuka A. *J. Am. Chem. Soc.* 2005; **127**: 8030-8031.

41. Rath H, Aratani N, Lim JM, Lee JS, Kim D, Shinokubo H and Osuka A. *Chem. Commun.* 2009: 3762-3764.

42. Zhu XJ, Fu ST, Wong WK and Wong WY. *Tetrahedron Lett.* 2008; **49**: 1843-1846.

43. Cha WY, Lim JM, Yoon MC, Sung YM, Lee BS, Katsumata S, Suzuki M, Mori H, Ikawa Y, Furuta H, Osuka A and Kim D. *Chem. Eur. J.* 2012; **18**: 15838-15844.

44. Misra R and Chandrashekar TK. *Acc. Chem. Res.* 2008; **41**: 265-279.

45. Rambo BM and Sessler JL. *Chem. Eur. J.* 2011; **17**: 4946-4959.

46. Mori S, Shimizu S, Shin JY and Osuka A. *Inorg. Chem.* 2007; **46**: 4374-4376.

47. Pospisilova S, Brazda V, Kucharikova K, Luciani MG, Hupp TR, Skladal P, Palecek E and Vojtesek B. *Biochem. J.* 2004; **378**: 939-947.

48. Rodrigues JMM, Farinha ASF, Muteto PV, Woranovicz-Barreira SM, Paz FAA, Neves MGPMS, Cavaleiro JAS, Tome AC, Gomes MTSR, Sessler JL and Tome JPC. *Chem. Commun.* 2014; **50**: 1359-1361.

49. Ellis JS, Xu SQ, Wang X, Herzog G, Arrigan DWM and Thompson M. *Bioelectrochemistry* 2010; **79**: 6-10.

5. Final remarks and conclusions.

5. Final remarks and conclusions.

The major aim of this project was to synthesize new expanded porphyrins based either on the functionalization of small oligipyrrolic units (BP, DPM), or by functionalization of *meso*-pentafluorophenyl expanded macrocycles which were first synthesized by our laboratory. Furthermore, we were also interested in determining their applicability in anion binding or PDI. The synthesis of bipyrrolic units **2.16** and **2.17** with different Knoevenagel nucleophile indane-1,3-dione and malononitrile proved a lack of generality in the procedure and a discrepancy in the yields. The solubility problems on the bipyrrolic synthons and the differences in the nucleophiles reactivity may be the cause for this inconsistency.

For the remaining DPM **2.18**-**2.20**, this methodology showed to destabilize dipyrromethane **2.13**, when more reactive nucleophiles are used (*e.g.* malononitrile) yielding complex mixtures, which failed to exhibit any features of a typical functionalized DPM. However compound **2.18** was isolated in a relatively low yield.

Interestingly, DPM **2.14** undergoes Knoevenagel reaction in very good yields and the products proved to be very stable in the solid state (**2.19** and **2.20**). The effortless manner on how these reactions run with this DPM, indeed shows that this synthon can be a subject of more studies on its reactivity in the α-positions. These new sensors (**2.16**, **2.17**, **2.19** and **2.10**)showed high affinity constants for fluoride, acetate and dihydrogen phosphate anions. It is also important to note that sensor **2.17** exhibited an affinity constant ratio $KAcO^-/H_2PO_4^-$ of 36.7. Furthermore, these showed to be highly chromogenic having color variation upon addition of anions.

Moreover, other functionalization attempts, specifically via D-A reactions, revealed to be unsuccessful and the diformyl-bipyrrolic intermediate employed **2.11** was generally inert to the exposed conditions. Also, all attempts to make this unit more reactive showed to be ineffective as well, from which several other problems arise, such as the instability of the key intermediates for D-A reaction with **3.18** and the difficulties in the isolation of protected intermediates. In fact, most of the results from the reaction attempts making a diene to react with a dienophyle resulted in efficient Michael Addition reactions, regarding the easy accessibility to compounds **3.19** and **3.20**. Another route towards D-A adducts, was in this instance via reaction of DMAD with macrocycle **3.31**, instead of the first approach demonstrated in section 3.1. However, DMAD moiety reacted inside the

macrocycle core furnishing **3.37**. These findings are supported by the higher field signals presented in the ^{1}H-NMR spectra attributed to the substitution pattern involved in this reaction, showing that the signals attributed to the DMAD moiety is surrounded by a strong diamagnetic ring (**3.37**). While it was not possible to determine which isomer we obtained from this reaction, attempts in the synthesis of isomer **3.37c** by rational synthesis were performed without the expected success (**3.38**). In fact the chemistry presented in chapter 3 show the complications of working with building blocks and the unpredictability of expanded porphyrins when attempts are made to synthesize them or when they are subject to reactions revealing a vast amount of possibilities, which are not taken into account when synthesizing their tetrapyrrolic counterparts. The substitution on compound **3.37** was corroborated with anion binding tests confirming an extra obstruction in its inner core, when compared with **3.31**, which is in total concordance with the expected results.

When derivative **2.12** was subject to cyclization reactions with **3.32**, the result from this reaction revealed to be a scrambling product from the reaction of tripyrromethane **3.32** with the product of its own decomposition mediated by acidic media. These compounds are in fact a specific class of expanded porphyrins where their characteristics proved rather complicated to work with. Their stability and reactivity is diminished when compared to tetrapyrrolic analogues and consequently isolation of the products also prooved to be rather tedious and complex. This is unquestionable consistent with the number of publications around this family of macrocycles which compared to other analogues is fairly low.

Synthetically, incorporating these structural modifications into *N*-fused pentaphyrins and hexaphyrins periphery proved to be a substantial challenge. The major problem arises with their oxidation/reduction behavior in basic media and their stability, which compared with other porphyrinoid compounds namely, porphyrins and phthalocyanines is diminished.

Regarding the functionalization of expanded porphyrins complete substitution of the *para* fluorines of compounds **1.101** and **1.137** were successfully achieved along with the corresponding reduction of the starting material in the same reaction. The use of MnO_2 showed to be efficient in their oxidation and it allowed complete oxidation of all reduced version of hexaphyrins, with exception for **4.25**. In fact, MnO_2 diminished the amount of possible collateral reactions. The unpredictable behavior of these compounds towards the reactional media led us to attempt variations of these macrocycles either by metallation

(**Zn.1.137**) or by inducing *N*-confusion on compounds **1.137** or **4.24**. None of these resulted the expected outcome. Metallation reactions on **1.137** proved to eliminate the aromatic character of compound **1.137**, and while there is some interesting aspects to be further explored on this macrocycle, related to the absence of the anion coordinated to the two zincs of **Zn1.137**, its synthesis was abandoned.

On the other side compound **4.24** was achieved and characterized evidencing that *N*-confusion of *para* substituted [26]hexaphyrins is possible to be induced in the same manner as in **1.152**. However its cationization showed the same exact problems as we had in most of the macrocycles tested (**4.13, 4.14**, and **4.26)**. There is much to explore with these macrocycles and pyridine moieties allow their applicability in other areas than PDI, as it is for instance catalysis. The possibility to coordinate several metals into these sites seems to be an interesting area to explore. Also derivatives **4.28**, **4.29** and **4.30** with diamine moieties at the periphery of the macrocycle, increasing the number of binding sites of these compounds, were synthesized. The compounds were characterized by different spectroscopy technique and are in accordance with all the material published about these compounds. These new compounds displayed interaction with several anions in solvents like $CHCl_3$ and DMSO.

Antagonistically, the results demonstrate that anion complexation with hydrogen-bonding receptors in a competitive solvent is enhanced. The role of the solvent may take in this phenomena is of high relevance either due the structure that [28]hexaphyrins may acquire when dissolved in this media and/or the possibility of participating in process of binding itself. In both cases the competitive solvent adds to the overall complexation energy and thereby strengthens binding affinity. These compounds especially compounds **4.28** and **4.29** in DMSO exhibits a pronounced constant ratio $KAcO^-/H_2PO_4^-$, 61.44 and 459.9, respectively.

Further insights towards new methodologies to detect and remove anions from aqueous media led us to use piezoelectric crystals coated with compounds **1.138**, **4.28** and **4.29**. The deposition of these compounds is a fashionable methodology to surpass some problems encountered with chemosensors that are not soluble in aqueous media, or that can be difficult to study by other analytical method.

As long term goals, since we did not have enough time to explore the pyridyl expanded porphyrinoids as molecular frameworks building blocks, we are planning to

carry on this work in collaboration with other interested groups in new ligands for catalysis.